Functional and genetic characterisation of Tcp plasmid maintenance and conjugation systems in *Clostridium perfringens*

Sarah Alyce Revitt-Mills

BSc (Hons)

A thesis submitted for the degree of Doctor of Philosophy at

Monash University in 2019

Department of Microbiology

Monash Biomedicine Discovery Institute

Copyright notice

Table of Contents

Abstract

Clostridium perfringens is an important pathogen in both humans and animals. The disease-causing capabilities of this bacterium lie in its arsenal of 20 or more toxins and extracellular enzymes, many of which are located on highly-stable, conjugative plasmids. With the exception of a few, most toxin genes are carried on a family of plasmids related to the tetracycline-resistance plasmid pCW3, which all possess a 35 kb plasmid backbone that is highly conserved. Within this backbone, genetic loci involved in plasmid maintenance and conjugative transfer have been identified and characterised. However, there still are gaps in our knowledge and understanding of the fundamental processes of plasmid biology utilised by this family of plasmids, including replication, conjugation and stability. This thesis investigates several of these processes.

The pCW3-like plasmids utilise the Tcp conjugation system for conjugative transfer. However, it remains unclear whether all components of this system have been identified. Located upstream of the *tcp* locus are genes that remain highly conserved across *C. perfringens* plasmids of the pCW3 family. It was postulated that these conserved genes or genetic regions may play important roles in conjugative transfer. To investigate the involvement of uncharacterised pCW3 genes in conjugative transfer, a panel of mutants were constructed, and their conjugation phenotype determined. Deletion of the conserved *srtD* and *tcpN* genes resulted in a significantly reduced conjugation efficiency, providing evidence that two genes located outside of the *tcp* locus are involved in mediating the efficient conjugative transfer of pCW3 (Chapter Two).

The pCW3-like plasmids are highly stable, as yet only a few maintenance systems have been characterised. To investigate mechanisms of pCW3 plasmid stability, mutants were constructed in two genes predicted to be involved in plasmid maintenance. Through this work it has been demonstrated that a putative multimer resolution system, encoded by the gene *resP* is essential for pCW3 maintenance

(Chapter Three) and that pCW3 relies on a novel gene, *srm*, that is unique to the clostridia, to mediate a stable inheritance pattern (Chapter Four).

The Tcp conjugation system has been well characterised, with key components of the DNA-processing relaxosome and the membrane associated DNA-translocation machinery identified. Whilst previous studies have determined the location of some key components of the conjugation apparatus within the *C. perfringens* cell, resolution has been limited. To increase the resolution and to investigate the location of other Tcp proteins, location of functional epitope-tagged derivatives of six Tcp proteins was determined using StimulaTed Emission Depletion (STED) super resolution microscopy (Chapter Five). This work has provided invaluable insight into the spatial location of the Tcp conjugation event. Overall, the work of this thesis has expanded our knowledge of how pCW3-like plasmids are maintained within *C. perfringens* cells and has deepened our knowledge of the Tcp conjugation process.

Declaration

Thesis is an original work of my research and contains no material which has been accepted for the award of any other degree or diploma at any university or equivalent institution and that, to the best of my knowledge and belief, this thesis contains no material previously published or written by another person, except where due reference is made in the text of the thesis.

Signature: Date: 15/05/19

Sarah Revitt-Mills

Publications during enrolment

Revitt-Mills, S. A, Vidor, C. J., Watts, T. D., Lyras, D., Rood, J. I, & Adams, V. (2019) Virulence plasmids of the pathogenic clostridia. *Microbiology Spectrum* **7**(3), GPP3-0034-2018

Revitt-Mills, S.A., Rood, J.I. and Adams, V.A. (2015) *Clostridium perfringens* extracellular toxins and enzymes: 20 and counting. *Microbiology Australia* **36**(3), 114-117.

Acknowledgements

This PhD journey has certainly been a tough one, and without any reservations, I can truly say I have enjoyed every minute of it. The unknown challenges and new discoveries that come along each and every day keep me going; but there is no way I could have done this on my own. I have been so fortunate to receive an abundance of support from many people throughout this PhD adventure. Without this support most certainly the PhD would have been unobtainable.

First and foremost, I would like to thank my extraordinary supervisors, Julian, Vicki and Dena. Your support throughout the difficulties I have faced during this PhD has been invaluable. Your compassion, kindness and understanding have helped me through and has allowed me to achieve my ultimate goal. To Julian, thank you for inviting me to be a part of your lab for the last five years. I have greatly enjoyed learning under the guise of a teacher so well renowned in his field. Your meticulous manner and constant encouragement to think of what comes next has challenged me to be a better thinker and scientist.

To Vic, our plasmid mum. Your incredible knowledge knows no bounds-except maybe on Mondays. Thank you for your belief in me. Thank you for your continuous encouragement and guidance; you have certainly shaped me into a more confident person and researcher.

To Dena, you are a role model. Thank you for taking on the position of my PhD co-supervisor. I thank you for your insightful contributions to my projects and reminders to think of the big picture. You are a role model for women in science and I aspire to be like you.

I would like to acknowledge the contributions of others in the guidance and undertaking of the experimental work and analysis throughout this PhD project. Particularly, Dr. Alex Fulcher who provided expertise, training and assistance using the STED microscope. Dr. Milena Awad who provided guidance for microscopy sample preparation techniques and methods. Dr. Volker Hilsenstein and Dr. Juan Nunez-Iglesias who designed image analysis pipelines and provided expertise to analyses. A special

mention to Dr. Daouda Traore, who sacrificed much of his time teaching me protein expression and purification methods, which in the end were to little avail. To my academic panel, Daouda, John Boyce and Milena thank you for your guidance at each step along the PhD path. Thank you to the Australian Government for funding this research by an Australian Government Research Training Program (RTP) Scholarship. A special thank you to Sherrie for making the PhD process an absolute breeze.

To the Rood and Lyras lab members, you are all wonderful welcoming people and have helped make this lab my home over these years. A special shout out to my dearest Team Plasmid: Jacob Amy, Callum Vidor, Tom Stent, Sam Munn and Tom Watts. Thank you for sharing this journey, for being real and honest though times of struggle. Thank you for being such incredible support. Friday Freggs catch-ups and pBae drinks nights will forever be the fondest memories of the PhD. To my desk and lab bench buddy, T.D. Watts, this adventure has been fun and, although I don't want to admit it, it has been partly thanks to you. The coffee breaks and procrasta-talks are truly valued.

My greatest network of love, support and encouragement has been my family, who mean so much to me. Firstly, my brothers, my rocks. To my big brother Nic, I thank you for the sacrifices you have made to assist me in my academic pursuit. Uprooting yourself to move back in with your little sister while she studies isn't quite what a man in his mid-twenty's dreams. But you did it anyway. To my little brother Paul, hopefully now I live up to that glorious title of 'nerd' you constantly call me. To the both of you, your unceasing love, encouragement and support is what drives me, and I could not have done this without you.

To my dearest Dad Dad, you have always encouraged me to dream big. You have never allowed me to be held back from any of my pursuits. Thank you for everything and I hope I have made you proud.

To my wonderful mum Sue, I am so glad you are a part of my life. Your love and support have been paramount to my success. Thank you. And to my younger siblings, Eden and Eamon, I aspire to be a role model for you both, with hope this is a good first step.

To my loving grandparents, Lindsay and Pauline, your undying interest in what I am doing drives me to do more. Whilst we often need a dictionary on hand when discussing my work, this has never held you back from trying to learn, understand and seek more from me. I thank you for your love and encouragement.

To my mum, Cheryll, I miss you with all my heart. You are my inspiration. You are my guide. Thank you for all you gave me, and all you sacrificed for me. Thank you for you and for the time we had together, even if it was too short.

Thank you to the many others who have supported me along the way, including Michelle, Cameron, Jess and Frankie, my new Bakker family Gerardo, Vilma, Gerrit, Jacinta, Geri and Adam and my uncles Mark and Ron.

Finally, to my newly minted husband, Steve, whom without your love and support I would not be where I am or who I am today. Thank you for all you have done to help me to achieve my goals. I admire your willingness and courage to take this journey with me as I chase my dreams. You encourage me and build me up, I could not have asked for a better person to do life with.

List of abbreviations

µm	Micrometre
2YT	2 x Yeast Tryptone
AA	Amino Acid
ADP	Adenosine diphosphate
Amp	Ampicillin
AMV	Avian Myeloblastosis Virus
ATP	Adenosine Triphosphate
BCA	Bicinchoninic Acid Assay
BHI	Brain Heart Infusion
BLItz	Biolayer Interferometry
bp	Base Pairs
CCR	Central Control Region
cDNA	Complementary DNA
ChIP-seq	Chromatin Immunoprecipitation- Sequencing
Chl	Saturated Potassium Chlorate
Cm	Chloramphenicol
CPE	*C. perfringens* Enterotoxin
ddPCR	Digital Droplet PCR
DIG	Digoxigenin
DNA	Deoxyribonucleic Acid
dNTP	Deoxyribonucleotide Triphosphate
dsDNA	Double Stranded DNA
DSF	Differential Scanning Fluorimetry
DTBP	Di-*tert*-butyl Peroxide
DTT	Dithiothreitol
DUF	Domain of Unknown Function
Em	Erythromycin
FTG	Fluid Thioglycolate
G_6	hexaglycine
GFP	Green Fluorescent Protein
HA	Haemagglutinin

HI	Heart Infusion
HTH	Helix-Turn-Helix
IDT	Integrated DNA Technologies©
IR	Inverted Repeat
kb	Kilobases
kDa	Kilodaltons
Kn	Kanamycin
LHS	Left Hand Side
MPF	Mating Pair Formation
mRNA	Messenger Ribonucleic Acid
MS	Mass Spectrometry
MW	Molecular Weight
N/A	Not Applicable
NA	Nutrient Agar
Nal	Nalidixic Acid
NEB	New England Biolabs®
ng	Nanograms
NTPase	Nucleoside-triphosphatase
OD	Optical Density
ORF	Open Reading Frame
oriT	Origin of Transfer
oriV	Origin of Replication
Par	Partitioning
PBS	Phosphate Buffered Saline
PCR	Polymerase Chain Reaction
PVDF	Polyvinylidene Diflouride
RAM	Retrotransposition-Activated Selectable Marker
RHS	Right Hand Side
Rif	Rifampicin
RNA	Ribonucleic Acid
RNA-seq	RNA-Sequencing
RT	Room Temperature
RT-PCR	Reverse Transcription- Polymerase Chain Reaction

SD	Standard Deviation
SEM	Standard Error of the Mean
SP	Signal Peptide
SPR	Surface Plasmon Resonance
ssDNA	Single Stranded Deoxyribonucleic Acid
STED	StimulaTed Emission Depletion
Str	Streptomycin
T4SS	Type IV Secretion System
TA	Toxin-Antitoxin
Tc	Tetracycline
tcp	Transfer Clostridial Plasmid
Tm	Thiamphenicol
TMD	Transmembrane Domain
TPG	Tryptone, Peptone, Glucose
TPGY	Tryptone, Peptone, Glucose and Yeast
T-strand	Transfer Strand
TT	TargeTron
UV	Ultraviolet
VC	Vector Control
WGA	Wheat Germ Agglutinin

List of tables

List of figures

Chapter 1

Chapter 2

Chapter 3

Chapter One

Introduction

Clostridium perfringens infection and toxins

Clostridium perfringens is a Gram-positive anaerobic pathogen that is ubiquitously distributed amongst animals, humans and in the environment (McClane *et al.*, 2013). Although often found as a common commensal in the gastrointestinal tract of mammals, this spore-forming rod is also the causative agent of numerous infections in both humans and animals (Uzal *et al.*, 2014, McClane, 2014). The diseases caused by *C. perfringens* range from mild, self-limiting food poisoning, to the more severe pathologies of gas-gangrene, enterotoxaemia and necrotic enteritis (Uzal *et al.*, 2014). What makes *C. perfringens* such a proliferate pathogen is its impressive ability to encode and produce up to 20 different toxins and extracellular enzymes, many of which are associated with conjugative plasmids (Katayama *et al.*, 1996, Revitt-Mills *et al.*, 2015, Li *et al.*, 2013).

C. perfringens strains differ in their carriage and expression of toxin genes. As several toxins have been proven essential for *C. perfringens*-mediated disease (Awad *et al.*, 1995, Sarker *et al.,* 1999, Sayeed *et al.*, 2008, Keyburn *et al.*, 2008), they provide the basis for the toxinotype classification scheme in *C. perfringens* (Rood *et al.*, 2018, Petit *et al.*, 1999). In this scheme *C. perfringens* strains are classified into seven toxinotypes based on the differential production of six typing toxins: α-toxin, β-toxin, ε-toxin, ι-toxin, enterotoxin (CPE) and NetB-toxin (Table 1.1) (Rood *et al.*, 2018). A unique feature of the *C. perfringens* classification scheme is the association of particular 'types' with specific diseases (Rood *et al.*, 2018). For example, type A strains are known to cause gas gangrene in humans, whereas type G strains are closely associated with necrotic enteritis in chickens (Rood *et al.*, 2018).

Table 1.1: *C. perfringens* toxinotypes and associated diseases in humans and animals.

Toxinotype	α	β	ε	ι	CPE	NetB	Associated Disease
A	+	-	-	-	-	-	Human myonecrosis Myonecrosis in sheep, cattle and horses Enteritis in dogs, pigs, horses and goats
B	+	+	+	-	-	-	Necrotic enteritis and enterotoxaemia in sheep, cattle and horses
C	+	+	-	-	+/-	-	Enteritis necroticans in humans Necrotic enteritis and enterotoxaemia in pigs, lambs, calves and foals
D	+	-	+	-	+/-	--	Enterotoxaemia in sheep, goats and cattle
E	+	-	-	+	+/-	-	Enteritis in rabbits, lambs and cattle
F	+	-	-	-	+	-	Food poisoning in humans Non-foodborne diarrhoea in humans
G	+	-	-	-	-	+	Avian necrotic enteritis

Table adapted from (Rood *et al.*, 2018), (+) produced, (-) not produced, (+/-) produced in some strains

In addition to the typing toxins, *C. perfringens* can express a range of other toxins such as β2-toxin, δ-toxin, λ-toxin, κ-toxin, μ-toxin, perfringolysin O, NetE, NetF, NetG, TpeL, BEC and chromosomally encoded sialidases in various combinations (Gibert *et al.*, 1997, Yonogi *et al.*, 2014, Alouf & Jolivet-Reynaud, 1981, Jin *et al.*, 1996, Canard *et al.*, 1994, Mehdizadeh Gohari *et al.*, 2015, Paredes-Sabja *et al.*, 2011, Dupuy *et al.*, 1997, Chakravorty *et al.*, 2011, Chiarezza *et al.*, 2009).

The toxins of *C. perfringens* can be categorised into four groups based on their mechanism of function: β-pore-forming toxins, intracellular toxins, membrane damaging enzymes and hydrolytic enzymes (Petit *et al.*, 1999). For the purpose of this review, the toxins of *C. perfringens* will only be mentioned briefly, as their mechanism of function and genetic location are summarised in Table 1.2. Through sequencing and genetic analysis, many of the toxins produced

by *C. perfringens* have been found to be encoded extrachromosomally on large conjugative plasmids (Bannam *et al.*, 2011, Gurjar *et al.*, 2010, Katayama *et al.*, 1996, Keyburn *et al.*, 2008, Li *et al.*, 2007, Popoff & Bouvet, 2013, Sayeed *et al.*, 2007, Sayeed *et al.*, 2010, Li *et al.*, 2013, Hughes *et al.*, 2007, Brynestad *et al.*, 2001). Interestingly the enterotoxin gene, *cpe*, can be found both chromosomally and on plasmids, with the location of the gene playing a role in the epidemiology of disease (Collie & McClane, 1998; Cornillot *et al.*, 1995). Typically, *C. perfringens* food poisoning isolates possess a chromosomally encoded *cpe* gene; by contrast, isolates from non-food borne gastrointestinal infections possess plasmid encoded *cpe* genes (Collie & McClane, 1998). The reason for this difference and its relation to pathogenesis has not yet been determined (Collie & McClane, 1998). However, it is likely that the presence of toxin genes on conjugative plasmids plays a significant role in disease dissemination, as transfer of toxin genes from virulent strains to commensal strains eliminates the need for efficient bacterial colonisation in order to produce disease (Bannam *et al.*, 2006, Lacey *et al.*, 2017, Brynestad *et al.*, 2001).

Plasmids and horizontal gene transfer

Bacterial genomes are vastly plastid, constantly adapting and changing to overcome new environmental pressures (Ochman *et al.*, 2000). This genetic diversity arises through the ability of bacterial cells to naturally share DNA through the horizontal transfer of mobile genetic elements, including plasmids (Frost *et al.*, 2005, Thomas & Nielsen, 2005). Plasmids are non-essential, extrachromosomal DNA molecules that autonomously replicate within bacterial cells (Tolmasky, 2017). These genetic elements are extremely diverse and can vary in size, host range and copy number (Smillie *et al.*, 2010, Tolmasky, 2017), and will often encode genes necessary for self-replication and partitioning (Frost *et al.*, 2005, Ochman *et al.*, 2000). Most importantly, plasmids can also encode various antibiotic resistance, metabolic and pathogenic determinants (Frost *et al.*, 2005, Ochman *et al.*, 2000). The transfer of plasmids from one bacterium to another can occur via three mechanisms: transduction, transformation and conjugation, with conjugation

Table 1.2: Properties of *C. perfringens* toxins.

Toxin	Gene	Toxin category and activity	Genetic location
α-toxin	*plc*	Membrane damaging; phospholipase C and sphingomyelinase activities	Chromosome
β-toxin	*cpb*	Pore-forming toxin	Plasmid
ε-toxin	*etx*	Pore-forming toxin	Plasmid
ι-toxin	*iap, ibp*	Intracellular toxin; actin-specific ADP ribosyltransferase	Plasmid
CPE	*cpe*	Pore-forming toxin	Chromosome or Plasmid
NetB	*netB*	Pore-forming toxin	Plasmid
BEC	*becA, becB*	Intracellular toxins; actin-specific ADP-ribosyltransferase	Plasmid
α-clostripain	*ccp*	Hydrolytic enzymes; cysteine protease	Chromosome
κ-toxin	*colA*	Hydrolytic enzymes; collagenase	Chromosome
β2-toxin	*cpb2*	Putative pore-forming toxin	Plasmid
δ-toxin	*cpd*	Pore-forming toxin	Plasmid
λ-toxin	*lam*	Hydrolytic enzymes; protease	Plasmid
μ-toxin	*nagH*	Hydrolytic enzyme; hyaluronidase	Chromosome
NanI	*nanI*	Hydrolytic enzymes; sialidase	Chromosome
NanJ	*nanJ*	Hydrolytic enzymes; sialidase	Chromosome
NetE	*netE*	Putative pore-forming toxin	Plasmid
NetF	*netF*	Pore-forming toxin	Plasmid
NetG	*netG*	Putative pore-forming toxin	Plasmid
perfringolysin O or θ-toxin	*pfoA*	Pore-forming toxin; cholesterol-dependent cytolysin	Chromosome
TpeL	*tpeL*	Intracellular toxins; Ras-specific mono-glucosyltransferase	Plasmid
Urease	*ureABC*	Hydrolytic enzymes; urease	Plasmid

This table was adapted from (Revitt-Mills *et al.*, 2015).

being the most common mechanism (Thomas & Nielsen, 2005, Schröder & Lanka, 2005). Conjugative plasmids encode all the genes necessary for self-transfer and can autonomously transfer to recipient cells (Schröder & Lanka, 2005). This movement of DNA molecules between bacterial cells is of importance, as it can lead to the rapid dissemination of virulence, metabolic and antibiotic resistance determinants within a bacterial population (Norman *et al.*, 2009).

C. perfringens plasmid diversity

Plasmids were first described in *C. perfringens* in 1973 with the identification of the small non-conjugative bacteriocin plasmid pIP404 (Ionesco & Bouanchaud, 1973, Solberg *et al.*, 1981). Early studies on *C. perfringens* plasmid biology were focussed on the identification and characterisation of plasmids encoding bacteriocins and antibiotic resistance determinants (Brefort *et al.*, 1977, Rood *et al.*, 1978, Rokos *et al.*, 1978). At the time, many antibiotic resistance and bacteriocin plasmids were identified (Ionesco & Bouanchaud, 1973, Mihelc *et al.*, 1978, Rood *et al.*, 1978, Abraham & Rood, 1985a). However, since the discovery of toxin genes on plasmids, the focus of *C. perfringens* plasmid research has shifted to the identification and characterisation of plasmids encoding virulence determinants (Li *et al.*, 2013, Katayama *et al.*, 1996).

The era of genome sequencing has identified an extensive number of toxin- and antibiotic-resistance plasmids from different *C. perfringens* strains (Bannam *et al.*, 2006, Bannam *et al.*, 2011, Gurjar *et al.*, 2010, Parreira *et al.*, 2012, Sayeed *et al.*, 2007, Sayeed *et al.*, 2010, Shimizu *et al.*, 2002, Yonogi *et al.*, 2014). Many of these sequenced plasmids share a high degree of homology, approximately 35 kb, with the archetypal conjugative tetracycline resistance plasmid pCW3 (Figure 1.1) (Bannam *et al.*, 2006, Li *et al.*, 2013). Located within this conserved region are genes involved in plasmid replication, maintenance, regulation and conjugative transfer (Bannam *et al.*, 2006, Brynestad *et al.*, 2001, Miyamoto *et al.*, 2006). All of the plasmid-encoded toxin genes, apart from *becAB*, have been identified on plasmids similar to pCW3 (Bannam *et al.*, 2011, Gurjar *et al.*, 2010, Katayama *et al.*, 1996, Keyburn *et al.*, 2008, Li *et al.*, 2007, Sayeed *et al.*, 2007, Sayeed *et al.*,

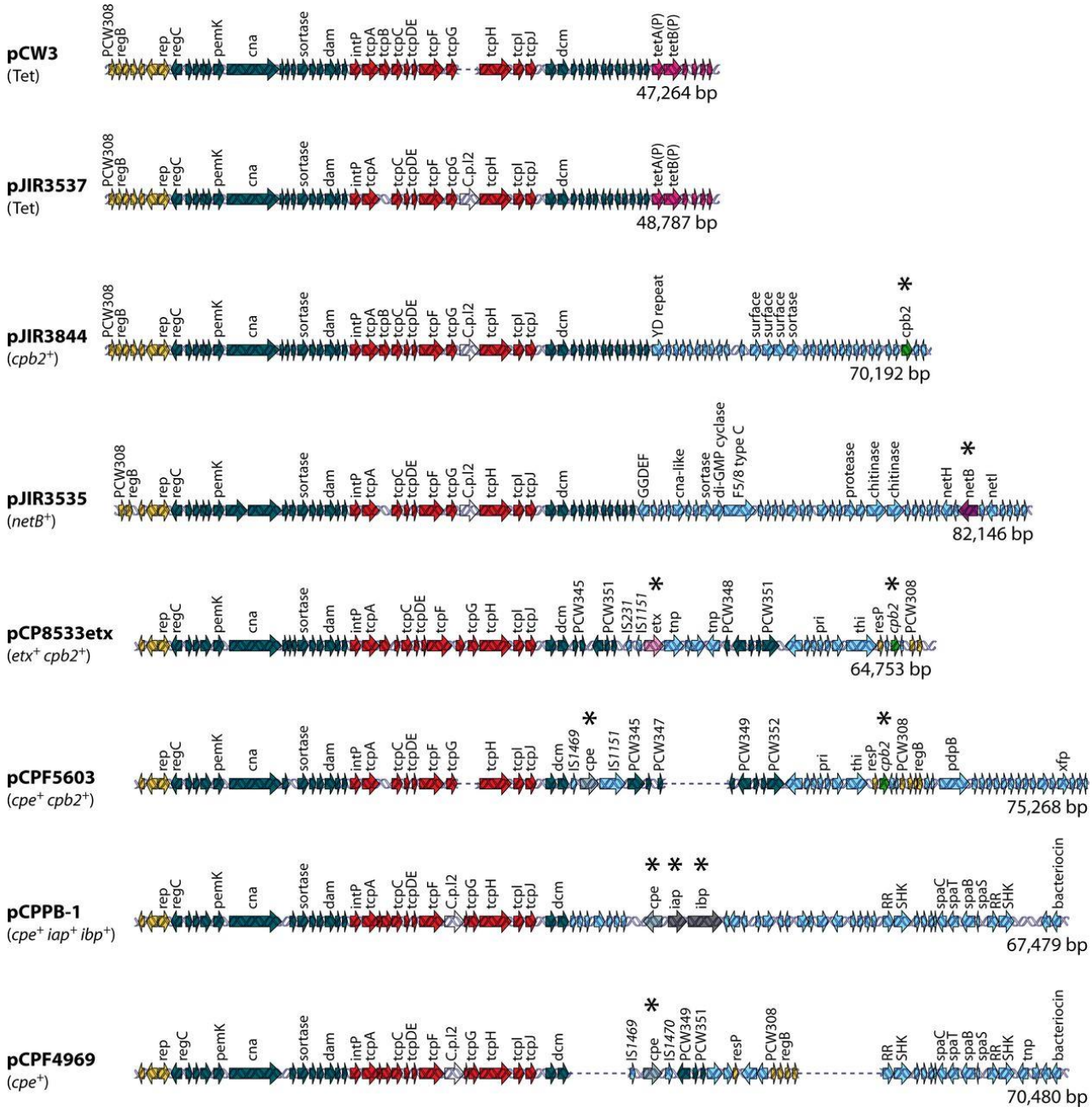
pCW3
(Tet)
47,264 bp
pJIR3537
(Tet)
48,787 bp
pJIR3844
(cpb2+)
70,192 bp
pJIR3535
(netB+)
82,146 bp
pCP8533etx
(etx+ cpb2+)
64,753 bp
pCPF5603
(cpe+ cpb2+)
75,268 bp
pCPPB-1
(cpe+ iap+ ibp+)
67,479 bp
pCPF4969
(cpe+)
70,480 bp

Figure 1.1: Comparative alignment of *C. perfringens* pCW3-like plasmid sequences. Shown are sequence alignments for pCW3 (Bannam *et al.*, 2006); pJIR3537 (*tet*$^{+}$), pJIR3844 (*cpb2*$^{+}$), and pJIR3535 (*netB*$^{+}$) (Bannam *et al.*, 2011); pCP8533etx (*etx cpb2*$^{+}$) (Miyamoto *et al.*, 2008); pCPF5603 (*cpe*+ *cpb2*$^{+}$) (Miyamoto *et al.*, 2006); pCPPB-1 (*cpe*+ *iota*$^{+}$) (Miyamoto *et al.*, 2011); and pCPF4969 (*cpe*$^{+}$) (Miyamoto *et al.*, 2006). Each arrow represents an open reading frame (ORF); ORF arrows shown are as follows: red arrows, the conserved *tcp* locus; dark blue arrows, other conserved ORFs shared by these plasmids; yellow arrows, plasmid replication region; light purple arrows, tetracycline resistance gene; green arrows, the *cpb2* toxin gene; purple arrow, the *netB* toxin gene; pink arrows, the *etx* gene; grey arrows, the *cpe* gene; dark grey arrows, the iota-toxin genes; light blue arrows, regions unique to each plasmid. Asterisks denote a toxin gene. Image and figure legend adapted from (Li *et al.*, 2013).

2010, Bannam *et al.*, 2006, Parreira *et al.*, 2012, Brynestad *et al.*, 2001, Cornillot *et al.*, 1995, Miyamoto *et al.*, 2002, Miyamoto *et al.*, 2006). Due to the high level of sequence conservation, as well as the presence of shared or similar replication and conjugation functions, these plasmids have been classified into the pCW3-like family of *C. perfringens* plasmids. Based on current knowledge, the plasmids of *C. perfringens* can be broadly characterised into three families: the well characterised pCW3-like plasmids, the pCP13-like plasmids, and the pIP404-like plasmids, a family of small non-conjugative plasmids that usually encode a bacteriocin (*bcn*).

The pCP13-like plasmids

Whole genome sequence analysis of *C. perfringens* strain 13 identified the 54 kb plasmid, pCP13 (Shimizu *et al.*, 2002). At the time of its discovery, pCP13 was not considered of importance to toxin gene carriage, as the *cpb2* toxin gene located on this plasmid was defective, due to the presence of a premature stop codon (Shimizu *et al.*, 2002). However, the pCP13-like family of plasmids is gaining more interest as a toxin-carrying plasmid family in *C. perfringens* as further sequence data becomes available. Initial bioinformatic analysis of pCP13 revealed the presence of 63 open reading frames (ORFs), many of which encode hypothetical proteins (Shimizu *et al.*, 2002). At the time of discovery, pCP13 shared very little homology to any other characterised *C. perfringens* plasmids (Shimizu *et al.*, 2002). As such, characterisation of this plasmid type was largely overlooked.

More recently, multiple outbreaks of *C. perfringens*-mediated food poisoning were associated with strains that did not encode the CPE toxin, the toxin commonly associated with *C. perfringens* food-borne disease (Yonogi *et al.*, 2014, Irikura *et al.*, 2015). Analysis of the causative strains identified the presence of a novel binary enterotoxin named BEC (or CPILE), which was harboured on large plasmids (Yonogi *et al.*, 2014, Irikura *et al.*, 2015). Sequencing of two BEC encoding plasmids revealed that they shared considerable sequence homology to pCP13 and were among the first toxin plasmids of *C. perfringens* to be classified into the new family of pCP13-

like plasmids (Yonogi *et al.*, 2014). The BEC plasmids and pCP13 share a region of 38 kb, which is thought to comprise the common backbone of pCP13-like plasmids (Yonogi *et al.*, 2014).

The conserved region of pCP13-like plasmids encodes several genes hypothesised to be involved in plasmid partitioning and multimer resolution (Shimizu *et al.*, 2002). However, until recently, no replication or conjugation genes were identified (Shimizu *et al.*, 2002). Recent work on another pCP13-like plasmid, the bacteriocin encoding plasmid pBCNF5603, has identified a replication gene that is highly related to *orf63* from pCP13, homologues of which are also carried on the BEC plasmids (Miyamoto *et al.*, 2015).

Initial analysis suggested that pCP13 was non-conjugative, as the plasmid sequences had no similarities to other characterised conjugation loci (Shimizu *et al.*, 2002). However, the recent identification and characterisation of a new conjugation locus on the plasmid pCS1-1 from *Paeniclostridium sordelii* (previously *Clostridium sordellii*), revealed a significant degree of homology between the *P. sordellii* transfer (*cst*) locus to a region found on pCP13, challenging the notion that pCP13 is non-conjugative (Vidor *et al.*, 2018). Subsequent analysis of pCP13 demonstrated the existence of a functional conjugation locus, denoted the Pcp locus, and showed that pCP13 was conjugative (Watts *et al.*, 2019). Examination of the Pcp locus among other members of the pCP13-like plasmid family revealed a high degree of conservation, indicating that other members of this plasmid family, including the BEC plasmids, are likely to be conjugative (Watts *et al.*, 2019). The recent discoveries that pCP13-like plasmids are independently mobile and can harbour virulence genes emphasises the importance of this mostly ignored plasmid family in toxin gene spread and warrants further study.

The pCW3-like plasmids

The pCW3-like plasmids (or Tcp plasmids) comprise the largest characterised plasmid family in *C. perfringens*. Plasmids within this family have significant conservation across a 35 kb region that is highly similar to the tetracycline resistance plasmid pCW3 (Figure 1.1) (Bannam *et al.*, 2011, Li

et al., 2013, Parreira *et al.*, 2012). This conserved region makes up the common backbone of all pCW3-like plasmids, as it contains genes involved in plasmid replication, maintenance, regulation and conjugative transfer (Li *et al.*, 2013). To date, only two key loci of the common backbone have been characterised: the replication and partitioning region and the *tcp* conjugation locus (Figure 1.2). The replication region encodes several genes involved in plasmid regulation, maintenance and replication (Parreira *et al.*, 2012, Adams *et al.*, 2015, Watts *et al.*, 2017, Bannam *et al.*, 2006). The genes located within this region remain conserved between the Tcp plasmids, with the only significant changes occurring in the nucleotide sequences of the *parMRC*-like partitioning locus (Parreira *et al.*, 2012, Adams *et al.*, 2015). These nucleotide differences form the basis for plasmid incompatibility groups in *C. perfringens* (Adams *et al.*, 2015, Watts *et al.*, 2017).

The *tcp* locus encodes a novel transfer locus that is unique to the Tcp plasmids of *C. perfringens* (Wisniewski & Rood, 2017). To date, five large toxin plasmids and numerous antibiotic resistance plasmids have been shown experimentally to be conjugative (Bannam *et al.*, 2011, Brynestad *et al.*, 2001, Hughes *et al.*, 2007, Brefort *et al.*, 1977, Rood *et al.*, 1978, Rood, 1983, Abraham & Rood, 1985b, Abraham *et al.*, 1985, Han *et al.*, 2015). Furthermore, sequencing, pulsed field gel electrophoresis and Southern hybridisation have demonstrated that all of the large toxin plasmids carry a *tcp* locus that is closely related to that of pCW3, meaning that these plasmids are also highly likely to be conjugative (Bannam *et al.*, 2011, Brynestad *et al.*, 2001, Hughes *et al.*, 2007, Sayeed *et al.*, 2010, Sayeed *et al.*, 2007, Li *et al.*, 2007, Gurjar *et al.*, 2010, Miyamoto *et al.*, 2006, Mehdizadeh Gohari *et al.*, 2016). The precise mechanism of conjugation utilised by *C. perfringens* has yet to be fully characterised. However, functional analysis of the proteins encoded within the pCW3 *tcp* locus, has begun to build a picture of the conjugative mechanism, which will be discussed in further detail later in this chapter.

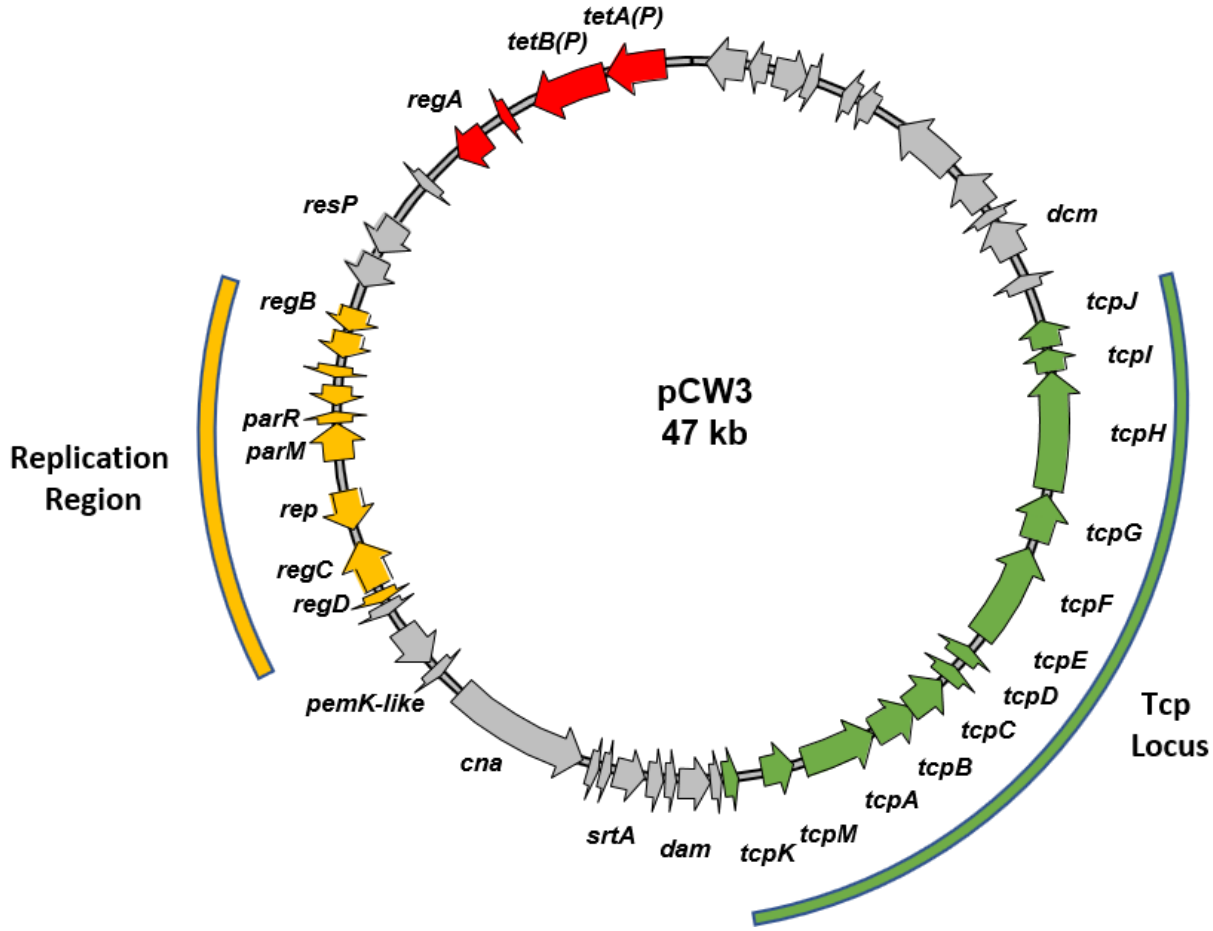

Figure 1.2: Genetic organisation of the archetypal tetracycline resistance plasmid pCW3. A circular map of pCW3 is shown. ORFs are indicated by the arrows. Genetic regions are indicated as follows: the replication region (yellow), the conjugation locus (Tcp locus; green) and the unique region, including the tetracycline resistance genes *tetAB(P)*, are shown in red. Grey arrows indicate conserved ORFs

Conjugation

Conjugation is one of the most utilised mechanisms of DNA transfer amongst bacterial cells and involves the movement of genetic elements, such as plasmids, between two bacterial cells (Cabezón *et al.*, 2015, Norman *et al.*, 2009, Thomas & Nielsen, 2005). For conjugative plasmid transfer to occur, direct cell-to-cell contact is required (Waksman & Orlova, 2014). In Gram-negative bacteria this contact is initiated through the formation of a pilus structure that extends from the donor cell surface to the recipient cell (Schröder & Lanka, 2005). In Gram-positive bacteria the mechanism of initial cellular contact has not yet been elucidated, however, it has been postulated that cell surface adhesins initiate this contact, rather than a pilus structure (Christie *et al.*, 2017, Alvarez-Martinez & Christie, 2009, Bhatty *et al.*, 2013, Goessweiner-Mohr *et al.*, 2014). Upon cellular contact, DNA is then transferred through a specialised conjugation apparatus (Christie *et al.*, 2014).

The conjugative apparatus facilitates transfer of DNA *via* the assembly of a multiprotein complex at the surface of a bacterial donor cell (Grohmann *et al.*, 2018, Llosa *et al.*, 2002). This complex is comprised of two distinct subunits, the cytoplasmic relaxosome and the membrane-associated transferosome, which are linked by a coupling protein (Figure 1.3) (Christie *et al.*, 2014, Trokter *et al.*, 2014). The relaxosome is the DNA processing machinery of the conjugation apparatus and is typically comprised of a relaxase enzyme, which nicks the DNA in preparation for transfer, and accessory proteins, which process and protect plasmid DNA prior to transfer (Lanka & Wilkins, 1995, Wong *et al.*, 2012, Chandran Darbari & Waksman, 2015). The transferosome is a large multisubunit transmembrane channel, through which the DNA is pumped from the donor cell into a recipient cell (Chandran Darbari & Waksman, 2015, Grohmann *et al.*, 2018). Conjugative plasmids of Gram-negative bacteria employ a specialised subfamily of Type IV secretion systems (T4SSs) as transferosome complexes (Grohmann *et al.*, 2018, Chandran Darbari & Waksman, 2015). However, due to differences in cell wall composition, Gram-positive bacteria use a similar,

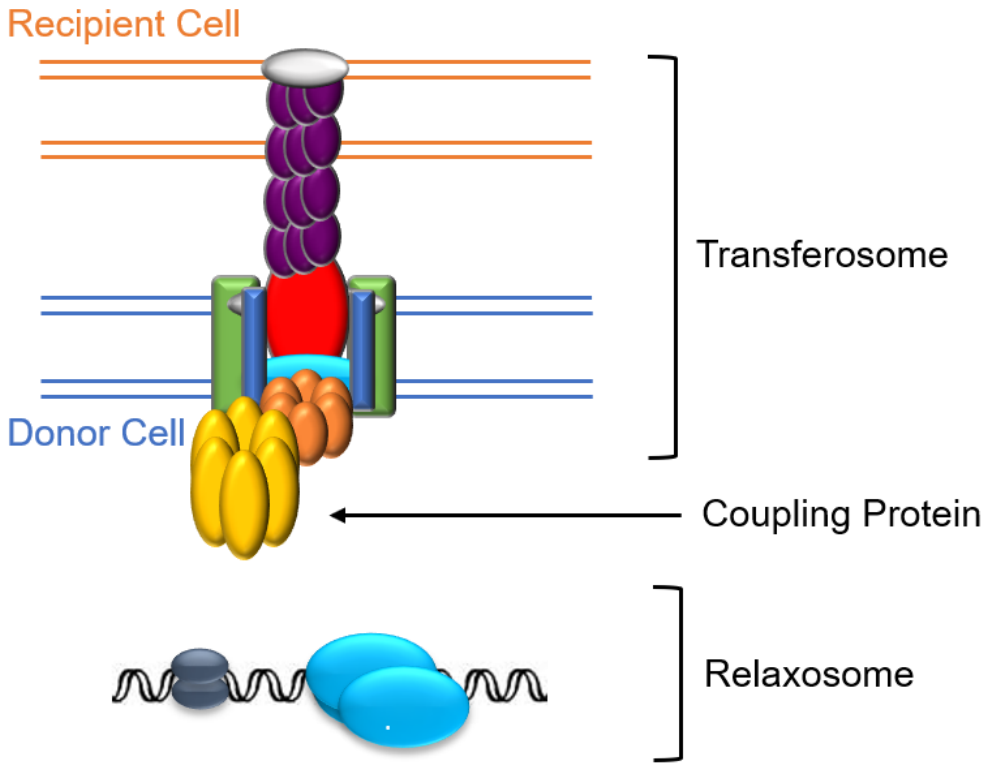

Figure 1.3: Simplified schematic of the Gram-negative conjugative type IV secretion system. The thick red and blue lines represent bacterial membranes. The transferosome transverses both membranes linking the donor cell to the recipient, protein components are depicted in red, green, purple, grey and orange and blue. The relaxase is represented as the blue oval shape. Relaxosome auxiliary proteins are seen in dark blue. The hexameric coupling protein is represented as a hexamer in yellow, anchored to the inner membrane. DNA is represented by the thin double black lines. Image and figure legend adapted from (Llosa *et al.*, 2002).

but modified, form of Type IV secretion system (T4SS) (Goessweiner-Mohr *et al.*, 2014, Grohmann *et al.*, 2017, Gomis-Rüth *et al.*, 2002). The multimeric coupling protein interacts directly with the relaxosome and transferosome complexes, linking them and facilitating the active transport of plasmid DNA through the transferosome *via* its ATPase activity (Gomis-Rüth *et al.*, 2002, Gomis-Ruth *et al.*, 2004, Guglielmini *et al.*, 2013).

Relaxosome structure and function

The relaxosome is the cytoplasmic substrate-processing machinery of conjugative T4SS (Zechner *et al.*, 2017, Lanka & Wilkins, 1995). For transfer to occur, DNA must first be processed into a physical state that allows for conjugative transport (Lanka & Wilkins, 1995, Wong *et al.*, 2012). In most cases, this involves the production of single stranded DNA (Lanka & Wilkins, 1995, Wong *et al.*, 2012). However, exceptions do occur whereby double stranded DNA is used as the conjugative substrate, as seen in some *Streptomyces* and *Mycobacterium* species (Pettis & Cohen, 2001, Possoz *et al.*, 2001, Wang *et al.*, 2003, Alvarez-Martinez & Christie, 2009). Plasmid DNA processing by the relaxosome is a conserved mechanism, initiated by the formation of the relaxosome complex at the plasmid origin of transfer (*oriT*) (Ilangovan *et al.*, 2017, Wong *et al.*, 2012, Llosa *et al.*, 2002, Llosa & de la Cruz, 2005). After complex formation, the relaxase enzyme catalyses strand-specific cleavage of the DNA at the *oriT* site through a transesterification reaction (Byrd & Matson, 1997). After nicking, plasmid DNA is unwound through the action of associated DNA transfer accessory factors, such as helicases, producing a single strand of DNA (also known as the T-strand) that is ready for conjugative transfer (de la Cruz *et al.*, 2010, Ding *et al.*, 2003). It is hypothesised that rolling circle replication then replaces the displaced T-strand (de la Cruz *et al.*, 2010, Waters & Guiney, 1993). Throughout DNA processing and transfer the relaxase enzyme remains covalently bound to the 5'-phosphate group of the T-strand (Byrd & Matson, 1997, de la Cruz *et al.*, 2010). The relaxase-DNA complex interacts with the transferosome and transport to the recipient cell is facilitated by the coupling protein (de la Cruz *et al.*, 2010).

In many Gram-negative systems, accessory proteins aid the formation and function of the relaxosome complex (Wong *et al.*, 2012). For example, the accessory protein TraH of the RP4 plasmid system stabilises the relaxosome complex, which allows for more efficient plasmid DNA processing (Pansegrau *et al.*, 1990). The F-plasmid encoded protein, TraM, increases the frequency of *oriT* DNA cleavage (Ragonese *et al.*, 2007), as well as enhancing the recruitment of the relaxosome to the transferosome (Disqué-Kochem & Dreiseikelmann, 1997). The F-plasmid system also encodes the accessory factor TraY, which has helicase-like activity and aids in the local unwinding of the plasmid DNA (Luo *et al.*, 1994). Accessory proteins can also stabilise the association of important processing subunits, as shown by MobB from R1162 (Parker & Meyer, 2007). Some Gram-positive systems also encode relaxosome accessory proteins, such as the MobC protein of the *Staphylococcal* pC221 system, which enables the relaxase to specifically recognise the *oriT* sequence (Caryl & Thomas, 2006, Smith & Thomas, 2004). The Aux1 and Aux2 accessory proteins from the *Bacillus subtilis* plasmid pLS20, facilitate essential interactions with the *oriT* DNA, thereby aiding relaxosome processing (Miguel-Arribas *et al.*, 2017).

Transferosome structure and function

The transferosome machinery has been best characterised in Gram-negative organisms, especially the VirB/D4 system of *Agrobacterium tumefaciens* (Figure 1.4) (Ilangovan *et al.*, 2015, Waksman & Orlova, 2014). This system is comprised of three multiprotein subcomplexes: the cytoplasmic inner-membrane complex, the core complex, and the pilus complex (Waksman & Orlova, 2014). The inner-membrane complex has two major components, intracellular ATPases (VirD4, VirB4 and VirB11) that power complex formation and translocation, and the inner membrane channel complex (VirB3, VirB6 and VirB8), which is linked to the core complex (Ilangovan *et al.*, 2015, Waksman & Orlova, 2014). The core complex (VirB7, VirB9 and VirB10) spans the inner and outer membranes, and the pilus complex (VirB2 and VirB5) extends from the cell surface, mediating cell-to-cell contact (Waksman & Orlova, 2014). Many other Gram-negative

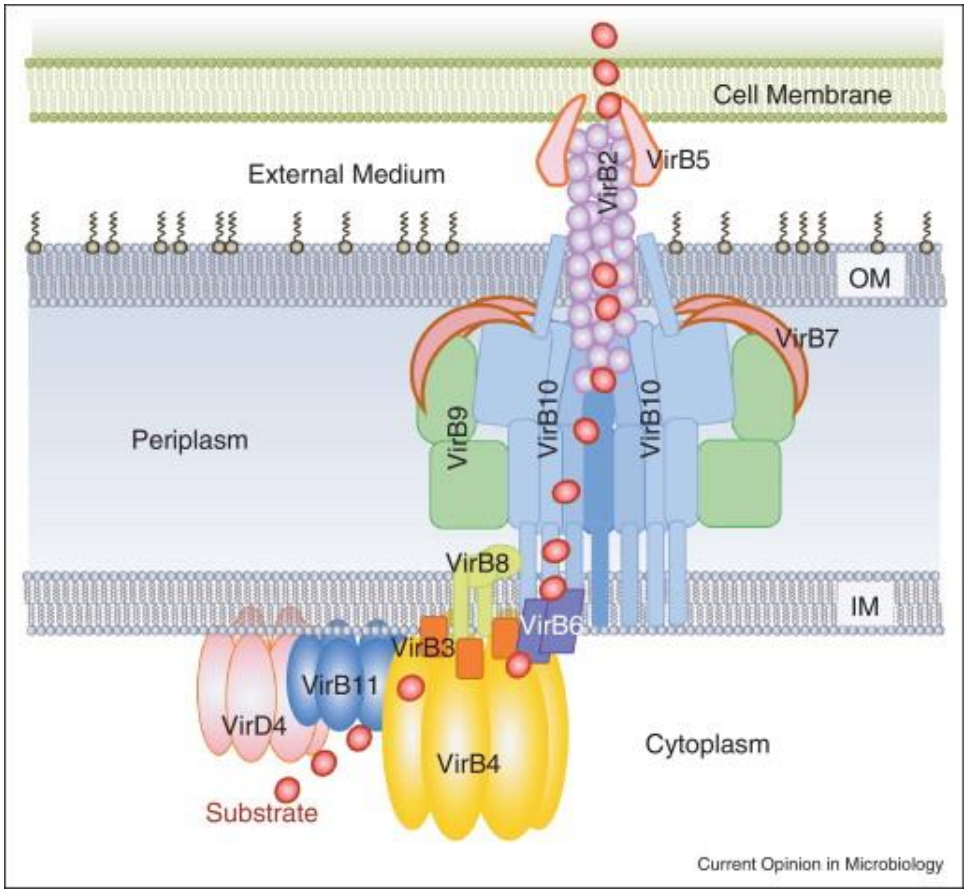

Figure 1.4: Organisation of the T4SS of *Agrobacterium tumefaciens*. VirD4 (pink), VirB11 (blue), VirB4 (gold) ATPases, polytopic VirB6 (purple), bitopic VirB8 (light green) and VirB3 (orange) form the cytoplasmic inner membrane part of the complex. VirB7 (brown), VirB9 (green), and VirB10 (blue) compose the periplasmic part of the secretion system. VirB2 and VirB5 constitute the outer part of the secretion system. Red dots indicate the proposed path of the substrate through the machinery as established by Cascales and Christie, 2003. Image and figure legend reproduced from (Waksman & Orlova, 2014).

conjugative plasmid systems, such as the F-plasmid and RP4 systems of *Escherichia coli*, have been found to encode proteins with conserved structures and functions similar to those of the VirB/D4 system (Arutyunov *et al.*, 2010, Farrand *et al.*, 1996). As a result, the VirB/D4 T4SS is used as a reference for the nomenclature of orthologs and homologues found in other conjugative systems (Bhatty *et al.*, 2013, Cabezón *et al.*, 2015). Gram-positive T4SS are not as extensively studied as their Gram-negative counterparts. However, Gram-positive bacteria are proposed to utilise a novel conjugative T4SS. The transferosome complex needs only to span a single cell membrane, but must also navigate a thick peptidoglycan layer, in contrast to the double membrane of Gram-negative bacteria (Goessweiner-Mohr *et al.*, 2014, Grohmann *et al.*, 2017). It has been established that several protein structures and functions remain conserved across a range of Gram-positive and Gram-negative T4SS (Goessweiner-Mohr *et al.*, 2014, Grohmann *et al.*, 2017). Notably, homologs of the inner-membrane proteins VirD4, VirB4, VirB6 and VirB8 have been described in many Gram-positive systems, suggesting functional conservation (Goessweiner-Mohr *et al.*, 2013, Goessweiner-Mohr *et al.*, 2014). Homologs of the outer-membrane channel proteins have yet to be found in Gram-positive systems (Goessweiner-Mohr *et al.*, 2014, Grohmann *et al.*, 2018).

The mechanism by which plasmid DNA is transferred into a recipient cell has best been described by Llosa *et al.* (2002), who first proposed that conjugative transport of DNA occurs in an energy-dependent two-step manner (Figure 1.5). The first step involves the active transport of the relaxase covalently bound to the T-strand through the transferosome facilitated by ATPase activity. Following relaxase transport, the remaining T-strand is then actively pumped into the recipient, in an energy dependent manner facilitated by the function of the coupling protein. After T-strand transfer into the recipient cell, the relaxase acts on the initial *nic* site resulting in a closed circular ssDNA molecule (Lanka & Wilkins, 1995, Llosa *et al.*, 2002). By an unknown mechanism, the complementary strand is then synthesised until the plasmid is complete, resulting in both the donor and recipient cells possessing identical plasmids (Llosa *et al.*, 2002, Byrd & Matson, 1997).

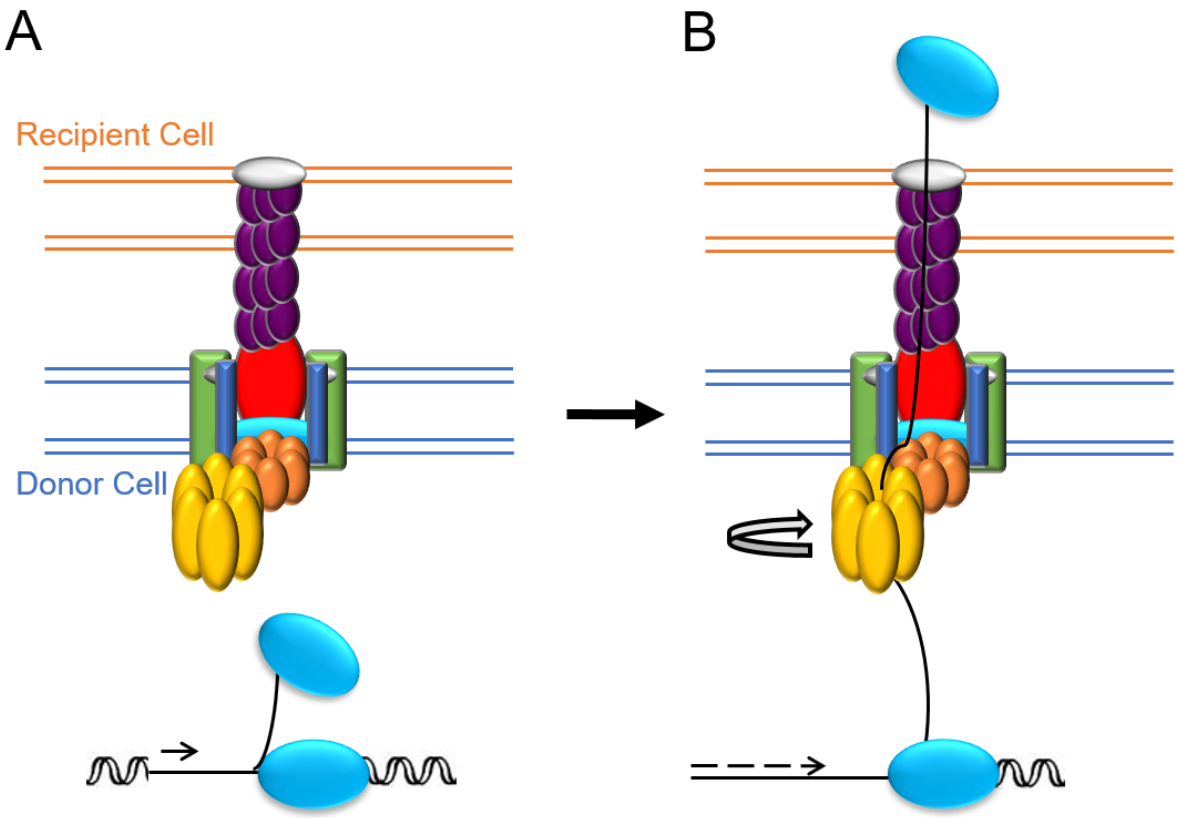

Figure 1.5: Two-step model for conjugal DNA transport. Horizontal thick blue and red lines represent bacterial membranes, traversed by green and red cylinders that represent the T4SS. An ATPase enzyme is depicted in dark blue. The relaxase is represented as the blue oval shape; the coupling protein is represented as a hexamer in yellow, with an orange-like shape, anchored to the inner membrane. DNA is represented by a thin black line; newly replicated DNA, by a dashed arrow. Curved arrows indicate postulated motion forces required for DNA movement. **A.** The coupling protein links the T4SS and the relaxosome; a relaxase monomer covalently linked to the nicked T-strand is the substrate for T4SS secretion. **B.** The coupling protein pumps out the T-strand as it is displaced from the donor plasmid. Image and figure legend adapted from Llosa and de la Cruz, 2005.

The current model for Tcp mediated conjugative transfer

The original bioinformatic analysis of pCW3 proposed that the genetic region spanning from *tcpM* (previously *intP*) though to *tcpJ* forms an operon that was likely to encode a conjugation system, since the products of several ORFs shared low-level homology to products of the *Enterococcus faecalis* conjugative transposon, Tn*916* (Bannam *et al.*, 2006, Roberts & Mullany, 2009). Many of the genes within this locus were predicted to encode components of the transferosome complex; by contrast, no relaxase or other relaxosomal components were identified from these initial investigations (Bannam *et al.*, 2006). Systematic mutagenesis and complementation studies on each of the genes located within this locus confirmed the involvement of these gene products in pCW3 conjugation. (Bannam *et al.*, 2006, Bantwal *et al.*, 2012, Parsons *et al.*, 2007, Porter *et al.*, 2012, Steen *et al.*, 2009, Teng *et al.*, 2008, Wisniewski *et al.*, 2015a, Wisniewski *et al.*, 2015b). Therefore, this locus was denoted the transfer clostridial plasmid (*tcp*) locus and remains unique to the pCW3-like plasmids of *C. perfringens* (Figure 1.6A) (Bannam *et al.*, 2006).

The pCW3 relaxosome

Prior to transport into the recipient cell, pCW3 DNA must first be processed by the relaxosome. Typically, a relaxosome complex is comprised of a relaxase enzyme, which nicks the DNA, the origin of transfer (*oriT)* DNA of the plasmid to be transferred, and accessory proteins (Lanka & Wilkins, 1995, Gomis-Rüth & Coll, 2006). Initial analysis of the pCW3 *tcp* locus did not identify a typical relaxase gene, nor were any sequences identified with similarity to known *oriT* sites (Bannam *et al.*, 2006). However, the first gene encoded in the putative *tcp* operon, *tcpM*, encoded a protein that shared limited similarity to tyrosine recombinase enzymes and was hypothesised to function as an atypical relaxase (Bannam *et al.*, 2006, Li *et al.*, 2013, Wisniewski *et al.*, 2015b). Mutagenesis and complementation studies have confirmed that TcpM is necessary for efficient transfer (Wisniewski *et al.*, 2015b). Subsequent complementation with site-directed mutants

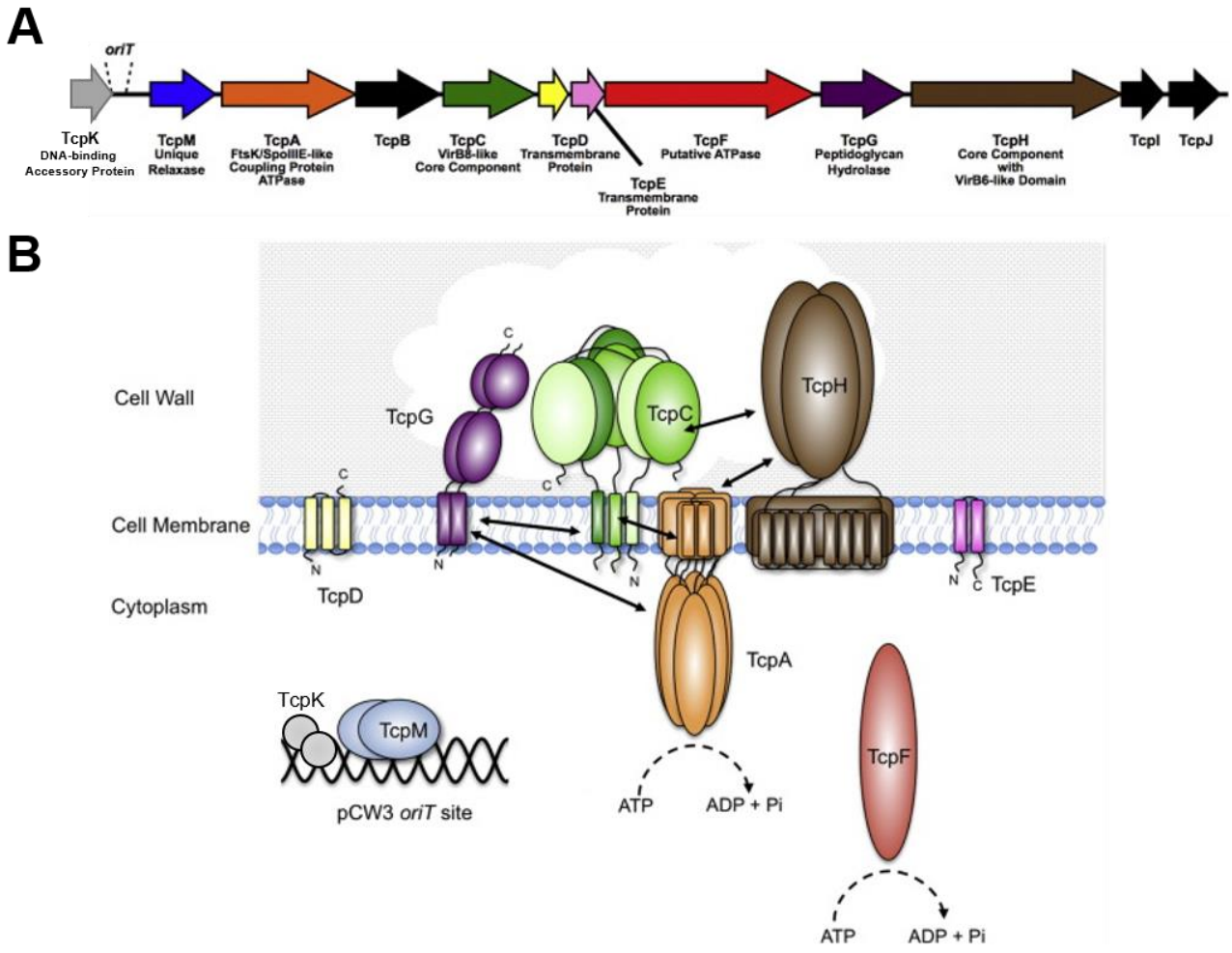

Figure 1.6: Schematic representation of the pCW3 *tcp* locus and Tcp conjugation system. A. The *tcp* locus. Genes are denoted by arrows. The name and proposed function of the proteins encoded by each gene are labelled below. Genes not required for conjugative transfer are coloured black. Image adapted from (Wisniewski & Rood, 2017). **B.** Model of localisations and interactions of the pCW3 Tcp conjugation apparatus, as determined by protein interaction studies and bioinformatic analysis. Confirmed protein-protein interactions are denoted by the black arrows. Proteins are coloured corresponding to the gene as shown in Figure 1.6A. Image and figure legend adapted from (Wisniewski & Rood, 2017).

determined that a single C-terminal tyrosine residue (Y259) was essential for TcpM function, in contrast to typical tyrosine recombinases, which require seven conserved arginine, histidine and tyrosine residues for full catalytic function (Wisniewski *et al.*, 2015b, Gibb *et al.*, 2010). Therefore, it was concluded that TcpM is a unique relaxase that shares similarity to tyrosine recombinase enzymes, but initiates nucleophilic attack on the DNA within the *oriT* of pCW3 *via* a modified catalytic site (Wisniewski *et al.*, 2015b). In many conjugative systems, the *oriT* site is located adjacent to genes involved in the relaxosome complex (de la Cruz *et al.*, 2010). With this knowledge, it was postulated that the pCW3 *oriT* site was located within a 391 bp intergenic region located upstream of *tcpM* (Wisniewski *et al.*, 2015b). Mobility assays using the 391 bp region cloned into a non-conjugative shuttle vector confirmed that the *oriT* sequence was located within this region (Wisniewski *et al.*, 2015b). Further analysis defined the minimal *oriT* to be within a 150 bp fragment in the *tcpK-tcpM* intergenic region (Wisniewski *et al.*, 2015b).

In other conjugation systems, accessory proteins form critical components of the cytoplasmic relaxosome complex. TcpK is a small protein with no predicted functional domains and is encoded by a gene located upstream of *tcpM* (Traore *et al.*, 2018). Mutational analysis determined that TcpK is required for the efficient transfer of pCW3 (Traore *et al.*, 2018). To gain insight into its function, the structure of TcpK was determined using X-ray crystallography. TcpK was shown to resemble a winged helix-turn-helix (wHTH) protein, similar to transcriptional regulators (Traore *et al.*, 2018). Additional studies determined that TcpK recognises and binds as a dimer to specific sequences within the pCW3 *oriT*, denoted 'TcpK boxes' (Traore *et al.*, 2018). The findings of this study have expanded the characterised *tcp* locus to 12 genes and defined TcpK as a unique DNA binding protein required for the efficient conjugative transfer of pCW3; it is likely to function as an accessory factor within the relaxosome (Traore *et al.*, 2018).

The pCW3 transferosome

Transferosomes are large multi-protein membrane-associated complexes that physically transfer plasmid DNA into a recipient cell utilising ATPase activity (Chandran Darbari & Waksman, 2015, Cascales & Christie, 2003). Initial bioinformatic analysis of the pCW3 *tcp* locus identified several putative proteins predicted to assemble as part of the transferosome complex (Bannam *et al.*, 2006). TcpF and TcpH were the first proteins tested for their involvement in pCW3 conjugation, due to their functional similarities to other transferosome proteins (Bannam *et al.*, 2006). TcpF is a putative ATPase enzyme, and was postulated to power DNA translocation as well as to assist in the formation of the transferosome complex (Bannam *et al.*, 2006). TcpH is a putative structural protein, that is predicted to comprise a large proportion of the transmembrane channel that spans from the donor cell into the recipient (Bannam *et al.*, 2006). Mutation and subsequent conjugation analysis demonstrated that both the TcpF and TcpH proteins are essential for the conjugative transfer of pCW3 (Bannam *et al.*, 2006). In a later study, it was shown that a region located between amino acids 514-581 was essential for TcpH function (Teng *et al.*, 2008). Although essential for pCW3 transfer, TcpF remains to be functionally or structurally characterised.

tcpG and *tcpI* were both predicted to encode peptidoglycan hydrolase enzymes (Bannam *et al.*, 2006), which function to produce localised openings in the peptidoglycan layers of bacterial cells. It was predicted that these enzymes would function to clear the thick peptidoglycan layers of the donor and recipient cells to allow for the formation of the transferosome. Mutation and complementation analysis determined that TcpG, but not TcpI, was required for efficient pCW3 transfer (Bantwal *et al.*, 2012). Further analysis confirmed the peptidoglycan hydrolase activity of TcpG in an *in vitro* plate assay (Bantwal *et al.*, 2012).

tcpC, tcpD, tcpE and *tcpJ* all encode hypothetical proteins of no known function (Bannam *et al.*, 2006, Porter *et al.*, 2012, Wisniewski *et al.*, 2015a). With the exception of *tcpJ*, all are required for pCW3 transfer. Analysis of the of the C-terminal portion of the TcpC crystal structure showed that

although it had no conserved domains or similarities to other protein sequences, TcpC showed a structural similarity to VirB8, a structural protein of the *A. tumefaciens* T4SS (Porter *et al.*, 2012). The structural similarities between these proteins infer that TcpC plays a structural role in the transferosome of pCW3 (Porter *et al.*, 2012). The small transmembrane proteins TcpD and TcpE are essential for pCW3 transfer, as plasmids with mutations in either the *tcpD* or *tcpE* genes were unable to support plasmid transfer (Wisniewski *et al.*, 2015a). Their function in conjugation remains to be elucidated, however, immunofluorescence imaging has determined that these proteins localise to the cellular poles (Wisniewski *et al.*, 2015a) as was demonstrated for TcpF and TcpH (Teng *et al.*, 2008). Since these proteins localise to the same subcellular region as other transferosome proteins, and are predicted to be membrane associated, it is highly likely that TcpD and TcpE also comprise part of the Tcp transferosome.

The third gene in the *tcp* operon, *tcpA,* encodes a putative integral membrane protein with a conserved FtsK/SpoIIIE domain (Parsons *et al.*, 2007). Proteins within the FtsK/SpoIIIE family functionally bind DNA as part of cellular processes such as chromosomal segregation and the transfer of genetic material into the forespore during sporulation (Massey *et al.*, 2006). Due to its putative involvement in DNA transfer, TcpA was hypothesised to function as the coupling protein in the pCW3 conjugative transfer apparatus (Parsons *et al.*, 2007). Subsequent mutation and complementation analysis confirmed that functional TcpA was essential for pCW3 transfer (Parsons *et al.*, 2007). As a coupling protein it was assumed that TcpA would mediate a range of protein-protein interactions with other Tcp proteins in both the relaxosome and transferosome complexes (Steen *et al.*, 2009). Through chemical cross-linking and bacterial two-hybrid analysis, TcpA was found to self-associate, as well as to interact with the transferosome components TcpC, TcpG and TcpH (Steen *et al.*, 2009). At the time of that study no relaxosome components had been identified and thus interactions with pCW3 relaxosome components have not yet been assessed (Steen *et al.*, 2009).

Various combinations of protein-protein interactions have been analysed (Parsons *et al.*, 2007, Steen *et al.*, 2009, Teng *et al.*, 2008), and based on these findings a model for the conjugative apparatus utilised by pCW3 has been proposed (Figure 1.6B). However, this model remains limited and needs to be expanded by additional studies. The entire repertoire of interactions between the Tcp proteins, and others that have yet to be discovered, need to be assessed to produce a definitive model.

Although there has been a large body of work conducted on the *tcp* locus of pCW3, there remain large gaps in our knowledge and understanding of function and form of the conjugation apparatus. To date, it is unclear whether pCW3 DNA transport occurs in a single-stranded or double-stranded manner. Additionally, the precise processing reactions that are catalysed by the relaxosome remain uncharacterised, as the full protein composition of the relaxosome remains to be elucidated. Finally, the mechanism of direct cell-to-cell contact between *C. perfringens* donor and recipient cells remains elusive.

Plasmid maintenance mechanisms

Plasmids can confer beneficial attributes to bacterial cells, such as antibiotic resistance and virulence genes, however, they are typically not essential and can be easily lost (Hülter *et al.*, 2017). To survive, plasmids must ensure they are maintained during multiple cell division events (San Millan & MacLean, 2017). High copy number plasmids, those with a copy number of >15, are maintained by the random distribution or clustered aggregation of plasmid molecules within the cell prior to cell division (Wang *et al.*, 2016). Low copy number plasmids, such as the Tcp plasmids of *C. perfringens,* cannot solely rely on random diffusion to ensure faithful inheritance (Ebersbach & Gerdes, 2005). Instead, these plasmids have developed a range of mechanisms to ensure ordered and precise plasmid segregation prior to septum formation (Ebersbach & Gerdes, 2005). These plasmid stability mechanisms include: replication and copy number control, active partitioning, multimer resolution, post-segregational killing, and regulation (Figure 1.7)

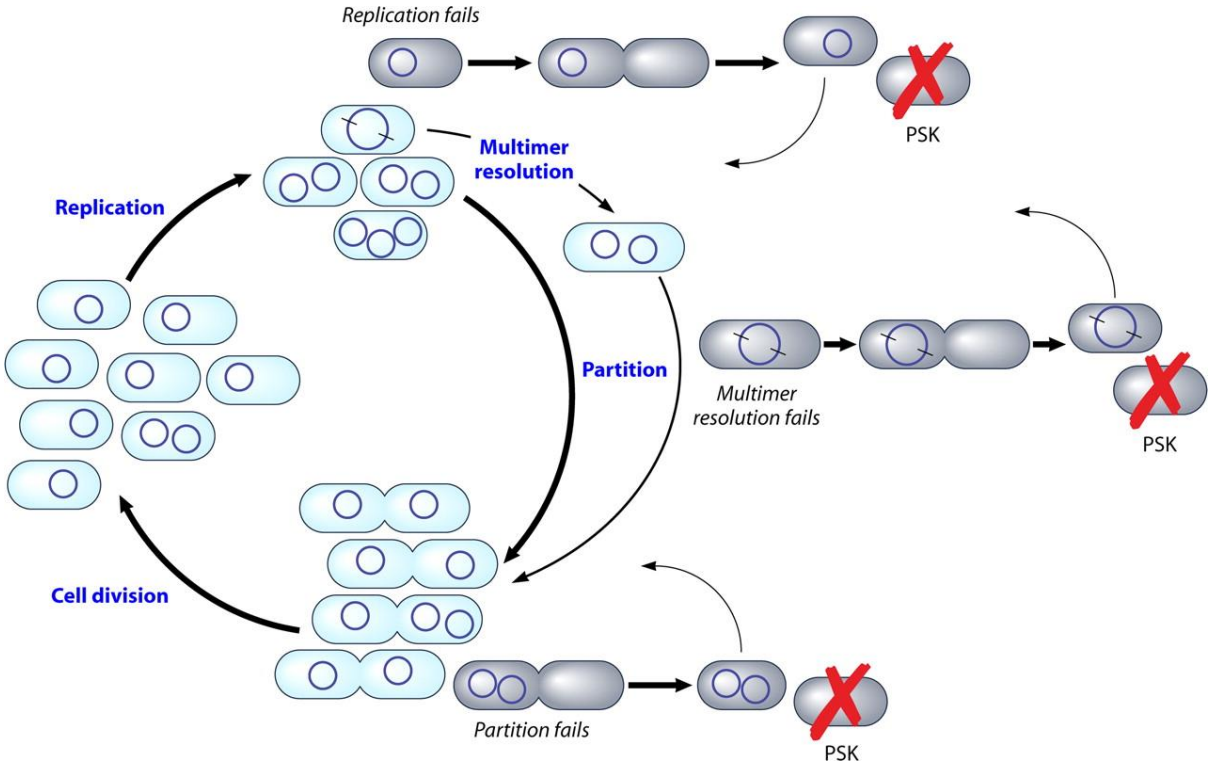

Figure 1.7: Diagram demonstrating how plasmid maintenance systems combine to achieve stable plasmid inheritance. The cell cycle of typical cells (blue cells) containing a low-copy-number plasmid is represented on the left. Plasmid replication doubles the number of plasmids in each cell. Some cells contain plasmid dimers formed by generalized recombination. These are reduced to monomers by the multimer resolution system. The replicated plasmids are subjected to active partition to opposite cell halves, ensuring that cell division produces two cells containing at least one plasmid copy. The grey cells represent those rare cells where the replication, multimer resolution, or partition system of the plasmid has failed to function properly. In each case, cell division produces one plasmid-containing cell that is returned to the general population and one that has no plasmid copy. Post segregational killing is triggered in the latter cells, killing them and thus ensuring that all viable cells in the population retain the plasmid. Figure and figure legend reproduced from (Sengupta & Austin, 2011).

(Tolmasky, 2017). Plasmids employ one or more of these mechanisms in concert to establish plasmid stability (Volante *et al.*, 2014, Bouet *et al.*, 2006).

The Tcp plasmids of *C. perfringens* encode several genes involved in putative plasmid maintenance mechanisms, such as partitioning, multimer resolution, regulation and toxin-antitoxin systems. Only some of these systems have been characterised (Bannam *et al.*, 2006, Adams *et al.*, 2015, Watts *et al.*, 2017).

Plasmid replication and copy number control

To be maintained within bacterial cells, plasmid molecules must replicate to ensure that more than one copy is available for each progeny cell prior to cell division (Pinto *et al.*, 2012). Plasmids replicate independently of the host chromosome and maintain a steady copy number within the bacterial cell (Tolmasky, 2017). Since replication of DNA molecules incurs a fitness cost, the plasmid replication process is tightly controlled (del Solar *et al.*, 1998). Plasmids can replicate *via* three alternate mechanisms: strand displacement, theta-replication, or rolling circle replication (del Solar *et al.*, 1998).

Rolling circle replication is initiated by the introduction of a nick at the replication-specific origin (*dso*) by the plasmid-encoded Rep protein (del Solar *et al.*, 1998, Ruiz-Masó *et al.*, 2015). The exposed 3'-OH group from a single strand is then used as a primer for elongation, requiring host encoded factors for initiation (Ruiz-Masó *et al.*, 2015). Theta replication involves the recognition of the origin of replication (*oriV*) by a plasmid-encoded replication initiation protein, Rep (del Solar *et al.*, 1998, Lilly & Camps, 2015). Similar to rolling circle replication, initiation often requires the presence of host proteins (Lilly & Camps, 2015). Plasmids that replicate *via* strand displacement have two single-stranded replication origins and encode all of the proteins essential for replication initiation (Sakai & Komano, 1996). Following initiation these plasmids replicate in either direction, synthesising a single strand continuously, resulting in the displacement of the complementary strand (Sakai & Komano, 1996). Continuous synthesis is also initiated on the

displaced strand through recognition of the single stranded origin (Lilly & Camps, 2015). As there is no requirement for host-encoded factors for replication initiation, these plasmids often have a broader host range than those that replicate through other mechanisms (del Solar *et al.*, 1998, Lilly & Camps, 2015).

pCW3 replication

Initial characterisation of the *C. perfringens* plasmid pCW3 did not identify any ORFs encoding products that shared homology to known replication initiation proteins (Bannam *et al.*, 2006). To delineate the pCW3 replication initiator a transposon mutagenesis approach was used (Bannam *et al.*, 2006). A single gene, designated *rep*, was found to be essential for pCW3 replication (Bannam *et al.*, 2006). Similar *rep* genes are encoded on other Tcp plasmids (Adams *et al.*, 2015). Additionally, repeated elements were identified within the intergenic region preceding *rep*; these repeats are likely to be iteron-like Rep binding sites that are involved in replication initiation (Bannam *et al.*, 2006). However, the mechanism of Tcp plasmid replication has not yet been examined further.

Plasmid partitioning systems

Plasmid partitioning involves the active and coordinated segregation of plasmids within the cell prior to cellular division (Gerdes *et al.*, 2010). These tripartite systems are considered the most important stability determinant of low copy number plasmids (Ebersbach & Gerdes, 2005). Although there are diverse types of partitioning (Par) systems, all function using similar mechanisms and are composed of three main elements: a *cis*-acting centromere site, a centromere DNA binding protein (adaptor) and a motor protein (NTPase) (Ebersbach & Gerdes, 2005). The active partitioning of plasmids requires specific binding of the adaptor protein to the plasmid-encoded centromere site, followed by interactions between the adaptor and motor proteins that links the DNA to the NTPase, allowing for active plasmid movement within the cell (Ebersbach & Gerdes, 2005, Gerdes *et al.*, 2010).

Active bacterial partitioning systems can be classified into three types, based on the NTPase motor protein family they encode (Ebersbach & Gerdes, 2005). Type I *parABS* systems consist of the centromere site *parS,* the DNA binding protein ParB and are defined by a P-loop ATPase (ParA) that possesses a variant Walker A motif (Gerdes *et al.*, 2010). This family of partitioning systems can be divided further on the basis of the presence (Type 1a) or absence (Type 1b) of a N-terminal helix-turn-helix DNA binding domain within the ParA protein (Gerdes *et al.*, 2010). Type I Par systems are the most widespread form of active segregation system and are thought to partition plasmids using a diffusion-rachet mechanism, whereby ParB bound plasmid moves across a ParA ATPase gradient produced by the switching of interaction states of ParA with the nucleoid (Figure 1.8A) (Hu *et al.*, 2017, Baxter & Funnell, 2015). Type II (*parMRC*) partitioning systems are the best-understood and involve the formation of unstable bidirectional filaments by the actin-like ATPase homologue ParM, which actively pushes ParR-bound plasmid molecules to either end of the bacterial cell (Figure 1.8B) (Salje *et al.*, 2010, Baxter & Funnell, 2015). Type III (*tubRZC*) systems encode tubulin homologues as their NTPase and function in a similar fashion to Type II systems, although filaments form *via* a treadmilling mechanism, whereby new filament monomers are continuously added at one end whilst being disassembled at the other (Figure 1.8C) (Larsen *et al.*, 2007, Gerdes *et al.*, 2010). In addition to these partitioning types, there is one more unique Par system, that of the *Staphylococcus aureus* plasmid pSK1 (Simpson *et al.*, 2003). pSK1 encodes a single partitioning protein that has been shown to increase the segregational stability of mini-replicons (Simpson *et al.*, 2003). However, the mechanism of action of this unique Par protein remains to be elucidated.

The active partitioning system of pCW3

The Tcp plasmids of *C. perfringens* all encode a Type II *parMRC*-like partitioning system (Adams *et al.*, 2015). A recent survey of all available Tcp plasmid sequences identified the presence of ten distinct *parMRC* families (A-J) (Adams *et al.*, 2015). As yet, no two plasmids possessing the same

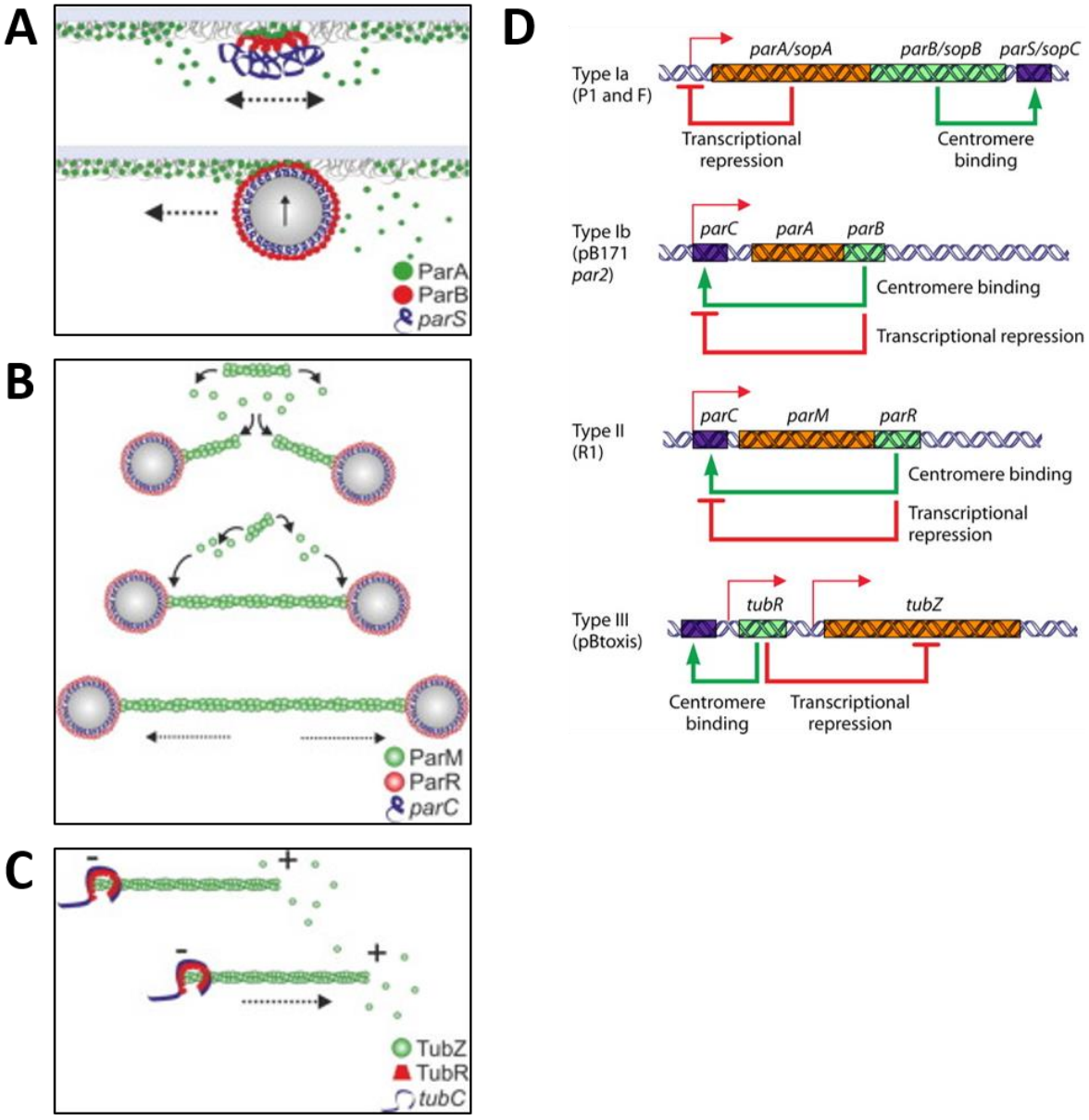
A
ParA
ParB
parS
B
ParM
ParR
parC
C
TubZ
TubR
tubC
D
Type Ia
(P1 and F)
parA/sopA
parB/sopB
parS/sopC
Transcriptional
repression
Centromere
binding
Type Ib
(pB171
par2)
parC
parA
parB
Centromere binding
Transcriptional repression
Type II
(R1)
parC
parM
parR
Centromere binding
Transcriptional
repression
Type III
(pBtoxis)
tubR
tubZ
Centromere
binding
Transcriptional
repression

Figure 1.8: Plasmid partition systems and their mechanisms. A. Diffusion rachet mechanism as exhibited by the *parABS* Type I partitioning system. ParB (red) loads onto the plasmid at *parS* (blue) to form the partition complex. ParA (green) interacts with the nucleoid carpet (grey) in an ATP -dependent switching manner. The changes in ParA interaction state with the nucleoid forms a ParA gradient along the cell. ParB bound plasmid then moves across the gradient and is postioned to one end of the cell. **B.** Bi-directional filament formation by the Type II *parMRC* partitioning system. The partition complex is formed by ParR (red) interactions with plasmid associated *parC* (blue). Dynamic ParM (green) filaments form between two partition complex, continuous filament elongation pushes the complexes apart, effectively positioning them at either end of the cell. **C.** Treadmilling mechanism of partitioning as exhibited by the *tubZRC* Type III partitioning system. Partition complexes of TubR (red) loaded plasmid at *tubC* (blue) are partitioned within the cell by the continuous addition of TubZ (green) monomers at a single end (+) of the growing filament. Concurrently TubZ monomers are removed from the filament at the opposite (-) end, resulting in a treadmill like movement. Figures (A, B and C) taken from (Brooks & Hwang, 2017) and figure legends adapted. **D.** Genetic organisation of the different types of plasmid partitioning systems. The green boxes and the orange boxes represent the centromere binding protein and the motor protein, respectively. The centromere sequences have been marked by the purple boxes. Red arrows mark the direction of transcription. Transcriptional repression and centromere binding have been marked in each case. Figure and figure legend reproduced from (Sengupta & Austin, 2011).

parMRC family type have been found in the same strain, suggesting that these families are important in determining pCW3-like plasmid incompatibility (Adams *et al.*, 2015). More recent work has confirmed this hypothesis, demonstrating experimentally that plasmids with shared partitioning systems are unable to stably co-exist within the same cell (Watts *et al.*, 2017). This work has demonstrated that the *parMRC* partitioning systems of the Tcp plasmids forms the basis of plasmid incompatibility in *C. perfringens* (Watts *et al.*, 2017).

Multimer resolution systems

Plasmid replication and subsequent recombination can result in the formation of multimeric plasmids (Austin *et al.*, 1981), which are covalently closed DNA molecules comprised of tandem repeats of a monomeric plasmid (Bedbrook & Ausubel, 1976). The formation of multimers dilutes the number of plasmids available for segregation, thus reducing the chance of the successful inheritance of a plasmid by daughter cells following cell division (Austin *et al.*, 1981). To overcome the potential plasmid loss, plasmids encode site-specific recombinase systems to resolve plasmids into their monomeric states (Austin *et al.*, 1981, Zielenkiewicz & Ceglowski, 2001). Multimer resolution systems are comprised of a site-specific recombinase (resolvase) and a *res* sequence that is located on the plasmid and is specifically recognised by the resolvase enzyme (Sengupta & Austin, 2011, Ebersbach & Gerdes, 2005, Zielenkiewicz & Ceglowski, 2001). Recombination between repeated *res* sites on plasmid multimers resolves plasmids to their monomeric state (Zielenkiewicz & Ceglowski, 2001).

Multimer resolution can be performed by either a plasmid-borne or chromosomally-encoded recombinase (Sengupta & Austin, 2011). Recombinase enzymes of plasmid-borne multimer resolution systems belong to two distinct families: the tyrosine recombinase family, which includes the enzymes Rsd from pSDL2 (Krause & Guiney, 1991) and Cre from plasmid P1 (Austin *et al.*, 1981); and the serine recombinase family, which includes proteins such as ParA from RK2/RP4 (Eberl *et al.*, 1994) and Res from pSK41 (LeBard *et al.*, 2008). Whilst enzymes of both families perform the same overall role in resolving DNA, the method of recombination used is vastly different (Grindley *et al.*, 2006).

Tyrosine recombinase enzymes are defined by a highly conserved C-terminal region that contains catalytic histidine, arginine and tyrosine residues (Grindley *et al.*, 2006, Rajeev *et al.*, 2009). Recombination by these enzymes involves a two-step DNA breakage reaction and results in the transient formation of a complex Holliday junction at the recombination site (Grindley *et al.*, 2006). By contrast, recombination by serine recombinases occurs by a simpler mechanism, whereby a single-step four-stranded DNA break is induced by four recombinase enzymes simultaneously (Grindley *et al.*, 2006, McPherson *et al.*, 2015). Recombinase bound DNA is then rotated and re-ligated, resulting in the resolution of the DNA molecules.

Multimer resolution and pCW3

pCW3 encodes a gene, *resP*, whose putative product shares sequence similarity to members of the serine recombinase family of site-specific recombinases (Bannam *et al.*, 2006). *resP* genes are present on all *C. perfringens* plasmid types, suggesting a conserved function amongst these plasmids (Bannam *et al.*, 2006, Shimizu *et al.*, 2002, Garnier *et al.*, 1987). However, to date no studies have been carried out to determine the importance of the putative multimer resolution system to the stability of pCW3.

Toxin-antitoxin systems

Toxin-antitoxin (TA) systems, also known as post-segregational killing systems, ensure plasmid stability by actively killing any plasmid-free daughter cells that arise following cell division (Page & Peti, 2016, Yamaguchi *et al.*, 2011). These systems rely on the differential stability of a cognate toxin and antitoxin pair (Page & Peti, 2016). When a TA-encoding plasmid is within the cell, the antitoxin supresses the activity of the toxin, acting as an antidote (Page & Peti, 2016). In daughter cells that have not received a plasmid, the short-lived antitoxin degrades, allowing for the more stable toxin to exert its toxicity and kill the plasmid-free cell (Page & Peti, 2016).

There are several types of post-segregational killing systems, differentiated primarily by the nature of the antitoxin molecule, which can be either RNA or protein (Yamaguchi *et al.*, 2011). Type I TA systems, such as *hok/sok* from plasmid R1, function through antisense RNA regulation (Zhang *et al.*, 2004),

whereby the unstable antisense *sok* RNA binds to *hok* mRNA inhibiting translation of the toxic product (Gerdes *et al.*, 1997). By contrast, the antitoxins of Type II TA systems are proteins, and form a stable antitoxin/toxin protein complex that inhibits the activity of the toxin (Yamaguchi *et al.*, 2011).

The best characterised plasmid Type II TA system is the *ccd* system from the F plasmid (Ogura & Hiraga, 1983). This system encodes a stable DNA gyrase inhibitor CcdB and the antitoxin CcdA (Couturier *et al.*, 1998). CcdA interacts with CcdB, ultimately blocking CcdB from making detrimental interactions with DNA gyrase (Couturier *et al.*, 1998). In a plasmid-free daughter cell, the antitoxin can be proteolytically degraded, allowing for the toxin to exert its effects within the cell.

Type III TA systems involve an RNA antitoxin that directly inhibits the toxicity of its cognate toxin (Yamaguchi *et al.*, 2011). The ToxI/ToxN TA system that is encoded by a cryptic plasmid present in the plant pathogen *Erwina carotovora,* is the best described Type III TA model (Fineran *et al.*, 2009). Several other TA system types (IV-VI) have been described, however no plasmid encoded systems within these types have yet been identified (Aakre *et al.*, 2013, Wang *et al.*, 2012, Brown & Shaw, 2003, Page & Peti, 2016).

Toxin-antitoxin systems on pCW3

All Tcp plasmids encode a putative protein that shares significant homology (60% amino acid sequence identity) to the Type II TA toxin PemK (Bannam *et al.*, 2006). The *pemI-pemK* system is a TA system encoded by the *E. coli* plasmid R100 and is essential for plasmid stability (Tsuchimoto *et al.*, 1988). PemK inhibits protein synthesis through its endoribonuclease activity and the cognate antitoxin, PemI, blocks this activity (Zhang *et al.*, 2004). The involvement of the *pemK*-like gene in pCW3 stability has not been tested. However, preliminary evidence suggests this region may be toxic to some bacterial cells, as attempts to clone this region in *Escherichia coli* without transcriptional control were unsuccessful (S. Revitt-Mills, V. Adams and J. Rood, unpublished). As yet, no *pemI* homologue on pCW3 has been identified.

Plasmid regulation

To ensure that plasmid-encoded functions do not result in an unfavourable burden on the bacterial cell, plasmids employ numerous regulatory networks to control gene expression (del Solar *et al.*, 1998). Replication control is required to ensure a steady plasmid copy number within the cell at any one time. A low plasmid copy number can lead to plasmid loss, whereas too many plasmids can be detrimental to the host cell (del Solar *et al.*, 1998). Control of replication occurs at the initiation phase and is most commonly achieved *via* negative feedback loops that control the expression of replication initiator (Rep) proteins through the use of antisense RNAs (Brantl & Behnke, 1992, del Solar *et al.*, 1998). Replication antisense RNA molecules are often encoded on the complementary strand to *rep* mRNA (Pluta & Espinosa, 2018). Through complementary base pairing, translation of Rep is attenuated (Pluta & Espinosa, 2018). Control of Rep production can be mediated by antisense RNA alone or through the concerted effects of layers of other regulatory factors (del Solar *et al.*, 1998). This phenomenon has been observed for plasmid pMV158, which, in addition to having an antisense RNA, also encodes an additional transcriptional repressor, CopG, that binds to the *rep* promoter blocking transcription (del Solar *et al.,* 2002, Pluta & Espinosa, 2018). In some systems, Rep production can be autoregulated, as has been demonstrated for plasmid pUB110 (Müller *et al.,* 1995).

Autoregulation is also utilised for the control of plasmid encoded stability mechanisms. For example, active partitioning systems generally are autoregulated, usually by the centromere binding protein sterically blocking transcription from the *par* promoter (Figure 1.8D) (Sengupta & Austin, 2011). Toxin-antitoxin systems are constitutively expressed, meaning they are not regulated at a transcriptional level (Yamaguchi *et al.*, 2011). However, these systems autoregulate their toxic effects though the antitoxin function (Yamaguchi *et al.*, 2011). These systems only become "dysregulated" when the antitoxin is no longer present, as is seen in plasmid-free daughter cells (Yamaguchi *et al.*, 2011).

The regulation of plasmid functions can also be achieved by plasmid-encoded global or master regulators (Bingle & Thomas, 2001). For the *S. aureus* plasmid pSK41, the plasmid encoded protein ArtA has been shown to repress the expression of genes involved in partitioning and conjugative transfer (Ni

et al., 2009). Similarly, for the broad-host-range plasmid RK2, conjugation, replication and stability are controlled by a coordinated regulatory network, comprised of four master regulators: KorA, KorB, KorC and TrbA (Bingle & Thomas, 2001, Zatyka *et al.*, 1994, Zatyka *et al.*, 2001, Kostelidou *et al.*, 1999). Plasmid genes can also be under the control of host regulators, as is seen for the plasmid-encoded toxin genes *etx* and *cpb*, which were shown to be under control of the chromosomally-encoded Agr-like quorum sensing system (Chen *et al.,* 2001, Chen & McClane, 2012, Vidal *et al.,* 2012). Host regulatory control of plasmid genes has also been observed for the genes *cnaB* and *cpb2* on the *C. perfringens* plasmid pCP13, which were shown to be under control of the host two-component VirR/VirS regulatory system (Ohtani *et al.*, 2003).

Methylation of DNA is another mechanism utilised to control the expression of plasmid-encoded genes. Methylation of either adenosine (Dam methylation) or cytosine (Dcm methylation) bases has been shown to modulate gene expression (Adhikari & Curtis, 2016, Løbner-Olesen *et al.*, 2005). For both the *Salmonella* virulence plasmid pSLT, and the F-like plasmid R100, conjugal transfer is repressed by Dam methylation, which blocks binding of the host regulator Lrp, an activator of conjugation (Camacho *et al.*, 2010, Camacho & Casadesús, 2005).

Putative regulatory networks of pCW3

pCW3 encodes numerous genes that could be involved in regulation, including four genes (*regA, regB, regC* and *regD)* that are predicted to encode proteins that may function as transcriptional regulators, due to the presence of DNA binding motifs commonly associated with regulation (Bannam *et al.*, 2006). RegC, a LexA-like protein, has been shown to regulate conjugation and plasmid stability (T. Stent, X. Han, V. Adams, R. Moore and J. Rood, unpublished), although the precise mechanism of regulation has not yet been determined.

Many of the key plasmid processes are likely to be regulated, as described for other plasmid systems. For example, it is postulated that pCW3 replication is under the direct control of a recently identified rep_{AS} antisense molecule (V. Adams, C. Lao and J. Rood, unpublished). It is also predicted that the type II

parMRC partitioning system is autoregulatory, as has been described for other homologous systems (Adams *et al.*, 2015, Watts *et al.*, 2017, Salje *et al.*, 2010, Brantl, 2002, Kwong *et al.*, 2017).

pCW3 encodes two methyltransferase enzymes, Dam and Dcm, that could potentially regulate key plasmid functions. Previous work has examined the role of pCW3-encoded *dam* in pCW3 conjugation and found no significant alteration in conjugation frequency between mutant and wild-type strains (S. Revitt-Mills, V. Adams and J. Rood, unpublished). However, the function of Dam and Dcm in other plasmid functions remains to be assessed. pCW3 also encodes several hypothetical proteins (Bannam *et al.*, 2006). These genes remain highly conserved amongst the Tcp plasmids and may play critical roles in the regulation of pCW3.

Objectives of this study

This study aims to investigate two major facets of *C. perfringens* plasmid biology: conjugative transfer and plasmid stability. In Chapter Two, the involvement in conjugative transfer of highly conserved genes within the backbone of pCW3-like plasmids was investigated, which lead to the identification of two genes that appear to be required for efficient transfer of pCW3. In Chapter Three, the role of the putative multimer resolution protein, ResP, in maintaining pCW3 stability was established. In Chapter Four, a novel stability factor, Srm, was discovered and its essential role in maintaining pCW3 stability examined. In Chapter Five, the subcellular localisation of various Tcp conjugation proteins was investigated using Super Resolution Microscopy techniques, providing insight into the formation of the Tcp conjugation complex on the surface of *C. perfringens* cells. Taken together, these studies have expanded our knowledge of how the large toxin and antibiotic resistance plasmids of *C. perfringens* undertake key plasmid processes such as conjugative transfer and maintenance.

References

Aakre, Christopher D., Phung, Tuyen N., Huang, D., and Laub, Michael T. (2013) A bacterial toxin inhibits DNA replication elongation through a direct interaction with the β sliding clamp. *Molecular Cell* **52**: 617-628.

Abraham, L.J., and Rood, J.I. (1985a) Cloning and analysis of the *Clostridium perfringens* tetracycline resistance plasmid, pCW3. *Plasmid* **13**: 155-162.

Abraham, L.J., and Rood, J.I. (1985b) Molecular analysis of transferable tetracycline resistance plasmids from *Clostridium perfringens*. *Journal of Bacteriology* **161**: 636-640.

Abraham, L.J., Wales, A.J., and Rood, J.I. (1985) Worldwide distribution of the conjugative *Clostridium perfringens* tetracycline resistance plasmid, pCW3. *Plasmid* **14**: 37-46.

Adams, V., Watts, T.D., Bulach, D.M., Lyras, D., and Rood, J.I. (2015) Plasmid partitioning systems of conjugative plasmids from *Clostridium perfringens*. *Plasmid* **80**: 90-96

Adhikari, S., and Curtis, P.D. (2016) DNA methyltransferases and epigenetic regulation in bacteria. *FEMS Microbiology Reviews* **40**: 575-591.

Alouf, J.E., and Jolivet-Reynaud, C. (1981) Purification and characterization of *Clostridium perfringens* delta-toxin. *Infection and Immunity* **31**: 536-546.

Alvarez-Martinez, C.E., and Christie, P.J. (2009) Biological diversity of prokaryotic type IV secretion systems. *Microbiology and Molecular Biology Reviews* **73**: 775-808.

Arutyunov, D., Arenson, B., Manchak, J., and Frost, L.S. (2010) F plasmid TraF and TraH are components of an outer membrane complex involved in conjugation. *Journal of Bacteriology* **192**: 1730-1734.

Austin, S., Ziese, M., and Sternberg, N. (1981) A novel role for site-specific recombination in maintenance of bacterial replicons. *Cell* **25**: 729-736.

Awad, M.M., Bryant, A.E., Stevens, D.L., and Rood, J.I. (1995) Virulence studies on chromosomal α-toxin and Θ-toxin mutants constructed by allelic exchange provide genetic evidence for the essential role of α-toxin in *Clostridium perfringens*-mediated gas gangrene. *Molecular Microbiology* **15**: 191-202.

Bannam, T.L., Teng, W.L., Bulach, D., Lyras, D., and Rood, J.I. (2006) Functional identification of conjugation and replication regions of the tetracycline resistance plasmid pCW3 from *Clostridium perfringens*. *Journal of Bacteriology* **188**: 4942-4951.

Bannam, T.L., Yan, X.-X., Harrison, P.F., Seemann, T., Keyburn, A.L., Stubenrauch, C., Weeramantri, L.H., Cheung, J.K., McClane, B.A., Boyce, J.D., Moore, R.J., and Rood, J.I. (2011) Necrotic enteritis-derived *Clostridium perfringens* strain with three closely related independently conjugative toxin and antibiotic resistance plasmids. *mBio* **2**: e00190-11.

Bantwal, R., Bannam, T.L., Porter, C.J., Quinsey, N.S., Lyras, D., Adams, V., and Rood, J.I. (2012) The peptidoglycan hydrolase TcpG is required for efficient conjugative transfer of pCW3 in *Clostridium perfringens*. *Plasmid* **67**: 139-147.

Baxter, J.C., and Funnell, B.E., (2015) Plasmid partition mechanisms. In: Plasmids: Biology and Impact in Biotechnology and Discovery. American Society of Microbiology, pp. 135-155

Bedbrook, J.R., and Ausubel, F.M. (1976) Recombination between bacterial plasmids leading to the formation of plasmid multimers. *Cell* **9**: 707-716.

Bhatty, M., Laverde Gomez, J.A., and Christie, P.J. (2013) The expanding bacterial type IV secretion lexicon. *Research in Microbiology* **164**: 620-639.

Bingle, L.E.H., and Thomas, C.M. (2001) Regulatory circuits for plasmid survival. *Current Opinion in Microbiology* **4**: 194-200.

Bouet, J.-Y., Bouvier, M., and Lane, D. (2006) Concerted action of plasmid maintenance functions: partition complexes create a requirement for dimer resolution. *Molecular Microbiology* **62**: 1447-1459.

Brantl, S. (2002) Antisense RNAs in plasmids: control of replication and maintenance. *Plasmid* **48**: 165-173.

Brantl, S., and Behnke, D. (1992) The amount of RepR protein determines the copy number of plasmid pIP501 in Bacillus subtilis. *Journal of Bacteriology* **174**: 5475-5478.

Brefort, G., Magot, M., Ionesco, H., and Sebald, M. (1977) Characterization and transferability of *Clostridium perfringens* plasmids. *Plasmid* **1**: 52-66.

Brooks, A.C., and Hwang, L.C. (2017) Reconstitutions of plasmid partition systems and their mechanisms. *Plasmid* **91**: 37-41.

Brown, J.M., and Shaw, K.J. (2003) A novel family of *Escherichia coli* toxin-antitoxin gene pairs. *Journal of Bacteriology* **185**: 6600-6608.

Brynestad, S., Sarker, M.R., McClane, B.A., Granum, P.E., and Rood, J.I. (2001) Enterotoxin plasmid from *Clostridium perfringens* is conjugative. *Infection and Immunity* **69**: 3483-3487.

Byrd, D.R., and Matson, S.W. (1997) Nicking by transesterification: the reaction catalysed by a relaxase. *Molecular Microbiology* **25**: 1011-1022.

Cabezón, E., Ripoll-Rozada, J., Peña, A., de la Cruz, F., and Arechaga, I. (2015) Towards an integrated model of bacterial conjugation. *FEMS microbiology reviews* **39**: 81-95.

Camacho, E.M., Camacho, E.M., Serna, A., and Casadesús, J. (2010) Regulation of conjugal transfer by Lrp and Dam methylation in plasmid R100. *International Microbiology* **8**: 279-285.

Camacho, E.M., and Casadesús, J. (2005) Regulation of *traJ* transcription in the Salmonella virulence plasmid by strand-specific DNA adenine hemimethylation. *Molecular Microbiology* **57**: 1700-1718.

Canard, B., Garnier, T., Saint-Joanis, B., and Cole, S.T. (1994) Molecular genetic analysis of the *nagH* gene encoding a hyaluronidase of *Clostridium perfringens*. *Molecular and General Genetics MGG* **243**: 215-224.

Caryl, J.A., and Thomas, C.D. (2006) Investigating the basis of substrate recognition in the pC221 relaxosome. *Molecular Microbiology* **60**: 1302-1318.

Cascales, E., and Christie, P.J. (2003) The versatile bacterial type IV secretion systems. *Nature Reviews Microbiology* **1**: 137-149.

Chakravorty, A., Awad, M.M., Hiscox, T.J., Cheung, J.K., Carter, G.P., Choo, J.M., Lyras, D., and Rood, J.I. (2011) The cysteine protease α-Clostripain is not essential for the pathogenesis of *Clostridium perfringens*-mediated myonecrosis. *PLoS ONE* **6**: e22762.

Chandran Darbari, V., and Waksman, G. (2015) Structural biology of bacterial Type IV secretion systems. *Annual Review of Biochemistry* **84**: 603-629.

Chen, J., and McClane B.A. (2012) Role of the Agr-like quoroum sensing system in regulating toxin production by *Clostridium perfringens* type B strain CN1793 and CN1795. *Infection and Immunity* **80**: 3008-3017.

Chen, J., Rood, J. I., and McClane B.A. (2011) Epsilon-toxin production by *Clostridium perfringens* type D strain CN3718 is dependent upon the *arg* operon but not the VirS/VirR two-component regulatory system. *mBio* **2**: e00275-00211.

Chiarezza, M., Lyras, D., Pidot, S.J., Flores-Díaz, M., Awad, M.M., Kennedy, C.L., Cordner, L.M., Phumoonna, T., Poon, R., Hughes, M.L., Emmins, J.J., Alape-Girón, A., and Rood, J.I. (2009) The NanI and NanJ sialidases of *Clostridium perfringens* are not essential for virulence. *Infection and Immunity* **77**: 4421-4428.

Christie, P.J., Gomez Valero, L., and Buchrieser, C., (2017) Biological diversity and evolution of Type IV secretion systems. In: Type IV Secretion in Gram-Negative and Gram-Positive Bacteria. S. Backert & E. Grohmann (eds). Cham: Springer International Publishing, pp. 1-30.

Christie, P.J., Whitaker, N., and González-Rivera, C. (2014) Mechanism and structure of the bacterial type IV secretion systems. *Biochimica et Biophysica Acta (BBA) - Molecular Cell Research* **1843**: 1578-1591.

Collie, R.E, and McClane, B.A. (1998) Evidence that the enterotoxin gene can be episomal in *Clostridium perfringens* isolates associated with non-food-borne human gastrointestinal diseases. *Journal of Clinical Microbiology* **36**: 30-36.

Cornillot, E., Saint-Joanis, B., Daube, G., Katayama, S.-i., Granum, P.E., Canard, B., and Cole, S.T. (1995) The enterotoxin gene (*cpe*) of *Clostridium perfringens* can be chromosomal or plasmid-borne. *Molecular Microbiology* **15**: 639-647.

Couturier, M., Bahassi, E.M., and Van Melderen, L. (1998) Bacterial death by DNA gyrase poisoning. *Trends in Microbiology* **6**: 269-275.

de la Cruz, F., Frost, L.S., Meyer, R.J., and Zechner, E.L. (2010) Conjugative DNA metabolism in Gram-negative bacteria. *FEMS Microbiol Rev* **34**: 18-40.

del Solar, G., Hernández-Arriaga, A.M., Gomis-Rüth, F.X., Coll, M., and Espinosa, M. (2002) A genetically economical family of plasmid-encoded transcriptional repressors involved in control of plasmid copy number. *Journal of Bacteriology* **184**: 4943-4951.

del Solar, G., Giraldo, R., Ruiz-Echevarría, M.J., Espinosa, M., and Díaz-Orejas, R. (1998) Replication and control of circular bacterial plasmids. *Microbiology and Molecular Biology Reviews* **62**: 434-464.

Ding, Z., Atmakuri, K., and Christie, P.J. (2003) The outs and ins of bacterial type IV secretion substrates. *Trends in Microbiology* **11**: 527-535.

Disqué-Kochem, C., and Dreiseikelmann, B. (1997) The cytoplasmic DNA-binding protein TraM binds to the inner membrane protein TraD in vitro. *Journal of Bacteriology* **179**: 6133-6137.

Dupuy, B., Daube, G., Popoff, M.R., and Cole, S.T. (1997) *Clostridium perfringens* urease genes are plasmid borne. *Infection and Immunity* **65**: 2313-2320.

Eberl, L., Kristensen, C.S., Givskov, M., Grohmann, E., Gerlitz, M., and Schwab, H. (1994) Analysis of the multimer resolution system encoded by the *parCBA* operon of broad-host-range plasmid RP4. *Molecular Microbiology* **12**: 131-141.

Ebersbach, G., and Gerdes, K. (2005) Plasmid segregation mechanisms. *Annual Review of Genetics* **39**: 453-479.

Farrand, S.K., Hwang, I., and Cook, D.M. (1996) The *tra* region of the nopaline-type Ti plasmid is a chimera with elements related to the transfer systems of RSF1010, RP4, and F. *Journal of Bacteriology* **178**: 4233-4247.

Fineran, P.C., Blower, T.R., Foulds, I.J., Humphreys, D.P., Lilley, K.S., and Salmond, G.P.C. (2009) The phage abortive infection system, ToxIN, functions as a protein–RNA toxin–antitoxin pair. *Proceedings of the National Academy of Sciences* **106**: 894-899.

Frost, L.S., Leplae, R., Summers, A.O., and Toussaint, A. (2005) Mobile genetic elements: the agents of open source evolution. *Nature Reviews Microbiology* **3**: 722-732.

Garnier, T., Saurin, W., and Cole, S.T. (1987) Molecular characterization of the resolvase gene, *res*, carried by a multicopy plasmid from *Clostridium perfringens*: common evolutionary origin for prokaryotic site-specific recombinases. *Molecular Microbiology* **1**: 371-376.

Gerdes, K., Gultyaev, A.P., Franch, T., Pedersen, K., and Mikkelsen, N.D. (1997) Antisense RNA-regulated programmed cell death. *Annual Review of Genetics* **31**: 1-31.

Gerdes, K., Howard, M., and Szardenings, F. (2010) Pushing and pulling in prokaryotic DNA segregation. *Cell* **141**: 927-942.

Gibb, B., Gupta, K., Ghosh, K., Sharp, R., Chen, J., and Van Duyne, G.D. (2010) Requirements for catalysis in the Cre recombinase active site. *Nucleic Acids Research* **38**: 5817-5832.

Gibert, M., Jolivet-Reynaud, C., and Popoff, M.R. (1997) Beta2 toxin, a novel toxin produced by *Clostridium perfringens*. *Gene* **203**: 65-73.

Goessweiner-Mohr, N., Arends, K., Keller, W., and Grohmann, E. (2013) Conjugative type IV secretion systems in Gram-positive bacteria. *Plasmid* **70**: 289-302.

Goessweiner-Mohr, N., Arends, K., Keller, W., and Grohmann, E. (2014) Conjugation in Gram-positive bacteria. *Microbiology* Spectrum **2**: PLAS-0004-2013.

Gomis-Rüth, F.X., and Coll, M. (2006) Cut and move: protein machinery for DNA processing in bacterial conjugation. *Current Opinion in Structural Biology* **16**: 744-752.

Gomis-Rüth, F.X., de la Cruz, F., and Coll, M. (2002) Structure and role of coupling proteins in conjugal DNA transfer. *Research in Microbiology* **153**: 199-204.

Gomis-Ruth, F.X., Sola, M., Cruz, F.d.l., and Coll, M. (2004) Coupling factors in macromolecular Type-IV secretion machineries. *Current Pharmaceutical Design* **10**: 1551-1565.

Grindley, N.D.F., Whiteson, K.L., and Rice, P.A. (2006) Mechanisms of site-specific recombination. *Annual Review of Biochemistry* **75**: 567-605.

Grohmann, E., Christie, P.J., Waksman, G., and Backert, S. (2018) Type IV secretion in Gram-negative and Gram-positive bacteria. *Molecular Microbiology* **107**: 455-471.

Grohmann, E., Keller, W., and Muth, G., (2017) Mechanisms of conjugative transfer and Type IV secretion-mediated effector transport in Gram-positive bacteria. In: Type IV Secretion in Gram-Negative and Gram-Positive Bacteria. S. Backert & E. Grohmann (eds). Cham: Springer International Publishing, pp. 115-141.

Guglielmini, J., de la Cruz, F., and Rocha, E.P. (2013) Evolution of conjugation and type IV secretion systems. *Molecular Biology and Evolution* **30**: 315-331.

Gurjar, A., Li, J., and McClane, B.A. (2010) Characterization of toxin plasmids in *Clostridium perfringens* type C isolates. *Infection and Immunity* **78**: 4860-4869.

Han, X., Du, X.-D., Southey, L., Bulach, D.M., Seemann, T., Yan, X.-X., Bannam, T.L., and Rood, J.I. (2015) Functional analysis of a bacitracin resistance determinant located on ICE*Cp1*, a novel Tn*916*-like element from a conjugative plasmid in *Clostridium perfringens Antimicrobial Agents and Chemotherapy* **59**: 6855-6865.

Hu, L., Vecchiarelli, A.G., Mizuuchi, K., Neuman, K.C., and Liu, J. (2017) Brownian ratchet mechanism for faithful segregation of low-copy-number plasmids. *Biophysical Journal* **112**: 1489-1502.

Hughes, M.L., Poon, R., Adams, V., Sayeed, S., Saputo, J., Uzal, F.A., McClane, B.A., and Rood, J.I. (2007) Epsilon-toxin plasmids of *Clostridium perfringens* type D are conjugative. *Journal of Bacteriology* **189**: 7531-7538.

Hülter, N., Ilhan, J., Wein, T., Kadibalban, A.S., Hammerschmidt, K., and Dagan, T. (2017) An evolutionary perspective on plasmid lifestyle modes. *Current Opinion in Microbiology* **38**: 74-80.

Ilangovan, A., Connery, S., and Waksman, G. (2015) Structural biology of the Gram-negative bacterial conjugation systems. *Trends in Microbiology* **23**: 301-310.

Ilangovan, A., Kay, C.W.M., Roier, S., El Mkami, H., Salvadori, E., Zechner, E.L., Zanetti, G., and Waksman, G. (2017) Cryo-EM structure of a relaxase reveals the molecular basis of DNA unwinding during bacterial conjugation. *Cell* **169**: 708-721.e712.

Ionesco, H., and Bouanchaud, D.H. (1973) Production of bacteriocin linked to the presence of a plasmid in *Clostridium perfingens* type A. *Compte Rendus Hebdomadariess des Seance de l'Academie des Sciences Serie D* **276**: 2855-2857.

Irikura, D., Monma, C., Suzuki, Y., Nakama, A., Kai, A., Fukui-Miyazaki, A., Horiguchi, Y., Yoshinari, T., Sugita-Konishi, Y., and Kamata, Y. (2015) Identification and characterization of a new enterotoxin produced by *Clostridium perfringens* isolated from food poisoning outbreaks. *PLOS One* **10**: e0138183.

Jin, F., Matsushita, O., Katayama, S., Jin, S., Matsushita, C., Minami, J., and Okabe, A. (1996) Purification, characterization, and primary structure of *Clostridium perfringens* lambda-toxin, a thermolysin-like metalloprotease. *Infection and Immunity* **64**: 230-237.

Katayama, S., Dupuy, B., Cole, S.T., Daube, G., and China, B. (1996) Genome mapping of *Clostridium perfringens* strains with I-CeuI shows many virulence genes to be plasmid-borne. *MGG Molecular & General Genetics* **251**: 720-726.

Keyburn, A.L., Boyce, J.D., Vaz, P., Bannam, T.L., Ford, M.E., Parker, D., Di Rubbo, A., Rood, J.I., and Moore, R.J. (2008) NetB, a new toxin that is associated with avian necrotic enteritis caused by *Clostridium perfingens*. *PLoS Pathogens* **4**: e26.

Kostelidou, K., Jones, A.C., and Thomas, C.M. (1999) Conserved C-terminal region of global repressor KorA of broad-host-range plasmid RK2 is required for co-operativity between KorA and a second RK2 global regulator, KorB11. *Journal of Molecular Biology* **289**: 211-221.

Krause, M., and Guiney, D.G. (1991) Identification of a multimer resolution system involved in stabilization of the *Salmonella dublin* virulence plasmid pSDL2. *Journal of Bacteriology* **173**: 5754-5762.

Kwong, S.M., Ramsay, J.P., Jensen, S.O., and Firth, N. (2017) Replication of staphylococcal resistance plasmids. *Frontiers in Microbiology* **8**: 2279.

Lacey, J.A., Keyburn, A.L., Ford, M.E., Portela, R.W., Johanesen, P.A., Lyras, D., and Moore, R.J. (2017) Conjugation-mediated horizontal gene transfer of *Clostridium perfringens* plasmids in the chicken gastrointestinal tract results in the formation of new virulent strains. *Applied and Environmental Microbiology* **83**: e01814-17.

Lanka, E., and Wilkins, B.M. (1995) DNA processing reactions in bacterial conjugation. *Annual Reviews Biochemistry* **64**: 141-169.

Larsen, R.A., Cusumano, C., Fujioka, A., Lim-Fong, G., Patterson, P., and Pogliano, J. (2007) Treadmilling of a prokaryotic tubulin-like protein, TubZ, required for plasmid stability in *Bacillus thuringiensis*. *Genes & Development* **21**: 1340-1352.

LeBard, R.J., Jensen, S.O., Arnaiz, I.A., Skurray, R.A., and Firth, N. (2008) A multimer resolution system contributes to segregational stability of the prototypical staphylococcal conjugative multiresistance plasmid pSK41. *FEMS Microbiology Letters* **284**: 58-67.

Li, J., Adams, V., Bannam, T.L., Miyamoto, K., Garcia, J.P., Uzal, F.A., Rood, J.I., and McClane, B.A. (2013) Toxin plasmids of *Clostridium perfringens*. *Microbiol Mol Biol Rev* **77**: 208-233.

Li, J., Miyamoto, K., and McClane, B.A. (2007) Comparison of virulence plasmids among *Clostridium perfringens* type E isolates. *Infection and Immunity* **75**: 1811-1819.

Lilly, J., and Camps, M. (2015) Mechanisms of theta plasmid replication. *Microbiology Spectrum* **3**: PLAS-0029-2014.

Llosa, M., and de la Cruz, F. (2005) Bacterial conjugation: a potential tool for genomic engineering. *Research in Microbiology* **156**: 1-6.

Llosa, M., Gomis-Rüth, F.X., Coll, M., and Cruz, F.d.l. (2002) Bacterial conjugation: a two-step mechanism for DNA transport. *Molecular Microbiology* **45**: 1-8.

Løbner-Olesen, A., Skovgaard, O., and Marinus, M.G. (2005) Dam methylation: coordinating cellular processes. *Current Opinion in Microbiology* **8**: 154-160.

Luo, Y., Gao, Q., and Deonier, R.C. (1994) Mutational and physical analysis of F plasmid *traY* protein binding to *oriT*. *Molecular Microbiology* **11**: 459-469.

Massey, T.H., Mercogliano, C.P., Yates, J., Sherratt, D.J., and Löwe, J. (2006) Double-Stranded DNA Translocation: Structure and Mechanism of Hexameric FtsK. *Molecular Cell* **23**: 457-469.

McClane, B., Robertson, S., and Li, J. (2013) *Clostridium perfringens*. *Food Microbiology: fundamentals and frontiers, 4th ed. ASM Press, Washington, DC*.

McClane, B.A., (2014) *Clostridium perfringens*. In: Encyclopedia of Toxicology (Third Edition). P. Wexler (ed). Oxford: Academic Press, pp. 987-988.

McPherson, A.L., Olorunniji, F.J., Stark, W.M., Pavlou, H.J., McIlwraith, M.J., Brazier, J.A., and Cosstick, R. (2015) Nicked-site substrates for a serine recombinase reveal enzyme–DNA

communications and an essential tethering role of covalent enzyme–DNA linkages. *Nucleic Acids Research* **43**: 6134-6143.

Mehdizadeh Gohari, I., Kropinski, A.M., Weese, S.J., Parreira, V.R., Whitehead, A.E., Boerlin, P., and Prescott, J.F. (2016) Plasmid characterization and chromosome analysis of two *netF*+ *Clostridium perfringens* isolates associated with foal and canine necrotizing enteritis. *PLOS One* **11**: e0148344.

Mehdizadeh Gohari, I., Parreira, V.R., Nowell, V.J., Nicholson, V.M., Oliphant, K., and Prescott, J.F. (2015) A novel pore-forming toxin in Type A *Clostridium perfringens* is associated with both fatal canine hemorrhagic gastroenteritis and fatal foal necrotizing enterocolitis. *PLOS One* **10**: e0122684.

Miguel-Arribas, A., Hao, J.-A., Luque-Ortega, J.R., Ramachandran, G., Val-Calvo, J., Gago-Córdoba, C., González-Álvarez, D., Abia, D., Alfonso, C., Wu, L.J., and Meijer, W.J.J. (2017) The *Bacillus subtilis* conjugative plasmid pLS20 encodes two ribbon-helix-helix type auxiliary relaxosome proteins that are essential for conjugation. *Frontiers in Microbiology* **8**: 2138.

Mihelc, V.A., Duncan, C.L., and Chambliss, G.H. (1978) Characterization of a bacteriocinogenic plasmid in *Clostridium perfringens* CW55. *Antimicrobial Agents and Chemotherapy* **14**: 771-779.

Miyamoto, K., Chakrabarti, G., Morino, Y., and McClane, B.A. (2002) Organization of the plasmid *cpe* locus in *Clostridium perfringens* Type A isolates. *Infection and Immunity* **70**: 4261-4272.

Miyamoto, K., Fisher, D.J., Li, J., Sayeed, S., Akimoto, S., and McClane, B.A. (2006) Complete sequencing and diversity analysis of the enterotoxin-encoding plasmids in *Clostridium perfringens* type A non-food-borne human gastrointestinal disease isolates. *Journal of Bacteriology* **188**: 1585-1598.

Miyamoto, K., Li, J., Sayeed, S., Akimoto, S., and McClane, B.A. (2008) Sequencing and diversity analyses reveal extensive similarities between some epsilon-toxin-encoding plasmids and the pCPF5603 *Clostridium perfringens* enterotoxin plasmid. *Journal of Bacteriology* **190**: 7178-7188.

Miyamoto, K., Seike, S., Takagishi, T., Okui, K., Oda, M., Takehara, M., and Nagahama, M. (2015) Identification of the replication region in pBCNF5603, a bacteriocin-encoding plasmid, in the enterotoxigenic *Clostridium perfringens* strain F5603. *BMC Microbiology* **15**: 1-12.

Miyamoto, K., Yumine, N., Mimura, K., Nagahama, M., Li, J., McClane, B.A., and Akimoto, S. (2011) Identification of novel *Clostridium perfringens* Type E strains that carry an iota toxin plasmid with a functional enterotoxin gene. *PLOS One* **6**: e20376.

Müller, A.K., Rojo, F., and Alonso, J.C. (1995) The level of the pUB110 replication initiator protein is autoregulated, which provides an additional control for plasmid copy number. *Nucleic Acids Research* **23**: 1894-1900.

Ni, L., Jensen, S.O., Ky Tonthat, N., Berg, T., Kwong, S.M., Guan, F.H.X., Brown, M.H., Skurray, R.A., Firth, N., and Schumacher, M.A. (2009) The *Staphylococcus aureus* pSK41 plasmid-encoded ArtA protein is a master regulator of plasmid transmission genes and contains a RHH motif used in alternate DNA-binding modes. *Nucleic Acids Research* **37**: 6970-6983.

Norman, A., Hansen, L.H., and Sørensen, S.J. (2009) Conjugative plasmids: vessels of the communal gene pool. *Philos Trans R Soc Lond B Biol Sci* **364**: 2275-2289.

Ochman, H., Lawrence, J.G., and Groisman, E.A. (2000) Lateral gene transfer and the nature of bacterial innovation. *Nature* **405**: 299-304.

Ogura, T., and Hiraga, S. (1983) Mini-F plasmid genes that couple host cell division to plasmid proliferation. *Proceedings of the National Academy of Sciences* **80**: 4784-4788.

Ohtani, K., Kawsar, H.I., Okumura, K., Hayashi, H., and Shimizu, T. (2003) The VirR/VirS regulatory cascade affects transcription of plasmid-encoded putative virulence genes in *Clostridium perfringens* strain 13. *FEMS Microbiology Letters* **222**: 137-141.

Page, R., and Peti, W. (2016) Toxin-antitoxin systems in bacterial growth arrest and persistence. *Nature Chemical Biology* **12**: 208.

Pansegrau, W., Balzer, D., Kruft, V., Lurz, R., and Lanka, E. (1990) *In vitro* assembly of relaxosomes at the transfer origin of plasmid RP4. *Proceedings of the National Academy of Sciences* **87**: 6555-6559.

Paredes-Sabja, D., Sarker, N., and Sarker, M.R. (2011) *Clostridium perfringens tpeL* is expressed during sporulation. *Microbial Pathogenesis* **51**: 384-388.

Parker, C., and Meyer, R.J. (2007) The R1162 relaxase/primase contains two, type IV transport signals that require the small plasmid protein MobB. *Molecular Microbiology* **66**: 252-261.

Parreira, V.R., Costa, M., Eikmeyer, F., Blom, J., and Prescott, J.F. (2012) Sequence of two plasmids from *Clostridium perfringens* chicken necrotic enteritis isolates and comparison with *C. perfringens* conjugative plasmids. *PLOS One* **7**: e49753.

Parsons, J.A., Bannam, T.L., Devenish, R.J., and Rood, J.I. (2007) TcpA, an FtsK/SpoIIIE homolog, is essential for transfer of the conjugative plasmid pCW3 in *Clostridium perfringens*. *Journal of Bacteriology* **189**: 7782-7790.

Petit, L., Gibert, M., and Popoff, M.R. (1999) *Clostridium perfringens*: toxinotype and genotype. *Trends in Microbiology* **7**: 104-110.

Pettis, G.S., and Cohen, S.N. (2001) Unraveling the essential role in conjugation of the Tra protein of *Streptomyces lividans* plasmid pIJ101. *Antonie van Leeuwenhoek* **79**: 247-250.

Pinto, U.M., Pappas, K.M., and Winans, S.C. (2012) The ABCs of plasmid replication and segregation. *Nature Reviews Microbiology* **10**: 755.

Pluta, R., and Espinosa, M. (2018) Antisense and yet sensitive: Copy number control of rolling circle-replicating plasmids by small RNAs. *Wiley Interdisciplinary Reviews: RNA* **9**: e1500.

Popoff, M.R., and Bouvet, P. (2013) Genetic characteristics of toxigenic Clostridia and toxin gene evolution. *Toxicon* **75**: 63-89.

Porter, C.J., Bantwal, R., Bannam, T.L., Rosado, C.J., Pearce, M.C., Adams, V., Lyras, D., Whisstock, J.C., and Rood, J.I. (2012) The conjugation protein TcpC from *Clostridium perfringens* is structurally related to the type IV secretion system protein VirB8 from Gram-negative bacteria. *Molecular Microbiology* **83**: 275-288.

Possoz, C., Ribard, C., Gagnat, J., Pernodet, J.-L., and Guérineau, M. (2001) The integrative element pSAM2 from Streptomyces: kinetics and mode of conjugal transfer. *Molecular Microbiology* **42**: 159-166.

Ragonese, H., Haisch, D., Villareal, E., Choi, J.-H., and Matson, S.W. (2007) The F plasmid-encoded TraM protein stimulates relaxosome-mediated cleavage at *oriT* through an interaction with TraI. *Molecular Microbiology* **63**: 1173-1184.

Rajeev, L., Malanowska, K., and Gardner, J.F. (2009) Challenging a Paradigm: the Role of DNA Homology in Tyrosine Recombinase Reactions. *Microbiology and Molecular Biology Reviews* **73**: 300-309.

Revitt-Mills, S.A., Rood, J.I., and Adams, V. (2015) *Clostridium perfringens* extracellular toxins and enzymes: 20 and counting. *Microbiology Australia* **36**: 114-117.

Roberts, A.P., and Mullany, P. (2009) A modular master on the move: the Tn*916* family of mobile genetic elements. *Trends in Microbiology* **17**: 251-258.

Rokos, E.A., Rood, J.I., and Duncan, C.L. (1978) Multiple plasmids in different toxigenic types of Clostridium perfringens. *FEMS Microbiology Letters* **4**: 323-326.

Rood, J.I. (1983) Transferable tetracycline resistance in Clostridium perfringens strains of porcine origin. *Canadian Journal of Microbiology* **29**: 1241-1246.

Rood, J.I., Adams, V., Lacey, J., Lyras, D., McClane, B.A., Melville, S.B., Moore, R.J., Popoff, M.R., Sarker, M.R., Songer, J.G., Uzal, F.A., and Van Immerseel, F. (2018) Expansion of the *Clostridium perfringens* toxin-based typing scheme. *Anaerobe* **53**: 5-10.

Rood, J.I., Maher, E.A., Somers, E.B., Campos, E., and Duncan, C.L. (1978) Isolation and characterization of multiply antibiotic-resistant *Clostridium perfringens* strains from porcine feces. *Antimicrobial Agents and Chemotherapy* **13**: 871-880.

Ruiz-Masó, J.A., Machón, C., Bordanaba-Ruiseco, L., Espinosa, M., Coll, M., and del Solar, G., (2015) Plasmid rolling-circle replication. In: Plasmids: Biology and Impact in Biotechnology and Discovery. American Society of Microbiology, pp. 45-69.

Sakai, H., and Komano, T. (1996) DNA replication of IncQ broad-host-range plasmids in Gram-negative bacteria. *Bioscience, Biotechnology, and Biochemistry* **60**: 377-382.

Salje, J., Gayathri, P., and Löwe, J. (2010) The ParMRC system: molecular mechanisms of plasmid segregation by actin-like filaments. *Nature Reviews Microbiology* **8**: 683.

San Millan, A., and MacLean, R.C. (2017) Fitness costs of plasmids: A limit to plasmid transmission. *Microbiology Spectrum* **5**: MTBP-0016-2017.

Sarker, M.R., Carman, R.J., and McClane, B.A. (1999) Inactivation of the gene (*cpe*) encoding *Clostridium perfringens* enterotoxin eliminated the ability of two *cpe*-positive *C. perfringens* type A human gastrointestinal disease isolates to affect rabbit ileal loops. *Molecular Microbiology* **33**: 946-958.

Sayeed, S., Li, J., and McClane, B.A. (2007) Virulence plasmid diversity in *Clostridium perfringen*s type D isolates. *Infection and Immunity* **75**: 2391-2398.

Sayeed, S., Li, J., and McClane, B.A. (2010) Characterization of virulence plasmid diversity among *Clostridium perfringens* type B isolates. *Infection and Immunity* **78**: 495-504.

Sayeed, S., Uzal, F.A., Fisher, D.J., Saputo, J., Vidal, J.E., Chen, Y., Gupta, P., Rood, J.I., and McClane, B.A. (2008) Beta toxin is essential for the intestinal virulence of Clostridium perfringens type C disease isolate CN3685 in a rabbit ileal loop model. *Molecular Microbiology* **67**: 15-30.

Schröder, G., and Lanka, E. (2005) The mating pair formation system of conjugative plasmids—a versatile secretion machinery for transfer of proteins and DNA. *Plasmid* **54**: 1-25.

Sengupta, M., and Austin, S. (2011) Prevalence and significance of plasmid maintenance functions in the virulence plasmids of pathogenic bacteria. *Infection and Immunity* **79**: 2502-2509.

Shimizu, T., Ohtani, K., Hirakawa, H., Ohshima, K., Yamashita, A., Shiba, T., Ogasawara, N., Hattori, M., Kuhara, S., and Hayashi, H. (2002) Complete genome sequence of *Clostridium perfringens*, an anaerobic flesh-eater. *Proceedings of the National Academy of Sciences* **99**: 996-1001.

Simpson, A.E., Skurray, R.A., and Firth, N. (2003) A single gene on the Staphylococcal multiresistance plasmid pSK1 encodes a novel partitioning system. *Journal of Bacteriology* **185**: 2143-2152.

Smillie, C., Garcillán-Barcia, M.P., Francia, M.V., Rocha, E.P.C., and de la Cruz, F. (2010) Mobility of plasmids. *Microbiol Mol Biol Rev* **74**: 434-452.

Smith, M.C.A., and Thomas, C.D. (2004) An accessory protein is required for relaxosome formation by small Staphylococcal plasmids. *Journal of Bacteriology* **186**: 3363-3373.

Solberg, M., Blaschek, H.P., and Kahn, P. (1981) Plasmids in *Clostridium perfingens*. *Journal of Food Safety* **3**: 267-289.

Steen, J.A., Bannam, T.L., Teng, W.L., Devenish, R.J., and Rood, J.I. (2009) The putative coupling protein TcpA interacts with other pCW3-encoded proteins to form an essential part of the conjugation complex. *Journal of Bacteriology* **191**: 2926-2933.

Teng, W.L., Bannam, T.L., Parsons, J.A., and Rood, J.I. (2008) Functional characterization and localization of the TcpH conjugation protein from *Clostridium perfringens*. *Journal of Bacteriology* **190**: 5075-5086.

Thomas, C.M., and Nielsen, K.M. (2005) Mechanisms of, and barriers to, horizontal gene transfer between bacteria. *Nature Reviews Microbiology* **3**: 711-721.

Tolmasky, M.E., (2017) Plasmids. In: Reference Module in Life Sciences. Elsevier, pp. 1485–1490.

Traore, D.A.K., Wisniewski, J.A., Flanigan, S.F., Conroy, P.J., Panjikar, S., Mok, Y.-F., Lao, C., Griffin, M.D.W., Adams, V., Rood, J.I., and Whisstock, J.C. (2018) Crystal structure of TcpK in complex with *oriT* DNA of the antibiotic resistance plasmid pCW3. *Nature Communications* **9**: 3732.

Trokter, M., Felisberto-Rodrigues, C., Christie, P.J., and Waksman, G. (2014) Recent advances in the structural and molecular biology of Type IV secretion systems. *Current Opinion in Structural Biology* **27**: 16-23.

Tsuchimoto, S., Ohtsubo, H., and Ohtsubo, E. (1988) Two genes, *pemK* and *pemI*, responsible for stable maintenance of resistance plasmid R100. *Journal of Bacteriology* **170**: 1461-1466.

Uzal, F.A., Freedman, J.C., Shrestha, A., Theoret, J.R., Garcia, J., Awad, M.M., Adams, V., Moore, R.J., Rood, J.I., and McClane, B.A. (2014) Towards an understanding of the role of *Clostridium perfringens* toxins in human and animal disease. *Future Microbiology* **9**: 361-377.

Vidal, J.E., Ma, M., Saputo, J., Garcia, J. Uzal, F. A., and McClane, B.A. (2012) Evidence that the Agr-like quorum sensing system regulates the toxin production, cytotoxicity and pathogenicity of *Clostridium perfringens* type C isolate CN3685. *Molecular Microbiology* **83**: 179-194.

Vidor, C.J., Watts, T.D., Adams, V., Bulach, D., Couchman, E., Rood, J.I., Fairweather, N.F., Awad, M., and Lyras, D. (2018) *Clostridium sordellii* pathogenicity locus plasmid pCS1-1 encodes a novel Clostridial conjugation locus. *mBio* **9:** e0761-17.

Volante, A., Soberón, N.E., Ayora, S., and Alonso, J.C. (2014) The interplay between different stability systems contributes to faithful segregation: *Streptococcus pyogenes* pSM19035 as a model. *Microbiology Spectrum* **2:**PLAS-0007-2013.

Waksman, G., and Orlova, E.V. (2014) Structural organisation of the type IV secretion systems. *Current Opinion in Microbiology* **17**: 24-31.

Wang, J., Parsons, L.M., and Derbyshire, K.M. (2003) Unconventional conjugal DNA transfer in mycobacteria. *Nature Genetics* **34**: 80-84.

Wang, X., Lord, D.M., Cheng, H.-Y., Osbourne, D.O., Hong, S.H., Sanchez-Torres, V., Quiroga, C., Zheng, K., Herrmann, T., Peti, W., Benedik, M.J., Page, R., and Wood, T.K. (2012) A new type V toxin-antitoxin system where mRNA for toxin GhoT is cleaved by antitoxin GhoS. *Nature Chemical Biology* **8**: 855.

Wang, Y., Penkul, P., and Milstein, J.N. (2016) Quantitative localization microscopy reveals a novel organization of a high-copy number plasmid. *Biophysical Journal* **111**: 467-479.

Waters, V.L., and Guiney, D.G. (1993) Processes at the nick region link conjugation, T-DNA transfer and rolling circle replication. *Molecular Microbiology* **9**: 1123-1130.

Watts, T.D., Johanesen, P.A., Lyras, D., Rood, J.I., and Adams, V. (2017) Evidence that compatibility of closely related replicons in *Clostridium perfringens* depends on linkage to parMRC-like partitioning systems of different subfamilies. *Plasmid* **91**: 68-75.

Watts, T.D., Vidor, C.J., Awad, M.M., Lyras, D., Rood, J.I., and Adams, V. (2019) pCP13, a representative of a new family of conjugative toxin plasmids in *Clostridium perfringens*. *Plasmid* **102**: 37-45.

Wisniewski, J.A., and Rood, J.I. (2017) The Tcp conjugation system of *Clostridium perfringens*. *Plasmid* **91**: 28-36.

Wisniewski, J.A., Teng, W.L., Bannam, T.L., and Rood, J.I. (2015a) Two novel membrane proteins, TcpD and TcpE, are essential for conjugative transfer of pCW3 in *Clostridium perfringens*. *Journal of Bacteriology* **197**: 774-781.

Wisniewski, J.A., Traore, D.A., Bannam, T.L., Lyras, D., Whisstock, J.C., and Rood, J.I. (2015b) TcpM, a novel relaxase that mediates transfer of large conjugative plasmids from *Clostridium perfringens*. *Molecular Microbiology* **99**: 884-896.

Wong, J.J., Lu, J., and Glover, J. (2012) Relaxosome function and conjugation regulation in F-like plasmids–a structural biology perspective. *Molecular Microbiology* **85**: 602-617.

Yamaguchi, Y., Park, J.-H., and Inouye, M. (2011) Toxin-antitoxin systems in bacteria and archaea. *Annual Review of Genetics* **45**: 61-79.

Yonogi, S., Matsuda, S., Kawai, T., Yoda, T., Harada, T., Kumeda, Y., Gotoh, K., Hiyoshi, H., Nakamura, S., Kodama, T., and Iida, T. (2014) BEC, a novel enterotoxin of *Clostridium perfringens* found in human clinical isolates from acute gastroenteritis outbreaks. *Infection and Immunity* **82**: 2390-2399.

Zatyka, M., Bingle, L., Jones, A.C., and Thomas, C.M. (2001) Cooperativity between KorB and TrbA repressors of broad-host-range plasmid RK2. *Journal of Bacteriology* **183**: 1022-1031.

Zatyka, M., Jagura-Burdzy, G., and Thomas, C.M. (1994) Regulation of transfer genes of promiscuous IncPα plasmid RK2: repression of Tra1 region transcription both by relaxosome proteins and by the Tra2 regulator TrbA. *Microbiology* **140**: 2981-2990.

Zechner, E.L., Moncalián, G., and de la Cruz, F., (2017) Relaxases and plasmid transfer in Gram-negative bacteria. In: Type IV Secretion in Gram-Negative and Gram-Positive Bacteria. S. Backert & E. Grohmann (eds). Cham: Springer International Publishing, pp. 93-113.

Zhang, J., Zhang, Y., Zhu, L., Suzuki, M., and Inouye, M. (2004) Interference of mRNA function by sequence-specific endoribonuclease PemK. *Journal of Biological Chemistry* **279**: 20678-20684.

Zielenkiewicz, U., and Ceglowski, P. (2001) Mechanisms of plasmid stable maintenance with special focus on plasmid addiction systems. *Acta Biochimica Poloncia* **48**: 1003-1023.

Chapter Two

The role of conserved hypothetical genes in the biology of pCW3

Introduction

The pCW3-like plasmids (or Tcp plasmids) comprise the largest characterised plasmid family in *C. perfringens*. These plasmids are defined by a high level of conservation across a 35 kb region that is closely related to the archetypal plasmid pCW3 (Bannam *et al.*, 2011, Li *et al.*, 2013, Parreira *et al.*, 2012). This conserved region makes up the common backbone for all pCW3-like plasmids, as it contains genes involved in plasmid replication, maintenance, regulation and conjugative transfer (Figure 2.1A) (Li *et al.*, 2013).

To date, only two key loci of the common backbone of pCW3-like plasmids have been characterised: the replication region and the *tcp* conjugation locus (Figure 2.1A). The replication region spans from a putative regulator**,** *regB*, through to the putative transcriptional repressor *regD* and contains some genes that are essential for pCW3 replication, regulation and maintenance (Parreira *et al.*, 2012, Bannam *et al.*, 2006, Watts *et al.*, 2017). Bioinformatic analysis has revealed that the genetic organisation of this region is conserved in the Tcp plasmids, with only significant changes occurring in the nucleotide sequences of the *parMRC*-like partitioning locus (Adams *et al.*, 2015, Parreira *et al.*, 2012). Recent work has shown that the differences in *parMRC* sequences form the basis for plasmid incompatibility groups in *C. perfringens* (Adams *et al.*, 2015, Watts *et al.*, 2017).

Located just outside of the replication region are genes encoding two other putative plasmid maintenance mechanisms: a putative multimer resolution system encoded by r*esP* and a putative toxin-antitoxin system partly encoded by a *pemK*-like gene (Bannam *et al.*, 2006). Whilst the predicted products of these genes have not yet been functionally characterised, significant homology to proteins of known function provides evidence for their role in pCW3 biology.

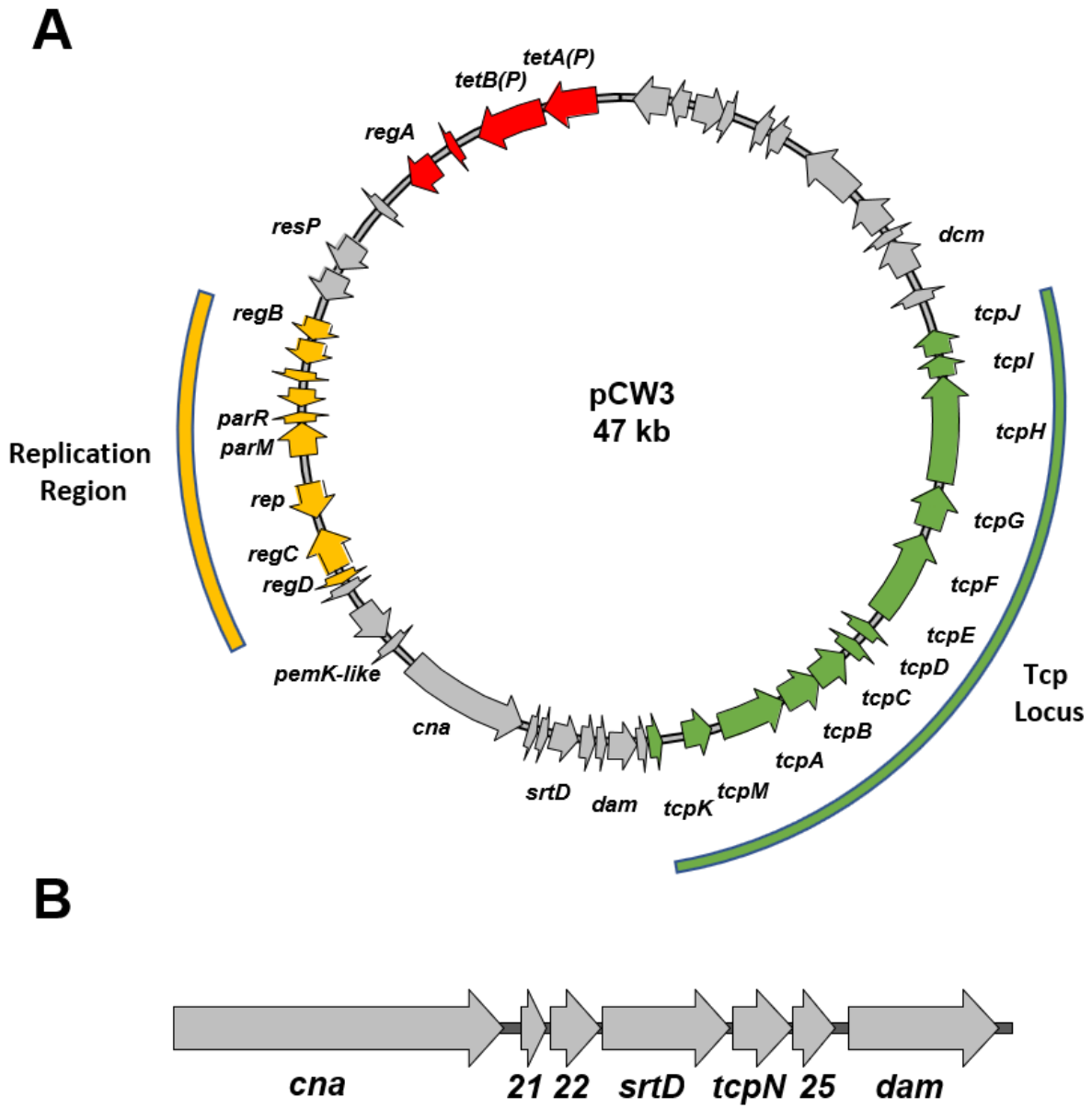

Figure 2.1: Genetic organisation of the archetypal tetracycline resistance plasmid pCW3. **A.** A circular map of pCW3 is shown. ORFs are indicated by the arrows. Genetic regions are indicated as follows: the replication region (yellow arrows), the conjugation locus (Tcp locus; green arrows) and the unique region, including the *tetAB(P)* tetracycline resistance genes is shown in red. Grey arrows indicate conserved ORFs. **B.** A genetic map of the conserved CnaC region of pCW3 is shown. ORFs are indicated by the arrows and genes labelled below.

The other well characterised region within the pCW3 backbone is the Tcp locus, which facilitates the conjugative transfer of pCW3-like plasmids (Wisniewski & Rood, 2017, Bannam *et al.*, 2006). The Tcp locus encodes 12 genes, *tcpK, tcpM,*and *tcpA* through to *tcpJ,* of which *tcpD, tcpE, tcpF and tcpH* are essential for conjugative transfer (Wisniewski & Rood, 2017, Parsons *et al.*, 2007, Porter *et al.*, 2012, Wisniewski *et al.*, 2015a, Bannam *et al.*, 2006, Bantwal *et al.*, 2012, Traore *et al.*, 2018, Wisniewski *et al.*, 2015b). Amongst pCW3-like plasmids the genetic organisation of the key features of the Tcp locus is conserved (Bannam *et al.*, 2006). Only minor differences have been noted in some plasmids, such as the absence of the non-essential gene *tcpB*, as well as the insertion of additional open reading frames and Group II introns (Wisniewski & Rood, 2017, Bannam *et al.*, 2006).

Many of the genes that are encoded on the common backbone of the Tcp plasmids have been well characterised or their functions proposed based on homology to known proteins (Watts *et al.*, 2017, Adams *et al.*, 2015, Parsons *et al.*, 2007, Porter *et al.*, 2012, Wisniewski *et al.*, 2015a, Bannam *et al.*, 2006, Bantwal *et al.*, 2012, Traore *et al.*, 2018, Wisniewski *et al.*, 2015b). However, there are many conserved genes whose function remains unclear. One of the remaining regions yet to be functionally studied has been designated as the CnaC region (Bannam *et al.*, 2006, Bannam *et al.*, 2011, Parreira *et al.*, 2012, Mehdizadeh Gohari *et al.*, 2016, Mehdizadeh Gohari *et al.*, 2017).

The CnaC region, spans from *cnaC* through to the *dam* gene (nucleotides 17927-24024 of pCW3) and contains six genes, four of which encode hypothetical proteins of various sizes (Figure 2.1B) (Bannam *et al.*, 2006). A putative sortase enzyme is also encoded within this region and is hypothesised to anchor the putative adhesion protein, CnaC, to the surface of *C. perfringens* cells, based on the presence of a sortase recognition sequence within CnaC (Bannam *et al.*, 2006, Bhatty *et al.*, 2013). Previous work has determined that CnaC is required for efficient transfer of pCW3 between *C. perfringens* cells of different strain backgrounds (S. Revitt-Mills, V. Adams and J. Rood,

unpublished). The genetic location of the CnaC region, just prior to the start of the Tcp locus, suggested that these genes may play a role in the conjugation of pCW3-like plasmids.

In this study the objectives were to mutate the genes within the conserved CnaC region of pCW3 and to elucidate their function. Unfortunately, the results did not lead to the unequivocal determination of the biological function of these genes. However, these findings do provide preliminary evidence that pCW3 conjugation requires the *srtD* and *tcpN* genes for efficient conjugative transfer.

Materials and Methods

Bacterial strains and culture conditions

C. perfringens strains and plasmids are listed in Table 2.1**.** *C. perfringens* was cultured at 37°C in pre-boiled fluid thioglycolate (FTG) medium (Difco), tryptone-peptone glucose (TPG) broth (Rood *et al.*, 1978a), heart infusion (HI) or brain heart infusion (BHI) broth or agar (Oxoid), or nutrient agar (NA) (Rood, 1983) supplemented with glucose (0.375% w/v). As required, media were supplemented with antibiotics (Sigma) at the following concentrations: tetracycline (Tc; 10 μg/ml), rifampicin (Rif; 10 μg/ml), nalidixic acid (Nal; 10 μg/ml), erythromycin (Em; 50 μg/ml), thiamphenicol (Tm; 10 μg/ml), streptomycin (Str; 1 mg/ml) or saturated potassium chlorate (Chl; 1% v/v). *C. perfringens* agar cultures were incubated in anaerobic jars (Oxoid) in an atmosphere of 10% (v/v) H_2, 10% (v/v) CO_2 and 80% (v/v) N_2.

Escherichia coli strain DH5α (Life Technologies) was used to construct vectors for subsequent introduction into *C. perfringens* (Table 2.1). All *E. coli* cultures were maintained at 37°C in 2x Yeast extract/tryptone (2YT) medium/agar (Difco) and were supplemented with the following antibiotics as required: kanamycin (Kn; 20 μg/ml), chloramphenicol (Cm; 30 μg/ml) or erythromycin (Em; 150 μg/ml).

Table 2.1: Bacterial strains and plasmids used in this study

Strain	Description	Reference
E. coli		
DH5α	F-φ80*lacZ*ΔM15, Δ(*lac*ZYA-*argF*)U169, *rec*A1, *end*A1, *hsd*R17(r_k-, m_k+), *pho*A, *sup*E44, *thi*-1, *gyr*A96, *rel*A1 λ	Invitrogen/ Life Technologies
C. perfringens		
JIR39	Strain CW362 derivative, Sm^R Chl^R	(Johanesen *et al.*, 2001)
JIR325	Strain 13 derivative; Rif^R Nal^R	(Lyristis *et al.*, 1994)
JIR4195	JIR325 (pCW3); Rif^R Nal^R Tc^R	(Hughes *et al.*, 2007)
JIR4394	Strain 13 derivative; Sm^R Chl^R	(Bannam *et al.*, 2006)
JIR13211	JIR325(pCP13)$^-$; Rif^R Nal^R JIR325 cured of pCP13	(Watts *et al.*, 2019)
JIR13224	JIR13211(pCW3); Rif^R Nal^R Tc^R	This study
JIR13252	JIR13211(pJIR4521); Rif^R Nal^R Tc^R Em^R pCW3Δ*pcw321::erm*(Q)	This study
JIR13253	JIR13211(pJIR4522); Rif^R Nal^R Tc^R Em^R pCW3Δ*pcw321::erm*(Q), independent mutant	This study
JIR13254	JIR13211(pJIR4523); Rif^R Nal^R Tc^R Em^R pCW3Δ*pcw322::erm*(Q)	This study
JIR13255	JIR13211(pJIR4524); Rif^R Nal^R Tc^R Em^R pCW3Δ*pcw322::erm*(Q), independent mutant	This study
JIR13256	JIR13211(pJIR4525); Rif^R Nal^R Tc^R Em^R pCW3Δ*srtD::erm*(Q)	This study
JIR13257	JIR13211(pJIR4526); Rif^R Nal^R Tc^R Em^R pCW3Δ*srtD::erm*(Q), independent mutant	This study
JIR13258	JIR13211(pJIR4527); Rif^R Nal^R Tc^R Em^R pCW3Δ*tcpN::erm*(Q)	This study

JIR13259	JIR13211(pJIR4528); Rif^R Nal^R Tc^R Em^R pCW3Δ*tcpN::erm*(Q), independent mutant	This study
JIR13321	JIR13211(pJIR4583); Rif^R Nal^R Tc^R Em^R pCW3Δ*pcw325::erm*(Q)	This study
Plasmids		
pT7Blue	*E. coli* cloning vector, f1 origin, pUC origin, *lacZ* α-peptide, Amp^R	Novagen
pCW3	Conjugative tetracycline resistance plasmid	(Rood *et al.*, 1978b)
pJIR2715	Base plasmid for the construction of *C. perfringens* suicide vectors, Em^R Cm^R	(Bannam *et al.*, 2006)
pJIR3422	pJIR750*ΩattCI, E. coli-C. perfringens* shuttle and expression vector, Cm^R	(Adams *et al.*, 2014, Bantwal *et al.*, 2012)
pJIR3566	Clostridial TargeTron vector, pMTL9361 derivative, *lacZ* α-peptide, Cm^R	(Cheung *et al.*, 2010)
pJIR4503	pJIR2715 (XhoI/SacI) ΩJRP6249/JRP6250 (XhoI/SacI; 2817 bp, pCW3) downstream of *pcw321*	This study
pJIR4504	pJIR2715 (XhoI/SacI) ΩJRP6249/JRP6251 (XhoI/SacI; 2550 bp, pCW3) downstream of *pcw322*	This study
pJIR4505	pJIR2715 (XhoI/SacI) ΩJRP6249/JRP6252 (XhoI/SacI; 1894 bp, pCW3) downstream of *srtD*	This study
pJIR4506	pJIR2715 (XhoI/SacI) ΩJRP6249/JRP6253 (XhoI/SacI; 1583 bp, pCW3) downstream of *tcpN*	This study
pJIR4507	pJIR2715 (XhoI/SacI) ΩJRP6249/JRP6254 (XhoI/SacI; 2550 bp, pCW3) downstream of *pcw325*	This study
pJIR4508	pJIR4503 (SphI/BamHI) ΩJRP6243/JRP6244 (SphI/BamHI; 1556 bp, pCW3) *pcw321* suicide vector	This study
pJIR4509	pJIR4504 (SphI/BamHI) ΩJRP6243/JRP6245 (SphI/BamHI; 1704 bp, pCW3) *pcw322* suicide vector	This study

pJIR4510	pJIR4506 (SphI/BamHI) ΩJRP6243/JRP6247 (SphI/BamHI; 2626 bp, pCW3) *tcpN* suicide vector	This study
pJIR4511	pJIR4507 (SphI/BamHI) ΩJRP6243/JRP6248 (SphI/BamHI; 2932 bp, pCW3) *pcw325* suicide vector	This study
pJIR4515	pJIR4505 (SphI/BamHI) ΩJRP6243/JRP6246 (SphI/BamHI; 1971 bp, pCW3) *srtD* suicide vector	This study
pJIR4521	pCW3Δ*pcw321::erm*(Q)	Transformation of JIR13224 with pJIR4508
pJIR4522	pCW3Δ*pcw321::erm*(Q), independent mutant	Transformation of JIR13224 with pJIR4508
pJIR4523	pCW3Δ*pcw322::erm*(Q)	Transformation of JIR13224 with pJIR4509
pJIR4524	pCW3Δ*pcw322::erm*(Q), independent mutant	Transformation of JIR13224 with pJIR4509
pJIR4525	pCW3Δ*srtD::erm*(Q)	Transformation of JIR13224 with pJIR4515
pJIR4526	pCW3Δ*srtD::erm*(Q), independent mutant	Transformation of JIR13224 with pJIR4515
pJIR4527	pCW3Δ *tcpN::erm*(Q)	Transformation of JIR13224 with pJIR4510
pJIR4528	pCW3Δ *tcpN::erm*(Q), independent mutant	Transformation of JIR13224 with pJIR4510
pJIR4545	pT7Blue (EcoRV) ΩJRP6372/JRP6373 (661 bp, pCW3) *srtD+*	This study
pJIR4546	pT7Blue (EcoRV) ΩJRP6375/JRP6375 (316 bp, pCW3) *tcpN+*	This study

pJIR4547	pJIR3422 (PstI/BamHI) ΩpJIR4545 (PstI/BamHI; 661 bp, pCW3), *srtD+* complementation vector	This study
pJIR4549	pJIR3422 (PstI/BamHI) ΩpJIR4546 (PstI/BamHI; 316 bp, pCW3), *tcpN+* complementation vector	This study
pJIR4583	pCW3Δ*pcw325::erm*(Q)	Transformation of JIR13224 with pJIR4511
pJIR4584	pT7Blue (EcoRV) ΩJRP6472/JRP6475 (970 bp, pCW3) *srtD+, tcpN+*	This study
pJIR4586	pJIR3566 (BamHI/Asp718) ΩJRP6450/JRP6451 (BamHI/Asp718; 1688 bp, pCW3) *pCW321* to *pcw325* knock-in vector	This study
pJIR4587	pJIR3422 (PstI/BamHI) ΩJRP6450/JRP6449 (PstI/BamHI; 1687 bp, pCW3) *pcw321* to *pcw325* complementation vector	This study
pJIR4588	pJIR3422 (PstI/BamHI) ΩpJIR4584 (PstI/BamHI; 970 bp, pCW3), *srtD+* and *tcpN+* double complementation vector	This study

Chl^R- potassium chlorate resistance, Cm^R- chloramphenicol resistance, Em^R- erythromycin resistance, Nal^R- nalidixic acid resistance, Rif^R – rifampicin resistance, Sm^R- streptomycin resistance, Tc^R- tetracycline resistance, Tm^R – thiamphenicol resistance.

Molecular Techniques

Plasmid DNA was extracted from *E. coli* using QIAprep Spin Miniprep kit (Qiagen) as outlined by the manufacturer. Crude *C. perfringens* DNA was obtained as previously described (Bannam *et al.*, 2006)**.** *E. coli* cells were made chemically competent and transformed as previously described (Inoue *et al.*, 1990).

Oligonucleotides used in this study are outlined in Table 2.2 and were synthesised by Integrated DNA Technologies (IDT) or Sigma. PCR amplification was performed using *Taq* (Roche) or Phusion Polymerase (NEB) as recommended by the manufacturer. PCR products were purified using QIAquick PCR purification kit (Qiagen). Restriction enzymes were used according to the manufacturer's instructions (Roche and NEB). Sequencing was performed using Prism BigDye Terminator mix (Applied Biosystems) and separated using an Applied Biosystems 3730S capillary sequencer. Sequences were analysed using Vector NTI (Invitrogen).

Table 2.2: Oligonucleotides used in this study

Name	Sequence	Purpose
JRP1777	CATATGGTAAGTTTGAGATAG	*rpoA,* RT-PCR, F
JRP1778	CTATTAACTACGATTTCCATA	*rpoA,* RT-PCR, R
JRP4330	CTCAGTACTGAGAGGGAACTTAGATGGTAT	*catP* probe oligo, F
JRP4331	CCGGGATCCTTAGGGTAACAAAAAACACC	*catP* probe oligo, R
JRP6001	CCAGGAAAAGGTCATATAACAGAAGC	*erm*(Q) probe, F
JRP6002	CTAAGACGCAATCTACACTAGGC	*erm*(Q) probe, R
JRP6025	CACAGGAGTCAAAGGAGAGAATTAATG	*tcpN* RT-PCR, F
JRP6029	CCTAAAACTATAGGAGCTTTAACCCC	*srtD* RT-PCR, F
JRP6243	GGGGTACCGAAATACTGATACTAATAAGCTTGTAGAG	LHS DCO plus Asp716, F
JRP6244	CGGGATCCCCCATCTCCTTATTTTCTTATG	LHS *pcw321* DCO plus BamHI, F
JRP6245	CGGGATCCTTTTCTCACTCCCTTTTATTGTTG	LHS *pcw322* DCO plus BamHI, F
JRP6246	CGGGATCCAATTGACACCTAAACTGCTATATTATTAAAG	LHS *srtD* DCO plus BamHI, F

JRP6247	CGGGATCCTTATTTCCTCCTATTTTATTTTAAGTACC	LHS *tcpN 4* DCO plus BamHI, F
JRP6248	CGGGATCCATCTTATCTCTCCTTTCTTTTTAAC	LHS *pcw325* DCO plus BamHI, F
JRP6249	CCGAGCTCGTTTATTGAACCTATCTTCTGC	RHS DCO plus SacI, R
JRP6250	CCGCTCGAGTGAGAAAAATGAGTGAAAC	RHS *pcw321* DCO plus XhoI, F
JRP6251	CCGCTCGAGTGTCAATTATGATGAAGAAAGG	RHS *pcw322* DCO plus XhoI, F
JRP6252	CCGCTCGAGGAAATAAATGTGTATGAATAAGAATAC	RHS *srtD* DCO plus XhoI, F
JRP6253	CCGCTCGAGATATGGGATTTAGTTTAAGAAAG	RHS *tcpN* DCO plus XhoI, F
JRP6254	CCGCTCGAGAATAATCATATAAAACGAGTTGTTCTCC	RHS *pcw325* DCO plus XhoI, F
JRP6372	CCTGCAGAGGTGTCAATTATGATGAAGAAAGG	*srtD* complementation plus PstI, F
JRP6373	CGGGATCCTCCTATTTTATTTTAAGTACCAAG	*srtD* complementation plus BamHI, RT-PCR, R
JRP6374	CCTGCAGAGGAGGAAATAAATGTGTATGAATAAG	*tcpN* complementation plus PstI, F
JRP6375	CGGGATCCCTTATCTCTCCTTTCTTTTTAAC	*tcpN* complementation plus BamHI, RT-PCR, R
JRP6449	AAACTGCAGTGCCATAAGGTACTCTCTTAAG	*pcw321-25* complementation plus PstI, F
JRP6450	CGGGATCCCATTATTTAAGTTCTTGGAGAACAACTC	*pcw321-25* complementation plus BamHI, R
JRP6451	GGGGTACCGTGCCATAAGGTACTCTCTTAAG	*pcw321-25* complementation plus Asp718, F

F- forward primer, R- reverse primer, DCO-double crossover

Bioinformatic analysis

Sequences for *C. perfringens* plasmids were obtained from GenBank (Benson *et al.*, 2017), with the following ascension numbers: pCW3 (NC_010937), pCPPB-1 (NC_015712.1), pJIR3844 (NC_019257), pJIR3536 (NC_025042), pCPF4969 (NC_007772.1), pJFP838B (KT020842.1), pJFP838C (CP013040.1), pJFP838D (CP013039), pCFP5603 (AB236337.1) and pCFP4969 (AB236336.1).

Sequences were analysed using BLAST (Altschul *et al.*, 1990) and predicted homology to proteins within the conserved domains database (Marchler-Bauer *et al.*, 2015). Signal peptides were predicted using Signal P 4.1 server (Petersen *et al.*, 2011). Potential transmembrane domains were predicted using TMHMM Server v 2.0 (http://www.cbs.dtu.dk/services/TMHMM/). Predicted protein molecular weights were determined by using ExPasy Compute pI/Mw tool (Artimo *et al.*, 2012). Multiple sequence alignments and percent identity matrices were generated using Clustal Omega (McWilliam *et al.*, 2013). Sequence homology between pCW3-like plasmids and graphics were produced using Easyfig (Sullivan *et al.*, 2011).

For the phylogenetic analysis of sortase enzymes, the list of sortase sequences was taken from (Spirig *et al.*, 2011) and translated protein sequences were obtained from the NCBI database. Bacterial species names and associated protein accession numbers are as outlined in Table 2.3. Sequences were aligned using Clustal Omega and phylogeny inferred (McWilliam *et al.*, 2013). Inferred phylogeny was visualised as a radial unrooted phylogram using FigTree (available for download at: https://github.com/rambaut/figtree).

Table 2.3: Organisms and sortase accession numbers used for phylogenetic analysis

Organism	Accession number(s)
Actinomyces naeslundii	AAC13546
Bacillus anthracis	NP_847260; NP_843215; NP_846988
Bacillus cereus	NP_834511; NP_830752; NP_830495; NP_834250; NP_832268
Bacillus halodurans	NP_244463; NP_244878; NP_244160
Bacillus subtilis	NP_388801
Bifidobacterium longum	NP_695779
Clostridium botulinum	YP_001254630
Clostridium difficile	YP_001089230
Clostridium perfringens	YP_001967764.1, BAB79928.1, BAB78963.1, BAB80219.1, BAB82021.1
Corynebacterium diphtheriae	NP_940343, NP_940532, NP_940531, NP_938627, NP_940575, NP_938624
Corynebacterium glutamicum	NP_602126
Geobacillus sp.	YP_003672707
Listeria innocua	NP_470268; NP_471617
Listeria monocytogenes	NP_464454; NP_465705
Oceanobacillus iheyensis	NP_691253; NP_694114
Ruminococcus albus	ZP_06717336
Streptomyces avermitilis	NP_826393; NP_827770; NP_826840; NP_828474; NP_821266; NP_825513; NP_825514; NP_826383; NP_825510
Streptomyces coelicolor	NP_628037; NP_628038; NP_627928; NP_631498; NP_626722; NP_625233; NP_627070
Streptomyces griseus	YP_001825232; YP_001825235; YP_001826193; YP_001825236
Staphylococcus aureus	NP_375640; NP_374252
Staphylococcus epidermis	NP_765631
Streptococcus agalactiae	NP_687667; NP_687668; NP_687670; NP_688403; NP_688404
Streptococcus equi	YP_002746265
Streptococcus gordonii	YP_001450517
Streptococcus pyogenes	NP_802272; NP_801365
Tropheryma whipplei	NP_787692

Construction of mutants

The pCW3 genes *pcw321, pcw322, srtD, tcpN* and *pcw325* were replaced with an *erm*(Q) cassette using allelic exchange. Approximately 2 kb of upstream and downstream flanking regions for each gene were cloned into the *C. perfringens* suicide vector pJIR2715, on either side of the *erm*(Q) gene. For example, a 1556 bp fragment encompassing the 20046-21601 bp region from pCW3 was cloned into BamHI and SphI sites upstream of *erm*(Q), and a 2821 bp fragment from 21739-24559 bp was cloned into the XhoI and SacI sites downstream of *erm*(Q), to generate the *pcw321* suicide vector, pJIR4508. Other mutants were constructed in a similar manner, see Table 2.1 for specific plasmid constructs.

The suicide vectors were introduced independently into the *C. perfringens* strain JIR13224 by electroporation (Scott & Rood, 1989). To identify potential double crossover mutants, the resultant transformants were plated onto NA containing Em and Tc and cross-patched onto NA supplemented with Tm. The required mutants would be Tc^R, due to the inherent tetracycline resistance of pCW3, and both Em^R and Tm^S, due to the incorporation of the *erm*(Q) cassette into pCW3 as well as loss of the suicide vector. DNA preparations from Em^R Tm^S colonies were tested by PCR to confirm deletion of the target gene with the insertion of the *erm*(Q) cassette and the loss of the suicide plasmid. Southern blotting was used to confirm the resultant independent *srtA* and *tcpN* mutants.

Complementation of mutants

For complementation, PCR fragments containing the wild type *srtD* and *tcpN* genes were amplified by PCR and subsequently cloned into the cloning vector, pT7-Blue, as per the manufacturer's instructions (Novagen), generating pJIR4545 and pJIR4546, respectively. BamHI and Asp718 digested fragments containing *srtD* and *tcpN* from pJIR4545 and pJIR4546 were subcloned into the BamHI and Asp718 sites of the *E. coli-C. perfringens* shuttle vector pJIR3422,

where their expression would be under the control of the P_{attCI} promoter (Adams *et al.*, 2014), to generate pJIR4547 and pJIR4548, respectively.

For complementation with both the *srtD* and *tcpN* genes, a 970 bp fragment encoding wild type *srtD* and *tcpN* was generated by PCR and cloned into the PstI and BamHI sites of pJIR3422, to generate pJIR4584. For complementation with the entire genetic region spanning from *pcw321* to *pcw325*, a PCR fragment encompassing this region was generated and cloned into the PstI and BamHI sites of pJIR3422 to generate pJIR4587. All complementation vectors were confirmed by restriction analysis and sequencing.

Complementation vectors were introduced into respective mutant strains *via* electroporation and transformants selected for on NA with Em and Tm. The presence of the complementation plasmids was confirmed by restriction analysis and sequencing following plasmid rescue in *E. coli.*

For unmarked complementation *in cis*, to reverse the original mutation, a mutagenesis plasmid was constructed by cloning a 1688 bp PCR fragment encompassing *pcw321* through to *pcw325* into the BamHI and Asp718 sites of pJIR3566 to produce pJIR4586. The mutagenesis plasmid was introduced separately into the *srtD* and *tcpN* mutants *via* electroporation. Transformants were selected on NA with Tm, to select for transformants with the mutagenesis plasmid. Subsequent transformants were cross-patched onto NA with Tc, to select for the pCW3 plasmid, and NA with Em, to identify strains that no longer possess the *erm*(Q) gene and NA with Tm to detect the presence of the mutagenesis plasmid. The predicted restored mutant strains would be Tc^R, due to the inherent tetracycline resistance of pCW3, and both Tm^S and Em^S, due to loss of the *erm*(Q) cassette from pCW3 as well as loss of the knock-in vector.

Conjugation assays

Conjugative matings were conducted on solid media as previously described (Rood *et al.*, 1978a, Rood, 1983) with minor alterations. Briefly, short conjugation assays were plated onto thick HI

media and incubated at 37°C for four-hours, scraped from the plates using HI diluent and plated out to select for transconjugants as previously described (Rood *et al.*, 1978a, Rood, 1983). Overnight assays were conducted as previously described. The transfer frequency is defined as the number of transconjugants per donor cell.

Intrastrain matings were conducted using derivatives of JIR13224. A spontaneous Sm^R Chl^R derivative of strain 13, JIR4394, was used as a recipient. Transconjugants were selected for on NA with Str, Chl and Tc.

Interstrain matings were conducted using the same donor strains. A spontaneous Sm^R Chl^R resistant derivative of the *C. perfringens* strain CW362, JIR39 (Rood, 1983), was used as a recipient. Transconjugants were selected on NA supplemented with Str, Chl and Tc.

Statistical analysis was performed using a Mann-Whitney *u*-test on transfer frequencies, with statistical significance defined as $p < 0.05$.

Reverse Transcription- PCR (RT-PCR)

RNA was isolated using a modified and optimised TriZol extraction method, as described previously (Cheung & Rood, 2000, La Fontaine & Rood, 1996). Following Turbo DNase treatment, PCR was used to check for DNA contamination. RNA integrity was analysed by agarose gel electrophoresis on a 1% (w/v) agarose gel. RNA concentration and purity were determined by analysing samples on a NanoDrop™ spectrophotometer (Thermo Scientific) measuring absorbance at 260nm and noting the $OD_{260/280}$ ratio. A ratio value of 1.8-2.2 was considered to be high-quality RNA (Farrell Jr, 2010).

For RT-PCR, 200ng of total RNA was converted to cDNA using 100ng of random primers (Promega) and Avian Myeloblastosis Virus Reverse Transcriptase (AMV; Promega). Reactions with and without AMV-Reverse Transcriptase were performed simultaneously. PCR samples were set up to contain 5 µg of cDNA with gene specific primers at 520 nM.

Complementation vector stability assay

Complementation vector stability assays were performed on solid media as described for the conjugation assays. To assess complementation vector stability, samples were taken from overnight selection plates prior to FTG inoculation, following FTG incubation and following incubation on HI agar for either 4 or 12 hours. Samples were serially diluted and plated onto non-selective NA. Single colonies were patched onto NA and on NA with Tm; the latter was used to detect the presence of the complementation vector. Vector stability was determined by comparing the number of viable patches on NA Tm to those on NA alone.

pCW3 stability assay

To determine the stability of the wild-type and mutant plasmids, each strain was passaged continuously over the course of six days in HI broth. Pure cultures of each strain were obtained on NA supplemented with appropriate antibiotics and incubated anaerobically at 37°C overnight. On day 0, a smear was taken from the pure culture selection plates and resuspended in 500 µl of HI diluent (HI Broth (Oxoid) diluted 1:10). Samples (100 µl) were used to inoculate 20 mL of HI broth, which were incubated at 37°C for 6-8 hours. Following incubation, 100 µl of HI broth culture was used to inoculate fresh HI medium, which was incubated at 37°C overnight. Passaging was repeated continuously over the course of six days. For viable counts, a cell suspension of an overnight broth culture was serially diluted and 100 µl plated onto non-selective media and incubated anaerobically at 37°C overnight. Resultant colonies were cross-patched onto media containing Tc to detect the presence of pCW3. Viable counts were plated every second day (0, 2, 4 6) and plasmid stability was determined by comparing viable patches on media with and without Tc. Statistical analysis was performed on data obtained on a single day (either 0, 2, 4 or 6) and performing Mann-Whitney *u*-tests with statistical significance defined as $p < 0.05$.

Results

Updated bioinformatic analysis of the uncharacterised CnaC region of pCW3

Initial annotation of pCW3 (Bannam *et al.*, 2006) did not provide much insight into the potential function of the products encoded within the CnaC region (Figure 2.1B), but this analysis was carried out over 12 years ago. Therefore, it was decided to reanalyse the putative protein products encoded within this genetic region using BLASTp (Table 2.4).

BLAST analysis of ORFs within the CnaC region did not provide any further insight into the potential function of these genes; no new domains were identified, with the exception of a DUF4236 domain (domain of unknown function) present in the putative PCW325 protein. Proteins that contain DUF4236 domains are present in both bacteria and viruses, however, this family of proteins remains to be functionally characterised (Marchler-Bauer *et al.*, 2017).

The only other additional information gained from BLAST analysis of the CnaC region was the re-classification of the pCW3-encoded sortase. Previously annotated as encoding a class A sortase, the gene, previously designated as *srtA,* is now predicted to encode a subfamily 2 class D sortase enzyme, prompting a name change to *srtD* (YP_001967764.1).

To confirm the reclassification of this sortase, phylogenetic analysis was performed to compare the pCW3-encoded sortase with sortases from different classes. A reference library of sortase sequences, representative of all six classes (Spirig *et al.*, 2011), was analysed using multiple sequence alignment and subsequent phylogenetic analysis (Figure 2.2). As predicted, the pCW3-encoded sortase clustered amongst other class D sortases, within a subfamily that only included *C. perfringens* encoded sortases. This analysis confirmed the re-classification of the pCW3 encoded sortase as SrtD; terminology that will be used throughout this thesis.

Table 2.4: Summary of predicted genes within the CnaC region.

					pCW3-like plasmid homologues (AA Identity)								
pCW3 Gene	**MW (kDa)**	**SP**	**TMD**	**Predicted Function**	**pJIR3844**	**pJIR3536**	**pJIR838B**	**pJIR838C**	**pJIR838D**	**pCPPB-1**	**pCP8533*etx***	**pCPF4969**	**pCPF5603**
cnaC	132.5	Y	2 (AA 7-29) (AA 1158 – 1187)	Thioester-forming surface anchored protein, thioester domain, collagen binding domains	57.8%	99.6% 99.1%	99.2%	63.2%	97.8%	96.6%	98.7%	98.9%	99.1%
pcw321	5	N	1 (AA 2-21)	Unknown	90.5%	100%	100%	100%	100%	100%	97.6%	97.6%	97.6%
pcw322	10.5	N	0	Unknown	97.7%	100%	97.7%	98.8%	97.7%	97.7%	97.7%	97.7%	96.5%
srtD	24.3	N	1 (AA 5-23)	Subfamily 2 Class D sortase	92.2%	92.2%	96.7%	93.9%	99.5%	96.2%	98.1%	98.1%	96.7%
tcpN	11.9	N	0	Unknown	95%	100%	99%	98%	100%	98%	98%	99%	99%
pcw325	7.8	N	0	Unknown, DUF4236 domain	98.6%	100%	100%	98.6%	100%	96.8%	97.2%	98.6%	90.3%
dam	30	N	0	DNA adenine methyltransferase	98.0%	96.9%	97.6%	98.7%	97.6%	97.2%	97.2%	97.6%	97.6%

MW refers to molecular weight in kDa, SP refers to signal peptide, Y is yes, N is no, TMD refers to putative transmembrane domains and AA refers to amino acid.

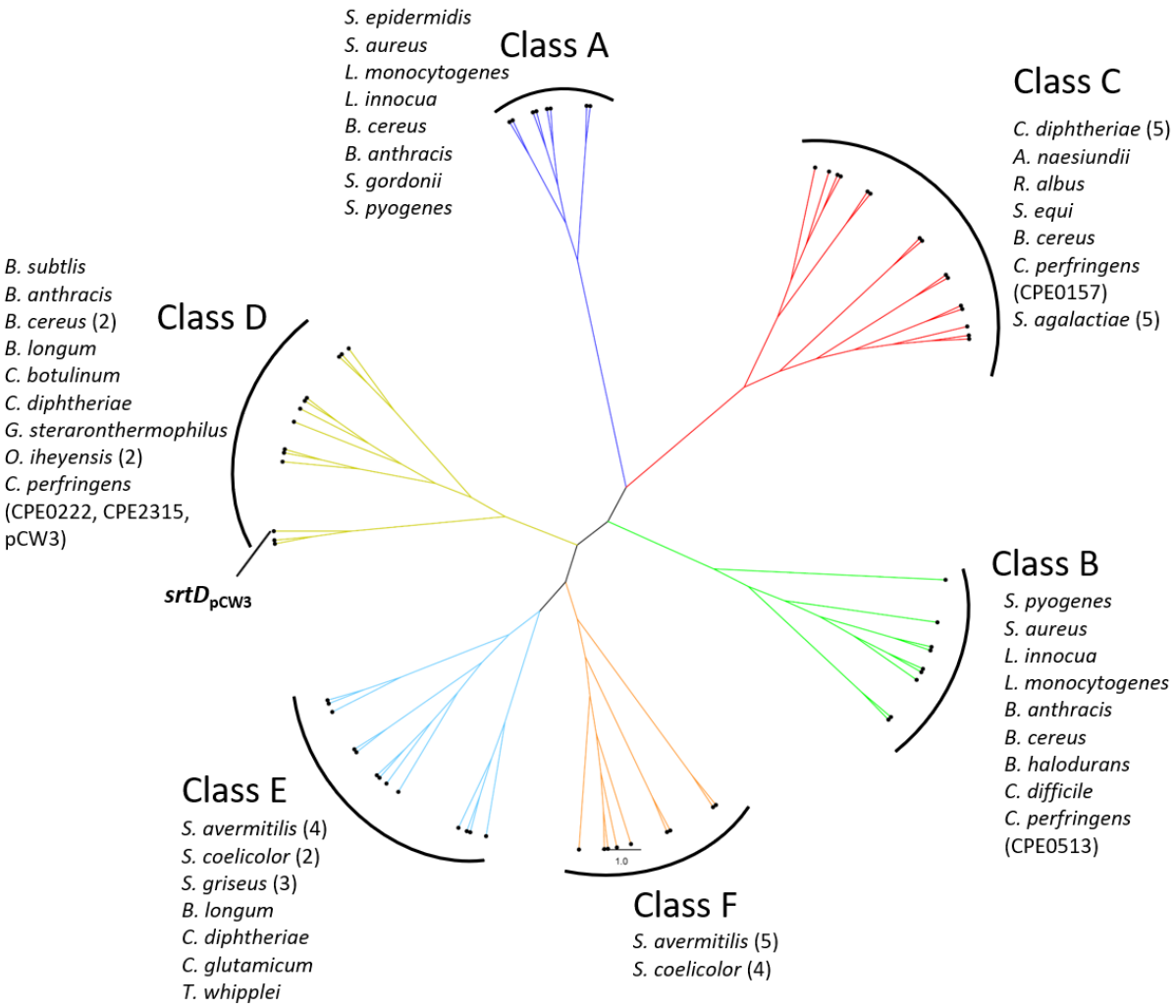

Figure 2.2: Phylogenetic tree showing the clustering of the six classes of sortases. A multiple sequence alignment using Clustal Omega was performed with sequences of 64 sortase proteins from different organisms. A phylogenetic tree was generated using the neighbour joining method and visualised as an unrooted phylogram using FigTree. The clades have been coloured based on sortase class groupings as indicated: A is blue, B is green, C is red, D is yellow, E is light blue and class F is orange. The branch and node representing the pCW3 encoded SrtD is indicated by a thick black line and labelled. The name of the bacterial species of the associated sortases are listed alongside the class names. Accession numbers of proteins analysed are listed in Materials and Methods.

Potential transmembrane domains were predicted within the products of *pcw321* and the *srtD* genes. Whilst the function of transmembrane domain in *pcw321* remains unknown, the presence of an N-terminal transmembrane domain within the predicted sortase enzyme agrees with the current understanding of sortase enzyme topology, whereby many sortase enzymes are membrane associated (Spirig *et al.*, 2011).

The CnaC region is highly conserved amongst the Tcp plasmids

To determine the level of conservation of the CnaC region amongst other pCW3-like plasmids the genetic profiles of nine pCW3-like plasmids were investigated by comparing genes located within the conserved regions of interest to the reference plasmid pCW3 (Table 2.4). Analysis was carried out using BLAST and multiple sequence alignments and visualised using EasyFig (Artimo *et al.*, 2012). The results showed that the CnaC region was highly conserved, as homologues of the genes *pcw321* through to *pcw325* were present on all plasmids analysed (Figure 2.3).

The genetic organisation of the CnaC region differs only slightly, with the addition of a small ORF between *pcw322* and *srtD* on pJFP838B, pJFP838C, pJIF3844 and pCP8533etx. A conserved sequence related to this ORF is found on pCPF5603, but it does not possess a start codon. This ORF encodes a small hypothetical protein that is also encoded on other Tcp plasmids pDel1_2 and pFORC.

Most variation within this region occurs within the *cnaC* gene product. CnaC ranges from 451 amino acids on pJIR3536 to 1187 AA on pCW3. Additionally, the *cnaC* from pCPPB-1 and pJIR3536 have premature stop codons, truncating the translated CnaC products. This analysis highlights that there may be multiple families of CnaC proteins, with those encoded on pJIR3844 and pJFP838C differing greatly from those encoded on the other pCW3-like plasmids analysed. Indeed, when assessed phylogenetically, the CnaC proteins from pJIR3844 and pJFP838C form a distinct clade, grouping closer to CnaB encoded on the unrelated plasmid pCP13 (Figure 2.4).

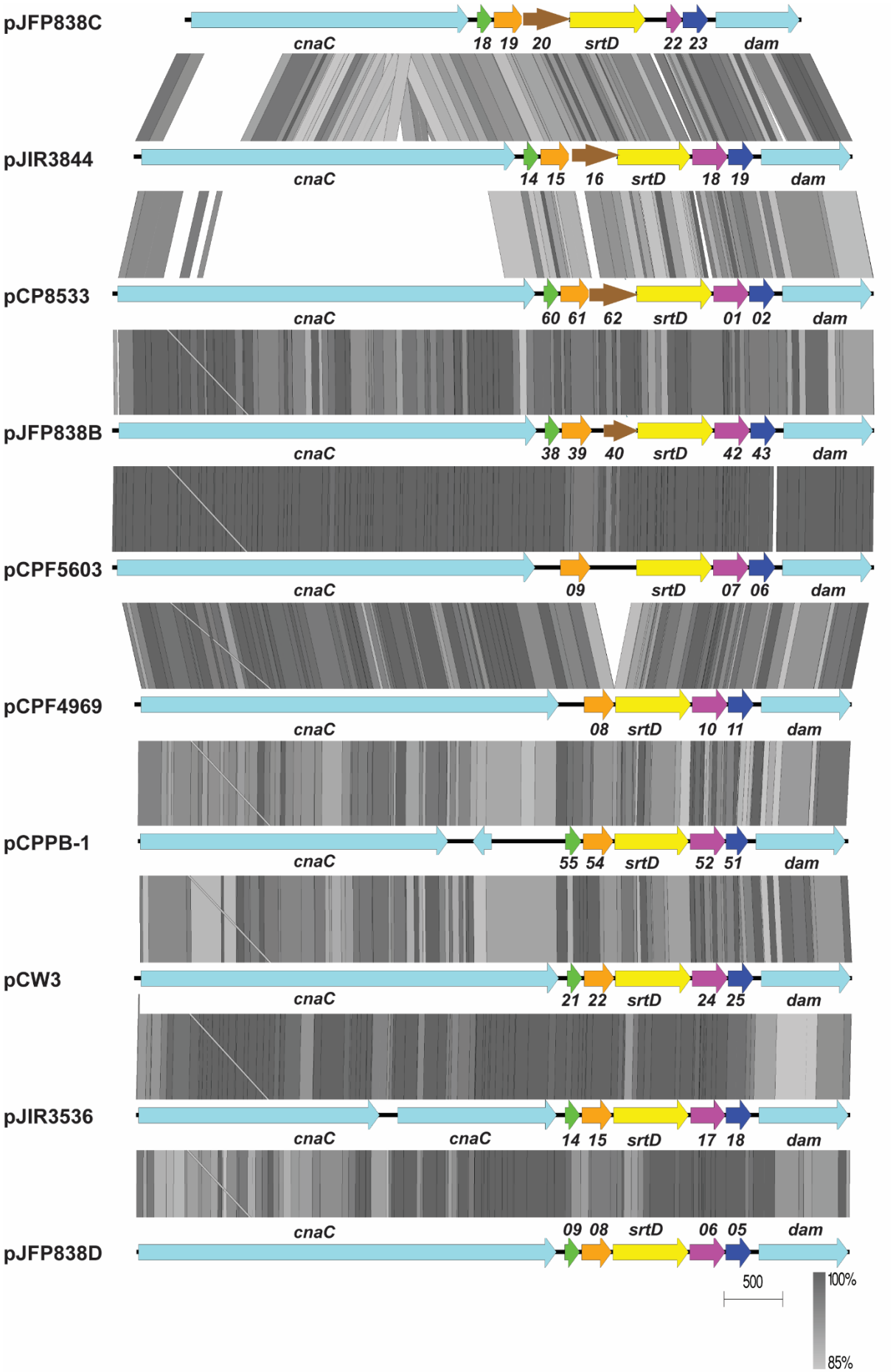
pJFP838C
cnaC
18 19 20
srtD
22 23
dam
pJIR3844
cnaC
14 15 16
srtD
18 19
dam
pCP8533
cnaC
60 61 62
srtD
01 02
dam
pJFP838B
cnaC
38 39 40
srtD
42 43
dam
pCPF5603
cnaC
09
srtD
07 06
dam
pCPF4969
cnaC
08
srtD
10 11
dam
pCPPB-1
cnaC
55 54
srtD
52 51
dam
pCW3
cnaC
21 22
srtD
24 25
dam
pJIR3536
cnaC
cnaC
14 15
srtD
17 18
dam
pJFP838D
cnaC
09 08
srtD
06 05
dam
500
100%
85%

Figure 2.3: Comparison of CnaC regions from ten pCW3-like plasmids. Shown are tBLASTx (Altschul *et al.*, 1990) alignments of the CnaC regions from ten Tcp plasmids, named beside the corresponding sequence in the figure. ORFs are coloured according to pCW3 gene homologue: *pcw321* in green, *pcw322* in orange, *srtD* in yellow, *pcw324* (*tcpN*) in pink and *pcw325* in dark blue. Other ORFs are labelled in light blue with the exception of a small ORF between *pcw322* and *srtD* on pJFP838B, pJFP838C, pJIF3844 and pCP8533etx which is coloured brown. Regions of amino acid sequence identity are represented by the grey bars. The amino acid sequence identity cut off was 85%, with a maximum e-value of 0.001. The intensity of grey colour represents the level of identity between sequences directly above and below as shown.

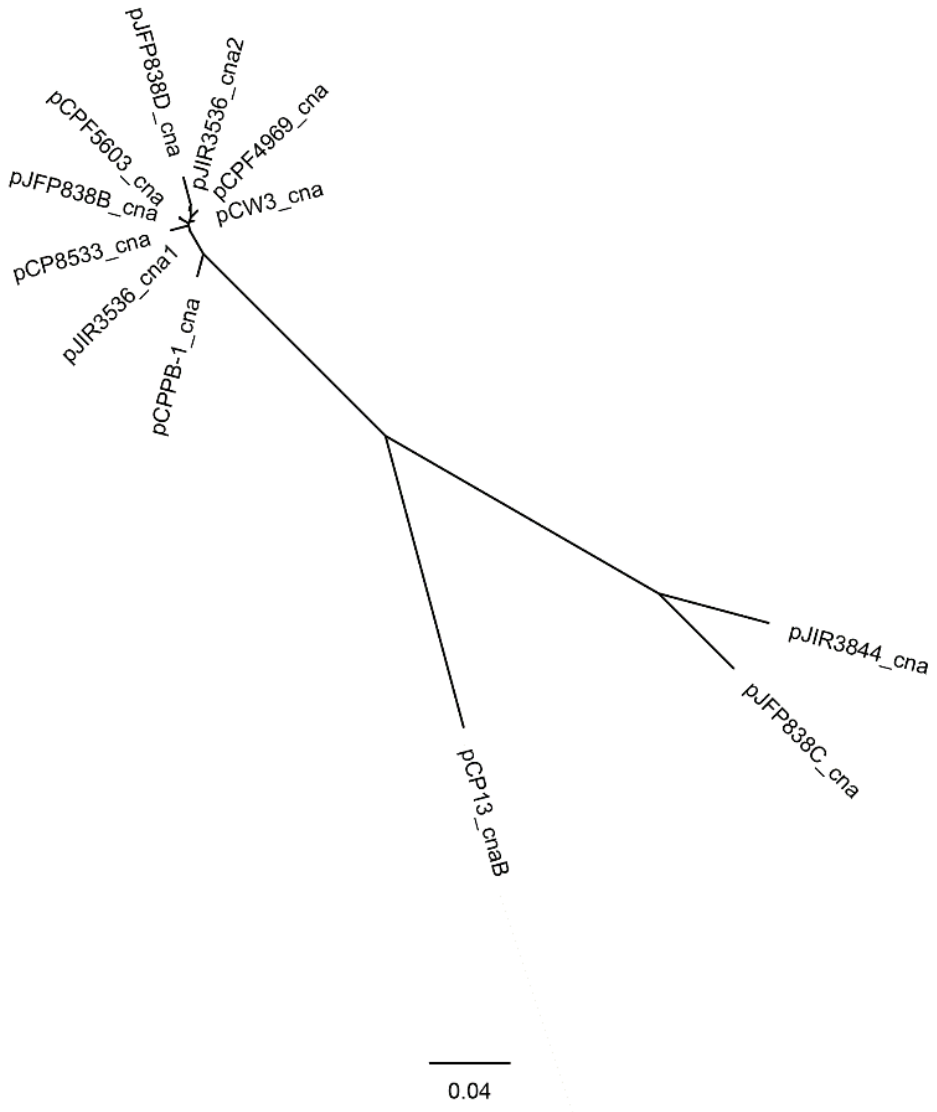

Figure 2.4: Phylogenetic analysis of CnaC proteins from eleven *C. perfringens* plasmids. A multiple sequence alignment using Clustal Omega was performed with ten CnaC proteins from various *C. perfringens* plasmids. A phylogenetic tree was generated using the neighbour joining method and visualised as an unrooted phylogram using FigTree. Plasmid names and accession numbers of proteins analysed are as follows: pCW3_cna (YP_001967761.1), pCP13_cna (NP_150050.1), pJIR3536 (WP_110439920.1), pJIR3844_cna (YP_006961226.1), pCPPB-1_cna (YP_007078907.1), pCP8533etx (YP_002291145.1), pJFP838B_cna (ALD82571.1), pJFP838C_cna (AMN30599.1), pJFP838D_cna (AMN30533.1), pCPF5603_cna (YP_473433.1) and pCPF4969_cna (YP_473370.1).

Finally, the genetic context of the CnaC region remains unchanged on all of the plasmids analysed; it was always located upstream of the *tcp* locus and directly downstream of a *pemK*-like gene. As this locus is highly conserved and present upstream of the conjugation *tcp* locus, it was postulated that the gene products encoded within this genetic region may play important roles in plasmid conjugative transfer.

Construction of mutants in the conserved CnaC region of pCW3

Conserved genes within the CnaC region of pCW3 were selected for mutant construction, Previous work has determined the involvement of the putative collagen adhesin protein CnaC in pCW3 conjugation (S. Revitt-Mills, V. Adams and J. Rood, unpublished), establishing its requirement for effective interstrain transfer of pCW3 and thus it was not included in this analysis. To investigate the role of the genes within this region, deletion mutants were constructed independently using allelic exchange, replacing the gene of interest with the *erm*(Q) gene, which encodes erythromycin resistance (Figure 2.5). Suicide vectors were constructed independently for each gene of interest, as outlined in the Materials and Methods. Following construction and confirmation by restriction analysis and sequencing (data not shown), the vectors were independently introduced into *C. perfringens* strain JIR13224, which contained wild-type pCW3. Potential mutants with the correct resistance profiles were obtained and the genotypes confirmed by PCR. The confirmation PCRs were performed on genomic DNA preparations using two primer pairs that would amplify products only when the gene of interest had been replaced with *erm*(Q). To confirm the loss of the suicide vector, a *catP* specific PCR was also performed. A representative example of the PCR results obtained for independent *pcw322* mutants is shown in Figure 2.6. All other mutant strains were confirmed by PCR (data not shown). Additionally, independent *srtD* and *tcpN* mutants also were confirmed by Southern blotting (Figure 2.7).

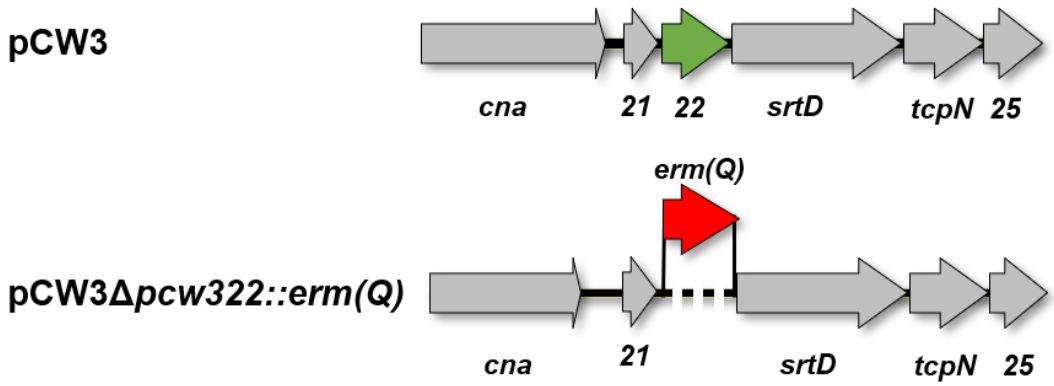

Figure 2.5: Diagram of the *pcw322* deletion mutant derived from a double crossover event.

A portion of the CnaC region from wild type (pCW3) and pCW3*Δpcw322::erm*(Q) mutant is shown. In the mutant, the entire *pcw321* gene (green) is replaced with the *erm*(Q) gene (red).

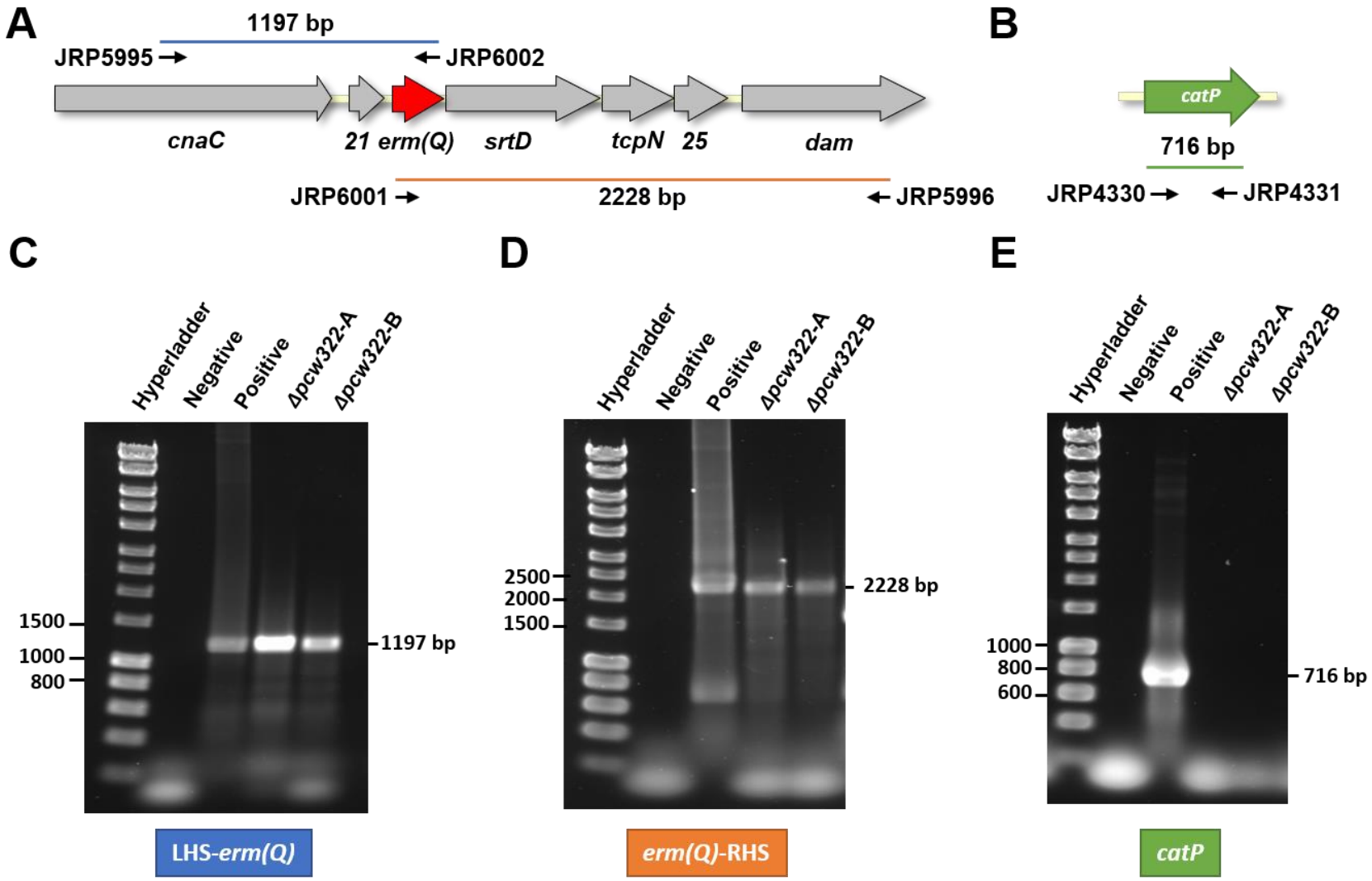
A
1197 bp
JRP5995
JRP6002
cnaC
21 erm(Q)
srtD
tcpN
25
dam
JRP6001
2228 bp
JRP5996
B
catP
716 bp
JRP4330
JRP4331
C
Hyperladder
Negative
Positive
Δpcw322-A
Δpcw322-B
1500
1000
800
1197 bp
LHS-erm(Q)
D
Hyperladder
Negative
Positive
Δpcw322-A
Δpcw322-B
2500
2000
1500
2228 bp
erm(Q)-RHS
E
Hyperladder
Negative
Positive
Δpcw322-A
Δpcw322-B
1000
800
600
716 bp
catP

Figure 2.6: PCR confirmation of pCW3Δ*pcw322::erm*(Q) mutant. A. A diagram of a portion of the CnaC region of the pCW3Δ*pcw322::erm*(Q) mutant is shown with primers used for PCR confirmation. Genes of interest are represented by the thick arrows. Primer positions are indicated by the short black arrows and are labelled alongside. The size of the expected products in base pairs (bp) are labelled above the corresponding coloured line. Genomic DNA was extracted from potential mutants (*Δpcw322*-A and *Δpcw322*-B) and the replacement of *pcw322* with *erm*(Q) was confirmed by two PCRs, using a primer specific for *erm*(Q) and an appropriate primer flanking the gene of interest: LHS- *erm*(Q) (indicated by the blue line) and *erm*(Q)-RHS (indicated by the orange line). **B.** Schematic representation of the *catP* gene is shown with primers used for PCR confirmation. The absence of the double crossover vector was determined using a primer pair specific for *catP,* which should not produce a product in a correct double crossover mutant **C.** PCR analysis of potential *pcw322* mutants using a LHS flanking primer and an *erm*(Q) specific primer. For correct mutants, a product of 1197 bp is expected. **D.** PCR analysis of potential *pcw322* mutants using an *erm*(Q) specific primer and a RHS flanking primer. For correct mutants, a product of 2228 bp is expected. **E.** PCR analysis of potential *pcw322* mutants using a *catP* specific primer pair, correct mutants should not produce a product. For all reactions, the positive control used was the *pcw321* specific suicide plasmid, pJIR4508, as template and the negative control did not have any template in the reaction. Hyperladder I DNA standards (Bioline) were used as a size standard.

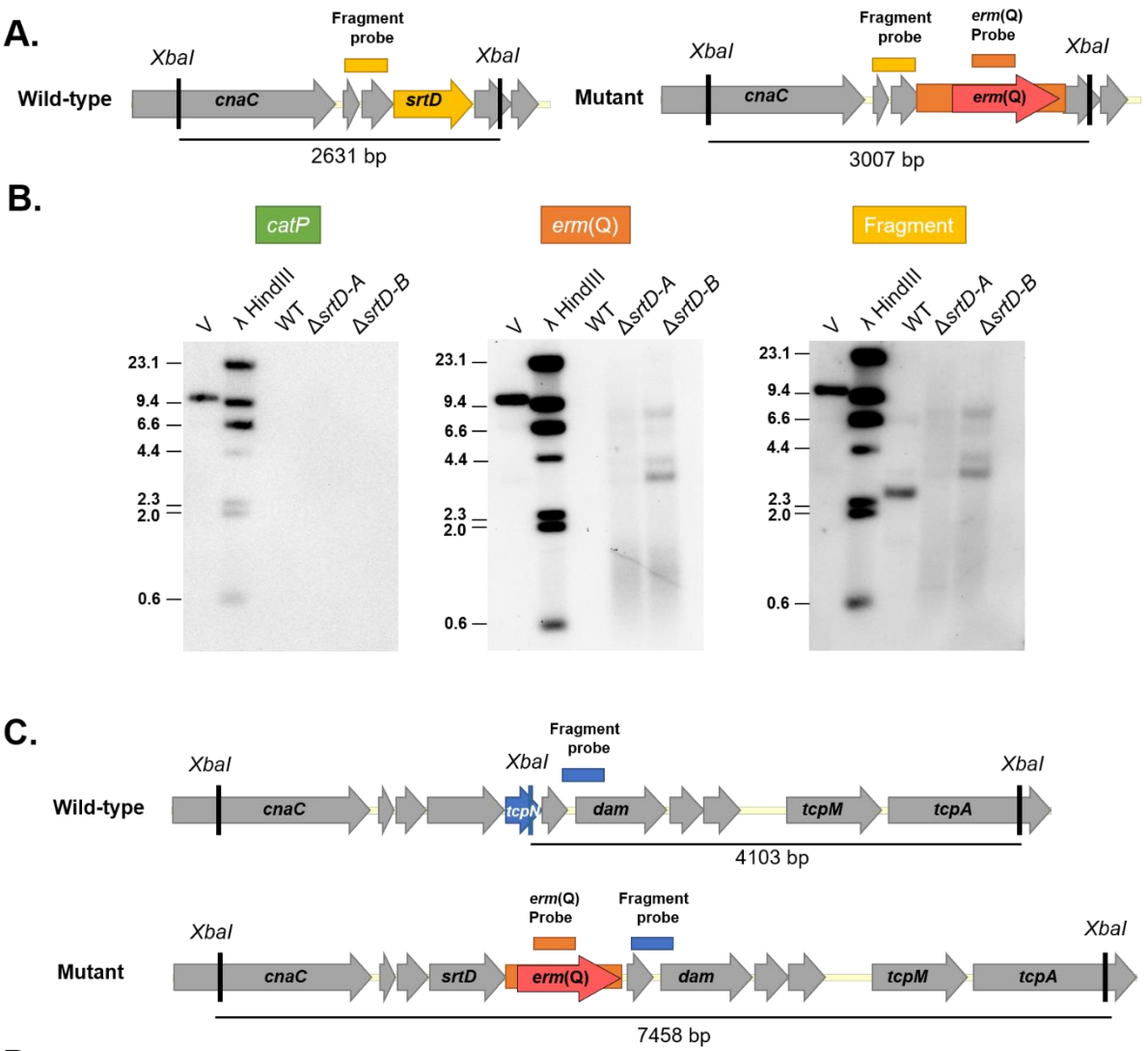
A.
Wild-type
XbaI
Fragment probe
cnaC
srtD
XbaI
2631 bp
Mutant
XbaI
Fragment probe
erm(Q) Probe
cnaC
erm(Q)
XbaI
3007 bp
B.
catP
erm(Q)
Fragment
V
λ HindIII
WT
ΔsrtD-A
ΔsrtD-B
23.1
9.4
6.6
4.4
2.3
2.0
0.6
C.
Wild-type
XbaI
Fragment probe
cnaC
tcpN
dam
tcpM
tcpA
4103 bp
Mutant
erm(Q) Probe
Fragment probe
srtD
erm(Q)
7458 bp
D.
catP
erm(Q)
Fragment
V
λ HindIII
WT
ΔtcpN-A
ΔtcpN-B

Figure 2.7: Confirmation of *srtD* and *tcpN* mutants by Southern. Genomic DNA was purified and digested with the enzyme XbaI. The Southern blots were probed with DIG-labelled DNA probes specific for *catP*, carried on the double-crossover vector backbone; *erm*(Q), located within the double crossover selection cassette, and a fragment of DNA adjacent to or containing the gene of interest. **A.** Schematic representation of wild-type and *srtD* mutant DNA fragments digested with XbaI. **B.** Confirmation of independent *srtD* mutants. Lanes are labelled as follows: V – XbaI-digested gene specific double crossover vector, λ HindIII- DIG-labelled λ HindIII molecular size markers (kilobases), WT- wild type *C. perfringens* JIR13224 DNA. The double crossover site is present on a fragment of 2631 bp for the wild type and 3007 bp for the mutant. Incomplete digestion has occurred and fragments of 3715 bp, 5524 bp, and 7110 bp were also detected. These are consistent with incomplete digest products predicted to be formed from this genetic region. **C.** Schematic representation of wild type and *tcpN* mutant DNA fragments digested with XbaI. **D.** Confirmation of independent *tcpN* mutants. The double crossover site is present on a fragment of 4103 bp for the wild type and 7458 bp for the mutant.

Mutation of *srtD* and *tcpN* decreased intrastrain conjugative transfer of pCW3.

Independent *pcw321, pcw322, srtD, tcpN* and *pcw325* mutants initially were assessed for their conjugative ability in four-hour mating experiments (Figure 2.8A). These intrastrain experiments were performed using genetically marked, isogenic strain 13 derivative for both the donor and recipient strains.

Mutation of *pcw321, pcw322* and *pcw325* did not have any significant effect on conjugation efficiency, with plasmid transfer occurring at levels similar to wild type pCW3. However, the *srtD* and *tcpN* mutants displayed five orders of magnitude reduction in conjugation efficiency in comparison to wild-type transfer. This finding suggests that the products of these genes are required for efficient transfer of pCW3. Thus, the gene *pcw324* was renamed *tcpN* as it is postulated to be a component of the Tcp conjugation system.

To assess if the transfer of *srtD* and *tcpN* mutants were still defective in a longer saturated mating, overnight mating assays were conducted (Figure 2.8B). Similar to what was observed in the four-hour assays, the independently derived *srtD* and *tcpN* mutants displayed a three order of magnitude reduction in conjugation efficiency in comparison to wild type, at a statistically significant level ($p \leq 0.03$), further supporting the notion that pCW3 requires these gene products for efficient conjugation.

Interstrain transfer of pCW3 is reduced by deletion of *srtD* and *tcpN*

The CnaC region mutants were then assessed using an interstrain mating; that is a mating between two different *C. perfringens* strain backgrounds. DNA transfer often occurs more efficiently between isogenic donor and recipient cells, as was demonstrated by (Rood, 1983), who reported up to a 5-log increase in mating frequency when an isogenic recipient of *C. perfringens* was used for mating assays. For this current study, the use of recipient cells from a different strain background was used to assess if any of these mutations played a role in facilitating efficient

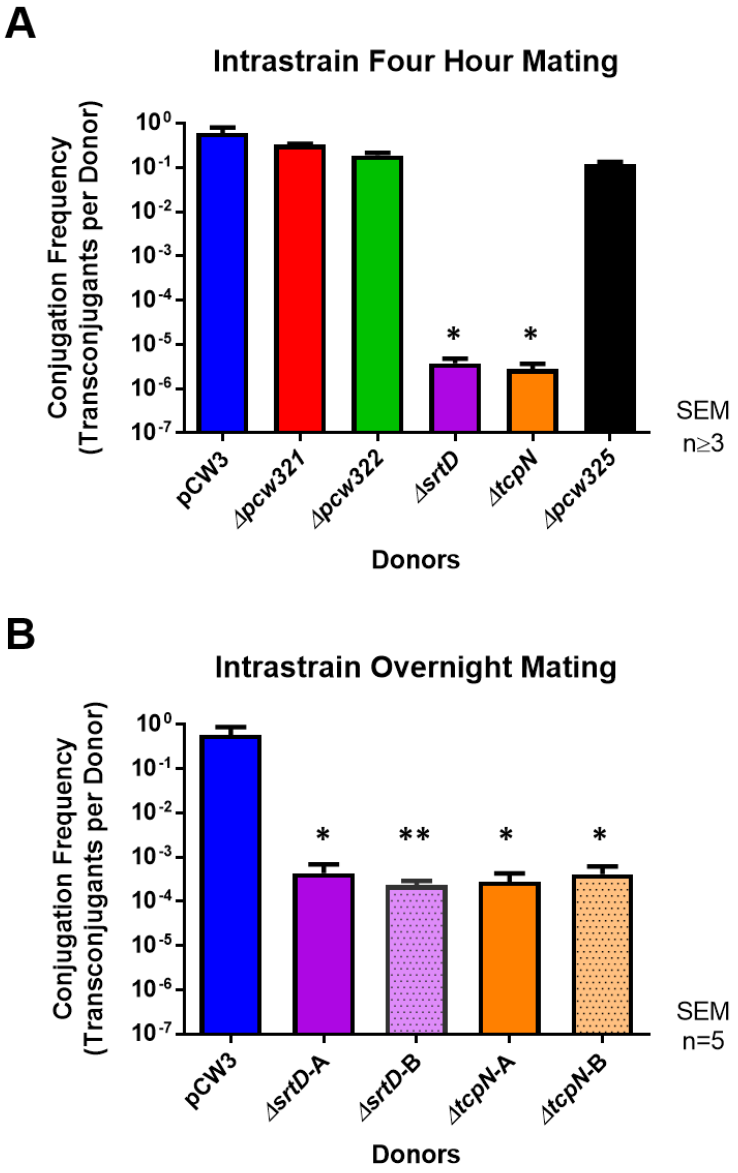

Figure 2.8: Intrastrain conjugation frequencies of independent CnaC region mutants. Mixed plate matings were conducted using JIR13224 derived strains as donors and the isogenic strain 13 derivative, JIR4394, as a recipient. Donor strains are labelled on the X-axis and the wild type strain is denoted as pCW3. The conjugation frequency is defined as the number of transconjugants per donor cell. **A.** Transfer frequencies of the *pcw321, pcw322, srtD, tcpN* and *pcw325* mutants in a four-hour intrastrain mating (n≥3). **B.** Transfer frequencies of independent *srtD* and *tcpN* mutant strains, denoted A and B, in an intrastrain overnight mating (n=5). One asterisk denotes statistical significance of $p<0.03$ and two asterisks denote $p<0.02$ compared to wild-type pCW3 as determined by a Mann-Whitney *u*-test.

transfer between cells of different strain types; a difference that is not observable using the intrastrain mating assay described above.

To conduct interstrain matings the *C. perfringens* strain CW362 derivative, JIR39, was used as a recipient. The mutant panel was first assessed in four-hour mating experiments (Figure 2.9A). A slight reduction in conjugation frequency was observed for the *pcw321*, *pcw322* and *pcw325* mutants, however, these differences were not statistically significant, with p-values of 0.12, 0.06 and 0.2, respectively. By contrast, no transconjugants were obtained for either the *srtD* or *tcpN* mutants in this assay; which highlights the potential importance of these gene products in facilitating interstrain conjugative transfer.

Independent *srtD* and *tcpN* mutants then were tested at conjugative saturation using the JIR39 derivative as a recipient. The *srtD* and *tcpN* mutants transferred at reduced levels after overnight mixed plate matings, roughly six orders of magnitude lower than wild-type transfer (Figure 2.9B).

Complementation *in trans* with the wild-type *srtD* and *tcpN* genes did not restore wild-type conjugative ability

To confirm the involvement of *srtD* and *tcpN* genes in conjugation, efforts were then made to complement the mutant derivatives *in trans*. The wild type *srtD* and *tcpN* genes were cloned independently into the *C. perfringens-E. coli* shuttle vector pJIR3422 (Adams *et al.*, 2014). The resultant plasmids, pJIR4547 and pJIR4549, were introduced into the *srtD* and *tcpN* mutants, respectively. The vector plasmid was introduced into the mutants as a negative control.

Conjugative transfer of the resultant derivatives was assessed in overnight intrastrain conjugation assays (Figure 2.10). All the mating experiments described for the remainder of this thesis were overnight intrastrain assays. The results showed that *in trans* complementation did not restore wild type conjugation efficiency. For both mutants, strains containing the respective complementation vector transferred at a slightly lower frequency to strains containing the empty

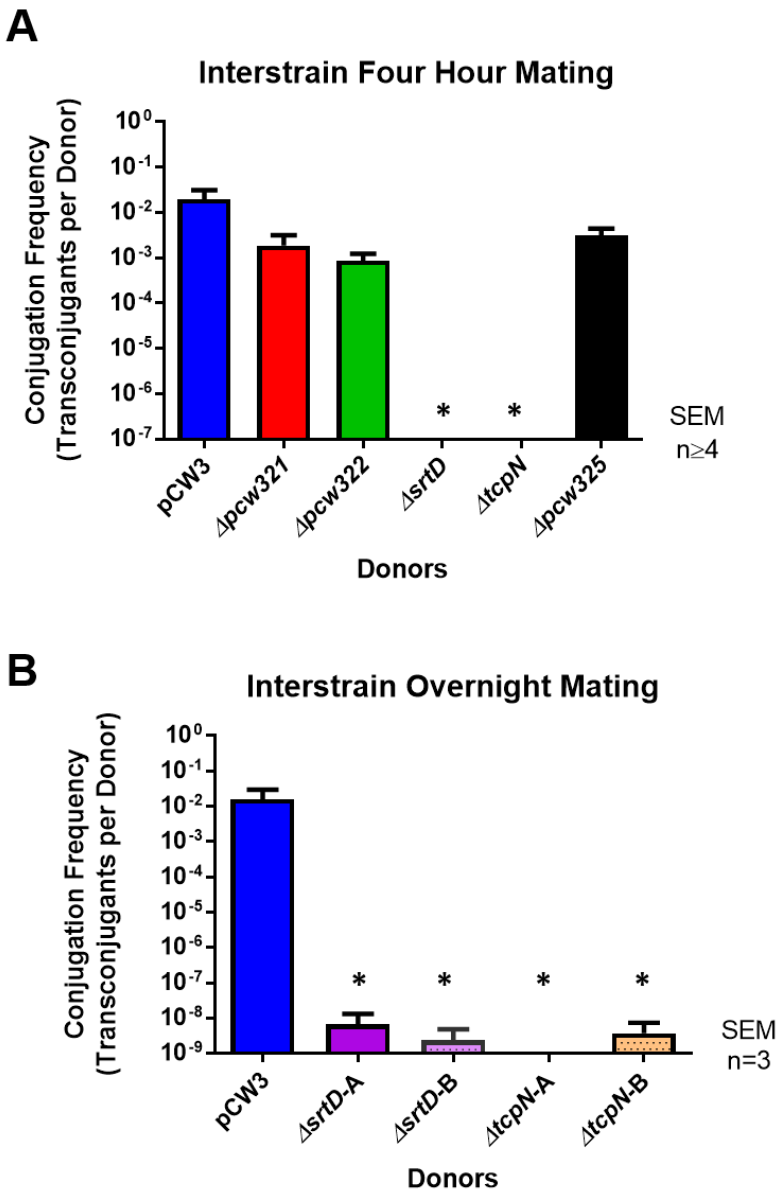

Figure 2.9: Interstrain conjugation frequencies of independent CnaC region mutants. Mixed plate matings were conducted using JIR13224 derived strains as donors and the CW562 derivative, JIR39, as a recipient. Donor strains are labelled on the X-axis and the wild type strain is referred to as pCW3. The conjugation frequency is defined as the number of transconjugants per donor cell. **A.** Transfer frequencies of the *pcw321, pcw322, srtD, tcpN* and *pcw325* mutants in a four-hour interstrain mating (n≥4). **B.** Transfer frequencies of independent *srtD* and *tcpN* mutant strains, denoted A and B, in an interstrain overnight mating (n=3). One asterisk denotes statistical significance of $p<0.03$ compared to wild type pCW3 as calculated by Mann-Whitney *u*-test.

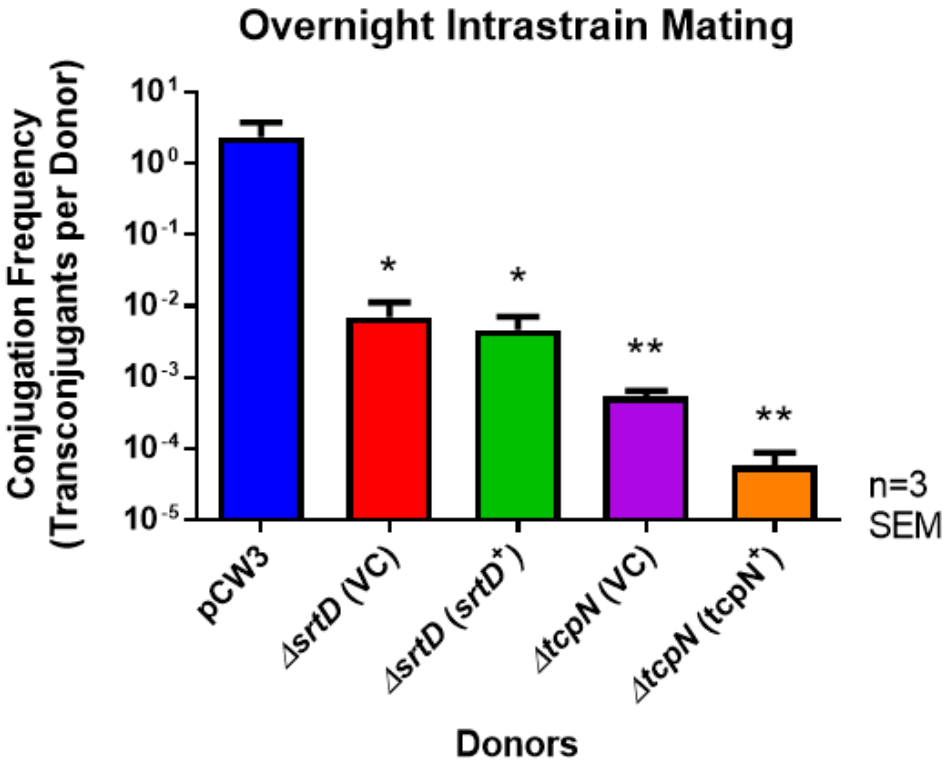

Figure 2.10: Conjugation frequency of complemented *srtD* and *tcpN* mutant strains. Transfer frequency of *srtD* and *tcpN* mutants and complemented derivatives in an overnight intrastrain mating (n=3). Mixed plate matings were conducted using JIR13224 derivative strains as donors and the isogenic strain 13 derivative JIR4394 as a recipient. Isogenic donor strains are labelled on the X-axis. The wild type strain is referred to as pCW3, *srtD* (VC) – JIR13256 with vector pJIR3422, *srtD* (*srtD*$^+$) – JIR13256 with pJIR3422 containing wild-type *srtD*, pJIR4547, *tcpN* (VC) – JIR13258 with pJIR3422, *tcpN* (*tcpN*$^+$) – JIR13258 with pJIR3422 containing wild-type *tcpN*, pJIR4549. Transfer frequencies are expressed as the number of transconjugants per donor cell and are reported on a $\log_{10}$ scale. One asterisk denotes statistical significance of $p<0.01$ and two asterisks denote $p=0.0002$ compared to wild-type pCW3 as calculated by Mann-Whitney *u*-test.

vector control. This reduced transfer may indicate that the complementation plasmids were not tolerated well by the *C. perfringens* cells.

Complementation plasmids were extracted from *C. perfringens* and introduced into *E. coli* before re-extraction and analysis *via* restriction digestion and sequencing. No changes in gene sequence or digestion patterns were observed for the *srtD* and *tcpN* complementation vectors (data not shown). These findings suggest that ineffective *in trans* complementation was not due to sequence errors on the complementation plasmids.

To determine if the complementation strains were expressing the desired genes, expression studies were conducted. RNA was extracted from wild-type, mutant, vector control and complemented strains and RT-PCR conducted using primers specific for the genes *rpoA* (as a control for RNA extraction)*, srtD* and *tcpN.*

As anticipated, PCR products for both *srtD* and *tcpN* were observed in the respective complementation strains, as well as the wild-type strain (Figure 2.11). The absence of a *srtD* transcript in the *srtD* mutant confirms the successful deletion of the gene. Likewise, the absence of a *tcpN* transcript in the respective mutant and vector control strains further confirms the mutation of that gene. Additionally, analysis of *srtD* mutant RNA with oligonucleotides specific for *tcpN* yielded products of the expected size (204 bp) for positive gene expression. The identification of downstream gene expression reduces the potential of genetic polar effects- that could occur as a result of the double crossover mutation- influencing the conjugation phenotype, however, this technique is not quantitative and further analysis would need to be conducted for confirmation. A similar result was obtained when the *tcpN* mutants were probed for *srtD* expression. In all *tcpN* mutants the *srtD* gene was expressed, demonstrating that the double-crossover mutation of *tcpN* was not affecting the expression of the upstream gene. The RT-PCR analysis demonstrated that *srtD* and *tcpN* genes were being transcribed from the

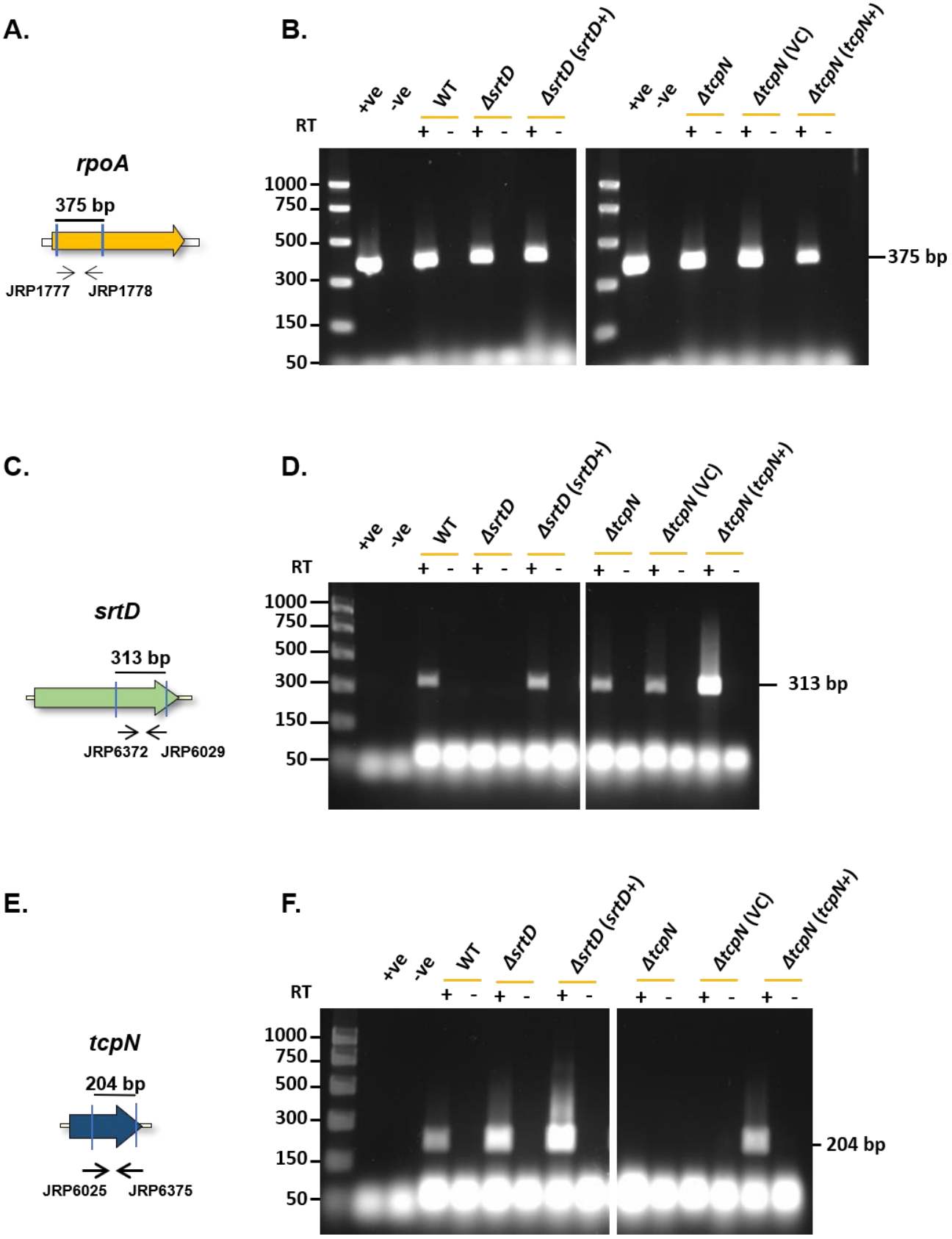
A.
rpoA
375 bp
JRP1777
JRP1778
B.
+ve
-ve
WT
ΔsrtD
ΔsrtD (srtD+)
ΔtcpN
ΔtcpN (VC)
ΔtcpN (tcpN+)
RT
1000
750
500
300
150
50
375 bp
C.
srtD
313 bp
JRP6372
JRP6029
D.
313 bp
E.
tcpN
204 bp
JRP6025
JRP6375
F.
204 bp

Figure 2.11: RT-PCR analysis of *srtD* and *tcpN* transcription in wild-type and mutant strains. A. C. and E. Schematic representation of the oligonucleotides used to analyse transcription in RT-PCR experiments: *rpoA* (A)*, srtD* (C) and *tcpN* (E). Genes of interest are represented by the thick coloured arrows. Primer positions are indicated by the vertical lines and are labelled below. Size of the expected products for each reaction are labelled above the ORF. **B., D., and F.,** 2% agarose gel electrophoresis of RT-PCR products specific for *rpoA* (B), *srtD* (D) and *tcpN* (F), conducted in the presence (+) or absence (-) of reverse transcriptase (RT). RT-PCR reactions were performed on total RNA extractions from the wild-type strain JIR13224, a *srtD* mutant – JIR13256, *srtD* (*srtD*$^{+}$) – JIR13256 with pJIR3422 containing the wild-type *srtD*$^{+}$ plasmid pJIR4547, a *tcpN* mutant – JIR13258, *tcpN* (VC) – JIR13258 with pJIR3422, *tcpN* (*tcpN*$^{+}$) – JIR13258 with pJIR3422 containing the wild-type *tcpN*$^{+}$ plasmid, pJIR4549. The positive control (+ve) was performed using JIR13224 genomic DNA as a template. The negative control (-ve) contained no template. PCR markers (Promega) were used as a size standard and are shown in base pairs (bp).

complementation vectors as desired, suggesting that ineffective complementation was not due to the absence of transcription.

To determine if the inability to complement the mutants was due to the instability of the complementation vectors, a stability assay was designed to mimic the length of time the cells were grown without selection during overnight mating assays. The stability of the complementation plasmids was measured by patching a sample of 100 colonies onto non-selective NA and NA supplemented with Tm (Figure 2.12).

For each construct, at least 80% of the population retained the complementation vectors following 18 hours non-selective culture. There was a population loss of roughly 20% of the *srtD* complementation vector, suggesting that overexpression of this gene was disadvantageous to the host *C. perfringens* cell. Despite this partial loss of the *srtD* complementation vector, the plasmids were considered stable enough for complementation in the mating assays, meaning that plasmid instability was not contributing significantly to the lack of complementation.

As the genes in the CnaC region appeared to be in a single operon (Figure 2.1), there is the potential for transcriptional or translational coupling, which may be hindering complementation attempts. The coordinate protein expression of SrtD and TcpN may be required to stabilise protein products following translation. This phenomenon has been observed previously for the F plasmid, whereby the TraQ protein processes the pilin subunit TraA into a stable form. When TraQ is absent, TraA is readily degraded (Maneewannakul *et al.*, 1993). To address this possibility, *in trans* complementation was attempted with vectors encoding the genetic region including both *srtD* and *tcpN* or with the entire CnaC region. The wild-type *srtD* to *tcpN* gene region was cloned into the complementation vector pJIR3422. The resultant plasmid, pJIR4588, was introduced into the *srtD* and *tcpN* mutant strains. Similarly, the wild-type region spanning from *pcw321* to *pcw325* was cloned into pJIR3422, producing pJIR4587, which was introduced into the *srtD* and *tcpN* deletion strains. Conjugation assays were conducted with all of these

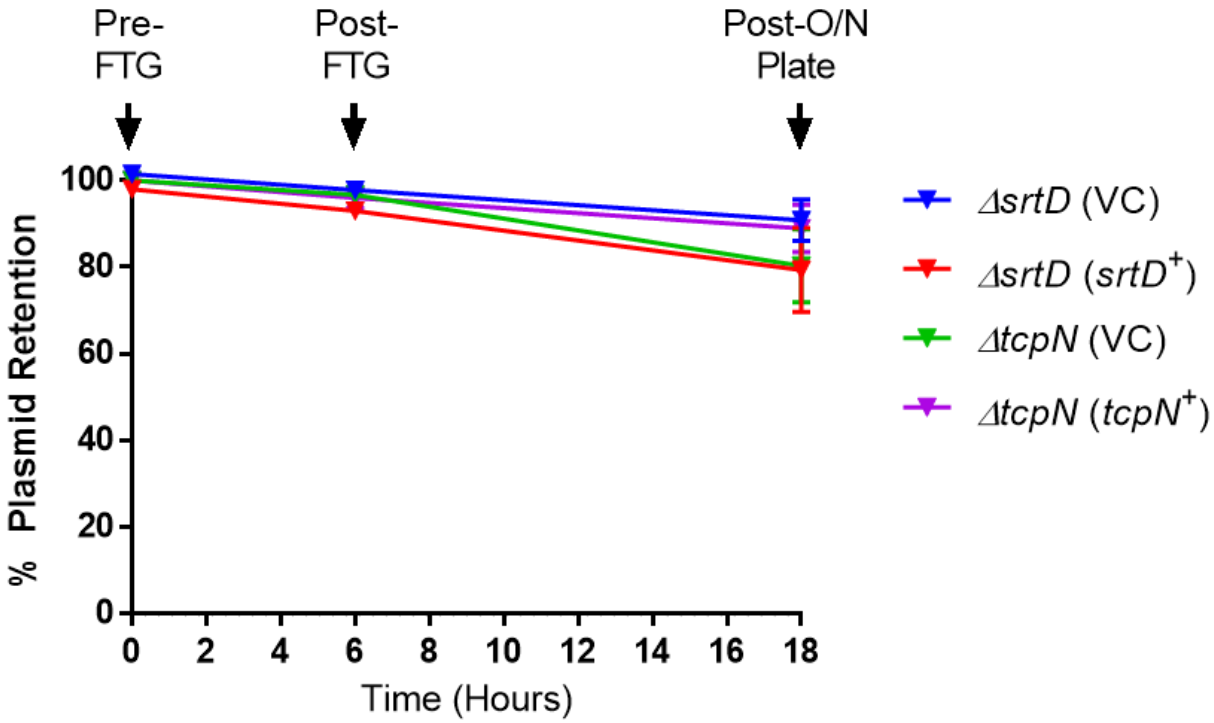

Figure 2.12: Complementation plasmid stability assays. Complementation plasmid stability was assessed over the course of mock mating assays simulating the overnight conjugation assays (SEM, n=3). Legend: *srtD* (VC) – JIR13256 with vector pJIR3422, *srtD* (*srtD*$^{+}$) – JIR13256 with pJIR3422 containing wild-type *srtD*, pJIR4547, *tcpN* (VC) – JIR13258 with pJIR3422, *tcpN* (*tcpN*$^{+}$) – JIR13258 with pJIR3422 containing wild-type *tcpN*, pJIR4549. Stability data were collected from pure culture selection plates prior to the assay start (Pre-FTG; t=0), following non-selective FTG propagation (Post-FTG; t=6 hrs) and following overnight (Post O/N plate; t=18 hrs) incubation on non-selective solid media. The stability of the complementation plasmids was measured by patching a sample of 100 colonies onto non-selective NA and NA supplemented with Tm.

complementation strains (Figure 2.13). As before, *in trans* complementation did not restore conjugative transfer in either mutant strain. However, when these new complementation plasmids were rescued in *E. coli* they could not be sequenced and did not produce the correct restriction profiles as they no longer possessed either of the inserted fragments. It is likely that the overexpression of genes from these constructs is unfavourable in. *C. perfringens*, and as such the vectors may have been altered *in vivo* to reduce the burden on the cell.

Complementation *in cis,* through the reversal of the original mutations

An alternative approach was to complement the *srtD* and *tcpN* mutants by reversing the double crossover mutation using a vector construct containing the wild-type genes (Figure 2.14). A mutagenesis reversal vector was produced by cloning a 1.6 kb wild-type region spanning *pcw321* to *pcw325* into a 5.2 kb fragment of the plasmid pJIR3566. This plasmid backbone was used as it confers chloramphenicol resistance, allowing for the easy identification of transformant strains, and it is also unstable in *C. perfringens* (Cheung *et al.*, 2010), which is beneficial for the quick elucidation of potential double crossover revertants. The resultant mutagenesis plasmid, pJIR4587, was introduced into the *srtD* and *tcpN* mutants *via* transformation. After passaging on solid media, 1000 single colonies from each transformation were patched onto NA, NA with Tm (to detect presence of the reversal vector) and NA with Em (to detect the original double crossover mutation). It was expected that correct revertants would exhibit sensitivity to both Tm and Em. Many patched colonies exhibited a loss of the mutagenesis vector as desired, however, they were resistant to erythromycin, indicating that reversion of the initial double crossover had not occurred. Subsequently, attempts were made to construct a reversal vector with a larger wild type gene fragment, increasing the possibility of a double crossover. Unfortunately, construction of these vectors proved difficult and complementation *in cis* was not achieved.

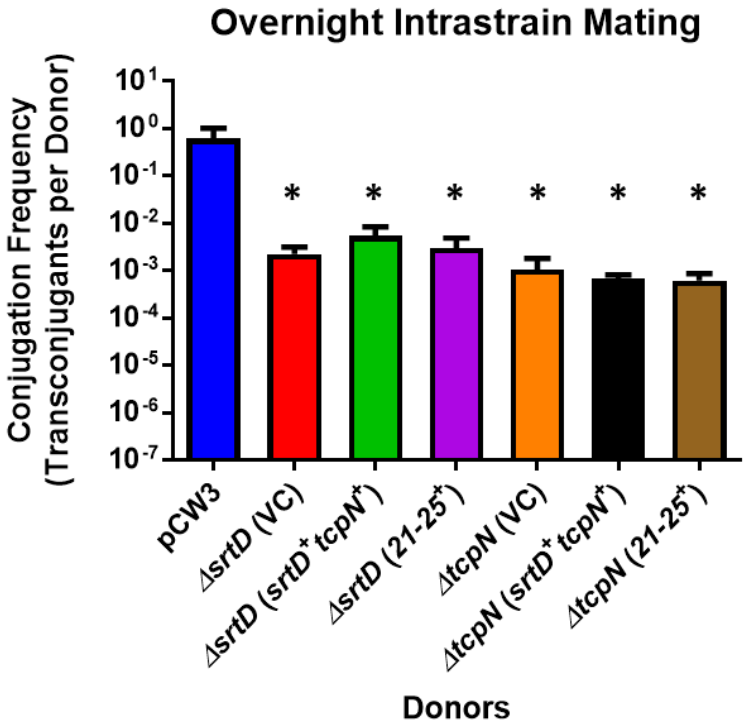

Figure 2.13: Conjugation frequency of complemented *srtD* and *tcpN* mutant strains. Transfer frequency of *srtD* and *tcpN* mutants and complemented derivatives in an overnight intrastrain mating (n=4). Mixed plate matings were conducted using JIR13224 derivative strains as donors and the isogenic strain 13 derivative JIR4394 as a recipient. Isogenic donor strains are labelled on the X-axis. The wild type strain is referred to as pCW3, *srtD* (VC) – JIR13256 with pJIR3422, *srtD* (*srtD*$^+$ *tcpN*$^+$) – JIR13256 with pJIR3422 containing wildtype *srtD* and *tcpN,* pJIR4588, *srtD* (*21-25*$^+$) – JIR13256 with pJIR3422 containing the genetic region spanning from *pcw321* to *pcw325,* pJIR4587, *tcpN* (VC) – JIR13258 with pJIR3422, *tcpN* (*srtA*$^+$ *tcpN*$^+$) – JIR13258 with pJIR3422 containing wildtype *srtD* and *tcpN,* pJIR4588 and *tcpN* (*21-25*$^+$) – JIR13258 with pJIR3422 containing the genetic region spanning from *pcw321* to *pcw325,* pJIR4587. Transfer frequencies are expressed as the number of transconjugants per donor cell. Means ± SEM are shown. One asterisk denotes statistical significance of ($p<0.05$) as compared to wild-type pCW3 as calculated by Mann-Whitney *u*-test.

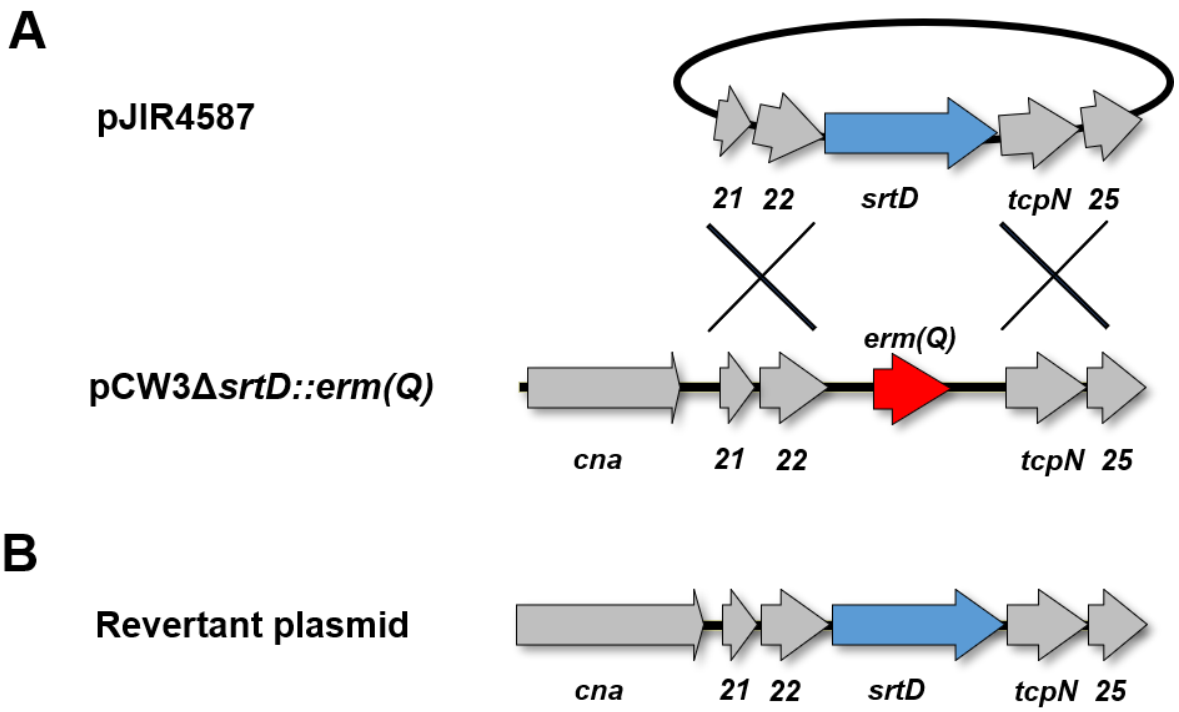

Figure 2.14: Schematic diagram of the *in cis* complementation approach for the *srtD* mutant. A. The mutagenesis plasmid pJIR4587 is shown, with ORFs corresponding to the cloned CnaC region represented by large arrows. A portion of the CnaC region from the pCW3*ΔsrtD::erm*(Q) mutant is also shown. In the mutant, the entire *srtD* gene is replaced with the *erm*(Q) gene (shown in red). Regions whereby homologous recombination could occur are denoted by the thick black crosses. **B.** The expected genetic profile of the revertant plasmid is shown, whereby the *srtD* gene has been replaced and reverted to wild type.

Mutation of genes within the CnaC region did not affect pCW3 stability

Another important factor in plasmid biology is the ability to maintain a stable population of plasmids during natural cellular replication. To test if the mutations in genes within the CnaC region resulted in an unstable plasmid phenotype, a single stability assay in broth was conducted (data not shown). All mutant plasmids tested showed wild-type stability over the course of six days of the experiment, suggesting these genes are not required for pCW3 plasmid maintenance.

Discussion

The CnaC region remains highly conserved amongst the pCW3-like plasmids of *C. perfringens,* however, the function of the products encoded within this region remains unknown. As this region is encoded directly upstream of the Tcp conjugation locus, it was hypothesised that these gene products may be involved in conjugation. Therefore, the involvement of *pcw321, pcw322, srtD, tcpN* and *pcw325* genes in pCW3 conjugation was assessed. This study suggested that both SrtD and TcpN are required for efficient pCW3 conjugative transfer (Figures 2.8 and 2.9). Independent *srtD* and *tcpN* double crossover mutants demonstrated a significant decrease in transfer frequency in comparison to wild type pCW3. To confirm the involvement of these genes, multiple complementation strategies *in trans* and *in cis* were attempted but were inconclusive. Although complementation was not achieved, this work provides preliminary evidence that both *srtD* and *tcpN* are involved in mediating the efficient conjugative transfer of pCW3.

What roles might SrtD and TcpN play in pCW3 conjugation? Bioinformatic analysis of the predicted product of *tcpN* did not provide insight into the potential function of this protein thereby the mechanism by which it is involved in conjugation remains a mystery. However, a mechanism by which SrtD may function in conjugation has been hypothesised. Sortase enzymes decorate Gram-positive bacterial cell walls through the covalent attachment of proteins that possess a sortase recognition motif (Clancy *et al.*, 2010, Spirig *et al.*, 2011). Sortases are phylogenetically grouped into six distinct classes, with each class playing different biological

roles. For example, Class C sortases are involved in pilin polymerisation, whereas Class B sortases typically attach haem-receptors to the cell surface (Spirig *et al.*, 2011). The pCW3-encoded sortase was originally annotated as SrtA. However, the BLAST and phylogenetic analysis reported in this chapter has reclassified this protein into the class D subfamily 2 of sortase enzymes (Table 2.4 and Figure 2.2). The subclass D2 is comprised exclusively of *C. perfringens* sortases and has only recently been defined (Suryadinata *et al.*, 2015). Only one sortase within this class has been functionally characterised and it is thought to be involved in attaching sporulation-related proteins to the cell surface (Suryadinata *et al.*, 2015).

Sortase genes are typically clustered in the same operon as the genes encoding proteins with which they interact (Spirig *et al.*, 2011, Clancy *et al.*, 2010). pCW3-encoded SrtD may attach sporulation-associated proteins to the cell surface, however, given the location of the pCW3 *srtD* gene, it is more likely to be involved in the attachment of plasmid-encoded proteins to the cell wall. Located upstream of *srtD* is *cnaC*, which is predicted to encode an adhesin protein that contains a derivative of the sortase recognition motif (Figure 2.1). It has been proposed for Gram-positive conjugation systems that target cell attachment is facilitated by the production of cell surface adhesins, such as TraO from pIP501 (Goessweiner-Mohr *et al.*, 2014, Bhatty *et al.*, 2013). Due to the close proximity of *srtD* and *cnaC* to the *tcp* conjugation genes, it has been postulated that SrtD anchors CnaC to the surface of *C. perfringens* cells, acting as an adhesion factor facilitating conjugative transfer (Bhatty *et al.*, 2013). This hypothesis is supported by the findings of this study, whereby mutation of *srtD* resulted in a reduction of intrastrain plasmid transfer (Figure 2.8). This phenotype was amplified when interstrain matings, between two different strains, were conducted (Figure 2.9).

Significant differences of conjugation frequencies between intrastrain and interstrain matings was observed for *srtD* and *tcpN* mutants. One theory for why transfer efficiency was altered is that the loss of plasmid-mediated adhesion may have been masked by favourable adhesion

interactions between cells of the same strain background. For example, the use of an intrastrain recipient may have overcome the loss of the plasmid specific adhesion factors that would have displayed on the surface of the donor by SrtD. This suggestion is partially supported by the findings of previous work that had demonstrated that mutation of *cnaC* (which encodes the adhesin proposed to be attached to the surface of cells *via* SrtD) resulted in a decreased conjugation frequency only during interstrain matings (S. Revitt-Mills, V. Adams and J. Rood, unpublished). The reduction, but not complete abrogation, of conjugation by mutation of *srtD* may also be due to functional redundancies, as a number of subclass D2 sortase enzymes are encoded on the *C. perfringens* strain 13 chromosome (Miyamoto *et al.*, 2006, Suryadinata *et al.*, 2015, Tamai *et al.*, 2017). No transconjugants were obtained for either the *srtD* or *tcpN* mutants in the four-hour interstrain assay (Figure 2.9A), indicating that the function of these gene products may be important in facilitating early transfer of pCW3 between *C. perfringens* cells-before cell densities are high- particularly for different stain backgrounds.

In this study, multiple complementation strategies were attempted, with little success. Difficulties experienced with complementation could be attributed to multiple events such as uncontrolled gene over expression, unfavourable expression conditions or secondary mutations. Each of these potential contributing factors now will be discussed in more detail.

Complementation was primarily attempted *in trans* on a multi-copy vector, with no regulatory control over gene expression. The use of this vector for complementation has been successful for many other *C. perfringens* mutagenesis studies on conjugation genes (Porter *et al.*, 2012, Wisniewski *et al.*, 2015a, Bantwal *et al.*, 2012, Traore *et al.*, 2018, Wisniewski *et al.*, 2015b), but not in this study. It is possible that uncontrolled over-expression of a membrane protein, such as SrtD, may be unfavourable to the cell. As such, future work should attempt to complement the mutation under the control of an inducible or native promoter, whereby expression may not be as detrimental to the cell. This phenomenon has been previously observed during

complementation analysis of the Δ*virB2* mutation in *Agrobacterium tumefaciens,* whereby full complementation was only achieved when *virB2* was expressed *in trans* under the control of the native *virB2* promoter (Berger & Christie, 1994). Expression of *srtD* and *tcpN* genes using their native pCW3 promoter may have been required for successful complementation.

The genetic organisation of the CnaC region may have contributed to the ineffective complementation of the *srtD* and *tcpN* mutations. The genes within the CnaC region are all transcribed on the sense strand, and *pcw321, pcw322* and *srtD* are encoded in the same reading frame (+3). The *tcpN* and *pcw325* genes are also encoded on the same reading frame (+1). At the time of this experimental work the transcriptional profile of pCW3 had not been investigated. However, recently obtained pCW3 transcriptomic data suggests that genes *pcw321* through to *pcw327* form an operon, with the predicted promoter located upstream of *pcw321* (T. Stent, X. Han, V. Adams, R. Moore and J. Rood, unpublished). The organisation of this genetic region in an operon suggests that potential transcriptional or translational coupling of these genes may be reasons for unsuccessful complementation.

In a study conducted on the type IV secretion system of *A. tumefaciens,* successful *in trans* complementation of some mutations required the presence of additional upstream or downstream genes (Berger & Christie, 1994). To address the potential requirement of surrounding gene products for successful complementation within this study, complementation with both *srtD* and *tcpN* genes on the same construct, as well as complementation with the entire *cnaC* genetic region was attempted. However, complementation with either construct was inconclusive, and the vectors were not tolerated well by the *C. perfringens* cells, suggesting that complementation with additional surrounding genes was not tolerated when transcription was driven by such a strong promoter. It is also possible that not all the additional genes necessary for complementation were included in these constructs. This could be addressed with the construction of larger complementation construct, however *in cis* complementation, through the

reversal of the *srtD* and *tcpN* mutations would be a more appropriate approach. The reversal of the *srtD* and *tcpN* mutations was attempted during this study, but revertant strains were not obtained, perhaps due to the small region of homology (1.6 kb in total, <800 bp on either side of the target gene) flanking the sites of mutagenesis. For double crossovers to occur efficiently in *C. perfringens* cells, large flanking regions of approximately 2 kb on either side of the gene to be replaced, are generally used (Awad *et al.*, 1995). Targeted gene deletion is then positively selected using antibiotic resistance, this approach could not be used in this situation, since the recombination event could only be detected by the loss of antibiotic resistance. To increase the possibility of a double crossover, future work could utilise a mutagenesis plasmid with a larger region of homology. To conclusively determine the involvement of both *srtD* and *tcpN* genes in pCW3 conjugation an effective *in cis* complementation strategy should be employed.

Another explanation for the phenotypes that could not be complemented within this study is the possibility of secondary mutations. For the mutants with an altered conjugation phenotype, secondary mutations could have arisen elsewhere on the pCW3 plasmid in regions that are required for efficient conjugative transfer, such as within the Tcp locus. Although possible, this scenario seems unlikely, as independently derived *srtD* and *tcpN* mutants possessed the same conjugation phenotypes whilst all other gene deletions created at the same time were unaffected (*pcw321, pcw322* and *pcw325*). The likelihood of the same secondary mutation arising in these four independently derived mutants and altering the conjugation phenotype in the same way seems low. Unless mutation of *srtD* and *tcpN* drive the formation of a particular secondary mutation – a compensatory mutation. To conclusively rule out the possibility of secondary mutations, mutant strains should be sequenced, and the genotypes confirmed.

Also located within the CnaC region, downstream of *pcw325,* is a putative adenine-specific DNA methyltransferase gene *(dam).* In bacteria, DNA methyltransferases are involved in the regulation of many important cellular functions such as virulence, gene expression, DNA replication and

DNA repair (Adhikari & Curtis, 2016). In plasmid systems such as pSLT and R100 from *Salmonella enterica* Serovar Typhimurium, Dam methylation of DNA has been shown to negatively regulate the conjugative transfer of plasmids (Camacho *et al.*, 2010, Camacho & Casadesús, 2005). Methylation of plasmid DNA was found to decrease the plasmid transfer frequency; when plasmids were mated in isogenic strains lacking Dam methylation, conjugal transfer of the R100 plasmid increased ten-fold in comparison to mating within a Dam^+ background (Camacho *et al.*, 2010). Previous work has examined the role of the pCW3-encoded *dam* gene in pCW3 conjugation and found no significant alteration in conjugation frequency (S. Revitt-Mills, V. Adams and J. Rood, unpublished). However, this previous study did not examine the effects of *dam* mutation in interstrain matings. Since the findings of the current study have demonstrated that some conjugation phenotypes are amplified in interstrain matings, future work should examine the *dam* mutants in interstrain conjugative transfer experiments.

The sequencing of new *C. perfringens* plasmids consistently reveals the conserved nature of many of the genes encoded within the pCW3-like plasmid backbone (Gurjar *et al.*, 2010, Li *et al.*, 2007, Li *et al.*, 2013, Mehdizadeh Gohari *et al.*, 2016, Miyamoto *et al.*, 2002, Miyamoto *et al.*, 2006, Miyamoto *et al.*, 2008), hinting at their likely importance in key plasmid functions. This work has analysed some of the genes located in the previously uncharacterised CnaC region of pCW3 and demonstrated that many of the genes within this region are highly conserved, despite the unknown nature of their function in plasmid biology. This work provides preliminary evidence that the products of *srtD* and *tcpN* are involved in conjugation, as independent mutation of these genes reproducibly results in a reduction in conjugative transfer. Furthermore, it is hypothesised that *srtD* may function to attach adhesin proteins to the cell surface, facilitating effective conjugative transfer. Further investigation of the genes that are conserved on the pCW3-like plasmid backbone is critical for our understanding of the nature of these plasmids, which often harbour disease-causing pathogenic traits in this important human and animal pathogen.

References

Adams, V., Bantwal, R., Stevenson, L., Cheung, J.K., Awad, M.M., Nicholson, J., Carter,

G.P., Mackin, K.E., Rood, J.I., and Lyras, D. (2014) Utility of the Clostridial site-specific recombinase TnpX to clone toxic-product-encoding genes and selectively remove genomic DNA fragments. *Applied and Environmental Microbiology* **80**: 3597-3603.

Adams, V., Watts, T.D., Bulach, D.M., Lyras, D., and Rood, J.I. (2015) Plasmid partitioning systems of conjugative plasmids from *Clostridium perfringens*. *Plasmid* **80**: 90-96.

Adhikari, S., and Curtis, P.D. (2016) DNA methyltransferases and epigenetic regulation in bacteria. *FEMS Microbiology Reviews* **40**: 575-591.

Altschul, S.F., Gish, W., Miller, W., Myers, E.W., and Lipman, D.J. (1990) Basic local alignment search tool. *Journal of Molecular Biology* **215**: 403-410.

Artimo, P., Jonnalagedda, M., Arnold, K., Baratin, D., Csardi, G., de Castro, E., Duvaud, S., Flegel, V., Fortier, A., Gasteiger, E., Grosdidier, A., Hernandez, C., Ioannidis, V., Kuznetsov, D., Liechti, R., Moretti, S., Mostaguir, K., Redaschi, N., Rossier, G., Xenarios, I., and Stockinger, H. (2012) ExPASy: SIB bioinformatics resource portal. *Nucleic Acids Research* **40**: W597-W603.

Awad, M.M., Bryant, A.E., Stevens, D.L., and Rood, J.I. (1995) Virulence studies on chromosomal α-toxin and Θ-toxin mutants constructed by allelic exchange provide genetic evidence for the essential role of α-toxin in *Clostridium perfringens*-mediated gas gangrene. *Molecular Microbiology* **15**: 191-202.

Bannam, T.L., Teng, W.L., Bulach, D., Lyras, D., and Rood, J.I. (2006) Functional identification of conjugation and replication regions of the tetracycline resistance plasmid pCW3 from *Clostridium perfringens*. *Journal of Bacteriology* **188**: 4942-4951.

Bannam, T.L., Yan, X.-X., Harrison, P.F., Seemann, T., Keyburn, A.L., Stubenrauch, C., Weeramantri, L.H., Cheung, J.K., McClane, B.A., Boyce, J.D., Moore, R.J., and Rood, J.I. (2011) Necrotic enteritis-derived *Clostridium perfringens* strain with three closely related independently conjugative toxin and antibiotic resistance plasmids. *mBio* **2**: e00190-11.

Bantwal, R., Bannam, T.L., Porter, C.J., Quinsey, N.S., Lyras, D., Adams, V., and Rood, J.I. (2012) The peptidoglycan hydrolase TcpG is required for efficient conjugative transfer of pCW3 in *Clostridium perfringens*. *Plasmid* **67**: 139-147.

Benson, D.A., Cavanaugh, M., Clark, K., Karsch-Mizrachi, I., Lipman, D.J., Ostell, J., and Sayers, E.W. (2017) GenBank. *Nucleic Acids Research* **45**: D37-D42.

Berger, B.R., and Christie, P.J. (1994) Genetic complementation analysis of the *Agrobacterium tumefaciens virB* operon: *virB2* through *virB11* are essential virulence genes. *Journal of Bacteriology* **176**: 3646-3660.

Bhatty, M., Laverde Gomez, J.A., and Christie, P.J. (2013) The expanding bacterial type IV secretion lexicon. *Research in Microbiology* **164**: 620-639.

Camacho, E.M., Camacho, E.M., Serna, A., and Casadesús, J. (2010) Regulation of conjugal transfer by Lrp and Dam methylation in plasmid R100. *International Microbiology* **8**: 279-285.

Camacho, E.M., and Casadesús, J. (2005) Regulation of *traJ* transcription in the Salmonella virulence plasmid by strand-specific DNA adenine hemimethylation. *Molecular Microbiology* **57**: 1700-1718.

Cheung, J.K., Keyburn, A.L., Carter, G.P., Lanckriet, A.L., Van Immerseel, F., Moore, R.J., and Rood, J.I. (2010) The VirSR two-component signal transduction system regulates NetB toxin production in *Clostridium perfringens*. *Infection and Immunity* **78**: 3064-3072.

Cheung, J.K., and Rood, J.I. (2000) Glutamate residues in the putative transmembrane region are required for the function of the VirS sensor histidine kinase from *Clostridium perfringens*. *Microbiology* **146**: 517-525.

Clancy, K.W., Melvin, J.A., and McCafferty, D.G. (2010) Sortase transpeptidases: Insights into mechanism, substrate specificity, and inhibition. *Peptide Science* **94**: 385-396.

Farrell Jr, R.E., (2010) Quality Control for RNA Preparations. In: RNA Methodologies (4th Edition). R.E. Farrell (ed). San Diego: Academic Press, pp. 139-154.

Goessweiner-Mohr, N., Arends, K., Keller, W., and Grohmann, E. (2014) Conjugation in Gram-positive bacteria. *Microbiology Spectrum* **2**: PLAS-0004-2013.

Gurjar, A., Li, J., and McClane, B.A. (2010) Characterization of toxin plasmids in *Clostridium perfringens* type C isolates. *Infection and Immunity* **78**: 4860-4869.

Hughes, M.L., Poon, R., Adams, V., Sayeed, S., Saputo, J., Uzal, F.A., McClane, B.A., and Rood, J.I. (2007) Epsilon-toxin plasmids of *Clostridium perfringens* type D are conjugative. *Journal of Bacteriology* **189**: 7531-7538.

Inoue, H., Nojima, H., and Okayama, H. (1990) High efficiency transformation of *Escherichia coli* with plasmids. *Gene* **96**: 23-28.

Johanesen, P.A., Lyras, D., Bannam, T.L., and Rood, J.I. (2001) Transcriptional analysis of the *tet*(P) operon from *Clostridium perfringens*. *Journal of Bacteriology* **183**: 7110-7119.

La Fontaine, S., and Rood, J.I. (1996) Organization of ribosomal RNA genes from the footrot pathogen *Dichelobacter nodosus*. *Microbiology* **142**: 889-899.

Li, J., Adams, V., Bannam, T.L., Miyamoto, K., Garcia, J.P., Uzal, F.A., Rood, J.I., and McClane, B.A. (2013) Toxin plasmids of *Clostridium perfringens*. *Microbiology and Molecular Biology Reviews* **77**: 208-233.

Li, J., Miyamoto, K., and McClane, B.A. (2007) Comparison of virulence plasmids among *Clostridium perfringens* type E isolates. *Infection and Immunity* **75**: 1811-1819.

Lyristis, M., Bryant, A.E., Sloan, J., Awad, M.M., Nisbet, I.T., Stevens, D.L., and Rood, J.I. (1994) Identification and molecular analysis of a locus that regulates extracellular toxin production in *Clostridium perfringens*. *Molecular Microbiology* **12**: 761-777.

Maneewannakul, K., Maneewannakul, S., and Ippen-Ihler, K. (1993) Synthesis of F pilin. *Journal of Bacteriology* **175**: 1384-1391.

Marchler-Bauer, A., Bo, Y., Han, L., He, J., Lanczycki, C.J., Lu, S., Chitsaz, F., Derbyshire, M.K., Geer, R.C., Gonzales, N.R., Gwadz, M., Hurwitz, D.I., Lu, F., Marchler, G.H., Song, J.S., Thanki, N., Wang, Z., Yamashita, R.A., Zhang, D., Zheng, C., Geer, L.Y., and Bryant, S.H. (2017) CDD/SPARCLE: functional classification of proteins via subfamily domain architectures. *Nucleic Acids Research* **45**: D200-D203.

Marchler-Bauer, A., Derbyshire, M.K., Gonzales, N.R., Lu, S., Chitsaz, F., Geer, L.Y., Geer, R.C., He, J., Gwadz, M., Hurwitz, D.I., Lanczycki, C.J., Lu, F., Marchler, G.H., Song, J.S., Thanki, N., Wang, Z., Yamashita, R.A., Zhang, D., Zheng, C., and Bryant, S.H. (2015) CDD: NCBI's conserved domain database. *Nucleic Acids Research* **43**: D222-D226.

McWilliam, H., Li, W., Uludag, M., Squizzato, S., Park, Y.M., Buso, N., Cowley, A.P., and Lopez, R. (2013) Analysis tool web services from the EMBL-EBI. *Nucleic Acids Research* **41**: W597-W600.

Mehdizadeh Gohari, I., Kropinski, A.M., Weese, S.J., Parreira, V.R., Whitehead, A.E., Boerlin, P., and Prescott, J.F. (2016) Plasmid characterization and chromosome analysis of two *netF*+ *Clostridium perfringens* isolates associated with foal and canine necrotizing enteritis. *PLOS One* **11**: e0148344.

Mehdizadeh Gohari, I., Kropinski, A.M., Weese, S.J., Whitehead, A.E., Parreira, V.R., Boerlin, P., and Prescott, J.F. (2017) NetF-producing *Clostridium perfringens*: Clonality and plasmid pathogenicity loci analysis. *Infection, Genetics and Evolution* **49**: 32-38.

Miyamoto, K., Chakrabarti, G., Morino, Y., and McClane, B.A. (2002) Organization of the plasmid *cpe* locus in *Clostridium perfringens* Type A isolates. *Infection and Immunity* **70**: 4261-4272.

Miyamoto, K., Fisher, D.J., Li, J., Sayeed, S., Akimoto, S., and McClane, B.A. (2006) Complete sequencing and diversity analysis of the enterotoxin-encoding plasmids in *Clostridium perfringens* type A non-food-borne human gastrointestinal disease isolates. *Journal of Bacteriology* **188**: 1585-1598.

Miyamoto, K., Li, J., Sayeed, S., Akimoto, S., and McClane, B.A. (2008) Sequencing and diversity analyses reveal extensive similarities between some epsilon-toxin-encoding plasmids and the pCPF5603 *Clostridium perfringens* enterotoxin plasmid. *Journal of Bacteriology* **190**: 7178-7188.

Parreira, V.R., Costa, M., Eikmeyer, F., Blom, J., and Prescott, J.F. (2012) Sequence of two plasmids from *Clostridium perfringens* chicken necrotic enteritis isolates and comparison with *C. perfringens* conjugative plasmids. *PLOS One* **7**: e49753.

Parsons, J.A., Bannam, T.L., Devenish, R.J., and Rood, J.I. (2007) TcpA, an FtsK/SpoIIIE homolog, is essential for transfer of the conjugative plasmid pCW3 in *Clostridium perfringens*. *Journal of Bacteriology* **189**: 7782-7790.

Petersen, T.N., Brunak, S., von Heijne, G., and Nielsen, H. (2011) SignalP 4.0: discriminating signal peptides from transmembrane regions. *Nature Methods* **8**: 785.

Porter, C.J., Bantwal, R., Bannam, T.L., Rosado, C.J., Pearce, M.C., Adams, V., Lyras, D., Whisstock, J.C., and Rood, J.I. (2012) The conjugation protein TcpC from *Clostridium perfringens* is structurally related to the type IV secretion system protein VirB8 from Gram-negative bacteria. *Molecular Microbiology* **83**: 275-288.

Rood, J.I. (1983) Transferable tetracycline resistance in *Clostridium perfringens* strains of porcine origin. *Canadian Journal of Microbiology* **29**: 1241-1246.

Rood, J.I., Maher, E.A., Somers, E.B., Campos, E., and Duncan, C.L. (1978a) Isolation and characterization of multiply antibiotic-resistant *Clostridium perfringens* strains from porcine feces. *Antimicrobial Agents and Chemotherapy* **13**: 871-880.

Rood, J.I., Scott, V.N., and Duncan, C.L. (1978b) Identification of a transferable tetracycline resistance plasmid (pCW3) from *Clostridium perfringens*. *Plasmid* **1**: 563-570.

Scott, P.T., and Rood, J.I. (1989) Electroporation-mediated transformation of lysostaphin-treated *Clostridium perfringens*. *Gene* **82**: 327-333.

Spirig, T., Weiner, E.M., and Clubb, R.T. (2011) Sortase enzymes in Gram-positive bacteria. *Molecular Microbiology* **82**: 1044-1059.

Sullivan, M.J., Petty, N.K., and Beatson, S.A. (2011) Easyfig: a genome comparison visualizer. *Bioinformatics (Oxford, England)* **27**: 1009-1010.

Suryadinata, R., Seabrook, S.A., Adams, T.E., Nuttall, S.D., and Peat, T.S. (2015) Structural and biochemical analyses of a *Clostridium perfringens* sortase D transpeptidase. *Acta Crystallographica Section D: Biological Crystallography* **71**: 1505-1513.

Tamai, E., Sekiya, H., Maki, J., Nariya, H., Yoshida, H., and Kamitori, S. (2017) X-ray structure of *Clostridium perfringens* sortase B cysteine transpeptidase. *Biochemical and Biophysical Research Communications* **493**: 1267-1272.

Traore, D.A.K., Wisniewski, J.A., Flanigan, S.F., Conroy, P.J., Panjikar, S., Mok, Y.-F., Lao, C., Griffin, M.D.W., Adams, V., Rood, J.I., and Whisstock, J.C. (2018) Crystal structure of TcpK in complex with *oriT* DNA of the antibiotic resistance plasmid pCW3. *Nature Communications* **9**: 3732.

Watts, T.D., Johanesen, P.A., Lyras, D., Rood, J.I., and Adams, V. (2017) Evidence that compatibility of closely related replicons in *Clostridium perfringens* depends on linkage to parMRC-like partitioning systems of different subfamilies. *Plasmid* **91**: 68-75.

Watts, T.D., Vidor, C.J., Awad, M.M., Lyras, D., Rood, J.I., and Adams, V. (2019) pCP13, a representative of a new family of conjugative toxin plasmids in *Clostridium perfringens*. *Plasmid* **102**: 37-45.

Wisniewski, J.A., and Rood, J.I. (2017) The Tcp conjugation system of *Clostridium perfringens*. *Plasmid* **91**: 28-36.

Wisniewski, J.A., Teng, W.L., Bannam, T.L., and Rood, J.I. (2015a) Two novel membrane proteins, TcpD and TcpE, are essential for conjugative transfer of pCW3 in *Clostridium perfringens*. *Journal of Bacteriology* **197**: 774-781.

Wisniewski, J.A., Traore, D.A., Bannam, T.L., Lyras, D., Whisstock, J.C., and Rood, J.I. (2015b) TcpM, a novel relaxase that mediates transfer of large conjugative plasmids from *Clostridium perfringens*. *Molecular Microbiology* **99**: 884-896..

Chapter Three

The pCW3-like plasmids of *Clostridium perfringens* require the *resP* gene to ensure stable inheritance

Introduction

Low copy-number plasmids rely on mechanisms such as active partitioning, post-segregational killing, multimer resolution and replication control to increase the likelihood of their vertical inheritance (Tolmasky, 2017). Many plasmids encode more than one stability mechanism to minimise plasmid loss following septum formation (Bouet *et al.*, 2006; Lobato-Márquez *et al.*, 2016). Typically, these mechanisms work in concert to ensure plasmid stability (Volante *et al.*, 2014).

Multimer resolution is a key mechanism utilised by plasmids to ensure faithful inheritance. Following replication, homologous recombination can result in the formation of multimeric plasmids (Bedbrook & Ausubel, 1976). Plasmid multimers decrease the plasmid copy number within a cell, reducing the chance of daughter cells successfully inheriting a plasmid (Summers, 1991). To overcome the instability induced by multimer formation, many plasmids encode site-specific recombinases, which resolve plasmid multimers into monomers (Austin *et al.*, 1981). These recombinase enzymes belong to two distinct families: the tyrosine recombinase family, which includes the enzymes Rsd from pSDL2 (Krause & Guiney, 1991) and Cre from P1 plasmid (Austin *et al.*, 1981), and the serine recombinase family, which includes proteins such as ParA from RK2/RP4 (Eberl *et al.*, 1994) and Res from pSK41 (LeBard *et al.*, 2008).

Bioinformatic analysis of the pCW3-like plasmids of *C. perfringens* has identified several potential stability mechanisms encoded on these plasmids, including an active partitioning system, putative regulators, and a putative multimer resolution system (Bannam *et al.*, 2006). Studies conducted on the active partitioning (Adams *et al.*, 2015; Watts *et al.*, 2017) and regulatory mechanisms (T. Stent, X. Han, V. Adams and J. Rood, unpublished) have demonstrated their involvement in plasmid stability and compatibility. However, to date no studies have been carried out on the role of the putative multimer resolution system in the stability of pCW3.

The pCW3 *resP* gene encodes a protein of 247 amino acids (AA), that has homology to site-specific serine recombinase enzymes (Bannam *et al.*, 2006). Plasmids from all three characterised *C. perfringens* plasmid families carry distinct resolvase genes, although they are distantly related. For example, there is only 29% AA sequence identity between the ResP proteins from pCP13 and pCW3 and 32% sequence identity between pCW3 and pIP404 ResP proteins (Bannam *et al.*, 2006; Garnier *et al.*, 1987; Shimizu *et al.*, 2002). The common carriage of putative resolvase systems highlights the potential importance of these stability mechanisms to the biology of *C. perfringens* plasmids. As yet, the involvement of multimer resolution systems in *C. perfringens* plasmid biology has not been investigated. This study provides functional evidence that pCW3 relies on a multimer resolution system encoded by the *resP* gene, which is essential for ensuring faithful plasmid inheritance.

Materials and Methods:

Bacterial strains, plasmids and culture conditions

C. perfringens strains and plasmids used in this study are listed in Table 3.1. *C. perfringens* cells were cultured as described in Chapter Two. *Escherichia coli* strains DH5α and DH12S (Life Technologies) were cultured at 37°C in 2X YT medium/agar and were supplemented with the following antibiotics as required: kanamycin (Kn; 20 μg/ml), chloramphenicol (Cm; 30 μg/ml) or erythromycin (Em; 150 μg/ml).

Molecular Techniques

Molecular techniques were performed as described in Chapter 2. Oligonucleotides used in this study are outlined in Table 3.2 and were synthesised by Integrated DNA Technologies (IDT) or Sigma.

Bioinformatic analysis

Sequences were analysed using BLAST (Altschul *et al.*, 1990) and predicted homology to proteins within the conserved domains database (Marchler-Bauer *et al.*, 2015). Multiple sequence alignments and percent identity matrices were generated using Clustal Omega (McWilliam *et al.*, 2013). For the phylogenetic analysis of ResP enzymes, translated protein sequences for *C. perfringens*-encoded ResP were obtained from the NCBI database. Protein accession numbers are outlined in Table 3.3. Sequences were aligned using Clustal Omega and phylogeny inferred (McWilliam *et al.*, 2013). Inferred phylogeny was visualised as a rectangular rooted phylogram using FigTree (available for download at: https://github.com/rambaut/figtree).

Construction of mutant strains and complementation

Allelic exchange was used to replace *resP* with an *erm*(Q) cassette using derivatives of the *C. perfringens* suicide vector pJIR2715 (Bannam *et al.*, 2006). Upstream and downstream flanking regions were generated by PCR and sequentially cloned into pJIR2715 using Asp718/BamHI sites upstream and XhoI/SacI sites downstream of the *erm*(Q) gene. A 1764 bp fragment encompassing the 5581-7344 bp region from pCW3 was cloned upstream of *erm*(Q), and a 2309 bp fragment from 7978-10286 bp was cloned downstream of *erm*(Q) to generate the *resP* suicide vector, pJIR4795.

The mutagenesis vector was introduced into the *C. perfringens* strain JIR4195 by electroporation and transformants selected on NA Em. To identify potential mutants, the resultant transformants were screened for resistance to tetracycline and erythromycin and sensitivity to thiamphenicol. DNA preparations from erythromycin-resistant thiamphenicol-sensitive colonies were tested by PCR and Southern blotting to confirm mutation of the target gene and the loss of the mutagenesis plasmid.

Table 3.1: Strains and plasmids used in this study

Strain	Description	Reference
E. coli		
DH5α	F-φ80*lacZ*ΔM15, Δ(*lac*ZYA-*argF*)U169, *rec*A1, *end*A1, *hsd*R17(r_k-, m_k+), *pho*A, *sup*E44, *thi*-1, *gyr*A96, *rel*A1 λ	Invitrogen/ Life Technologies
DH12S	φ80*lacZ*ΔM15, *mcrA* Δ(*mrr-hsdRMS-mcrBC*), *araD139* Δ(*ara, leu*)7697, Δ(*lacX74 galU galK rpsL)* (Str^R) *nupG, recA1/F,' proAB+, lacIqZ*ΔM15	Invitrogen/ Life Technologies
C. perfringens		
JIR325	Strain 13 derivative; Rif^R Nal^R	(Lyristis *et al.*, 1994)
JIR4195	JIR325 (pCW3); Rif^R Nal^R	(Hughes *et al.*, 2007)
JIR4394	Strain 13 derivative; Sm^R Chl^R	(Bannam *et al.*, 2006)
JIR13587	JIR4195(pJIR4796); Rif^R Nal^R Tc^R Em^R pCW3Δ*resP::erm*(Q)	This study
JIR13588	JIR4195(pJIR4797); Rif^R Nal^R Tc^R Em^R pCW3Δ*resP::erm*(Q), independent mutant	This study
Plasmids		
pCP13	54 kb plasmid from strain 13	(Shimizu *et al.*, 2002)
pCW3	Conjugative tetracycline resistance plasmid	(Rood *et al.*, 1978)
pJIR750	*E. coli-C. perfringens* shuttle vector, *catP+ lacZ* α-peptide	(Bannam & Rood, 1993)
pJIR2715	Base plasmid for the construction of *C. perfringens* suicide vectors, *erm*(Q)+ *catP+*	(Bannam *et al.*, 2006)
pJIR3844	Cpb2-toxin plasmid from NE-18	(Bannam *et al.*, 2011)
pJIR4794	pJIR2715 (EcoRI/XbaI) ΩJRP6797/JRP6798 (EcoRI/XbaI; 2039 bp, pCW3) downstream of *resP*	This study
pJIR4795	pJIR4794 (Asp718/BamHI) ΩJRP6799/JRP6800 (Asp718/BamHI; 1764 bp, pCW3), *resP* suicide vector	This study

pJIR4796	pCW3Δ*resP::erm*(Q)	Transformation of JIR4195 with pJIR4794
pJIR4797	pCW3Δ*resP::erm*(Q), independent mutant	Transformation of JIR4195 with pJIR4794
pJIR4798	pJIR750 (BamHI/Asp718) ΩJRP6844/JRP6845 (BamHI/Asp718; 1196 bp, pCW3) *resP*$^{+}$ complementation vector	This study
pJIR4809	pJIR750 (BamHI/Asp718) ΩJRP7195/JRP7196(BamHI/Asp718; 1117 bp, pJIR3844) *resP*$_{\text{pJIR3844}^{+}}$ complementation vector	This study
pJIR4810	pJIR750 (Asp718/BamHI) ΩJRP6866/JRP6867 (Asp718/BamHI; 744 bp; pCP13) *resP*$_{\text{pCP13}^{+}}$ complementation vector	This study
pJIR4833	pJIR2715 (Asp718/BamHI) ΩJRP7126/JRP7127 (Asp718/BamHI; 1176 bp, pCW3) Excision assay vector with one *res* site	This study
pJIR4834	pJIR4833 (XhoI/SacI) ΩJRP7128/JRP7129 (XhoI/SacI; 1176 bp, pCW3) Excision assay vector with two *res* sites flanking *erm*(Q)	This study
pJIR4835	pSU39 (Asp718/BamHI) ΩJRP6845/JRP6844 (Asp718/BamHI; 1196 bp, pCW3) ResP expression plasmid for excision assay	This study

Chl^{R}- potassium chlorate resistance, Cm^{R}- chloramphenicol resistance, Em^{R}- erythromycin resistance, Nal^{R}- nalidixic acid resistance, Rif^{R} – rifampicin resistance, Sm^{R}- streptomycin resistance, Tc^{R}- tetracycline resistance, Tm^{R} – thiamphenicol resistance

Table 3.2: Oligonucleotides used in this study

Name	Sequence	Purpose
JRP4330	CTCAGTACTGAGAGGGAACTTAGATGGTAT	*catP* probe oligo, F
JRP4331	CCGGGATCCTTAGGGTAACAAAAAACACC	*catP* probe oligo, R
JRP6001	CCAGGAAAAGGTCATATAACAGAAGC	*erm*(Q) probe, F
JRP6002	CTAAGACGCAATCTACACTAGGC	*erm*(Q) probe, R
JRP6797	CGGAATTCACTGGTGTAAAGGCTATGG	*resP* RHS plus EcoRI, F
JRP6798	CTTTTCTAGAGAATTTACTTTCTCAACG	*resP* RHS plus XbaI, R
JRP6799	CAGTTAAAGGTACCTTGAATAAATTAAGG	*resP* LHS plus KpnI, F
JRP6800	GCGGATCCTTATAACGCATTTTTATCACTCC	*resP* LHS plus BamHI, R
JRP6844	GGGGGTACCGTATAATGGTTCCTTAGTGTAATTCG	*resP* complementation plus Asp718, F
JRP6845	GCGGGATCCGAGCTTGACTCATAAACATACCTAAA C	*resP* complementation plus BamHI, R
JRP6866	CGGGTACCCAATAAAGTGGCGATTAAAAATCGTCA C	$resP_{pCP13}$ plus Asp718, F
JRP6867	CGGGGATCCCTAATAGATGTCCCCTGAGGACACC	$resP_{pCP13}$ plus BamHI, R
JRP7195	CGGGTACCGCTGGTTCATCCGTAGATATTTTGACC	$resP_{pJIR3844}$ plus Asp718, F
JRP7196	CGGGGATCCCAGCAAGTAAAATTGCTAAAATTATT GGAATTAACC	$resP_{pJIR3844}$ plus BamHI, R
JRP7126	GGGGTACCGAGCCAACAAGATGTATATCTTGTAGA AG	LHS *res* plus Asp718, F
JRP7127	CGGGATCCGATCTGAGTCACCATATACATAAGTCA AC	LHS *res* plus BamHI, R
JRP7128	CCGCTCGAGGAGCCAACAAGATGTATATCTTGTAG AAG	RHS *res* plus XhoI, F
JRP7129	CCGAGCTCGATCTGAGTCACCATATACATAAGTCA AC	RHS *res* plus SacI, R
JRP7156	GCTTCTGTTATATGACCTTTTCCTGG	Sequence out *erm*(Q), R
JRP7157	GCCTAGTGTAGATTGCGTCTTAG	Sequence out *erm*(Q), F
JRP7161	CTCTTTGCGCATATTTACATCTCCTTTAC	Sequence *res*, R
JRP7173	GACTCACTATAGGGAAAGCTCGGTACC	Sequence out LHS before MCS on pJIR2715, F
JRP7174	GCTCTAATACGACTCACTATAG	Sequence out LHS before MCS on pJIR2715, F

JRP7175	CCAGTGAATTGTGCGGCCGCGAGCTC	Sequence out RHS after MCS on pJIR2715, R
JRP7176	CTGCAAGGCGATTAAGTTGG	Sequence out RHS after MCS on pJIR2715, R

F- forward primer, R- reverse primer

Table 3.3: Plasmid names and accession numbers used for bioinformatic analysis

Plasmid	Accession number	Properties
pCP13	NP_150008.1	*cpb2*$^+$
pCP8533etx	YP_002291131.1	pCW3-like, *cpb2*$^+$, *etx*$^+$
pCPB2-CP1	NC_019687.1	pCW3-like, *cpb2*$^+$
pCPF4013	AB236338.1	pCW3-like, *cpb2*$^+$, *cpe*$^+$
pCPF4969	BAE79027.1	pCW3-like, *cpe*$^+$
pCPF5603	NC_007773.1	pCW3-like, *cpb2*$^+$, *cpe*$^+$
pCPPB-1	NC_015712.1	pCW3-like, *cpe*$^+$, *iap*$^+$, *ibp*$^+$
pCW3	YP_001967747.1	*tetAB*(P)$^+$
pDel1_2	NZ_CP019578.1	pCW3-like, *cpb2*$^+$
pDel1_4	NZ_CP019580.1	pCW3-like, *tetA*(P)$^+$
pF262A	NZ_CM001478.1	pCW3-like, *cpb2*$^+$, *tetAB*(P)$^+$
pF262B	NZ_CM001479.1	pCP13-like
pFORC3	NZ_CP009558.1	pCW3-like
pIP404	NP_040456.1	*bcn*$^+$
pJFP55F	CP013041.1	pCW3-like, *netE*$^+$, *netF*$^+$
pJFP55J	CP013044.1	pIP404-like, *bcn*$^+$
pJFP838B	CP013039.1	pCW3-like, *netG*$^+$
pJFP838C	AMN30663.1	pCW3-like, *netE*$^+$, *netF*$^+$
pJGS1987	NZ_ABDW01000020.1	pCW3-like, t*etAB*(P)$^+$
pJIR3537	NC_019259.1	pCW3-like, t*etAB*(P)$^+$
pJIR3844	NC_019257.1	pCW3-like, *cpb2*$^+$
pJIR4150	CRG98356.1	pCW3-like, *tpeL*$^+$, *bcrRABD*$^+$
pOS-1	YP_009023940.1	pCP13-like, *becAB*$^+$
pTS-1	YP_009023995.1	pCP13-like, *becAB*$^+$

Toxin and antibiotic resistance encoding genes are indicated in brackets: Beta2-toxin (*cpb2*), epsilon toxin (*etx*), enterotoxin (*cpe*), iota toxin (*iap, ibp*), tetracycline resistance (*tetAB*(P)), NetE toxin (*netE*), NetF toxin (*netF*), NetG toxin (*netG*), TpeL toxin (*tpeL*), bacitracin resistance (*bcn, bcrRABD*) and Bec toxin (*becAB*)

For complementation, a PCR fragment containing the wild-type *resP* gene was amplified by PCR and subsequently cloned into the BamHI/Aps718 sites of the *E. coli-C. perfringens* shuttle vector pJIR750, to generate pJIR4798. The *resP* genes, $resP_{pCP13}$ and $resP_{pJIR3844}$, were also amplified from the *C. perfringens* plasmids pJIR3844 and pCP13 and cloned into pJIR750 to generate pJIR4809 and pJIR4810, respectively. The complementation plasmids were introduced into the *C. perfringens resP* mutant by electroporation and transformants selected on NA Em Tm. The presence of the complementation plasmids was confirmed by restriction analysis and sequencing, following plasmid rescue in *E. coli.*

Mixed plate mating experiments

Overnight intrastrain conjugative transfer experiments were conducted as outlined in Chapter 2.

Stability experiments

C. perfringens strains were sub-cultured from glycerol stocks stored at either -20°C or -80°C into pre-boiled FTG media and incubated at 37°C for 6 hours. Strains were streaked onto NA supplemented with appropriate antibiotics and incubated anaerobically at 37°C overnight. Single colonies from overnight plates were sub-cultured onto NA supplemented with appropriate antibiotics and incubated anaerobically at 37°C overnight. To determine the stability of wild-type and mutant plasmids, each strain was passaged continuously over the course of six days in HI broth. For strains containing pJIR750-based complementation vectors, Tm was included in the broth to ensure the maintenance of the complementation plasmid. On day 0, a smear was taken from overnight selection plates and resuspended in 500 µl of HI diluent (HI Broth (Oxoid) diluted 1:10); then 100µl was used to inoculate 20 mL HI broths, which were incubated at 37°C for 6-8 hours. Following incubation, 100 µl of this culture was used to inoculate fresh HI media which were incubated at 37°C overnight. Passaging was repeated continuously over the course of six days. For viable counts, the cell suspension of the overnight broth culture was serially diluted and 100 µl plated onto non-selective media and incubated anaerobically at 37°C overnight. 100

resultant colonies were cross patched onto media containing tetracycline to detect the presence of pCW3. Viable counts were plated every second day (0, 2, 4 6) and plasmid stability was determined by comparing viable patches on media with and without tetracycline.

Excision assay

E. coli strains DH12S (pJIR2715), DH12S (pJIR4833, *res* LHS) and DH12S (pJIR4834, *res*) were made chemically competent as previously described (Adams *et al.*, 2006; Crellin & Rood, 1997). Strains were then transformed with pSU39 or pJIR4835, a pSU39 derivative carrying wild-type *resP*. Transformants were selected on 2YT Kn Cm agar. To assess loss of erythromycin resistance, 100 of the resultant colonies were cross-patched onto 2YT Cm or Em. The frequency of excision was determined by comparing the number of viable patches on 2YT Em to those on 2YT Cm. Plasmid DNA was then extracted from transformant colonies growing on Cm plates and subject to restriction analysis and sequencing.

Copy number analysis

Plasmid copy number was determined using digital droplet PCR (ddPCR) (Bio-Rad) on clarified whole cell extracts of *C. perfringens* strains. Briefly, pure cultures of *C. perfringens* strains were grown in HI broth for 6 hours at 37°C. Samples (3 mL) were taken and pelleted by centrifugation at 4000 x g at room temperature (RT). Cells were washed in 3 mL of TES buffer (10mM Tris-HCL, pH 8.0; 1mM EDTA; 0.1% SDS) and pelleted by centrifugation once more. Cells were resuspended in 1mL of TES buffer and either stored at -80°C or immediately lysed by bead beating using the Precellys 24 Tissue Homogeniser (Bertin Instruments) at 3 x 45 sec cycles at 6500 rpm. Cell debris was removed by centrifugation at 17000 x g for 15 mins at RT. The resultant clarified lysate was used at a 1 in 5000 dilution as the template for ddPCR.

All reactions were conducted as per the manufacturer's (Bio-Rad) instructions. Duplexed PCR samples contained 1 µl of DNA template with gene specific primers for *rpoA* and *tetB*(P) at 450 nM each and *rpoA* and *tetB*(P) probes at a concentration of 250 nM, along with an equal volume

of QX200™ddPCR™ Supermix for Probes (No dUTP) (BioRad). PCR reactions were converted to droplets in DG8™ cartridges (Bio-Rad) using the QX200™ droplet generator (Bio-Rad), and amplified in a C1000 Touch™ thermal cycler (Bio-Rad). Amplification events within individual droplets were measured by the QX200™ droplet reader (Bio-Rad) and the resulting data were analysed using QuantaSoft™ software (Bio-Rad). Plasmid copy number is defined as the number of reads for the chromosomal gene *rpoA* divided by the number of reads for the plasmid gene *tetB*(P). Statistical analysis was carried out using the Mann-Whitney *u*-test on four independent biological replicates.

Results

ResP, is a serine recombinase enzyme that is encoded by all *C. perfringens* plasmid family types

The pCW3 gene *resP* is predicted to encode a protein belonging to the serine recombinase family since it has a predicted serine recombinase catalytic domain making up the central portion (AA 48-183) of the 247 AA protein (Bannam *et al.*, 2006). Typically, serine recombinase enzymes possess a DNA binding helix-turn-helix (HTH) motif that allows them to bind specific DNA sequences prior to catalytic cleavage (Grindley *et al.*, 2006).

To confirm the classification of ResP as a serine recombinase, its sequence was compared to other members of the serine recombinase family (Figure 3.1). Analysis showed that ResP only had low level AA sequence identity to the well-characterised serine recombinases from transposons Tn*3* and γδ (Figure 3.1A). However, alignment of protein sequences from these recombinases demonstrated the conservation of key catalytic- and DNA binding-residues (Figure 3.1B), which suggests that ResP may function *via* a similar mechanism.

Analysis of *C. perfringens* plasmid sequences consistently identifies genes encoding homologues of ResP from pCW3 (Garnier *et al.*, 1987; Mehdizadeh Gohari *et al.*, 2016; Shimizu *et al.*, 2002;

A

	ResP (pCW3)	**TnpR** (*Tn* 3)	**TnpR** (γδ)
ResP (pCW3)	100	31.9	34.4
TnpR (*Tn* 3)	31.9	100	80.3
TnpR (γδ)	34.4	80.3	100

B

```
ResP  (YP_001967747.1)      MRYKLTYVYGDSDQKFTQTFSSKVLMESYIETGKDKDLRVINIESSKLYGYARVSSKEQN     60
Tn3   (YP_190221)           -------------------------------------------MRIFGYARVSTSQQS     15
γδ    (NP_061388)           -------------------------------------------MRLFGYARVSTSQQS     15
                                                                        :::******:.:*.

ResP  (YP_001967747.1)      LDRQIEALKEYGVNERDIITDKQSGKDFNREGYKTLKEQLLRSGDVLVIKELDRLGRNMA     120
Tn3   (YP_190221)           LDIQIRALKDAGVKANRIFTDKASGSSTDREGLDLLRM-KVEEGDVILVKKLDRLGRDTA     74
γδ    (NP_061388)           LDIQVRALKDAGVKANRIFTDKASGSSSDRKGLDLLRM-KVEEGDVILVKKLDRLGRDTA     74
                            ** *:.***: **: . *:*** **.. :*:* . *:   :..***:::*:******: *

ResP  (YP_001967747.1)      QIKEEWNDLQAKEINIVVIDTPILNTEGKSNLEKTLISNIVFELLSYMAEKERVKIKQRQ     180
Tn3   (YP_190221)           DMIQLIKEFDAQGVAVRFIDDGISTDG--------DMGQMVVTILSAVAQAERRRILERT     126
γδ    (NP_061388)           DMIQLIKEFDAQGVSIRFIDDGISTDG--------EMGKMVVTILSAVAQAERQRILERT     126
                            :: :  ::::*: : : .**  * .          :.::*. :** :*: ** :* :*

ResP  (YP_001967747.1)      AEGIANAKAKGKHLGRPRVEYPGNFKEVYDKWKAKEITGVKAMELMNLKKNSFYNLIKKY     240
Tn3   (YP_190221)           NEGRQEAKLKGIKFGRRRTVDRNVV---LTLHQKG-TGATEIAHQLSIARSTVYKILEDE     182
γδ    (NP_061388)           NEGRQEAMAKGVVFGRKRKIDRDAV---LNMWQQG-LGASHISKTMNIARSTVYKVINES     182
                             **  :*  **  :** *    . .      :    . .  . :.: :.:.*::::.

ResP  (YP_001967747.1)      EKEKKSI    247
Tn3   (YP_190221)           RAS----    185
γδ    (NP_061388)           N------    183
```

Figure 3.1: Alignment of amino acid sequences of Tn*3*, γδ and pCW3 ResP and percent identiy matrix. A. Percent identity matrix comparing pCW3-encoded ResP (YP_001967747.1) to the amino acid sequences of TnpR resolvase (YP_190221) from the Tn*3* transposon and TnpR from γδ transposon (NP_061388). **B.** Amino acid alignment of the serine recombinase enzymes TnpR from Tn*3*, TnpR from γδ and pCW3-encoded ResP, produced using Clustal Omega. The characterised nucleophilic serine from Tn*3* is highlighted in yellow. Other conserved Tn*3* catalytic residues are highlighted in green and residues involved in DNA binding are highlighted in pink.

Yonogi *et al.*, 2014). Phylogenetic comparison of ResP from different *C. perfringens* plasmids demonstrated that ResP proteins could be grouped based on the type of plasmid on which they are encoded (Figure 3.2). *C. perfringens* ResP proteins form two distinct clades, with ResP from pCP13-like and pIP404-like plasmids grouping together to form a discrete clade that is separate from ResP proteins encoded on pCW3-like plasmids. The large degree of dissimilarity between proteins from different plasmid families may indicate family specificity and separate evolutionary pathways of multimer resolution systems.

ResP is not required for the conjugative transfer of pCW3

To assess the function of ResP in pCW3 plasmid biology, individual mutants were constructed by allelic exchange, whereby the *resP* gene was replaced with an erythromycin gene, *erm*(Q). The genotypes of the resultant mutants were confirmed using PCR (data not shown) and Southern blotting (Figure 3.3).

To determine if ResP is required for conjugation, the mutant was assessed using a mixed plate mating assay (Figure 3.4). Deletion of *resP* from pCW3 did not alter the conjugation efficiency, indicating that *resP* is not required for the conjugative transfer of pCW3.

ResP is essential for pCW3 plasmid stability

As multimer resolution is a key mechanism utilised by plasmids for stability, the stability phenotype of one of the *resP* mutants was assessed using a non-selective stability assay. For this assay, strains were passaged continuously over the course of six days in broth alongside a wild-type control. To determine the stability of the various plasmids, viable counts were carried out every second day (0, 2, 4, 6) and 100 resulting colonies were cross-patched onto selective media containing tetracycline (to detect the presence of pCW3) and non-selective medium.

The results showed that the *resP* mutant plasmid was unstable in comparison to wild-type pCW3, with an average of 67.5±6% of the population retaining the plasmid following six days passage,

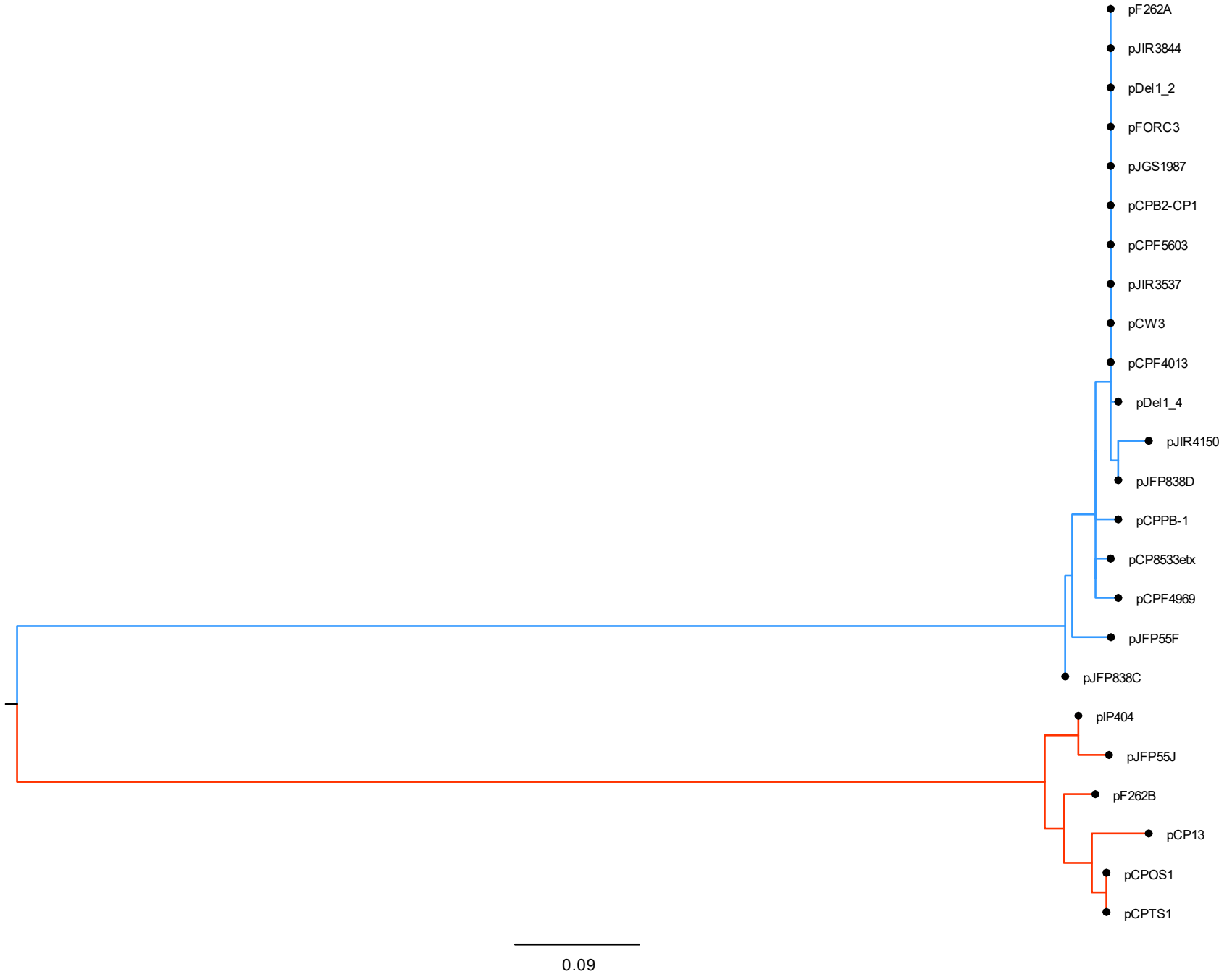
pF262A
pJIR3844
pDel1_2
pFORC3
pJGS1987
pCPB2-CP1
pCPF5603
pJIR3537
pCW3
pCPF4013
pDel1_4
pJIR4150
pJFP838D
pCPPB-1
pCP8533etx
pCPF4969
pJFP55F
pJFP838C
pIP404
pJFP55J
pF262B
pCP13
pCPOS1
pCPTS1
0.09

Figure 3.2: Phylogenetic tree showing the clustering of *C. perfringens*-encoded ResP proteins. A multiple sequence alignment using Clustal Omega was performed with sequences of 24 ResP proteins from various *C. perfringens* plasmids. A phylogenetic tree was generated using the neighbour joining method and visualised as a rooted phylogram using FigTree. The clades are coloured based on the plasmid family in which they belong; highlighted in blue are ResP from pCW3-like plasmids and in orange are ResP from pCP13-like and pIP404-like plasmids. Accession numbers of proteins analysed are listed in Materials and Methods.

A

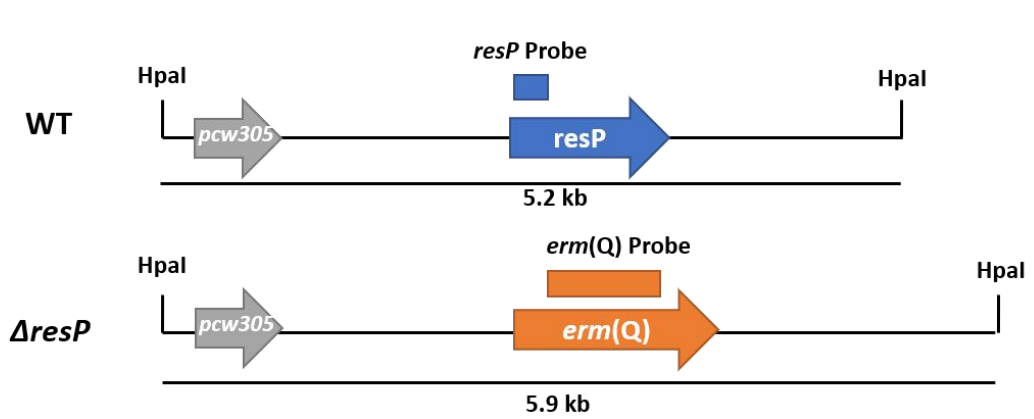
A
resP Probe
HpaI
HpaI
WT
pcw305
resP
5.2 kb
erm(Q) Probe
HpaI
HpaI
ΔresP
pcw305
erm(Q)
5.9 kb

B

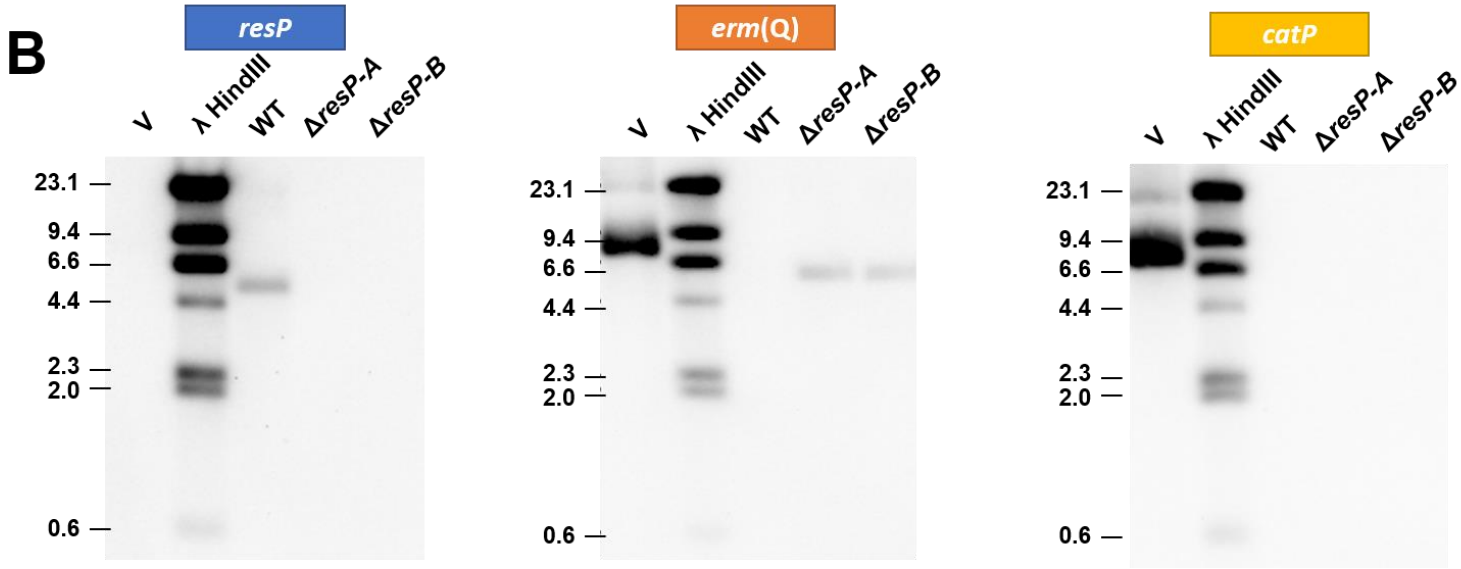
B
resP
V
λ HindIII
WT
ΔresP-A
ΔresP-B
23.1
9.4
6.6
4.4
2.3
2.0
0.6
erm(Q)
V
λ HindIII
WT
ΔresP-A
ΔresP-B
23.1
9.4
6.6
4.4
2.3
2.0
0.6
catP
V
λ HindIII
WT
ΔresP-A
ΔresP-B
23.1
9.4
6.6
4.4
2.3
2.0
0.6

Figure 3.3: Southern hybridisation confirmation of *resP* mutants. Genomic DNA was purified and digested with the enzyme HpaI. The Southern blots were probed with DIG-labelled DNA probes specific for *catP*, carried on the double-crossover vector backbone, *erm*(Q), encoded within the double crossover selection cassette, and the gene of interest, *resP*. **A.** Schematic representation of wild-type and *resP* mutant DNA fragments digested with HpaI**.** ORFs are represented by the thick arrows. **B.** Confirmation of independent *resP* mutants. Lanes are labelled as follows: V –undigested *resP* double crossover vector, λ HindIII - DIG-labelled Lambda HindIII molecular size markers (kilobases), WT- wild-type *C. perfringens* JIR4195 DNA. The double crossover site is present on a fragment of 5.2 kb for the wild type and 5.9 kb for the *correct* mutants. The *resP* gene was detected on a 5.2 kb fragment in the wild type, but not detected in the mutant strains, as expected. The *erm*(Q) gene was not detected in the wild type but was detected on a fragment of 5.9 kb in independent mutant strains. Lastly, the *catP* gene was not detected in the wild type or either of the mutant strains.

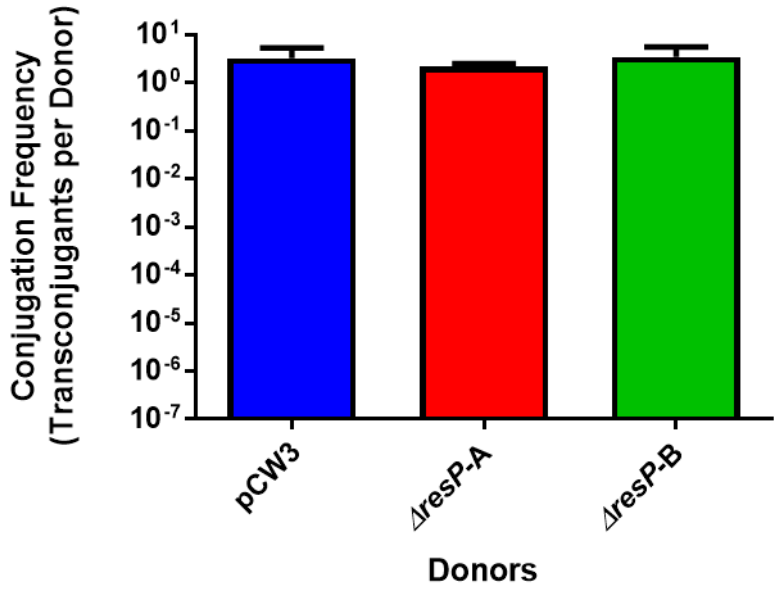

Figure 3.4: Conjugation frequencies of independently derived *resP* mutants. Mixed plate matings were conducted with JIR4195 derivative strains as donors and the isogenic strain 13 derivative JIR4394 as a recipient. Conjugation frequency is described as the number of transconjugants cells per donor cell. Donors are shown on the x-axis. The means and standard error of the mean are shown based on the results of at least two biological replicates.

in comparison to 93.3±1% for wild-type pCW3 (Figure 3.5). Complementation *in trans* with the wild-type *resP* gene on the multi-copy shuttle vector, pJIR750 (Bannam & Rood, 1993), restored plasmid stability to wild-type levels (95.3±1%). These results showed that *resP* is required for the stable inheritance of pCW3 under these conditions.

ResP functions in a plasmid family specific manner

Although ResP proteins are encoded by all three of the distinct plasmid families found in *C. perfringens* there remains a large variation in amino acid sequence identity (29% to 100%). To determine if ResP homologues from other *C. perfringens* plasmids could complement the mutation on pCW3, complementation vectors were constructed with *resP* sequences from pCP13 ($resP_{pCP13}$; 29% AA identity to pCW3 ResP) and the pCW3-like plasmid pJIR3844 ($resP_{pJIR3844}$; 98% AA identity) (Figure 3.5). Wild-type pCW3 remained stable over the course of the assay with 96.3±0.8% of the population retaining the plasmid on day 6. Complementation with *resP* from the pCW3-like plasmid, pJIR3844, restored plasmid stability to wild-type levels (94±2.4%), whereas complementation with the *resP* from pCP13 did not restore plasmid stability (69.3±4.8%) compared to the vector control (67.5±6%). These results imply that only closely related *resP* genes can complement a pCW3 *resP* mutation.

Deletion of *resP* from pCW3 does not affect pCW3 copy number

Digital droplet PCR was used to assess whether the instability conferred by loss of *resP* was due to an alteration in plasmid copy number. The results showed that there was no statistically significant difference between the copy number of *resP* mutant plasmids (4.7±0.3 copies per chromosome) and wild-type pCW3 plasmids (4.7±0.1 copies per chromosome) (Figure 3.6), which suggested that plasmid loss in the *resP* mutant strain was not linked to any changes in plasmid copy number.

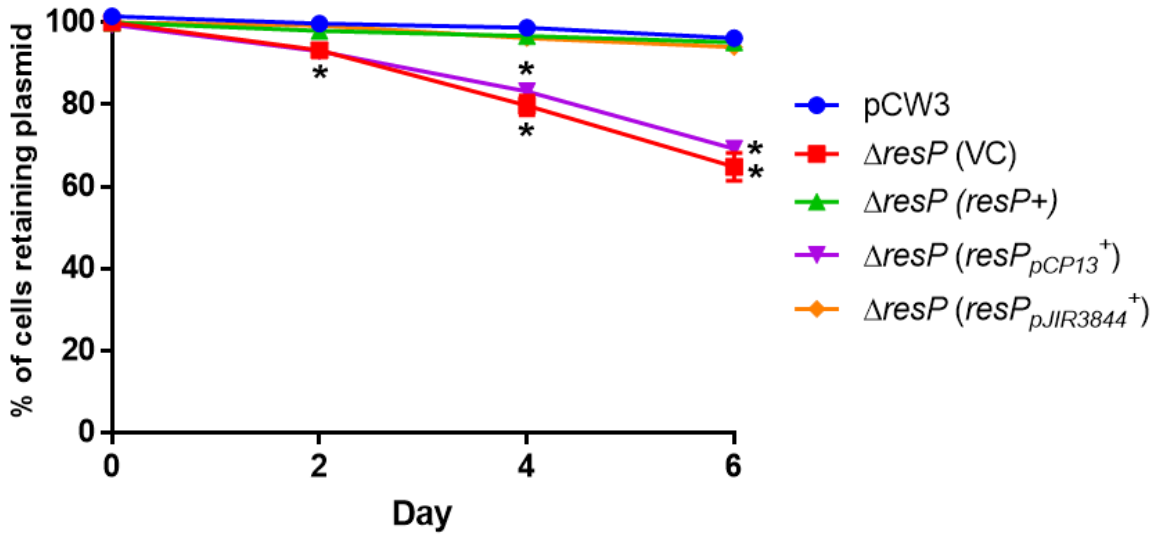

Figure 3.5: Plasmid stability of the *resP* mutant and complemented derivatives. The wild-type, the mutant with the vector alone (VC) and the complemented strains were passaged without selection over the course of six days. Plasmid stability is expressed as the percentage of cells still encoding Tc resistance. The means and standard error of the means are shown, based on results from at least four biological replicates. Statistical analysis was carried out using a Mann-Whitney *u*-test. An asterisk denotes statistical significance ($p < 0.05$) compared to wild-type pCW3.

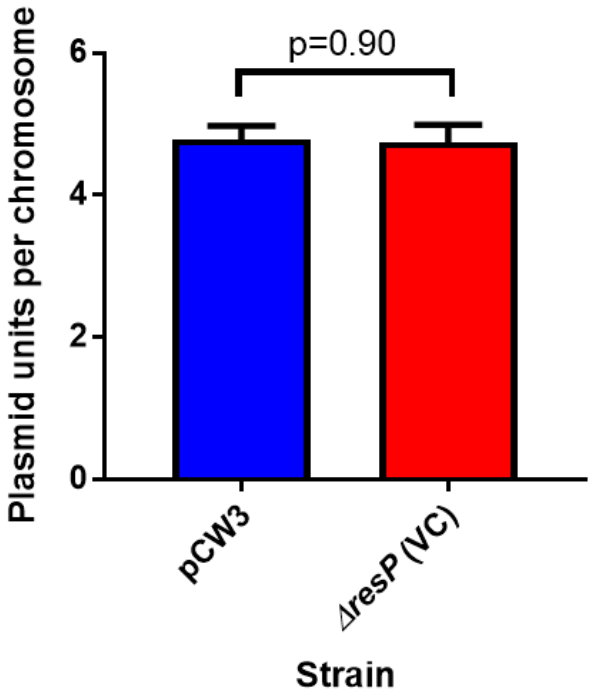

Figure 3.6: Plasmid copy number of independent *resP* mutants. Plasmid copy number was determined using ddPCR with probes targeting single copy chromosome (*rpoB*) and plasmid (*tetB(P)*) genes. Plasmid copy number is calculated by dividing relative reads for the plasmid marker by the values for chromosomal marker and is denoted as the number of plasmid units per chromosome. The means and standard error of the mean are shown based on the results of at least three biological replicates. Statistical analysis was conducted using a student's t-test.

Identification of a potential *res* site on pCW3 and related plasmids

Serine recombinase enzymes catalyse site-specific cleavage of DNA through the recognition of recombination sites (*res* sites) (Stark, 2015). The *res* sites of recombinases from transposons Tn*3* and γδ represent the more common recognition sites, and are characterised by three inverted repeat binding sites, termed sites I, II and III. The site for DNA crossover is located within the centre of site I, between an A and T nucleotide. Since resolvase recognition sites are typically located upstream of the resolvase gene, the sequence upstream of *resP* was analysed for inverted repeat (IR) sequences to identify a *res* site on pCW3 (Figure 3.7). Analysis revealed the presence of three inverted repeat structures directly upstream of the *resP* gene, but, unlike other characterised *res* sites, an AT dinucleotide was not present within the loop structure of site I, the inverted repeat farthest away from the resolvase gene. Instead, an AT sequence was present in the loop structure of site III, the inverted repeat closest to the start of the *resP* gene. All the three IRs contain a 10 base pair imperfect repeat with a consensus sequence, as shown in Figure 3.7 B.

To assess the conservation of this potential *res* site amongst other pCW3-like plasmids, the sequences upstream of *resP* from five pCW3-like plasmids was compared (Figure 3.8). The inverted repeat structures identified on pCW3 are highly conserved. Variation occurs within the loop regions of site I and site II, however, the loop region of site III, which contains an AT dinucleotide, is highly conserved, suggesting that this genetic region may be the site of recombination. The organisation of the repeat sequences upstream of *resP* indicates that the *res* site of pCW3 is similar to that of other serine recombinases. However, pCW3 *res* appears to be organised in the opposite orientation as shown by the location of the putative cleavage AT dinucleotide within site III. This finding implies that *C. perfringens* ResP may function by cleaving within the third inverted repeat, however, this hypothesis remains to be tested.

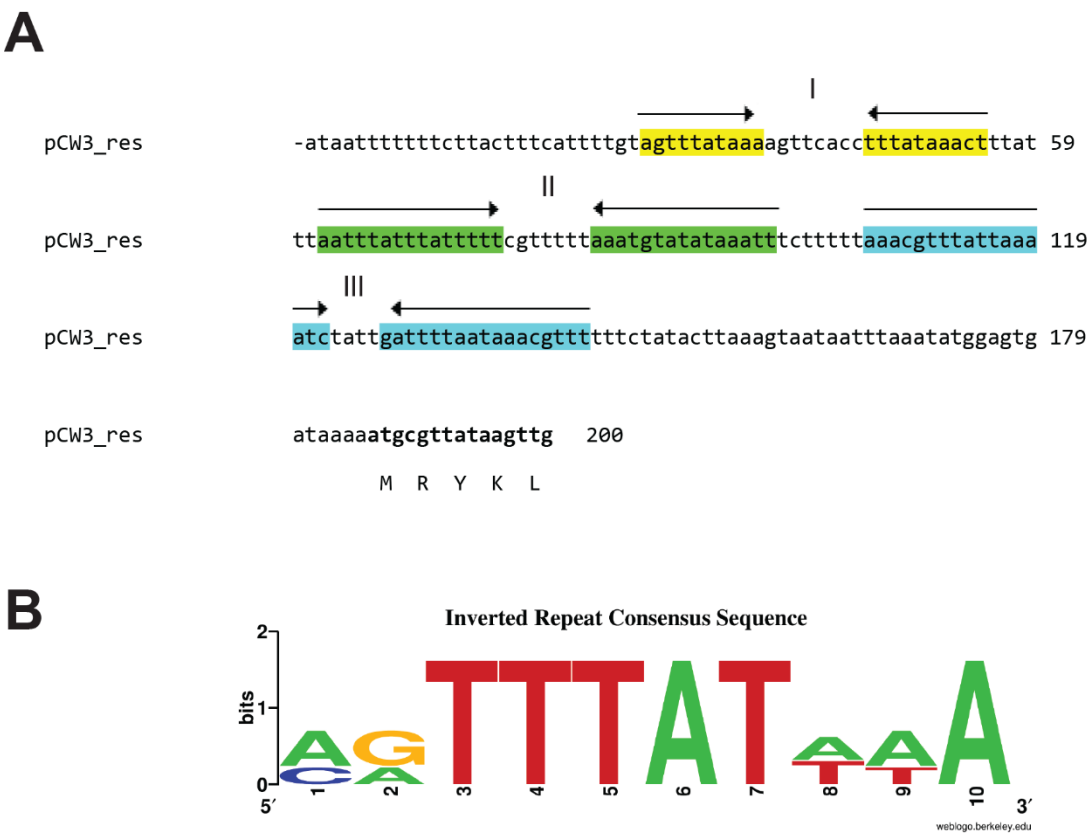

Figure 3.7: Genetic map of *resP* upstream region and inverted repeat consensus sequence. **A.** The nucleotide sequence of the region upstream of the *resP* gene and the first five amino acids of the ResP protein are shown. Inverted repeats are denoted by the arrows. The Site I inverted repeat is highlighted in yellow, the Site II inverted repeat is highlighted in green and the Site III is highlighted in blue. **B.** Inverted repeat consensus sequence image generated using WebLogo (Crooks *et al.*, 2004). Ten conserved nucleotides from left and right sides of each inverted repeat were aligned and a sequence logo generated. The overall height of each letter indicates the level of sequence conservation at that position.

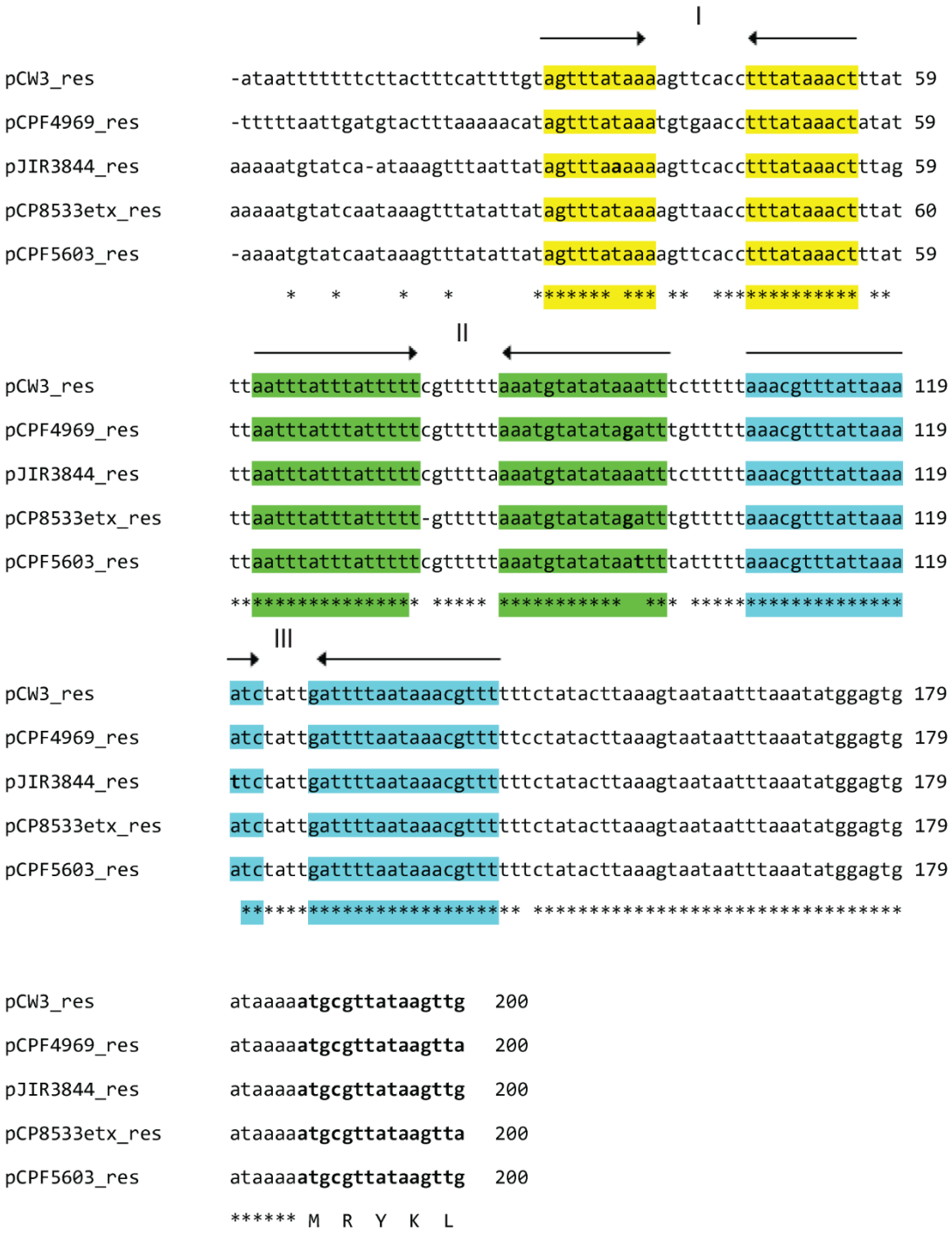

Figure 3.8: Multiple sequence alignment of putative *res* sites from five pCW3-like plasmids. Nucleotide sequences upstream of the *resP* genes from pCW3, pCPF4969, pJIR3844, pCP8533*etx* and pCPF5603 were aligned. Nucleotide conservation is denoted by an asterisk below the aligned sequences. Inverted repeats are denoted by arrows. The Site I inverted repeat is highlighted in yellow, the Site II inverted repeat is highlighted in green and the Site III is highlighted in blue.

ResP resolves DNA between two directly repeated *res* sites

Serine recombinase enzymes catalyse site-specific cleavage of DNA, through the recognition of two directly repeated *res* sites on the same DNA molecule (Stark, 2015). Since ResP was predicted to resolve plasmid multimers, pulsed field gel electrophoresis was used to assess plasmid multimer formation in the wild type and *resP* mutant strains. The results of this analysis were inconclusive (data not shown), because of the inherent difficulties associated with pulsed field gel electrophoresis and DNA resolution (Han & Craighead, 2000). Thus, the ability of ResP to recognise and resolve DNA containing directly repeated pCW3 *res* sites was assessed using an excision assay in *E. coli*. The pUC18-derived vector, pJIR2715 (encoding chloramphenicol and erythromycin resistance), was used as a base plasmid for the excision assay, as it possesses multiple cloning sites on either side of an *erm*(Q) gene, which confers erythromycin resistance (Figure 3.9A-1). To assess the requirement of multiple *res* sites for recombination two separate plasmids were constructed. The first plasmid, pJIR4833, contained a single *res* site that preceded the *erm*(Q) gene (Figure 3.9A-2). The second plasmid, pJIR4834, had two copies of the putative *res* site, located in direct orientation on either side of the *erm*(Q) gene (Figure 3.9A-3). In addition, the wild-type *resP* gene was cloned into a compatible pSU39 vector (encoding kanamycin resistance; Figure 3.9A-4), generating pJIR4835 (Figure 3.9A-5). For simplicity this plasmid will be referred to as pResP. In the presence of ResP, a loss of erythromycin resistance would be expected from pJIR4834, but not pJIR4833, as ResP would excise the *res-erm*(Q) cassette by acting at the directly repeated *res* sites (Figure 3.9B). Following the introduction of either pSU39 or pResP into *E. coli* strains harbouring the pJIR2715 derivative plasmids, the ability of ResP to excise the erythromycin cassette was assessed. After transformation, cells were plated onto media supplemented with Kn and Cm. From each transformation, 100 colonies were patched onto media supplemented with Em (to assess erythromycin resistance) and Cm (to confirm the presence of the pJIR2715 plasmid derivative). The percentage of excision was determined by comparing the number of colonies resistant to Em to those present on media with Cm. No loss of

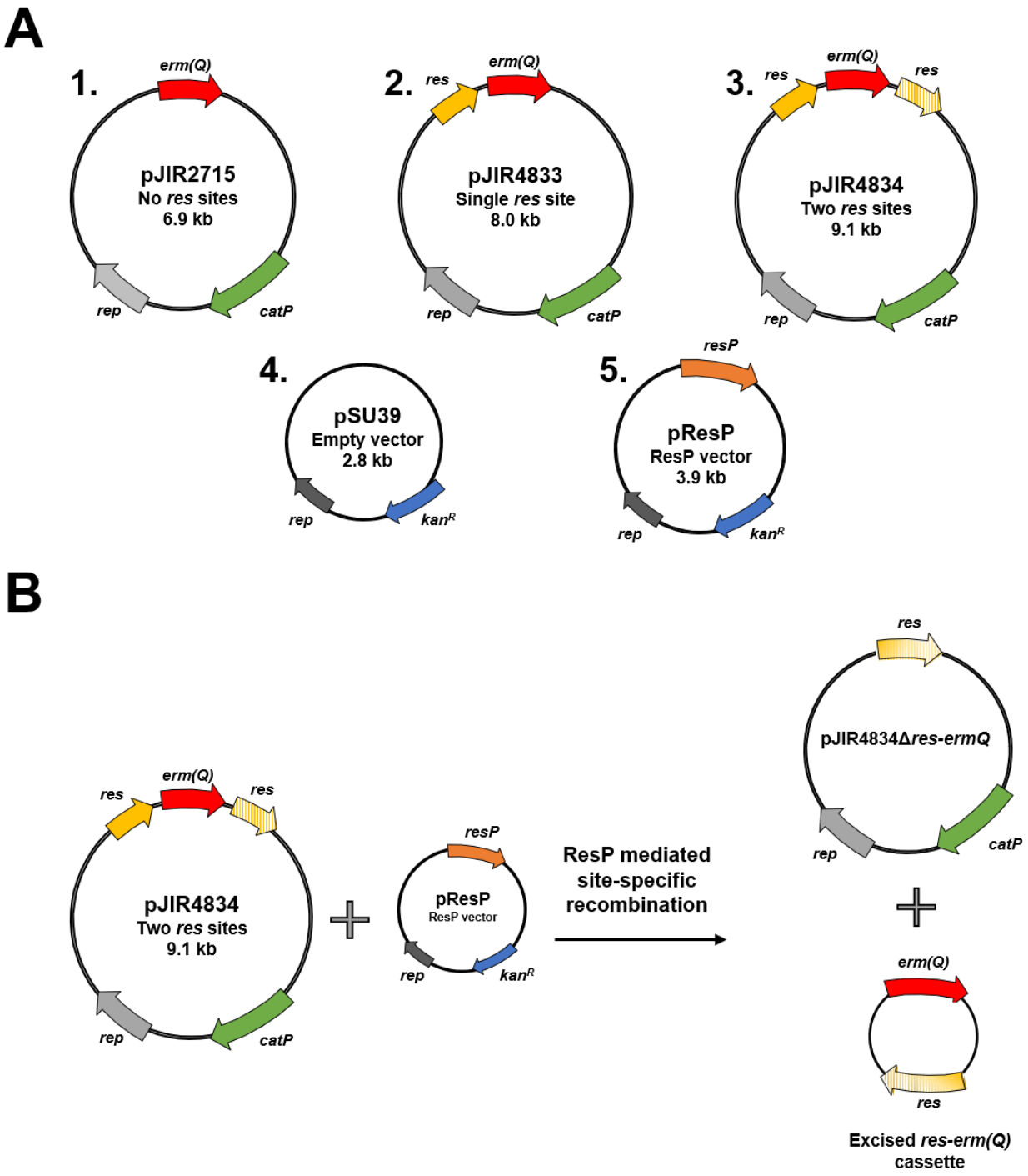
A
1.
erm(Q)
pJIR2715
No res sites
6.9 kb
rep
catP
2.
res
erm(Q)
pJIR4833
Single res site
8.0 kb
rep
catP
3.
res
erm(Q)
res
pJIR4834
Two res sites
9.1 kb
rep
catP
4.
pSU39
Empty vector
2.8 kb
rep
kanR
5.
resP
pResP
ResP vector
3.9 kb
rep
kanR
B
res
erm(Q)
res
pJIR4834
Two res sites
9.1 kb
rep
catP
resP
pResP
ResP vector
rep
kanR
ResP mediated
site-specific
recombination
res
pJIR4834Δres-ermQ
rep
catP
erm(Q)
res
Excised res-erm(Q)
cassette

Figure 3.9: Vector maps of the plasmids used in the excision assay and the mechanism of ResP-mediated excision of *erm*(Q) from pJIR4834. A. Diagrams of the plasmids constructed for this assay. 1. pJIR2715 base plasmid, 2. pJIR4833, pJIR2715 with a single *res* site preceding the *erm*(Q) gene, 3. pJIR4834, pJIR2715 with two directly repeated *res* sites flanking the *erm*(Q) gene, 4. pSU39 base plasmid and 5. pResP, pSU39 with wild-type *resP* gene. **B.** Schematic representation of proposed excision products of pJIR4834 produced following recombination by ResP.

erythromycin resistance was observed for strains containing pJIR2715 or pJIR4833 regardless of the presence or absence of ResP. For the pJIR2715 derivative with *res* sites flanking the *erm*(Q) gene (pJIR4834) there was no recorded loss of erythromycin resistance when the pSU39 base plasmid was introduced. However, in the presence of pResP, erythromycin resistance was lost at a frequency of 100%, demonstrating highly efficient ResP-mediated excision of the *res*-*erm*(Q) cassette (Table 3.4). The excision of *erm*(Q) was so efficient that construction of a strain containing these plasmids that was resistant to Em, Cm and Kn was not possible.

Plasmid DNA was extracted from the strains and assessed by restriction analysis, using the enzyme BamHI to linearise all of the plasmids (Figure 3.10). Plasmid DNA extracted from strains harbouring pJIR2715 or pJIR2715 with one *res* site did not show any changes in restriction pattern after introduction of ResP or the vector control (Figures 3.10A and B). Similarly, plasmid DNA extracted from the strain harbouring pJIR2715 with *res* sites flanking the *erm*(Q) gene was unchanged following introduction of the vector (Figure 3.10C). However, plasmid DNA extracted from the strain harbouring pResP and pJIR2715 with *res* sites flanking the *erm*(Q) gene was located at approximately 5000 bp, which is much lower than the pJIR4834 plasmid that was present in the strain prior to the addition of pResP. This size difference corresponds with the expected reduction in size that would be observed following excision of the *res*-*erm*(Q) cassette in this plasmid preparation (Figure 3.10C). To confirm the excision of the *res*-*erm*(Q) cassette from this strain sequencing across the *res*-*erm*(Q)-*res* region was performed. Sequencing was also performed on all other plasmid preparations derived from the excision assay. The results confirmed that there were no sequence changes in the pJIR4833 preparations, regardless of the presence or absence of ResP. Similarly, no sequence changes were observed for the pJIR4834 derivative following the addition of pSU39. However, sequencing confirmed the loss of the *res*-*erm*(Q) cassette from plasmid DNA extracted from the strain harbouring pResP and pJIR4834, as no sequence corresponding to *erm*(Q) was obtained. Instead, only the sequence of a single

Table 3.4: Results of the excision assay

Plasmid present in *E. coli* cells	% Em^R cells	
	pSU39 introduced	**pResP introduced**
pJIR2715 Vector control	100	100
pJIR4833 Single *res* site	100	100
pJIR4834 Two *res* sites	100	0

Following introduction of either pSU39 or pResP into *E. coli* strains harbouring pJIR2715 or a derivative, transformants were selected on media supplemented with Kn and Cm. 100 subsequent transformant colonies were concurrently patched onto media supplemented with Cm or Em. The number of viable patches on each plate was evaluated and the % of Em^R colonies calculated. Shown are the means based on at least four replicates. The standard error of the mean could not be calculated as the values obtained were identical in each replicate experiment.

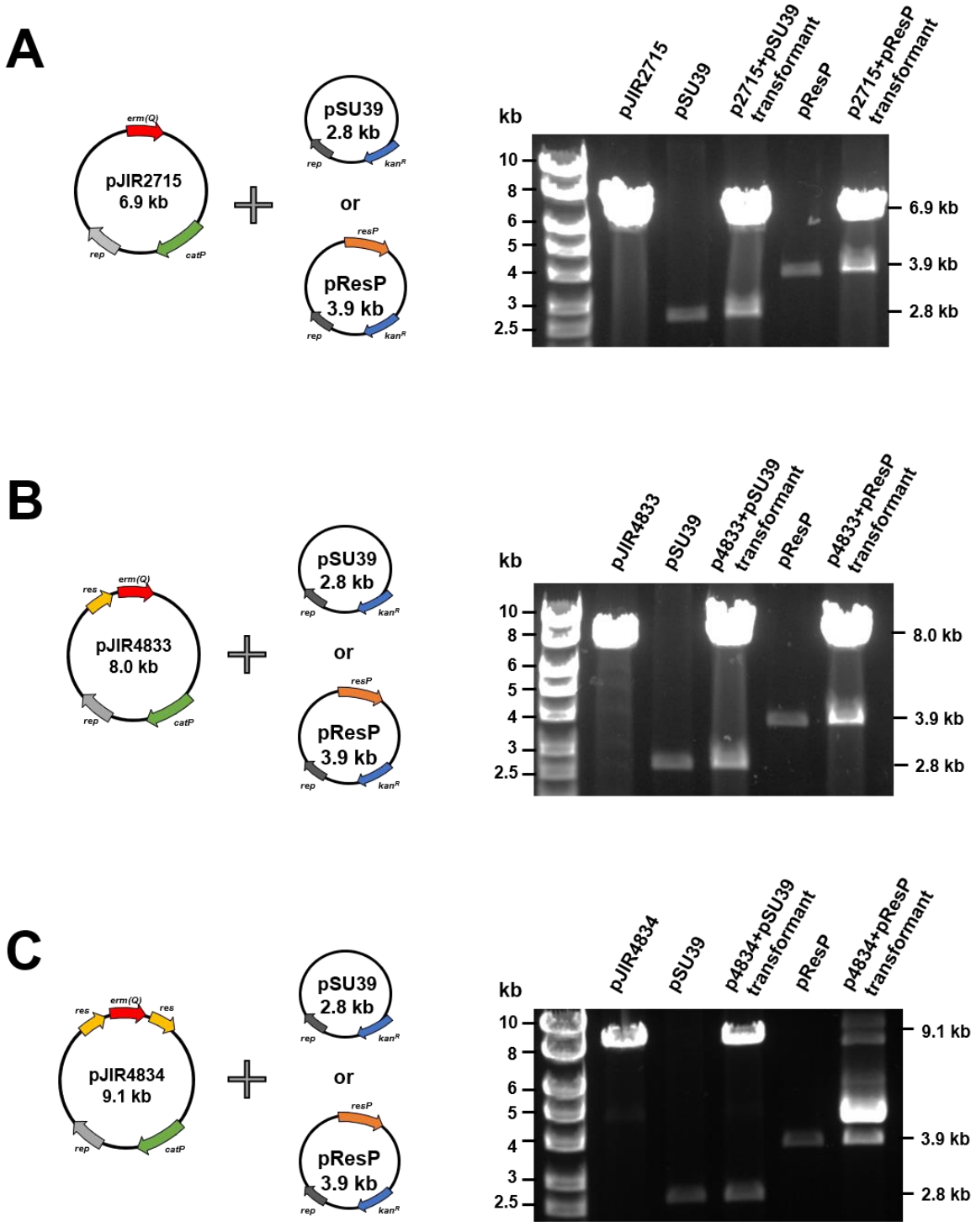
A
erm(Q)
pJIR2715
6.9 kb
rep
catP
pSU39
2.8 kb
rep
kanR
or
resP
pResP
3.9 kb
rep
kanR
pJIR2715
pSU39
p2715+pSU39 transformant
pResP
p2715+pResP transformant
kb
10
8
6
5
4
3
2.5
6.9 kb
3.9 kb
2.8 kb
B
erm(Q)
res
pJIR4833
8.0 kb
rep
catP
pSU39
2.8 kb
rep
kanR
or
resP
pResP
3.9 kb
rep
kanR
pJIR4833
pSU39
p4833+pSU39 transformant
pResP
p4833+pResP transformant
kb
10
8
6
5
4
3
2.5
8.0 kb
3.9 kb
2.8 kb
C
erm(Q)
res
res
pJIR4834
9.1 kb
rep
catP
pSU39
2.8 kb
rep
kanR
or
resP
pResP
3.9 kb
rep
kanR
pJIR4834
pSU39
p4834+pSU39 transformant
pResP
p4834+pResP transformant
kb
10
8
6
5
4
3
2.5
9.1 kb
3.9 kb
2.8 kb

Figure 3.10: Plasmid profiles obtained following excision assay. Schematic diagrams with the plasmid combinations tested in the excision assay are shown on the left. The corresponding gel images of plasmid profiles obtained following introduction of either pSU39 or pResP into *E. coli* strains harbouring pJIR2715 (**A**), pJIR4833 (**B**) or pJIR4834 (**C**) are shown beside the schematics. Hyperladder size standards are reported in kilobase pairs (kb). Plasmid profiles shown are representative of four replicate assays.

complete *res* site was acquired, which confirmed the occurrence of a site-specific recombination event between two *res* sites in this strain.

Discussion

This study has demonstrated the importance of the ResP resolvase for the stability of the *C. perfringens* plasmid pCW3. Mutation of *resP* resulted in a reduction in pCW3 stability, this phenotype was then rescued following *in trans* complementation. Analysis of the sequence of pCW3-encoded ResP protein revealed the presence of a domain highly similar to the serine recombinase family (Bannam *et al.*, 2006). Comparison of ResP to other characterised serine recombinases established the conservation of key residues required for enzymatic function (Figure 3.1). This result suggested that the mechanism of function of ResP was similar to other enzymes within this family.

Comparative analysis established that ResP proteins are encoded on all three plasmid types found within *C. perfringens*. When analysed phylogenetically, ResP proteins encoded on pCW3-like plasmids grouped separately to ResP from the pCP13-like plasmids and pIP404-like plasmids, forming a distinct clade (Figure 3.2). The low-level homology between ResP proteins encoded by different plasmid families speaks to the separate evolution of the multimer resolution systems utilised by these unrelated plasmids. This situation is reminiscent of the plasmids of *S. aureus* whereby some plasmids carry *sin* resolvase genes whereas others encode a distantly related, but mechanistically similar, Res protein (LeBard *et al.*, 2008; Paulsen *et al.*, 1994).

Until recently, only one *C. perfringens* plasmid multimer resolution protein had been studied; the Res enzyme that is encoded on the small bacteriocin plasmid pIP404 (Garnier *et al.*, 1987). However, due to the lack of available genetic tools for clostridial species at that time, the role of Res in the context of pIP404 plasmid stability was not examined (Garnier *et al.*, 1987). In this study, the role of ResP in the stability of pCW3 was examined. In the absence of ResP, pCW3 was unstable and readily lost from approximately 32.5% of the population following six days passage

(Figure 3.5). When ResP was provided *in trans,* pCW3 stability was restored to wild-type levels, providing evidence for the importance of ResP in pCW3 stability. ResP from another pCW3-like plasmid was also able to rescue the stability phenotype when provided *in trans* (Figure 3.5). When the distantly related ResP (29 % AA identity) from pCP13 was provided, pCW3 remained unstable (Figure 3.5), implying that the more divergent ResP protein is unable to function on pCW3. This finding further supports the argument of the separate evolution of the multimer resolution systems utilised by these unrelated plasmids (Watts *et al.*, 2019).

When multimer formation within the wild-type and *resP* mutant strains was assessed using pulsed field gel electrophoresis and subsequent Southern hybridisation the results were inconclusive. It remains unknown whether the inconclusive results were due to limitations in experimental procedure or whether pCW3 multimer formation occurs at a low frequency. This study then focused on demonstrating ResP function in a more amenable bacterial background. Serine recombinase mediated site-specific recombination requires the recognition of specific recombination sites, *res* sites. Analysis of the sequence upstream of ResP identified a region of 96 bp that contained three conserved inverted repeats, with dyad symmetry, hypothesised to be the pCW3 *res* site (Figure 3.9A). The organisation of the pCW3 *res* site was typical of other resolvase enzymes such as Tn*3* and γδ recombinases, which are characterised by three inverted repeat binding sites, termed site I, II and III. For the Tn*3* and γδ recombinases, cleavage and recombination of DNA occurs between an AT dinucleotide present within the loop region of site I; the inverted repeat furthest away from the start of the resolvase gene. When the loop region of the proposed site I of pCW3 *res* was examined, an AT dinucleotide was not present (Figure 3.9A). When the conservation of nucleotides within this loop structure amongst other pCW3-like plasmids was examined variation occurred most prominently within this site (Figure 3.8). When the loop structures of the other inverted repeats were analysed, it was noted that variation did not occur within the loop of site III, instead it remained highly conserved amongst the five plasmids analysed (Figure 3.8). In addition, the loop structure of site III contained an AT

dinucleotide, suggesting that this is where recombination occurs. The location of the putative cleavage site within site III (closest to the beginning of the resolvase gene) implies that the organisation of these sites on pCW3 is reversed in comparison to the organisation of characterised *res* sites, whereby site I would be the inverted repeat closest to the *resP* gene and site III the furthest. The two other sites, that do not possess a conserved loop structure, are likely to be accessory binding sites for the ResP protein, as is seen for other resolvase systems. For example, TnpR from transposon γδ, requires these two accessory sites for efficient site-specific recombination (Stark *et al.*, 1989b). These accessory sites also function by imposing a 'topological filter' to inhibit DNA inversion reactions and intermolecular recombination between separate DNA molecules possessing *res* sites (Grindley *et al.*, 2006; Stark *et al.*, 1989a; Stark *et al.*, 1989b).

The ability of ResP to recognise and recombine the putative pCW3 *res* site was examined using an excision assay (Table 3.4 and Figure 3.10). The results suggest that ResP can recognise directly repeated *res* sites on the same plasmid molecule and resolve the DNA between these sites, as evidenced by the highly efficient excision of the *res-erm*(Q) cassette from plasmids containing directly repeated *res* sites exposed to functional ResP. The *in vivo* plasmid excision assay model that was used demonstrated a highly efficient recombination mediated by ResP, as all cells analysed with this plasmid combination were no longer resistant to erythromycin. When a plasmid encoding functional ResP was introduced into cells with plasmids containing only a single *res* site, recombination did not occur, providing evidence that ResP recognises and recombines DNA only when two *res* sites are present on the same molecule. The recognition and recombination of multiple *res* sites on a single plasmid molecule is typical of resolvase enzymes, however, since pCW3 ResP is predicted to be a serine recombinase, a family of enzymes that can resolve or invert DNA, it would be pertinent to assess if ResP functions solely as a resolvase or can invert DNA sequences. Current evidence suggests that the *res* site on pCW3 is typical of resolvase only reactions, as evidenced by the presence of two putative accessory binding sites,

which are hypothesised to inhibit DNA inversion reactions (Stark *et al.*, 1989a; Stark *et al.*, 1989b).

Excision mediated by other serine recombinases from *C. perfringens* is not as efficient as reported here (Adams *et al.*, 2006; Bannam *et al.*, 1995; Crellin & Rood, 1997). However, the rate of excision mediated by ResP is on par with other recombinase enzymes involved in plasmid multimer resolution. In a similar experiment conducted on the Xer recombinase system of *E. coli,* complete excision was observed when vectors possessing two direct *psi* recombination sites flanking a kanamycin resistance gene were introduced into a Xer+ strain background (Blake *et al.*, 1997). This finding demonstrates that recombinase-mediated resolution of multimeric plasmids occurs at highly efficient rates, the reason for such fast recombination remains unknown, but would be an exciting avenue of investigation.

In conclusion, this study has demonstrated that the site-specific recombinase ResP is essential for pCW3 plasmid stability and is highly likely to function as part of a multimer resolution system. Overall the findings of this study have further defined the mechanisms by which the pCW3-like plasmids of *C. perfringens* stably maintain themselves within this pathogenic bacterium.

References

Adams, V., Lucet, I. S., Tynan, F. E., Chiarezza, M., Howarth, P. M., Kim, J., Rossjohn, J., Lyras, D. & Rood, J. I. (2006). Two distinct regions of the large serine recombinase TnpX are required for DNA binding and biological function. *Molecular Microbiology* **60**, 591-601.

Adams, V., Watts, T. D., Bulach, D. M., Lyras, D. & Rood, J. I. (2015). Plasmid partitioning systems of conjugative plasmids from *Clostridium perfringens*. *Plasmid* **80**, 90-96.

Altschul, S. F., Gish, W., Miller, W., Myers, E. W. & Lipman, D. J. (1990). Basic local alignment search tool. *Journal of Molecular Biology* **215**, 403-410.

Austin, S., Ziese, M. & Sternberg, N. (1981). A novel role for site-specific recombination in maintenance of bacterial replicons. *Cell* **25**, 729-736.

Bannam, T. L., Crellin, P. K. & Rood, J. I. (1995). Molecular genetics of the chloramphenicol-resistance transposon Tn4451 from *Clostridium perfringens*: the TnpX site-specific recombinase excises a circular transposon molecule. *Molecular Microbiology* **16**, 535-551.

Bannam, T. L. & Rood, J. I. (1993). *Clostridium perfringens-Escherichia coli* shuttle vectors that carry single antibiotic resistance determinants. *Plasmid* **29**, 233-235.

Bannam, T. L., Teng, W. L., Bulach, D., Lyras, D. & Rood, J. I. (2006). Functional identification of conjugation and replication regions of the tetracycline resistance plasmid pCW3 from *Clostridium perfringens*. *Journal of Bacteriology* **188**, 4942-4951.

Bannam, T. L., Yan, X.-X., Harrison, P. F., Seemann, T., Keyburn, A. L., Stubenrauch, C., Weeramantri, L. H., Cheung, J. K., McClane, B. A., Boyce, J. D., Moore, R. J. & Rood, J. I. (2011). Necrotic enteritis-derived *Clostridium perfringens* strain with three closely related independently conjugative toxin and antibiotic resistance plasmids. *mBio* **2**: e00190-11.

Bedbrook, J. R. & Ausubel, F. M. (1976). Recombination between bacterial plasmids leading to the formation of plasmid multimers. *Cell* **9**, 707-716.

Blake, J. A. R., Ganguly, N. & Sherratt, D. J. (1997). DNA sequence of recombinase-binding sites can determine Xer site-specific recombination outcome. *Molecular Microbiology* **23**, 387-398.

Bouet, J.-Y., Bouvier, M. & Lane, D. (2006). Concerted action of plasmid maintenance functions: partition complexes create a requirement for dimer resolution. *Molecular Microbiology* **62**, 1447-1459.

Crellin, P. K. & Rood, J. I. (1997). The resolvase/invertase domain of the site-specific recombinase TnpX is functional and recognizes a target sequence that resembles the junction of the circular form of the *Clostridium perfringens* transposon Tn*4451*. *Journal of Bacteriology* **179**, 5148-5156.

Crooks, G. E., Hon, G., Chandonia, J.-M. & Brenner, S. E. (2004). WebLogo: a sequence logo generator. *Genome research* **14**, 1188-1190.

Eberl, L., Kristensen, C. S., Givskov, M., Grohmann, E., Gerlitz, M. & Schwab, H. (1994). Analysis of the multimer resolution system encoded by the *parCBA* operon of broad-host-range plasmid RP4. *Molecular Microbiology* **12**, 131-141.

Garnier, T., Saurin, W. & Cole, S. T. (1987). Molecular characterization of the resolvase gene, *res*, carried by a multicopy plasmid from *Clostridium perfringens*: common evolutionary origin for prokaryotic site-specific recombinases. *Molecular Microbiology* **1**, 371-376.

Grindley, N. D. F., Whiteson, K. L. & Rice, P. A. (2006). Mechanisms of site-specific recombination. *Annual Review of Biochemistry* **75**, 567-605.

Gurjar, A., Li, J. & McClane, B. A. (2010). Characterization of toxin plasmids in *Clostridium perfringens* type C isolates. *Infection and Immunity* **78**, 4860-4869.

Han, J. & Craighead, H. G. (2000). Separation of long DNA molecules in a microfabricated entropic trap array. *Science* **288**, 1026-1029.

Hughes, M. L., Poon, R., Adams, V., Sayeed, S., Saputo, J., Uzal, F. A., McClane, B. A. & Rood, J. I. (2007). Epsilon-toxin plasmids of *Clostridium perfringens* type D are conjugative. *Journal of Bacteriology* **189**, 7531-7538.

Krause, M. & Guiney, D. G. (1991). Identification of a multimer resolution system involved in stabilization of the *Salmonella dublin* virulence plasmid pSDL2. *Journal of Bacteriology* **173**, 5754-5762.

LeBard, R. J., Jensen, S. O., Arnaiz, I. A., Skurray, R. A. & Firth, N. (2008). A multimer resolution system contributes to segregational stability of the prototypical staphylococcal conjugative multiresistance plasmid pSK41. *FEMS Microbiology Letters* **284**, 58-67.

Lobato-Márquez, D., Molina-García, L., Moreno-Córdoba, I., García-Del Portillo, F. & Díaz-Orejas, R. (2016). Stabilization of the virulence plasmid pSLT of *Salmonella* Typhimurium by three maintenance systems and its evaluation by using a new stability test. *Frontiers in Molecular Biosciences* **3**, 66-66.

Lyristis, M., Bryant, A. E., Sloan, J., Awad, M. M., Nisbet, I. T., Stevens, D. L. & Rood, J. I. (1994). Identification and molecular analysis of a locus that regulates extracellular toxin production in *Clostridium perfringens*. *Molecular Microbiology* **12**, 761-777.

Marchler-Bauer, A., Derbyshire, M. K., Gonzales, N. R., Lu, S., Chitsaz, F., Geer, L. Y., Geer, R. C., He, J., Gwadz, M., Hurwitz, D. I., Lanczycki, C. J., Lu, F., Marchler, G. H., Song, J. S., Thanki, N., Wang, Z., Yamashita, R. A., Zhang, D., Zheng, C. & Bryant, S. H. (2015). CDD: NCBI's conserved domain database. *Nucleic Acids Research* **43**, D222-D226.

McWilliam, H., Li, W., Uludag, M., Squizzato, S., Park, Y. M., Buso, N., Cowley, A. P. & Lopez, R. (2013). Analysis tool web services from the EMBL-EBI. *Nucleic Acids Research* **41**, W597-W600.

Mehdizadeh Gohari, I., Kropinski, A. M., Weese, S. J., Parreira, V. R., Whitehead, A. E., Boerlin, P. & Prescott, J. F. (2016). Plasmid characterization and chromosome analysis of two *netF+ Clostridium perfringens* isolates associated with foal and canine necrotizing enteritis. *PLOS One* **11**, e0148344.

Paulsen, I. T., Gillespie, M. T., Littlejohn, T. G., Hanvivatvong, O., Rowland, S.-J., Dyke, K. G. H. & Skurray, R. A. (1994). Characterisation of *sin*, a potential recombinase-encoding gene from *Staphylococcus aureus*. *Gene* **141**, 109-114.

Rood, J. I., Maher, E. A., Somers, E. B., Campos, E. & Duncan, C. L. (1978). Isolation and characterization of multiply antibiotic-resistant *Clostridium perfringens* strains from porcine feces. *Antimicrobial Agents and Chemotherapy* **13**, 871-880.

Shimizu, T., Ohtani, K., Hirakawa, H., Ohshima, K., Yamashita, A., Shiba, T., Ogasawara, N., Hattori, M., Kuhara, S. & Hayashi, H. (2002). Complete genome sequence of *Clostridium perfringens*, an anaerobic flesh-eater. *Proceedings of the National Academy of Sciences* **99**, 996-1001.

Stark, W. M. (2015). The serine recombinases. In *Mobile DNA III*: American Society of Microbiology.

Stark, W. M., Boocock, M. R. & Sherratt, D. J. (1989a). Site-specific recombination by Tn*3* resolvase. *Trends in Genetics* **5**, 304-309.

Stark, W. M., Sherratt, D. J. & Boocock, M. R. (1989b). Site-specific recombination by Tn*3* resolvase: Topological changes in the forward and reverse reactions. *Cell* **58**, 779-790.

Summers, D. K. (1991). The kinetics of plasmid loss. *Trends in Biotechnology* **9**, 273-278.

Tolmasky, M. E. (2017). Plasmids. In *Reference Module in Life Sciences*: Elsevier.

Volante, A., Soberón, N. E., Ayora, S. & Alonso, J. C. (2014). The interplay between different stability systems contributes to faithful segregation: *Streptococcus pyogenes* pSM19035 as a model. *Microbiology Spectrum* **2:**PLAS-0007-2013.

Watts, T. D., Johanesen, P. A., Lyras, D., Rood, J. I. & Adams, V. (2017). Evidence that compatibility of closely related replicons in *Clostridium perfringens* depends on linkage to *parMRC*-like partitioning systems of different subfamilies. *Plasmid* **91**, 68-75.

Watts, T. D., Vidor, C. J., Awad, M. M., Lyras, D., Rood, J. I. & Adams, V. (2019). pCP13, a representative of a new family of conjugative toxin plasmids in *Clostridium perfringens*. *Plasmid* **102**, 37-45.

Yonogi, S., Matsuda, S., Kawai, T., Yoda, T., Harada, T., Kumeda, Y., Gotoh, K., Hiyoshi, H., Nakamura, S., Kodama, T. & Iida, T. (2014). BEC, a novel enterotoxin of *Clostridium perfringens* found in human clinical isolates from acute gastroenteritis outbreaks. *Infection and Immunity* **82**: 2390-2399.

Chapter Four

Identification and analysis of *srm*, a gene involved in the stable inheritance of pCW3

Introduction

Plasmids are considered to be the major driving force for bacterial evolution, as they allow for easy and effective horizontal transfer of genetic information between bacterial cells (Tolmasky, 2017). Whilst plasmids can confer beneficial functions, such as antimicrobial resistance as well as virulence- and metabolic-factors, they are typically non-essential and can be lost from bacterial populations (Hülter *et al.*, 2017; San Millan & MacLean, 2017). To persist, plasmids must ensure they are maintained during the numerous cycles of cell division that occur with normal bacterial growth (San Millan & MacLean, 2017). High copy number plasmids can rely on random diffusion and clustered aggregation of plasmid DNA at septum formation (Wang *et al.*, 2016), lower copy number plasmids cannot rely solely on random segregation and, as such, have developed numerous mechanisms to ensure their faithful inheritance (Ebersbach & Gerdes, 2005). These plasmid stability mechanisms include: replication and copy number control, multimer resolution, post-segregational killing, active partitioning and regulation (Tolmasky, 2017). The tight control of replication is a key factor in plasmid stability, ensuring that the plasmid is not only being propagated and maintained at a consistent copy number, but also ensuring enough copies of the plasmid have been made prior to cell division (Pinto *et al.*, 2012).

Following replication, recombination can result in the formation of multimeric plasmids (Bedbrook & Ausubel, 1976). Plasmid multimers decrease the plasmid copy number within a cell, reducing the chance of daughter cells successfully inheriting a plasmid (Summers, 1991). Many plasmids encode site-specific recombinases, which resolve plasmid multimers into individual units, as discussed in the previous chapter (Austin *et al.*, 1981). Post-segregational killing systems are another mechanism plasmids can use to ensure stable inheritance, by creating an 'addiction' to the plasmid (Gerdes *et al.*, 1986). Active partitioning systems act to stabilise plasmids by actively positioning plasmid molecules at either end of the cell during septum formation, ensuring at least one copy of the plasmid will be maintained in each daughter progeny (Gerdes *et al.*, 2010).

Lastly, the regulation of key plasmid functions, including those mentioned above, ensures the metabolic burden of the plasmid on the cell does not become unfavourable and that the plasmid is successfully maintained within the cell (Bingle & Thomas, 2001). Regulation can be achieved through various means, including RNA interactions, as seen for plasmid R1 whereby Rep production is controlled by antisense RNA molecules (Nordström, 2006); and protein-DNA interactions, as demonstrated by the plasmid-encoded transcriptional regulator PagR, which controls virulence gene expression by binding to promoter regions on the *Bacillus anthracis* plasmid pXO1 (Mignot *et al.*, 2003).

This study focused on plasmid stability mechanisms of the tetracycline resistance plasmid, pCW3. The conserved backbone of pCW3-like plasmids incudes genes involved in replication, partitioning, conjugation and plasmid maintenance (Bannam *et al.*, 2011; Li *et al.*, 2013). Whilst the genes involved in replication (Bannam *et al.*, 2006), partitioning (Adams *et al.*, 2015; Watts *et al.*, 2017) and conjugation (Bannam *et al.*, 2006; Bantwal *et al.*, 2012; Parsons *et al.*, 2007; Porter *et al.*, 2012; Steen *et al.*, 2009; Teng *et al.*, 2008; Traore *et al.*, 2018; Wisniewski *et al.*, 2015a; Wisniewski *et al.*, 2015b) have been studied and characterised, little is known about other plasmid maintenance mechanisms encoded on pCW3.

Previous bioinformatic analysis of the pCW3 sequence identified genes that encode products that are strong candidates to function in plasmid maintenance. pCW3 also encodes four genes (*regA, regB, regC* and *regD)* whose products are predicted to function as transcriptional regulators, due to the presence of DNA binding motifs commonly associated with regulation (Bannam *et al.*, 2006). Due to the close proximity and divergent transcription of *regC* to the pCW3 replication gene, *rep*, it is hypothesised that RegC may be a key regulator of plasmid replication or stability functions. Recent analysis has demonstrated the importance of RegC to pCW3 plasmid stability, however, the mechanism of action remains elusive (T. Stent, X. Han, V. Adams, R. Moore, and J. Rood, unpublished).

Finally, there are large regions of pCW3 that remain uncharacterised; one such region is the *dcm* region, (nucleotides 38961-47068 of pCW3), which is located downstream of the *tcp* genes. The *dcm* region encodes ten genes, of which nine are predicted to be hypothetical proteins (Figure 4.1) (Bannam *et al.*, 2006). The putative cytosine-specific DNA methyltransferase encoded by the *dcm* gene is the only gene within this region that has a predicted function (Bannam *et al.*, 2006, Miyamoto *et al.*, 2006). Previous bioinformatic analysis of pCW3-like plasmids has shown that this region is an insertional and recombinational hotspot (Bannam *et al.*, 2011; Li *et al.*, 2007; Parreira *et al.*, 2012). However, there has been no further analysis conducted on the genes located within this genetic region. Despite the unknown function of these genes, they remain highly conserved amongst the Tcp plasmids and could be involved in key processes of pCW3 plasmid biology.

This study provides evidence that the stability of pCW3 involves a previously unreported mechanism potentially unique to *C. perfringens* plasmids. Mutagenesis and subsequent complementation studies demonstrated that pCW3 requires the presence of *pcw348*, a previously uncharacterised and conserved gene, to maintain plasmid stability. Thus, the gene was renamed *srm* for stability replication and maintenance, this broad title was given as the specific role of the gene product has not yet been demonstrated. Analysis also determined that deletion of *srm* increased pCW3 copy number and that recombinant Srm formed higher order oligomers. Overall, these studies have identified a gene essential for the stability of pCW3.

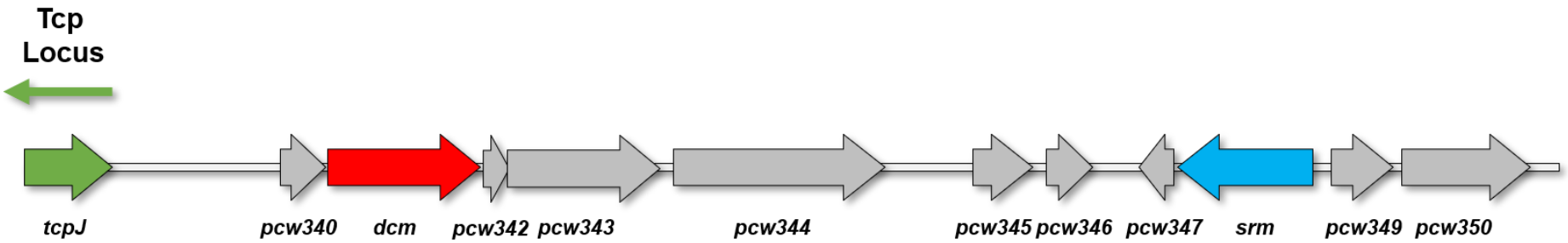

Figure 4.1: Schematic diagram of the *dcm* region of pCW3. A genetic map of the *dcm* region of pCW3 is shown. ORFs are indicated by the arrows and genes labelled below. ORFs labelled in grey encode hypothetical proteins. The *dcm* gene encoding a putative adenine-specific DNA methyltransferase is shown in red. The *srm* gene is shown in blue. The location of *tcpJ,* the last gene of the Tcp locus, is coloured in green and the positioning of the locus is denoted by an arrow.

Materials and Methods

Bacterial strains, plasmids and culture conditions.

C. perfringens strains and plasmids used in this study are listed in Table 4.1**.** *C. perfringens* was cultured as described in Chapter Two. As required, media was supplemented with antibiotics (Sigma) at the following concentrations: tetracycline (Tc; 10 μg/ml), rifampicin (Rif; 10 μg/ml), nalidixic acid (Nal; 10 μg/ml), erythromycin (Em; 50 μg/ml), thiamphenicol (Tm; 10 μg/ml), streptomycin (Str; 1 mg/ml) or saturated potassium chlorate (Chl; 1% v/v).

Escherichia coli strain DH5α (Life Technologies) were cultured at 37°C in 2X YT medium/agar and were supplemented with the following antibiotics as required: kanamycin (Kan; 20 μg/ml), chloramphenicol (Cm; 30 μg/ml) or erythromycin (Em; 150 μg/ml).

Table 4.1: Strains and plasmids used in this study

Strain	Description	Reference
E. coli		
DH5α	F-φ80*lacZ*ΔM15, Δ(*lac*ZYA-*argF*)U169, *rec*A1, *end*A1, *hsd*R17(r_k-, m_k+), *pho*A, *sup*E44, *thi*-1, *gyr*A96, *rel*A1 λ	Invitrogen/ Life Technologies
C41 (DE3)	BL21(DE3) derivative	(Miroux & Walker, 1996)
C. perfringens		
JIR325	Strain 13 derivative; Rif^R Nal^R	(Lyristis *et al.*, 1994)
JIR4195	JIR325 (pCW3); Rif^R Nal^R Tc^R	(Hughes *et al.*, 2007)
JIR4394	Strain 13 derivative; Sm^R Chl^R	(Bannam *et al.*, 2006)
JIR13187	JIR4195(pJIR4851); Rif^R Nal^R Tc^R Em^R pCW3Ω*regC::*targetron(TT), independent mutant	T. Stent, X. Han, V. Adams, R. Moore and J. Rood, unpublished
JIR13338	JIR4195(pJIR4593); Rif^R Nal^R Tc^R Em^R pCW3Δ*srm::erm*(Q)	This study

JIR13390	JIR4195(pJIR4621); Rif^R Nal^R Tc^R Em^R pCW3Δ*srm::erm*(Q), independent mutant	This study
Plasmids		
pT7-Blue	*E. coli* cloning vector, f1 origin, pUC origin, *lacZ* α-peptide, Amp^R	Novagen
pCP13	54 kb plasmid from strain 13	(Shimizu *et al.*, 2002)
pCW3	Conjugative tetracycline resistance plasmid	(Rood *et al.*, 1978)
pET22b+	*E. coli* expression vector, C-terminal His_6-Tag	Invitrogen
pJIR750	*E. coli-C. perfringens* shuttle vector, Cm^R	(Bannam & Rood, 1993)
pJIR2715	Base plasmid for the construction of *C. perfringens* suicide vectors, Em^R, Cm^R	(Bannam *et al.*, 2006)
pJIR3562	Clostridial targetron vector with P_{tet}, *ermB*-RAM	(Cheung *et al.*, 2010)
pJIR3844	Cpb2-toxin plasmid from EHE-NE-18	(Bannam *et al.*, 2011)
pJIR4067	Group II intron of pJIR3562 retargeted to the 152/153 site of *regC* gene	T. Stent, X. Han, V. Adams, R. Moore and J. Rood, unpublished
pJIR4353	pJIR750(Asp718/BamHI) ΩJRP5350/JRP5350 BamHI/Asp7118; 1200bp, pCW3) *regC*$^+$ complementation vector	T. Stent, X. Han, V. Adams, R. Moore and J. Rood, unpublished
pJIR4557	pJIR2715 (BamHI/Asp718) ΩJRP6414/JRP6418 BamHI/Asp718; 1643 bp, pCW3) downstream of *srm*	This study
pJIR4591	pJIR4557 (XhoI/EagI) ΩJRP6413/JRP6417 XhoI/EagI; 1851 bp, pCW3), *srm* suicide vector	This study
pJIR4593	pCW3Δ*srm::erm*(Q)	Transformation of JIR4195 with pJIR4591. This study
pJIR4621	pCW3Δ*srm::erm*(Q), independent mutant	Transformation of JIR4195 with pJIR4591 This study
pJIR4640	pT7-Blue (EcoRV) ΩJRP6563/JRP6564 (1615 bp, pCW3), *pCW347*$^+$, *srm*$^+$	This study

pJIR4641	pT7-Blue (EcoRV) ΩJRP6565/JRP6564 (1485 bp, pCW3), *srm*$^{+}$	This study
pJIR4653	pJIR750 (BamHI/Asp718) pJIR4640 (BamHI/Asp718; 1615 bp) *pCW347*$^{+}$, *srm*$^{+}$ complementation vector	This study
pJIR4654	pJIR750 (BamHI/Asp718) pJIR4641 (BamHI/Asp718; 1485 bp) *srm*$^{+}$ complementation vector	This study
pJIR4704	pT7-Blue (EcoRV) ΩJRP6564/JRP6638 (1180 bp, pCW3), *srm*$_{1\text{-}256}^{+}$	This study
pJIR4706	pJIR750 (BamHI/Asp718) pJIR4704 (BamHI/Asp718; 1180 bp) *srm*$_{1\text{-}256}^{+}$ complementation vector	This study
pJIR4724	pET22b+ (XhoI/NdeI) Ω JRP6670/JRP6671 (XhoI/NdeI; 902 bp, pCW3) Srm expression vector	This study
pJIR4800	pET22b+ (XhoI/NdeI) ΩJRP6783/JRP6670 (XhoI/NdeI; 770bp, pCW3) Srm$_{1\text{-}256}$ expression vector without putative HTH domain	This study
pJIR4812	pJIR750 (BamHI/Asp718) ΩJRP6564/JRP6865 (BamHI/Asp718; 1467 bp, pJIR3844) *srm*$_{\text{pJIR3844\_45}}^{+}$ complementation vector	This study
pJIR4813	pJIR750 (BamHI/Asp718) ΩJRP6564/JRP6864 (BamHI/Asp718; 1363 bp, pJIR3844) *srm*$_{\text{pJIR3844\_56}}^{+}$ complementation vector	This study
pJIR4851	pCW3Ω*regC*::targetron (TT)	T. Stent, X. Han, V. Adams, R. Moore and J. Rood, unpublished

Amp^{R}- ampicillin resistance, Chl^{R}- potassium chlorate resistance, Cm^{R}- chloramphenicol resistance, Em^{R}- erythromycin resistance, Kn^{R}- kanamycin resistance, Nal^{R}- nalidixic acid resistance, Rif^{R} – rifampicin resistance, Sm^{R}- streptomycin resistance, Tc^{R}- tetracycline resistance, Tm^{R} – thiamphenicol resistance.

Molecular Techniques

Plasmid DNA was extracted from *E. coli* using QIAprep Spin Miniprep kit (Qiagen) as outlined by the manufacturer. Crude *C. perfringens* DNA was obtained as previously described (Bannam *et al.*, 2006)**.** *E. coli* cells were made chemically competent and transformed as previously described (Inoue *et al.*, 1990).

Oligonucleotides used in this study are outlined in Table 4.2 and were synthesised by Integrated DNA Technologies (IDT) or Sigma. PCR amplification was performed using *Taq* (Roche) or Phusion Polymerase (NEB). PCR products were purified using QIAquick PCR purification kit (Qiagen). Restriction enzymes were used according to the manufacturer's instructions (Roche and NEB). Sequencing was performed using Prism BigDye Terminator mix (Applied Biosystems) and separated using an Applied Biosystems 3730S capillary sequencer. Sequences were analysed using Vector NTI (Invitrogen).

Bioinformatic Analysis

Sequences were analysed using BLAST (Altschul *et al.*, 1990) and predicted homology to proteins within the conserved domains database (Marchler-Bauer *et al.*, 2015). Sequences for *C. perfringens* plasmids were obtained from Genbank (Benson *et al.*, 2017), with the following accession numbers: pCW3 (NC_010937), pCPPB-1 (NC_015712.1), pJIR3844 (NC_019257), pJIR3536 (NC_025042), pCPF4969 (NC_007772.1), pJFP838B (KT020842.1), pJFP838C (CP013040.1), pJFP838D (CP013039), pCFP5603 (AB236337.1) and pCFP4969 (AB236336.1). Multiple sequence alignments and percent identity matrices were generated using Clustal Omega (McWilliam *et al.*, 2013). Sequences were aligned using Clustal Omega and phylogeny inferred (McWilliam *et al.*, 2013). Inferred phylogeny was visualised as a rectangular rooted phylogram using FigTree (available for download at: https://github.com/rambaut/figtree). Helix turn helix domains were predicted using the Network Protein Sequence Analysis (NPS@): Helix-turn-helix prediction tool (Dodd & Egan, 1990). Sequence logos were created using the WebLogo tool

Table 4.2: Oligonucleotides used in this study

Name	Sequence	Purpose
JRP4330	CTCAGTACTGAGAGGGAACTTAGATGGTAT	*catP* probe oligo, F
JRP4331	CCGGGATCCTTAGGGTAACAAAAAACACC	*catP* probe oligo, R
JRP6001	CCAGGAAAAGGTCATATAACAGAAGC	*erm*(Q) probe, F
JRP6002	CTAAGACGCAATCTACACTAGGC	*erm*(Q) probe, R
JRP6413	CGCCGGCCGACTTTTATTGTGATACAAAATG	*srm* LHS plus EagI, F
JRP6414	CCGGTACCAAAAAAGACTCTAAATTATAGAGTC	*srm* RHS plus Asp718, F
JRP6417	CGGCCTCGAGCATGAATAATAAATAAAAGGGGATTG	*srm* LHS plus XhoI, R
JRP6418	CGGGATCCGAAAAATTTCTTTTAAATTATCCTTCATATC	*srm* RHS plus BamHI, R
JRP6563	TTGGGATCCGCTATTCCACTATAATTCCCAACAATATAATAATTGTG	*srm* complementation plus BamHI, F
JRP6564	CCGGTACCGATCTGGGTAATATATCACAAGCTTATAGTCAA	*srm* complementation plus Asp718, R
JRP6565	TTGGGATCCGAGCAGTTCAATTTTCGGGATTTTG	*pcw347-srm* complementation plus BamHI, F
JRP6638	TTGGGATCCTTATTATGCTCCACGACTATTCTTTTTAG	$srm_{1\text{-}256}$ complementation without HTH plus BamHI, F
JRP6670	GCGCCATATGAAGGATAATTTAAAAGAAATTTTTCTAAATGAAC	*srm* expression plus NdeI, R
JRP6671	GGCCTCGAGTTCATGTAAAATTTTATGAATTACTCCAAAG	*srm* expression plus XhoI (no stop), F
JRP6783	GGCCTCGAGTGCTCCACGACTATTCTTTTTAG	$srm_{1\text{-}256}$ expression plus XhoI (no stop), F
JRP6864	TTGGGATCCCTATTAATACTAAAATAAAATCCATAATATCTCAAGCCAC	$srm_{pJIR3844\_56}$ plus Asp718, F
JRP6865	TTGGGATCCAACGATATAATAATTGTGAGCAGCATAAAAATAATAC	$srm_{pJIR3844\_45}$ plus Asp718, F

F- forward primer, R- reverse primer

(Crooks *et al.*, 2004). Signal peptides were predicted using Signal P 4.1 server (Petersen *et al.*, 2011). Potential transmembrane domains were predicted using TMHMM Server v 2.0 (http://www.cbs.dtu.dk/services/TMHMM/). Sequence homology between pCW3-like plasmids and graphics were produced using Easyfig (Sullivan *et al.*, 2011).

Construction of mutant strains and complementation

Allelic exchange was used to replace the *srm* gene with an *erm*(Q) cassette using a derivative of the *C. perfringens* suicide vector pJIR2715 (Bannam *et al.*, 2006). Upstream and downstream flanking regions were generated by PCR and sequentially cloned into pJIR2715 using Asp718/BamHI sites upstream and XhoI/SacI sites downstream of the *erm*(Q) gene. A 1643 bp fragment encompassing from 455613-47225 bp region from pCW3 was cloned upstream of *erm(Q)*, and an 1851 bp fragment from 42566-44716 bp was cloned downstream of *erm*(Q) to generate the *srm* suicide vector, pJIR4591. Attempts were made to construct double-crossover vectors for the pCW3 genes *pcw340, pcw342, pcw344, pcw345, pcw346, pcw347* and *pcw349*, however, despite successful cloning of the downstream regions for most of these vectors, cloning of the corresponding upstream regions was unsuccessful.

The *srm* mutagenesis vector was independently introduced by electroporation into the *C. perfringens* strain JIR4195, which carries pCW3, and transformants selected on NA supplemented with Em. To identify potential mutants, the resultant transformants were screened for resistance to Tc and Em and sensitivity to Tm. DNA preparations from Em-resistant, Tm-sensitive colonies were tested by PCR and Southern blotting to confirm mutation of the target gene and the loss of the mutagenesis plasmid.

For complementation, PCR fragments containing the wild-type *srm* gene were amplified by PCR and subsequently cloned into the BamHI/Aps718 sites of the *E. coli-C. perfringens* shuttle vector pJIR750, to generate pJIR4654. For *srm* deletion experiments, a PCR fragment without the coding region for the final 44 amino acids of Srm was cloned into pJIR750 to produce pJIR4706. For

cross-complementation analysis, the two *srm* genes from pJIR3844, $srm_{pJIR3844\_45}$ and $srm_{pJIR3844\_56}$, were amplified and cloned into pJIR750 to generate pJIR4812 and pJIR4813, respectively.

The complementation plasmids were introduced into the respective *C. perfringens* mutants by electroporation and transformants selected on NA supplemented with Em and Tm. The presence of the complementation plasmids was confirmed by restriction analysis and sequencing, following plasmid rescue in *E. coli.*

Mating, stability and copy number experiments

Overnight intrastrain conjugation experiments were conducted as outlined in Chapter Two.

Plasmid stability experiments were conducted as outlined in Chapter Three.

Plasmid copy number was determined using digital droplet PCR (ddPCR). Experiments were conducted as outlined in Chapter Three.

Expression and purification of recombinant proteins

E. coli expression vectors were constructed as follows: fragments containing the wild-type *srm* gene and the $srm_{1\text{-}256}$ gene were amplified by PCR and subsequently cloned into the NdeI/XhoI sites of the *E. coli* expression vector pET22b+, to generate pJIR4724 and pJIR4800, respectively. This cloning resulted in the construction of expression vectors encoding Srm proteins with a C-terminal hexa-histidine tag. The *E. coli* strain C41(DE3) pLysS was used as the expression host. Cells were grown in 2YT at 37°C until the OD_{600} reached 0.6 and induced with the addition of 1 mM IPTG (Thermo-Scientific) for four hours.

Cultures expressing recombinant protein were harvested and resuspended in lysis buffer (20 mM Tris-HCl (pH 7.4), 300 mM NaCl, 10% (v/v) glycerol), supplemented with Complete cocktail protease inhibitor (Roche) and 0.5 mg/mL DNaseI (Roche). Cells were lysed using a cell disrupter (Avestin) and the lysate cleared *via* centrifugation at 15, 000 x g for 20 mins at 4°C. Protein from this clarified lysate was purified using TALON resin (Clontech) equilibrated in lysis buffer. Protein

was allowed to bind to the resin overnight at 4°C. Unbound proteins were removed by washing the resin twice, once with 25 mL of lysis buffer with 5 mM imidazole then with 10 mL of lysis buffer with 10 mM imidazole. Protein was then eluted with the addition of lysis buffer with increasing concentrations of imidazole (50 mM-500 mM). Purified protein was stored in lysis buffer at 4°C, -20°C or -80°C. Protein concentrations were determined using the BCA assay (Pierce) as per the manufacturer's instructions. Protein samples were analysed on 12% (w/v) SDS-PAGE followed by staining in Coomassie Blue (Sigma-Aldrich) and Western blotting (Wisniewski *et al.*, 2015b) was performed using anti-His mouse monoclonal antibodies (Qiagen) and horseradish-peroxidase conjugated goat anti-mouse antibodies (Millipore). Blots were detected on the ChemiDoc XRS+ System (BioRad) using a Western Lighting detection kit (PerkinElmer) as per the manufacturer's instructions.

N-terminal sequencing

N-terminal sequencing of protein bands was performed as follows. Proteins of interest were run on 12% (w/v) SDS-PAGE and transferred to polyvinylidene difluoride (PVDF) membranes (Millipore) that had been washed in water, soaked in 100% methanol and equilibrated in Western transfer buffer (25mM Tris-HCl (pH 8.3), 200mM glycine, 20%(v/v) methanol). Following transfer, these membranes were washed three times in distilled water, incubated 5 minutes in N-terminal stain (Coomassie R-250) before being washed in 50% (v/v) methanol. Bands of interest were cut from the gel and analysed. The first ten amino acids from the N-terminus were sequenced using a Procise Protein Sequencer (Applied Biosystems) *via* the pulsed liquid-PVDF method.

Thermal stability assays

Purified protein in lysis buffer (20mM Tris-HCl (pH 7.4), 300 mM NaCl, 10% (v/v) glycerol) was concentrated to at least 1 mg/ml using Amicon Ultra-15 Centrifugal filter units with a 30 kDA cut off (Merck). The thermal stability of the protein samples was determined by Differential Scanning

Fluorimetry (DSF) in 14 different buffer conditions over a range of pH values at high and low salt concentrations. The data were analysed using a CFX96 RT-PCR (BioRad) machine and the results were analysed using BioRad CFX Software and the platform provided analysis datasheet Meltdown (Collaborative Crystallisation Centre, CSIRO).

Chemical crosslinking assays

Chemical crosslinking was performed as described previously (Teng *et al.*, 2008) with minor modifications. Purified protein was buffer exchanged into phosphate buffered saline (PBS; pH 7.4) and protein concentration estimated using the BCA assay. Purified protein was incubated with increasing concentrations (1-4 mM) of the chemical crosslinking agent DTBP (Pierce Biotechnology) and incubated at room temperature for 60 mins. Reactions were quenched by the addition of 50 mM Tris-HCl (pH 7.6) and then analysed by 12% (w/v) SDS-PAGE and Western blotting, as described earlier.

Results

The *dcm* region encodes numerous hypothetical proteins and is a recombination hotspot for the insertion of transposons and toxin genes

To expand on our knowledge of how Tcp plasmids maintain themselves within *C. perfringens* cells, bioinformatic analysis was performed on the uncharacterised *dcm* region of pCW3 to identify key candidates that may be involved in plasmid stability. The protein products encoded within the *dcm* region were assessed using BLASTp (Table 4.3).

Reannotation of the *dcm* region has provided new information since the original annotation in 2006 (Bannam *et al.*, 2006, Miyamoto *et al.*, 2006). A DUF4417 domain was predicted within the product of *pcw343*. The function of the DUF4417 domain remains to be characterised, however, members of this protein family possess a conserved glycine residue within this domain, which may be important for protein function (Marchler-Bauer *et al.*, 2017). The product of *pcw344* is predicted to contain an amidoligase domain; amidoligase enzymes catalyse the attachment of an amido group to proteins, in a mechanism analogous to ubiquitination in eukaryotes (Iyer *et al.*, 2009; Iyer *et al.*, 2008). The product of *srm* (previously designated as *pcw348*) is predicted to encode a Hin-like helix-turn-helix (HTH) domain, HTH domains are DNA binding domains unique to bacteria (Aravind *et al.*, 2005). This subfamily of HTH domains are represented by the Salmonella Hin recombinase. The Hin-like HTH domains are the simplest of the characterised HTH domains (Aravind *et al.*, 2005; Marchler-Bauer *et al.*, 2017). The presence of this domain suggests that this protein may play a role in regulation *via* direct interaction with DNA. Lastly, the product of *pcw350*, previously annotated as a conserved hypothetical protein with similarity to an uncharacterised gene found in the genome of *C. perfringens* strain 13, is predicted to be a transposase due to the presence of a PDDEXK_2 transposon domain (Marchler-Bauer *et al.*, 2017). BLAST analysis of the predicted products of genes *pcw340, pcw342, pcw345, pcw346, pcw347* and *pcw349* did not provide any

Table 4.3: Summary of predicted genes within the *dcm* locus.

					pCW3-like plasmid homologues (AA Identity)								
pCW3 Gene	**MW**	**SP**	**TMD**	**Predicted Function**	**pJIR3844**	**pJIR3536**	**pJIR838B**	**pJIR838C**	**pJIR838D**	**pCPPB-1**	**pCP8533etx**	**pCPF4969**	**pCPF5603**
pcw340	12.5	No	0	Unknown	99%	99.0%	97.0%	90.1%	98.0%	-	97.0%	-	98%
dcm	38.9	No	0	DNA cytosine methyltransferase	97.9%	97.9%	98.4%	95.5%* (199/339)	98.1%	95.8%* (96/339)	97.9%	98.2%	98.1%
pcw342	6.5	No	0	Unknown	100%	100%	98.3%	98.3%	100%	96.5%	100% ''	100% ''	100% ''
pcw343	39.3	No	0	Unknown, DUF4417 domain	96.9%	97.1%	95.9%	100%* (64/340)	84.4%* (109/340)	93.2%* (164/340)	96.2%	57.6%* (123/340)	93.6%* (109/340)
pcw344	53.4	No	0	Putative amidoligase enzyme	98.1%	98.1%	98.5%	97.0%	97.7%	92.8%* (365/468)	97.7%	97.3%* (186/468)	88.8%* (241/468)
pcw345	15.9	No	0	Unknown	98.5%	-	94.7%	84.1%* (63/133)	89.5%* (38/133)	94.3%* (35/133)	-	-	+
pcw346	12.6	No	0	Unknown	*052* 81.6% *043* 96.1%	93.2%	95.2%	80.4%* (46/103)	96.1%	62.3%* (77/103)	94.2%	+	97.1%
pcw347	9.3	No	2 (AA 5-27) (AA 47-69)	Unknown	*055* 75.3% *044* 96.1%	+	91.9%* (37/77)	96.1%	96.1%	57.8%* (45/77)	94.8% +	94.8%	100%
srm	35.7	No	0	Unknown, Hin-like HTH domain	*056* 93% *045* 97.7%	95.6%	99%	95.3%	97.3%	91.2%* (228/300)	*023* 96.7% *035* 97.3%	96.7%	98.7%
pcw349	15.9	No	0	Unknown	*046* 96.2% *057* 94% *067* 94.7%	97.8%	97%	94.8%	100%	97.8%	*035* 100% *024* 98.5%	96.3%	100%
pcw350	33.9	No	0	Rnp family recombination transposase	*047* 97.2% *058* 94.7% *068 92.5%*	97.2%	96.8%	96.1%	99%	96.8%	*025* 94% *037* 98.6%	96.8%	98.3%

(-) indicates no homologue present, ('') indicates previously unannotated ORF, (*) indicates truncated sequence, in brackets is the amino acid coverage, (+) indicates sequence present, but no start codon. In the case of multiple homologues, the gene identifier number is present in italics.

new information. However, this does not rule out the potential importance of these genes to pCW3. In contrast to the highly conserved *cnaC* region (discussed in Chapter Two), the gene arrangement within the *dcm* region was highly variable (Figure 4.2). However, key genes within this locus were present on all nine plasmids. Comparative analysis showed that homologues of *dcm, pcw342, srm, pcw349* and *pcw350* were the most conserved. PCW342 remains the most highly conserved product encoded within the *dcm* region, it was present on all plasmids analysed, with a high level of amino acid identity between homologues (96.5-100%). Many of the genes located within this region are subject to alteration by apparent recombination, many homologues of *pcw343, pcw344, pcw345* and *pcw346* were truncated on several plasmids. On some plasmids, such as pJIR3844 and pCP8533etx, duplication, or even triplication, of some genes was observed. Notably, the *pcw349* and *pcw350* genes are present in three copies on the plasmid pJIR3844, separated by large insertions. Although there has been a high level of recombination in this area, these specific genes are mostly intact, with only minor alterations occurring in the translated C-terminal portion of PCW350. Despite the *dcm* region being a recombination hotspot, many of the genes located in this region remain highly conserved (Table 4.3), suggesting that the products of some of these genes may be essential of the biology of Tcp plasmids.

Homologues of the putative regulator *srm* are present only on pCW3-like plasmids

As discussed earlier, the *srm* gene product was a candidate to be involved in the regulation of plasmid functions. To determine the level of conservation of this gene product encoded by the plasmids of *C. perfringens,* a broader search for homologues was performed. BLASTp analysis was used to identify proteins of similar sequence to that encoded by *srm*. Homologues with high-level amino acid identity (90% or above) to Srm were only present on pCW3-like plasmids (Table 4.4). No homologues were found on pCP13-like or pIP404-like plasmids, indicating the function of the translated product may be specific to the biology of pCW3-like plasmids. It was also noted that a

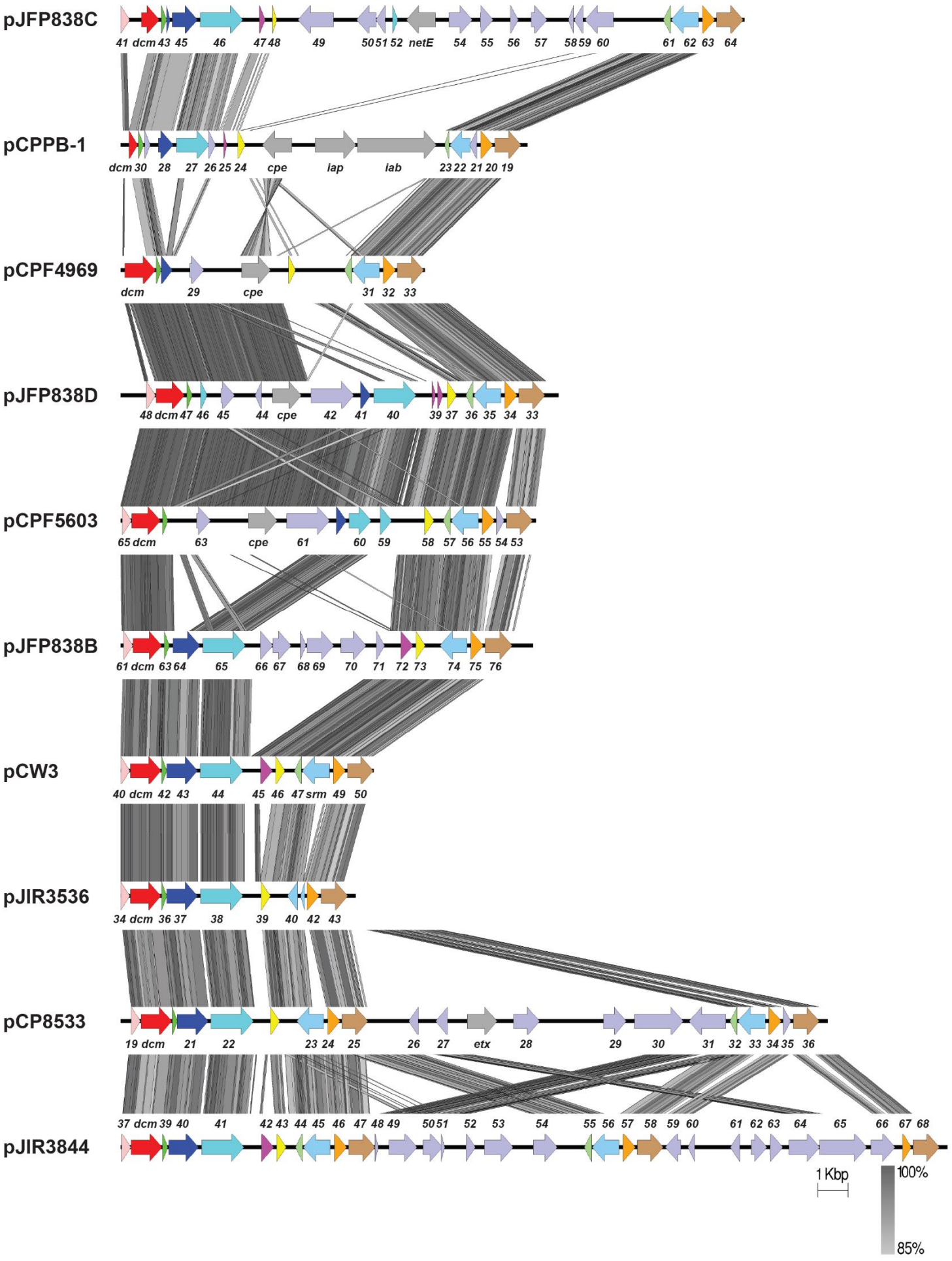
pJFP838C
41 dcm 43 45 46 47 48 49 50 51 52 netE 54 55 56 57 58 59 60 61 62 63 64
pCPPB-1
dcm 30 28 27 26 25 24 cpe iap iab 23 22 21 20 19
pCPF4969
dcm 29 cpe 31 32 33
pJFP838D
48 dcm 47 46 45 44 cpe 42 41 40 39 37 36 35 34 33
pCPF5603
65 dcm 63 cpe 61 60 59 58 57 56 55 54 53
pJFP838B
61 dcm 63 64 65 66 67 68 69 70 71 72 73 74 75 76
pCW3
40 dcm 42 43 44 45 46 47 srm 49 50
pJIR3536
34 dcm 36 37 38 39 40 42 43
pCP8533
19 dcm 21 22 23 24 25 26 27 etx 28 29 30 31 32 33 34 35 36
pJIR3844
37 dcm 39 40 41 42 43 44 45 46 47 48 49 50 51 52 53 54 55 56 57 58 59 60 61 62 63 64 65 66 67 68
1 Kbp
100%
85%

Figure 4.2: Comparison of *dcm* regions from nine pCW3-like plasmids. Shown are tBLASTx alignments of the *dcm* regions from pCW3-like plasmids indicated. ORFs are coloured according to pCW3 gene homologue: *pcw340* in pink, *dcm* in red, *pcw342* in green, *pcw343* in dark blue, *pcw344* in turquoise, *pcw345* in magenta, *pcw346* in yellow, *pcw347* in light green *srm* in light blue, *pcw349* in orange and *pcw350* in brown. Other ORFs are labelled in light purple and toxin genes in grey. If no conventional name is given to the ORF they are labelled with identifying locus tag numbers. Regions of amino acid identity are represented by the grey bars. The amino acid identity cut off was 85% with a maximum e-value of 0.001. The intensity of grey colour represents the level of identity between sequences, as illustrated by the legend.

Table 4.4: Identity matrix of Srm related proteins from *C. perfringens* pCW3-like plasmids

	Locus Tag	Plasmid	Accession Number	Amino acid identity %															
				1	2	3	4	5	6	7	8	9	10	11	12	13	14	15	16	17
1	CMR01_15525	pLLY_N11_3	ATD50155	100	92.2	95	95	91.7	91.3	92	91.3	92	92.3	92.3	93.7	92.7	93.3	93.3	93.3	93.3
2	pCpb2-CP1_53	pCpb2-CP1	YP_007078948	92.2	100	97.8	97.8	89.2	89.5	88.8	89.2	89.6	91.4	91.4	91.8	91.8	91	91	91	91
3	pBeta2_00056	pJIR3844	YP_006961269	95	97.8	100	100	91.3	91.6	91	91	91.7	93.3	93.3	94	93.7	93	93	93	93
4	BXT94_17120	pDel1_2	AQW28449	95	97.8	100	100	91.3	91.6	91	91	91.7	93.3	93.3	94	93.7	93	93	93	93
5	pJIR4150_049	pJIR4150	CRG98308	91.7	89.2	91.3	91.3	100	94	92	92.3	91.3	91.3	92	92	93	93.3	93.3	93.3	93.3
6	pCP8533etx_p23	pCP8533etx	YP_002291109	91.3	89.5	91.6	91.6	94	100	93.3	94.6	94	95.3	95.3	95.3	95.6	96.6	96.6	96.6	96.6
7	pJFP838C_C0062	pJFP838C	AMN30644	92	88.1	91	91	92	93.3	100	96	93	94.7	94.7	94.3	94	95.3	95.3	95.3	95.3
8	JFP55_pF0056	pJFP55F	AMN30720	91.3	89.2	91	91	92.3	94.6	96	100	93.7	96	96	95.7	95.3	96.7	96.7	96.7	96.7
9	pCP8533etx_p34	pCP8533etx	YP_002291120	92	89.6	91.7	91.7	91.3	94	93	93.7	100	94.7	94.7	95.7	96	97	97	97	97
10	JFP838_pD0035	pJFP838D	AMN30558	92.3	91.4	93.3	93.3	92	95.3	94.7	96	94.7	100	100	96.3	97.3	97.3	97.3	97.3	97.3
11	JFP55_pG0026	pJFP55G	AMN30768	92.3	91.4	93.3	93.3	92	95.3	94.7	96	94.7	100	100	96.3	97.3	97.3	97.3	97.3	97.3
12	pBeta2_00045	pJIR3844	YP_006961258	93.7	91.8	94	94	93	95.6	94.3	95.7	95.7	96.3	96.3	100	97.7	97.7	97.7	97.7	97.7
13	pCPF5603_56	pCPF5603	YP_473479	92.7	91.8	93.7	93.7	93.3	96.6	94	95.3	96	97.3	97.3	97.7	100	98.7	98.7	98.7	98.7
14	pCW3_0048	pCW3	YP_001967789	93.3	91	93	93	93.3	96.6	95.3	96.7	97	97.3	97.3	97.7	98.7	100	100	100	100
15	pTet_041	pTet	YP_006961342	93.3	91	93	93	93.3	96.6	95.3	96.7	97	97.3	97.3	97.7	98.7	100	100	100	100
16	FORC3_p009	pFORC3	ALG50275	93.3	91	93	93	93.3	96.6	95.3	96.7	97	97.3	97.3	97.7	98.7	100	100	100	100
17	CMR01_15610	pLLY_N11_3	ATD50171	93.3	91	93	93	93.3	96.6	95.3	96.7	97	97.3	97.3	97.7	98.7	100	100	100	100

number of these homologues were found in duplicate on some plasmids, as seen on pJIR3844 and pJIR8533etx. Phylogenetic analysis determined that the Srm proteins are closely related, with those encoded on pCW3, pTet, pFORC3 and pLLY_3 identical in sequence (Figure 4.3).

When the homologue search was broadened to include proteins with a lower amino acid sequence identity (41% or below), and to exclude homologues from *C. perfringens,* proteins from other clostridia were identified (Table 4.5). Unfortunately, the genetic context in which many of these homologue proteins are encoded could not be easily probed, as many sequences were from large sequencing studies whereby closed genomes have yet to be constructed or confirmed. Despite this limitation, analysis of these sequences determined that most of the proteins with similarity to Srm only shared a likeness to the putative Hin-like HTH motif and not necessarily any other protein region. Only one homologue shared identity to Srm outside of the predicted Hin-like HTH domain (40.59%). This hypothetical protein (Accession Number: KEH90511) is from the *Clostridium botulinum* C/D strain It1, and is encoded on the large plasmid, p3CbIt1 (Skarin & Segerman, 2014). Amino acid alignment showed conservation of a number of residues and motifs within the N-terminal portion of the protein, which may be important for protein function (Figure 4.4A). There is also a large deletion of 44 amino acids within the homologous protein. The *srm* gene homologue on p3Cb1t1, is located downstream of a DNA cytosine methyltransferase gene that is similar to that encoded on pCW3 (Figure 4.4B). No other proteins within this region had any significant similarity.

Figure 4.3: Phylogentic analysis of Srm homologues from pCW3-like plasmids. A multiple sequence alignment using Clustal Omega was performed with 18 homologues of Srm from various *C. perfringens* plasmids. A phylogenetic tree was generated using the neighbour joining method and visualised as a rooted phylogram using FigTree.

Table 4.5: Srm related proteins not including *C. perfringens* homologues

Accession Number	Organism	Amino Acids	% AA Identity to Srm
KEH90511.1	*Clostridium botulinum*	226	41.1
OKZ76301.1	*Clostridium sp. 27_14*	158	33.1
WP_099330195.1	*Clostridium paraputrificum*	129	33.9
WP_099330294.1	*Clostridium paraputrificum*	129	33.9
WP_066679372.1	*Clostridium septicum*	106	35.9
WP_002581204.1	*Clostridium butyricum*	153	33.6
WP_099328666.1	*Clostridium paraputrificum*	100	32.2
WP_012449980.1	*Clostridium botulinum*	81	41.3
WP_103673835.1	*Clostridium sp. 3-3*	138	31.5
WP_077711528.1	*Clostridioides difficile*	156	22.3
WP_077711540.1	*Clostridioides difficile*	156	23
WP_077711521.1	*Clostridioides difficile*	158	25
KLR50780.1	*Paeniclostridium sordellii 8483*	77	32.9

A

```
Srm                          ----------MKDNLKEIFLNELKNNKDTPKQEIIKLAEEYGIDFKPREA   40
p3CBIt1_0068_KEH90511        MDLNGDIKRCYNNINFGGIIMNDKFKEIFIDALNRSKEIKKDDIFNIVRECSLEIKPRTA   60
                                       *:*::****:: *:..*:  *::*::::..* .:::*** *

Srm                          KSKIIDKLVVAGEFDTIFNKFEKFGYIPTWTIADFYGVNTERIDQLHKIGAIKEIPVKRE   100
p3CBIt1_0068_KEH90511        KLKMIEAIAN-YNFNKLFKEFK-------------------------------------   81
                             * *:*: :.   :*:.:*::*:

Srm                          YYSRSSKSYYTVNTYPVSVLEYSREELEEAYNQTYGQEGFKFRIETNSKDEVEILINELR   160
p3CBIt1_0068_KEH90511        ------EFIYIANTYPIGILNYSKEELHNAYNKAFGQGWFKIRLETENREQFEKIVKEFK   135
                                   :  * .****:.:*:**:***.:***:::**  **:*:**:.::::.* :::*::

Srm                          KLFKIEKTPQIYERRNEGYNTYFTVKLLNNSEFEQNKFLSEIESLKNKNKETEEYYRDVL   220
p3CBIt1_0068_KEH90511        KIFLVENNPDVYERRNQGFNSYFKIQPLNNSSFEENKLLAEINKLRKTIEDFEERNANEI   195
                             *:* :*:.*::*****:*:*:**.:: ****.**:**:*:**:.*::. :: **   : :

Srm                          SGI----YKKFNVDSRMDLMRVSREYLELKEKSKKNSRGAGRKPRFTEEEKNIIRAQRKE   276
p3CBIt1_0068_KEH90511        KKIRKRYSDIFKVDTIFDLQKIKEEYDKLKE-----------------------------   226
                             . *     . *:**: :** ::..** :***

Srm                          GKTIKELAALNNCSFGVIHKILHE    300
p3CBIt1_0068_KEH90511        ------------------------    226
```

B

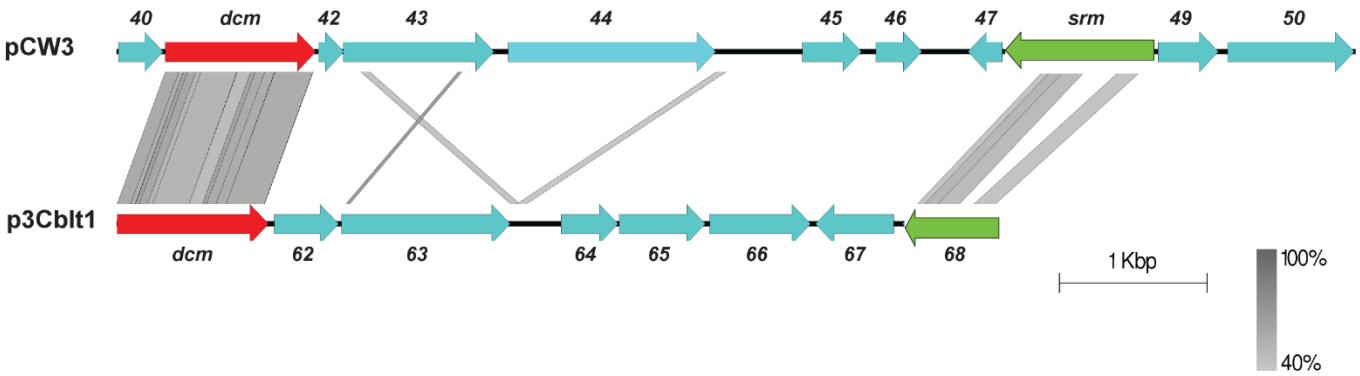

Figure 4.4: Alignment of amino acid sequences of Srm and P3CBIt1_0068 homologue and comparison of genetic loci from pCW3 and p3CbIt1. A. Alignment of amino acid sequences of Srm and P3CBIt1_0068 (KEH90511) produced using Clustal Omega. The putative Hin-like HTH motif of Srm is highlighted in yellow. **B.** Shown are tBLASTx alignments of the genetic regions from pCW3 and p3CbIt1 where *srm* and *p3CBIt1_0068* genes are located. ORFs are coloured according to pCW3 gene homologue: *dcm* in red and *srm* in green. All other ORFs are coloured in aqua. Regions of amino acid identity are represented by the grey bars. The amino acid identity cut off was 40% with a maximum e-value of 0.001. The intensity of grey colour represents the level of identity between sequences, as illustrated by the legend.

Construction of mutants within the *dcm* region of pCW3.

To determine if any genes within the *dcm* region are required for key plasmid processes, individual mutants were constructed by allelic exchange, whereby the genes of interest were replaced with an erythromycin resistance gene *erm*(Q). The approach was to construct suicide vectors independently for each gene of interest, as outlined in the Materials and Methods. Up to seven independent attempts were made to generate double crossover vectors for the *pcw340, pcw342-pcw347 and pcw349* genes, however, these efforts were unsuccessful because it was not possible to clone various downstream regions. A double crossover suicide vector was successfully constructed for the *srm* gene. Following construction and confirmation by restriction digest and sequencing (data not shown), the mutagenesis vector was independently introduced into *C. perfringens* strain JIR4195, containing wild type pCW3. The required mutants would be Tc^R, due to the inherent tetracycline resistance of pCW3, and Tm^S but Em^R, due to the acquisition of the *erm*(Q) cassette from the suicide vector. Potential mutant strains with the correct resistance profiles were obtained and the genotypes of resultant mutants were confirmed using PCR (data not shown) and Southern blotting (Figure 4.5). The Southern blots were probed with DIG-labelled DNA probes specific for: *catP*, carried on the double-crossover vector backbone, *erm*(Q), carried within the double crossover selection cassette and a fragment adjacent to the gene of interest, *srm*. A fragment adjacent to *srm* was probed to confirm the expected size difference that would be observed for mutant and wild type strains.

Srm is not required for the conjugative transfer of pCW3

The conjugative transfer of pCW3 occurs at high efficiency (Bannam *et al.*, 2006). In other plasmid systems, conjugative transfer is often regulated as it is considered a high energy expense to the cell (Zatyka *et al.*, 1994). It was postulated that the product of *srm* could function as a regulator, as indicated by the presence of a DNA binding motif, controlling key plasmid functions such as

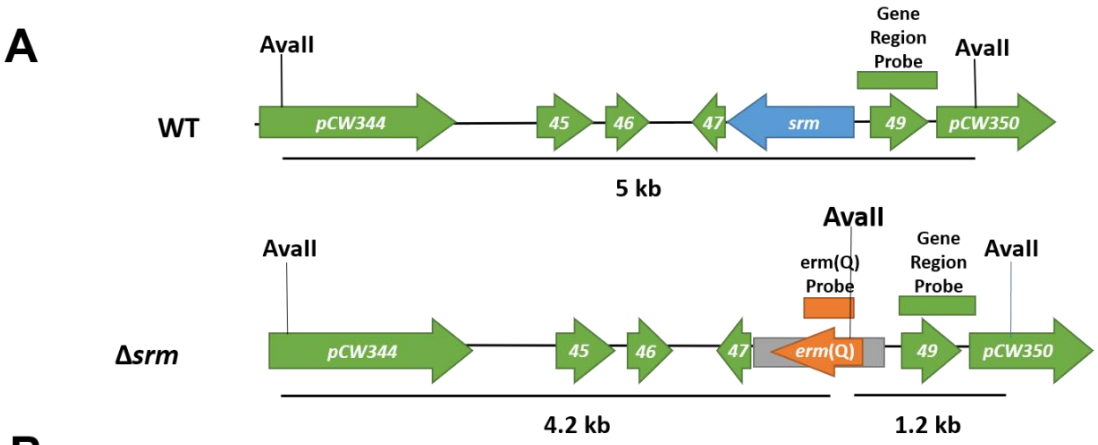
A
AvaII
Gene Region Probe
AvaII
WT
pCW344
45
46
47
srm
49
pCW350
5 kb
AvaII
AvaII
erm(Q) Probe
Gene Region Probe
AvaII
Δsrm
pCW344
45
46
47
erm(Q)
49
pCW350
4.2 kb
1.2 kb

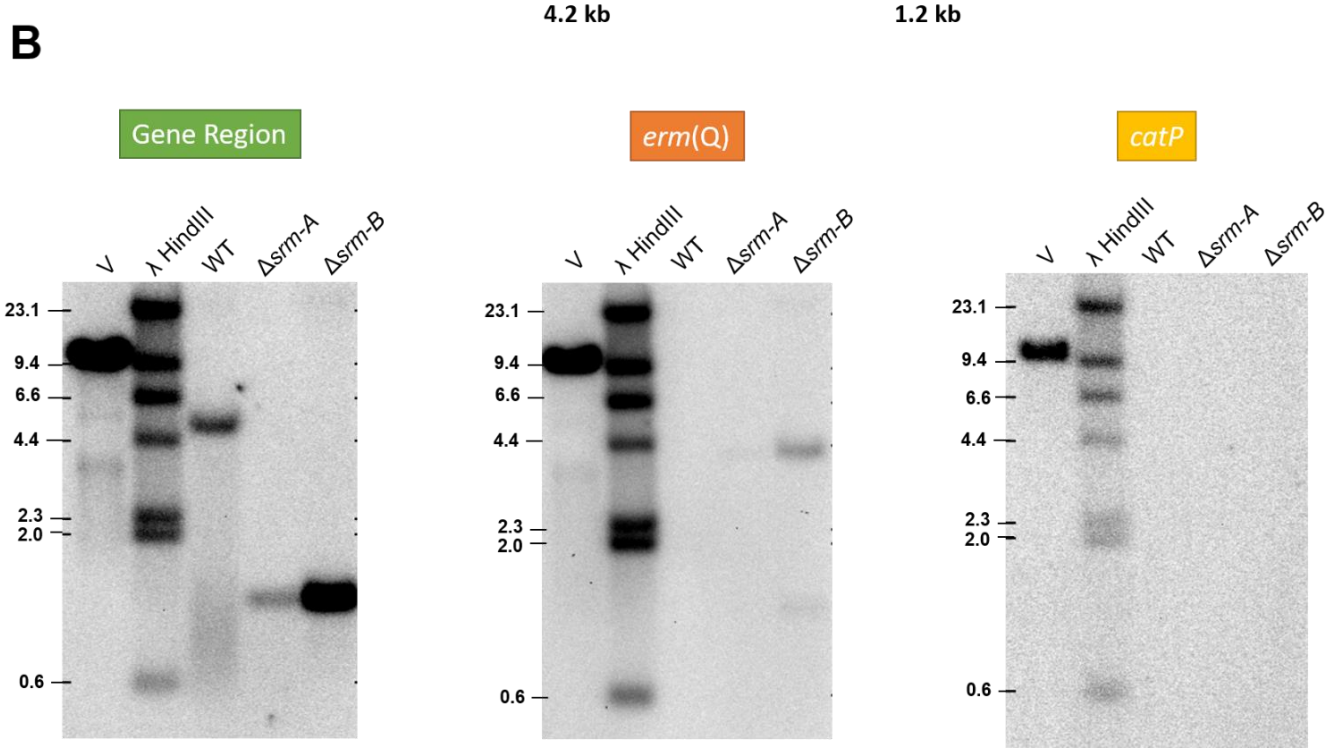
B
Gene Region
erm(Q)
catP
V
λ HindIII
WT
Δsrm-A
Δsrm-B
23.1
9.4
6.6
4.4
2.3
2.0
0.6

Figure 4.5: Southern hybridisation confirmation of *srm* mutants. Genomic DNA was purified and digested with the enzyme AvaII. The Southern blots were probed with DIG-labelled DNA probes specific for: *catP*, carried on the double-crossover vector backbone, *erm*(Q), carried within the double crossover selection cassette and a fragment adjacent to the gene of interest, *srm*. **A.** Schematic representation of wild-type and *srm* mutant DNA fragments digested with AvaII**.** Note an AvaII site in *erm*(Q) results in the production of two fragments that will hybridise with the *erm*(Q) probe. **B.** Confirmation of independent *srm* mutants. Lanes are labelled as follows: Vector –undigested *srm* double crossover vector, Lambda HindIII- DIG-labelled λ HindIII molecular size markers (kilobases), JIR4195- wild-type *C. perfringens* JIR4195 DNA. The double crossover site is present on a fragment of 5 kb for the wild-type and fragments of 4.2 kb and 1.2 kb for the correct mutants.

conjugation. To determine if Srm was required for conjugation, independent mutants were assessed using a mixed plate mating assay (Figure 4.6). Deletion of *srm* from pCW3 did not alter the conjugation efficiency, indicating that this gene is not required for the conjugative transfer of pCW3.

Srm is essential for pCW3 plasmid stability

This study then assessed the role of the Srm protein in the stability of pCW3. The stability phenotype of the *srm* mutants was assessed using a non-selective stability assay whereby independent mutant strains were passaged continuously over the course of six days in broth alongside a wild-type control. Viable counts were carried out every second day (days 0, 2, 4, 6) and 100 of the resulting colonies were cross-patched onto selective media containing tetracycline (to detect the presence of pCW3) and non-selective medium. The plasmid stability of each mutant was determined as the percentage of cells resistant to tetracycline.

When *srm* was mutated on pCW3, the plasmid was gradually lost over the course of the assay (Figure 4.7). Wild-type pCW3 was retained in 99.75% (±0.3%) of the population following six days passage, whereas approximately 66% (±7.7%) of the *srm* mutant population had lost the plasmid by day six.

As *srm* is located close to *pcw347* (Figure 4.1) it was unclear whether successful complementation of the *srm* mutation would require both genes. Subsequently, complementation vectors were constructed with wild-type *srm* alone or with *pcw347* and *srm* together on the multicopy vector pJIR750. *In trans* complementation with either construct restored plasmid stability to wild-type levels (Figure 4.7). These results showed that *srm* is required for the stable inheritance of pCW3, and that complementation did not require the presence of *pcw347.* As such, the gene *pcw348* was renamed *srm* for stability replication and maintenance, this broad title was given as the specific role of the gene product has not yet been demonstrated.

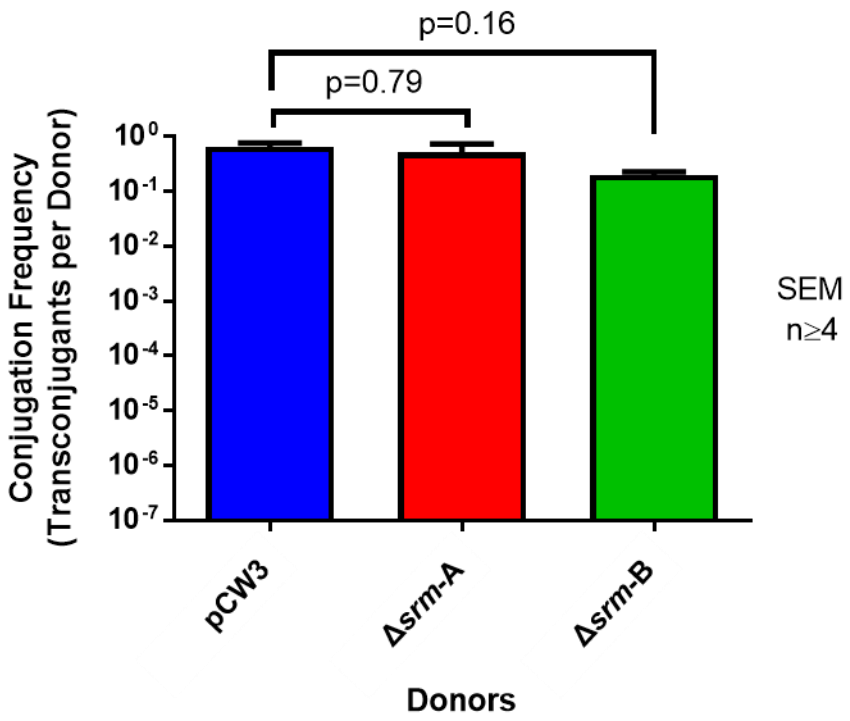

Figure 4.6: Conjugation frequencies of independent *srm* mutants. Conjugation frequency is described as the number of transconjugants cells per donor cell. Donors are shown on the x-axis. Donors are all isogenic derivatives of JIR4195. Two independent *srm* mutants are denoted by A and B, respectively. The means and standard error of the mean are shown based on the results of at least four biological replicates. Statistical analysis was conducted using the Mann-Whitney *u*-test.

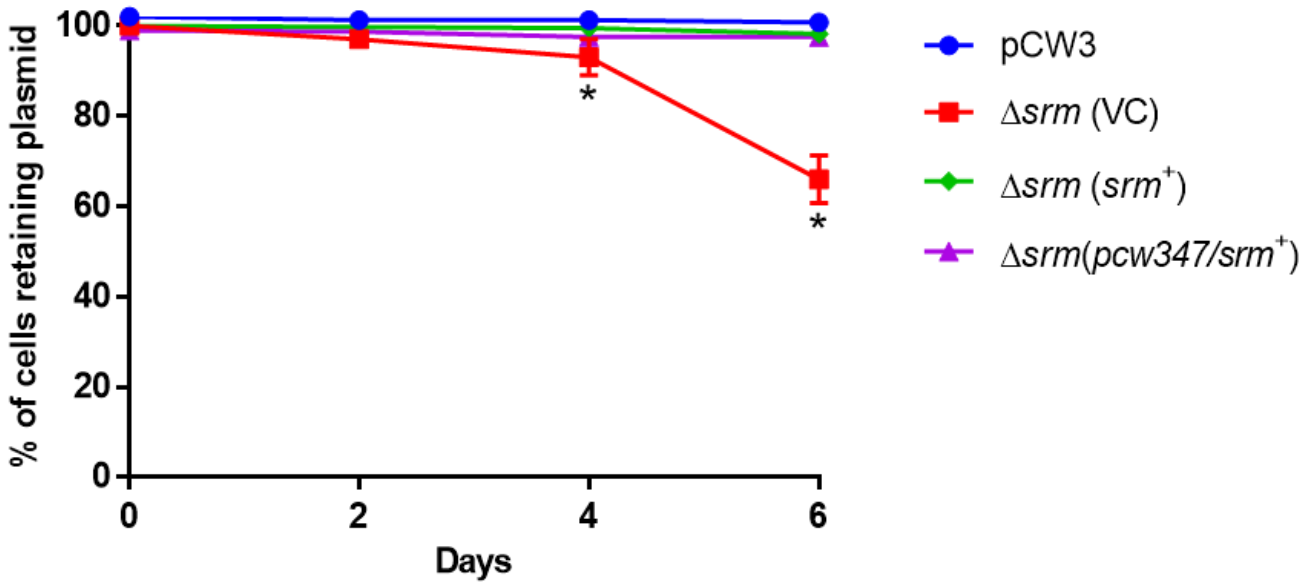

Figure 4.7: Plasmid stabilities of *srm* mutant strains and complemented derivatives. Wild-type, mutant with empty vector and complemented strains were passaged without selection over the course of six days. Plasmid stability is expressed as the percentage of cells retaining pCW3. The means and standard error of the means are shown, based on results from at least four biological replicates. Statistical analysis was carried out using a Mann-Whitney *u*-test. An asterisk denotes statistical significance ($p < 0.05$) compared to wild-type pCW3.

As determined by bioinformatic analysis, Srm was predicted to possess a Hin-like HTH motif. To assess whether this domain was essential for stability, a deletion derivative ($srm_{1\text{-}256}$) lacking the last 44 codons, which encoded the putative HTH motif, was constructed and used to complement the *srm* mutant. Complementation with the deletion construct restored plasmid stability (Figure 4.8). Although, the plasmid was lost from a small proportion of the population at day six (7.5±2.2%), these results indicated that the HTH domain was not essential for the functional role of Srm in maintaining pCW3 plasmid stability

Cross-Complementation with *srm* from other pCW3-like plasmids restores plasmid stability

srm genes are found on all surveyed pCW3-like plasmids, and their gene products have 91-100% amino acid sequence identity to the pCW3-encoded Srm protein. To test whether Srm from another pCW3-like plasmid could complement the *srm* mutation on pCW3, complementation vectors were constructed encoding two *srm* genes from pJIR3844, $srm_{\text{pJIR3844\_45}}$ and $srm_{\text{pJIR3844\_56}}$, with 95.32 % and 96.08% amino acid identity to pCW3 Srm, respectively (Figure 4.9). These two genes were chosen for analysis to determine if both the duplicates genes on this plasmid encoded functional proteins. Both constructs were able to restore plasmid stability back to wild-type levels. These results demonstrate that *srm* genes from other pCW3-like plasmids can complement the *srm* mutation on pCW3.

Deletion of *srm* has a minor effect on pCW3 copy number

Digital droplet PCR was used to assess whether the instability conferred by mutation of *srm* was due to an alteration in plasmid copy number (Figure 4.10). The *srm* mutant had a statistically significant ($p= 0.01$) increase in copy number (5.2±0.07) in comparison to wild-type pCW3 (4.0±0.13). This increase in plasmid copies per chromosome was reversed following complementation (4.2±0.10) ($p> 0.99$). When complemented with the Srm derivative lacking the

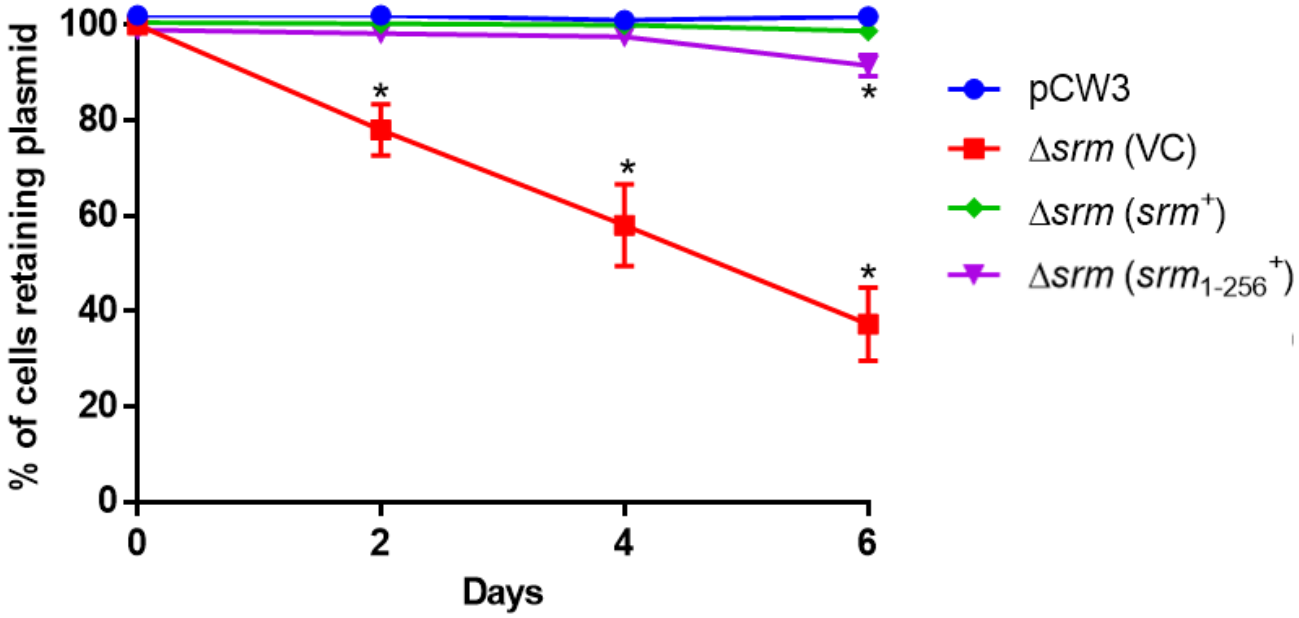

Figure 4.8: Plasmid stability of *srm* complemented derivatives. Wild-type, mutant with empty vector (VC) and complemented strains were passaged without selection over the course of six days. Plasmid stability is expressed as the percentage of cells retaining pCW3. The means and standard error of the means are shown, based on results from at least four biological replicates. Statistical analysis was carried out using a Mann-Whitney *u*-test. An asterisk denotes statistical significance ($p < 0.05$) compared to wild-type pCW3.

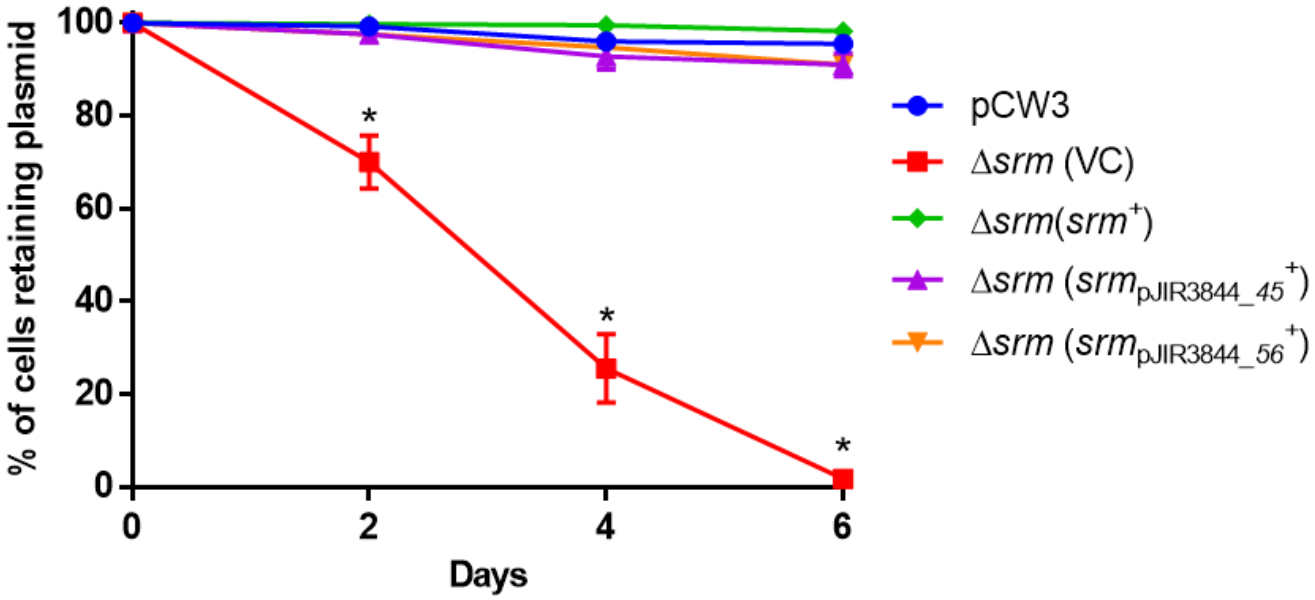

Figure 4.9: Plasmid stability of *srm* complemented derivatives. Wild-type, mutant with empty vector (VC) and complemented strains were passaged without selection over the course of six days. Plasmid stability is expressed as the percentage of cells retaining pCW3. The means and standard error of the means are shown, based on results from at least four biological replicates. Statistical analysis was carried out using a Mann-Whitney *u*-test. An asterisk denotes statistical significance ($p < 0.05$) compared to wild-type pCW3.

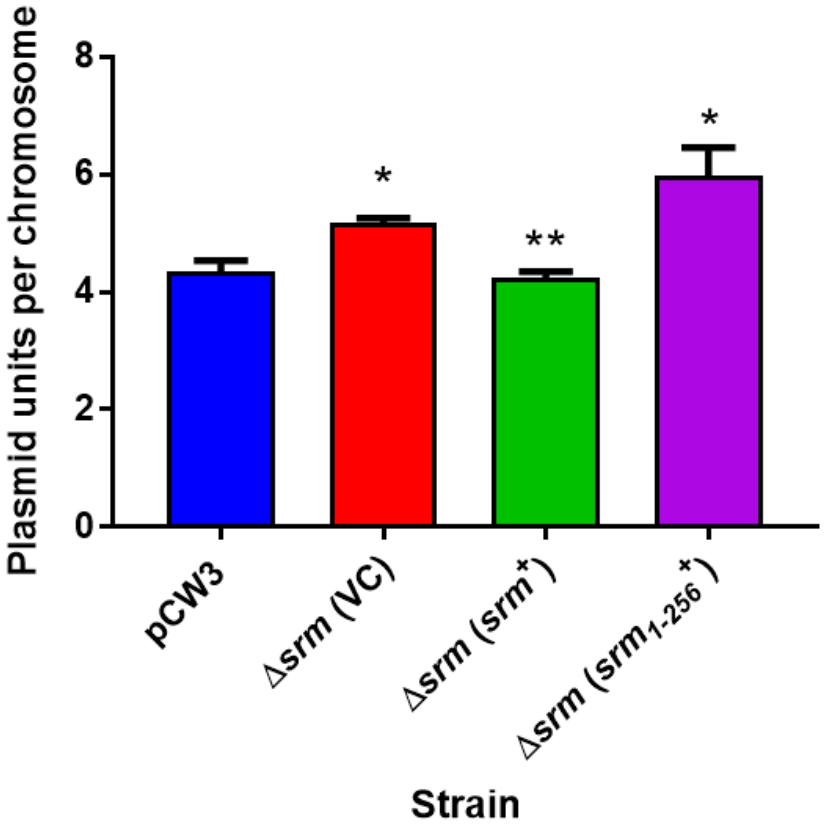

Figure 4.10: Plasmid copy number of *srm* mutant and complemented strains. Plasmid copy number was determined using ddPCR with probes targeting single copy chromosome (*rpoB*) and plasmid (*tetB(P)*) genes. Plasmid copy number is calculated by dividing relative reads for the plasmid marker by the values for chromosomal marker and is denoted as the number of plasmid units per chromosome. The means and standard error of the mean are shown based on the results of at least three biological replicates. Where applicable, statistical analysis was conducted using Mann-Whitney *u*-test. One asterisk denotes statistical significance ($p < 0.05$) compared to wild-type pCW3. Two asterisks denote statistical significance ($p < 0.05$) compared to the vector control strain.

putative HTH motif ($srm_{1\text{-}256}$) the plasmid copy number was increased further (6.0±0.48) (p=0.01), suggesting that the HTH motif may have a role in controlling plasmid copy number.

Attempted analysis of Srm function through protein purification and crystallisation studies

C. perfringens plasmid proteins can possess little amino acid sequence identity to proteins of known function, but subsequent crystallographic analysis can reveal strong structural homology to other characterised proteins (Porter *et al.*, 2012). As bioinformatic analysis did not provide much insight into the potential mechanism of action of the Srm protein, work focused on preliminary attempts of Srm protein structure determination in the hope that it would inform protein function. Srm proteins with ($Srm_{1\text{-}300}$) and without the putative HTH motif ($Srm_{1\text{-}256}$) were expressed as C-terminal His_6-tagged proteins in *E. coli* and subsequently purified using metal affinity chromatography using TALON cobalt resin. Attempts were made to concentrate proteins to concentrations high enough to begin crystallisation studies, but unfortunately both Srm proteins degraded following concentration (Figure 4.11A and B). Subsequent N-terminal sequencing of the degradation products determined that the C-terminal portion of the protein was being degraded as all four products sequenced produced the same ten amino acid sequences from the start of the protein (Figure 4.11C). No N-terminal sequenced products corresponded to any potential fragments that may have arisen from the degradation of the N-terminal end. Had any of these products been identified, the area of protein fragmentation could have been elucidated.

To determine more appropriate buffer conditions for crystallisation studies, protein thermal shift assays were conducted on purified $Srm_{1\text{-}300}$ and $Srm_{1\text{-}256}$ proteins. These assays would quantify protein denaturation patterns in varying conditions, potentially revealing a more appropriate condition for Srm protein studies. However, results from the thermal shift experiments were

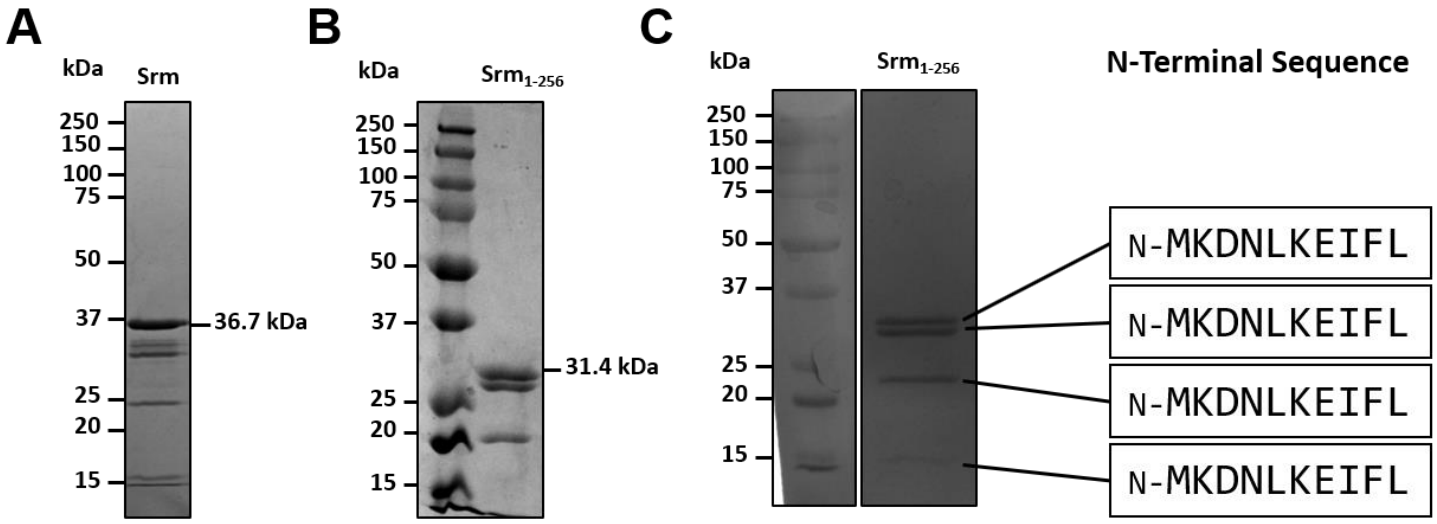

Figure 4.11: SDS-PAGE separation of degraded Srm_{1-300} and Srm_{1-256} proteins and N-terminal sequencing. A. Purified full length Srm_{1-300} protein was analysed using 12% SDS-PAGE and stained with Coomassie Brilliant Blue. Molecular size standards (Bio-Rad) are shown in kilodaltons (kDa). Full length Srm_{1-300} protein of 36.7 kDa can be observed along with degradation products of approximately 33.1, 31.4, 24.4 and 15.9 kDa in size. **B.** Purified Srm_{1-256} protein was analysed using 12% SDS-PAGE and stained in Coomassie Brilliant Blue. Srm_{1-256} protein of 31.4 kDa can be observed along with degradation products of approximately 27.1 and 20.3 kDa in size. **C.** PVDF membrane with Srm_{1-256} stained in Coomassie R250 prior to N-terminal sequencing. The corresponding ten amino acid N-terminal sequences determined from each protein band are labelled in the accompanying boxes.

variable and buffer changes did not improve protein stability. Further optimisation of crystallisation conditions was not attempted as the protein readily degraded.

Srm forms homooligomers

As protein purification at high concentrations proved difficult, work shifted to analyse the functional characteristics of the Srm protein. Many regulatory proteins function as higher order oligomeric forms (Dorman & Deighan, 2003; Gao *et al.*, 2007), to determine if Srm was able to form homooligmers, chemical-crosslinking assays were performed. Following treatment of purified Srm protein samples with increasing concentrations of the chemical crosslinker DTBP, protein-protein interactions were assessed through detection of His_6-tagged proteins *via* Western blot analysis with anti-His antibodies. In all reactions, monomeric Srm was detected at a size of 36.7 kDa (Figure 4.12A). In addition, in the presence of the crosslinker, a band of a higher molecular weight (~73.4 kDa) was observed. These results suggest that Srm can form a homodimer. However, the cross linkages formed in the presence of the cross-linker, DTBP should be reversed upon addition of the reducing agent DTT. This was not observed in this study, suggesting that the DTT used was not active or that the cross-linkages formed in Srm homodimers may be inaccessible to DTT cleavage.

To determine if the C-terminal HTH motif of Srm was required for homooligomerisation, chemical cross-linking experiments were conducted with the Srm_{1-256} derivative (Figure 4.12B). As seen for full length Srm, monomeric protein was detected in all lanes at a size of 31.4 kDa, the smaller size corresponding to the size expected for the truncated protein. Dimeric Srm_{1-256} can be seen in the lane without treatment of cross-linker, suggesting that this protein derivative may be more prone to forming dimers than full length protein. Following addition of increasing concentrations of chemical crosslinker numerous higher molecular weight bands were observed. These results suggest that the formation of Srm homooligomers is independent of the presence of the putative Hin-like HTH motif in the C-terminus of the protein. However, the presence of more higher-order

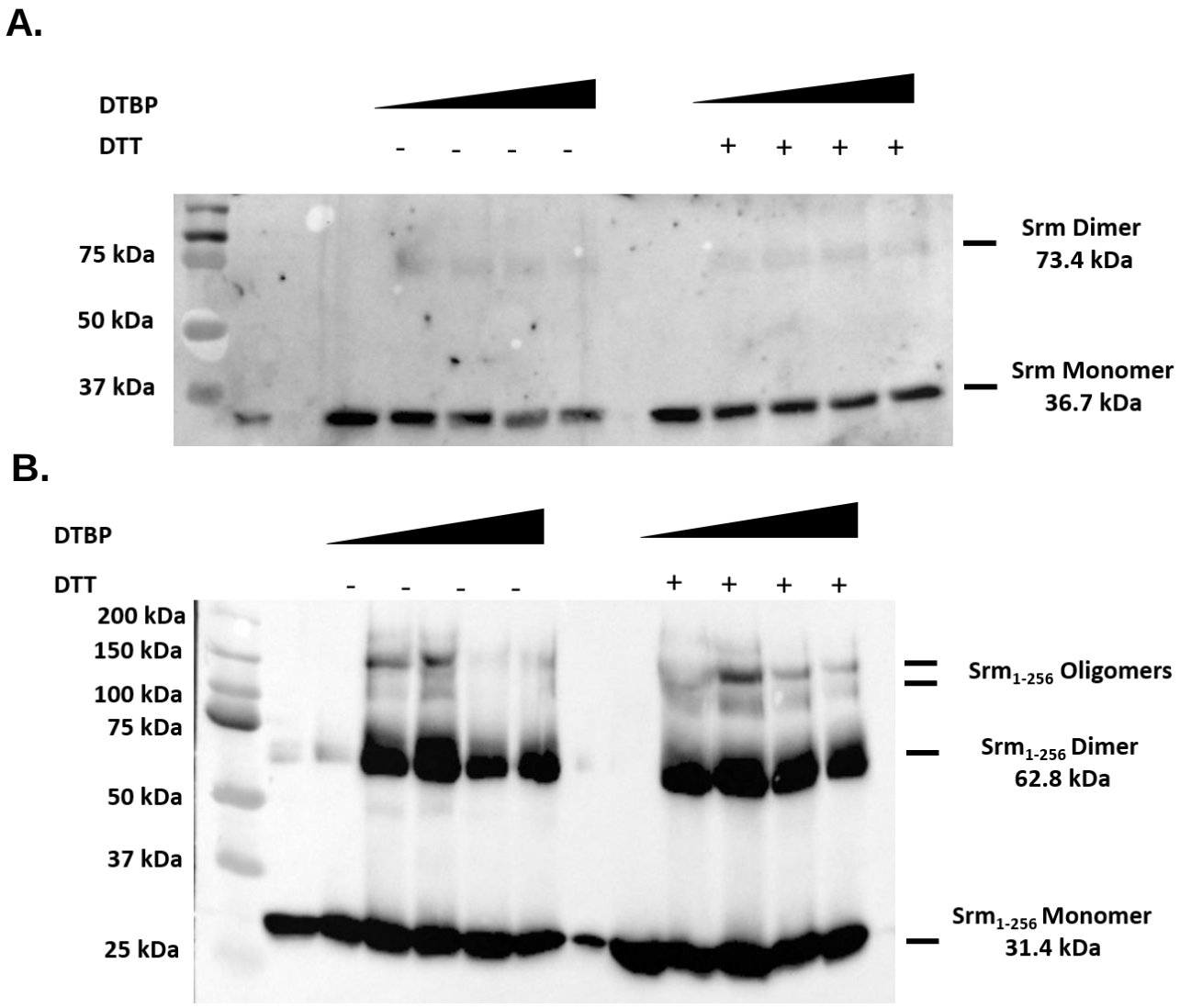

Figure 4.12: Chemical crosslinking of Srm_{1-300}-His_6 and Srm_{1-256}-His_6. Protein-protein interactions were examined by treatment of recombinant His-tagged protein (**A.** Srm_{1-300}; 0.17mg/mL) (**B.** Srm_{1-256}; 0.3mg/mL) with increasing concentrations of the chemical crosslinker DTBP. Chemical crosslinking was assessed using 12% acrylamide SDS-page in the presence (+) and absence (-) of the reducing agent DTT, followed by Western blotting with anti-His antibodies.

oligomeric forms observed for the Srm_{1-256} derivative does suggest that the putative HTH domain may hinder oligomerisation of the full length protein.

Mechanistic crosstalk between the RegC and Srm stability mechanisms: the *srm* gene complements a *regC* mutant.

The pCW3 regulator, RegC, has recently been shown to be involved in the regulation of plasmid stability (T. Stent, X. Han, V. Adams, R. Moore and J. Rood, unpublished). Similar to the *srm* and *resP* mutant studies in this thesis, a *regC* mutant is less stable than the wild type, a process that is reversed by complementation. It was postulated that inactivation of *regC* may have caused dysregulation of important plasmid stability genes, such as *srm* and *resP* (examined in Chapter Three and Four), which resulted in the unstable plasmid phenotype. To assess the ability of *srm* and *resP* to rescue plasmid stability in the *regC* mutant, the respective complementation vectors were introduced into a *regC* mutant, and the stability of the pCW3 derivative was determined (Figure 4.13A). Complementation with wild-type *regC* restored pCW3 stability, as previously described (T. Stent, X. Han, V. Adams, R. Moore and J. Rood, unpublished). Complementation with *resP* did not restore plasmid stability, suggesting that the instability of the *regC* mutant was not due to dysregulation of ResP. However, complementation of the *regC* mutant with the wild-type *srm* gene increased pCW3 stability in comparison to the vector control, with a statistically significant difference evident from day two. The *regC* mutant complemented with *srm* was maintained at levels similar to wild type until day six, where pCW3 was lost from approximately 24±3.7% of the population. Since complementation of the *regC* mutant with *srm* restored plasmid stability to levels similar to wild type, these data suggest that RegC may regulate Srm production.

Reciprocal complementation assays were conducted whereby the *srm* mutant was complemented with *regC* and *resP in trans* (Figure 4.13B). Complementation of the *resP* mutant with *srm* was also attempted. Complementation with *srm* was unable to restore plasmid stability to the *resP* mutant strain (Figure 4.13C), suggesting that Srm functions independently of ResP to ensure

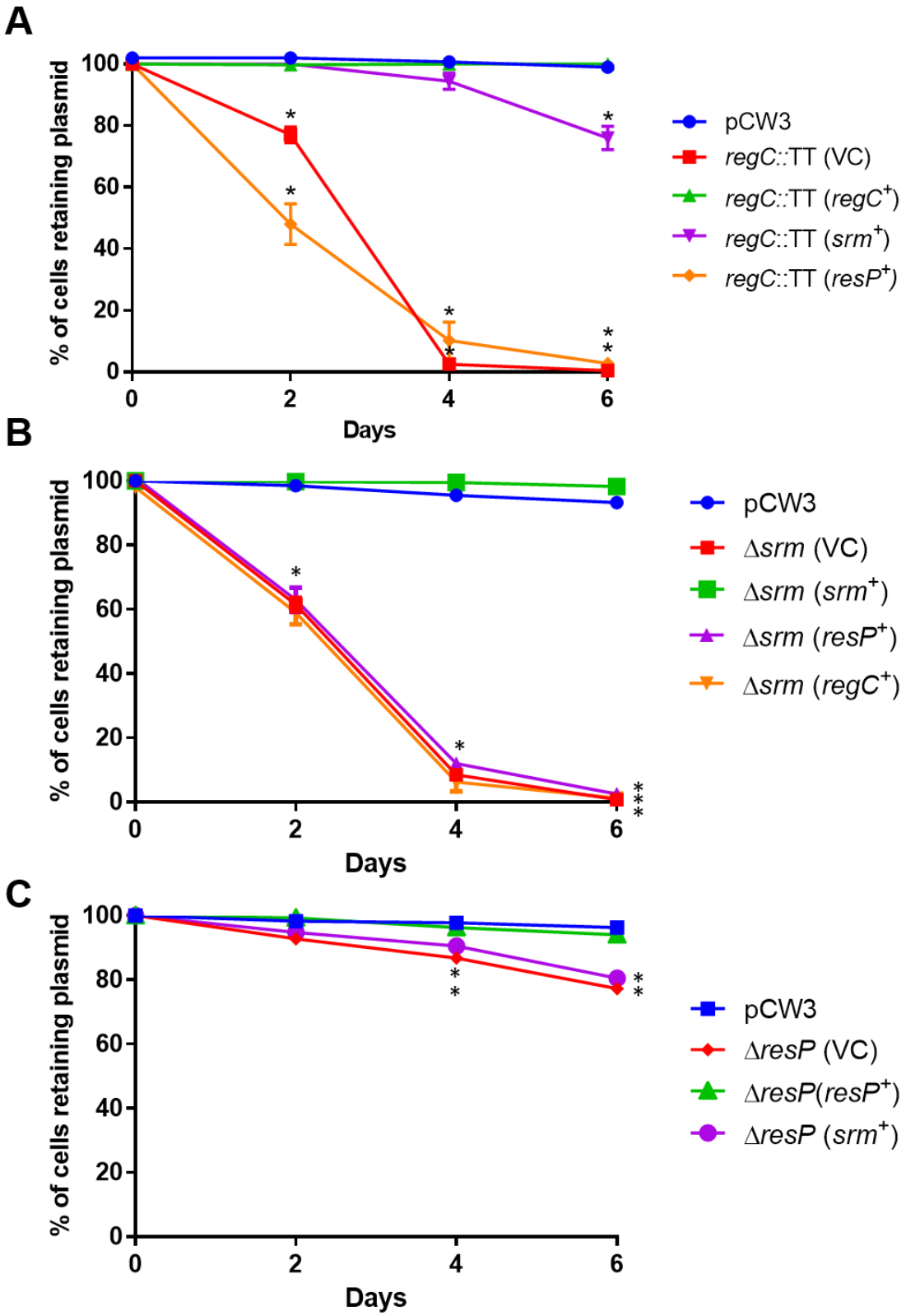
A
% of cells retaining plasmid
100
80
60
40
20
0
0
2
4
6
Days
pCW3
regC::TT (VC)
regC::TT (regC+)
regC::TT (srm+)
regC::TT (resP+)
B
% of cells retaining plasmid
Days
pCW3
Δsrm (VC)
Δsrm (srm+)
Δsrm (resP+)
Δsrm (regC+)
C
% of cells retaining plasmid
Days
pCW3
ΔresP (VC)
ΔresP(resP+)
ΔresP (srm+)

Figure 4.13: Stability assays of the *regC, srm,* and *resP* mutants and cross-complementation derivatives. A. Wild-type, *regC* mutant with empty vector (VC) and complemented strains were passaged without selection over the course of six days (n=4). Stability is expressed as the percentage of the population retaining tetracycline resistance. **B.** Wild-type, *srm* mutants with empty vector and complementation vectors were passaged without selection over the course of six days (n=4). **C.** Wild-type, *resP* mutants with empty vector and complementation vectors were passaged without selection over the course of six days (n=4). The means and standard error of the means are shown. Statistical analysis was carried out using Mann-Whitney *u*-test. An asterisk denotes statistical significance ($p < 0.05$) compared to wild-type pCW3.

plasmid stability. Additionally, *regC and resP* were unable to restore plasmid stability to the *srm* mutant, indicating that Srm does not act through control of these other mechanisms.

Discussion

In this study we provide evidence that the stability of the *C. perfringens* plasmid pCW3 involves a previously unreported mechanism that is potentially unique to the Tcp plasmid family. The *srm* gene, previously annotated as *pcw348*, is present on all surveyed pCW3-like plasmids, with many genes encoding proteins that were identical to Srm from pCW3. Bioinformatic analysis of Srm indicated that it had a Hin-like HTH motif, inferring that this protein may be involved in regulation through binding to DNA sequences. Subsequent analysis determined that Srm had little homology to any proteins outside of *C. perfringens*, with the exception of one plasmid-encoded protein from *C. botulinum.* The conservation of *srm* genes on pCW3-like plasmids and one other clostridial plasmid suggested a putative function in plasmid biology.

When *srm* was deleted from pCW3, plasmid stability was greatly reduced, and plasmid copy number increased slightly. Complementation *in trans* restored pCW3 stability and copy number to wild-type levels (Figures 4.6 and 4.9), highlighting the importance of Srm to both plasmid stability and perhaps fine-tuning copy number control. When an Srm derivative lacking the putative Hin-like HTH domain ($srm_{1\text{-}256}$), was introduced into the *srm* mutant, pCW3 stability was also restored, albeit at a lower level, suggesting that the putative DNA binding domain was not essential for function or may play a further regulatory role.

How might Srm regulate plasmid stability? The evidence acquired in this study suggests Srm may be involved in plasmid copy number control. Copy number control in theta replicating plasmids like pCW3, is achieved through the effective control of replication (Brantl, 2002), which relies on the production of the replication initiator protein, Rep (Del Solar & Espinosa, 2000). The production of Rep and control of plasmid copy number is largely regulated by antisense RNA mechanisms (Brantl, 2002). Unfortunately, the mechanism of pCW3-like plasmid replication and

replication control has not been thoroughly examined, although current work does suggest that pCW3 replication involves an antisense RNA molecule, termed rep_{AS} (V. Adams, C. Lao and J. Rood, unpublished). Typically, antisense RNA molecules are involved in the negative regulation of replication (Brantl, 2002). It would be interesting to examine if Srm is involved in the regulation of *rep* and rep_{AS} transcription. As replication control is a complex mechanism, and without further clarification of the replication process of pCW3-like plasmids, elucidating the role of Srm in plasmid copy number control remains difficult, but is an exciting avenue for future investigation.

Srm could also be influencing plasmid stability by regulating the plasmid maintenance systems present on pCW3, such as multimer resolution, active partitioning or post-segregational killing. It also is possible that Srm could function to directly influence plasmid stability *via* a mechanism that has not yet been characterised. To gain further insight into the function of Srm, determination of its crystal structure would prove invaluable.

Whilst Srm protein purification proved difficult, information regarding the biochemical traits of the Srm protein were obtained. Chemical cross-linking studies demonstrated that Srm did form oligomers, regardless of the presence of the putative Hin-like HTH domain (Figure 4.11). This finding suggested that oligomer formation does not rely on interactions within the last 44 amino acids of Srm. Additionally, since more higher-order oligomeric forms were observed for the Srm_{1-256} derivative than the full length protein, this suggests that the putative HTH domain may hinder oligomerisation of the full length protein. However, the formation of more Srm_{1-256} oligomers may have been an artefact of protein concentration, as the concentration of Srm_{1-256} protein used in this assay was much higher than that used for full length Srm. To further confirm the oligomeric state of Srm, analytical gel filtration and analytical ultracentrifugation analysis should be performed on purified protein.

Tight regulation of plasmid-encoded genes is essential to ensure plasmid maintenance, by reducing the metabolic burden of the plasmid on the cell. Previous studies have determined that

the LexA-like regulator, RegC, is involved in the control of a number of plasmid functions, including conjugation and stability (T. Stent, X. Han, V. Adams, R Moore and J. Rood, unpublished). The exact mechanism by which RegC regulates these plasmid functions has not yet been established. Based on its organisational similarity to the transcriptional repressor LexA, it is likely that RegC functions as an autocatalytic repressor having direct interaction with DNA *via* its C-terminal HTH motif. It was hypothesised that inactivation of *regC* may have caused dysregulation of plasmid stability genes, such as *srm* and *resP*, which resulted in the unstable plasmid phenotype. When the *regC* mutant was complemented *in trans* with the wild-type *srm* gene, plasmid stability was almost completely restored, with notable plasmid loss only observed after four days passage (Figure 4.14). These data support the hypothesis that the stability phenotype conferred by the *regC* mutation was due, at least in part, to its effects on *srm* gene expression, which then were rescued when *srm* was present on a multi-copy vector. The slight loss of the pCW3 *regC* plasmid later in the stability assay (Figure 4.12) indicates that RegC most likely regulates other stability mechanisms, which were not complemented by addition of the *srm* gene. Investigation of cross-complementation phenotypes amongst the *regC, resP* and *srm* mutants hints at the existence of a potential regulatory circuit utilised by pCW3 (further discussed in Chapter Six), whereby RegC is a master regulator, regulating the plasmid stability gene *srm*. The *resP* gene did not complement the instability of either the *regC* or *srm* mutants, indicating that RegC and Srm do not function through the control of the pCW3 multimer resolution system.

When complementation with the $srm_{1\text{-}256}$ derivative was examined using a copy number assay the copy number of pCW3 was increased in comparison to the wild type and the *srm* mutant strains, indicating the HTH domain may be important for Srm-mediated copy number control. Although, it is possible that partial restoration of plasmid stability with the $srm_{1\text{-}256}$ derivative could be an effect of over expression. Previous studies have shown that overexpression of proteins involved in regulation can result in a loss of coordinate control; as was observed for the VirSR two-component regulatory system of *C. perfringens* (Cheung *et al.*, 2009). In this study, *in trans*

overexpression of the *virR* gene resulted in independent activation of the phosphorelays controlled by this response regulator system (Cheung *et al.*, 2009). Controlled regulation was only achieved when the *virR* gene was introduced into the strain in single copy. It is possible that overexpression of the $srm_{1\text{-}256}$ derivative bypassed the regulatory controls governing proper Srm function and as a consequence copy number control, providing an explanation for the increased plasmid copy number in this complemented derivative.

Although this study primarily focused on the characterisation of *srm*, new information was obtained regarding the surrounding genetic region in which this gene is encoded. Within the *dcm* region, products of the *pcw343, pcw344,* and *pcw350* genes all showed at least some homology to known protein domains (Table 4.3). Whilst little is known about the DUF4417 domain found within the product of *pcw343,* the presence of an amidoligase domain in PCW344 is interesting. Amidoligase enzymes catalyse the attachment of an amido group to proteins (Iyer *et al.*, 2009; Iyer *et al.*, 2008). Why a plasmid requires a peptide tagging system remains to be determined, one hypothesis is that it could be involved in the regulation of proteins involved in key plasmid pathways. The product of *pcw350* is now classified as a transposase (Table 4.3) and similar transposase genes can be found in various other organisms, such as *Clostridium thermobutyricum*, *Romoboutsia timonensis*, and *C. botulinum.* Although *pcw350* encodes a putative transposase, it remains one of the most conserved genes within the *dcm* region and is found in one or more copies on the pCW3-like plasmids analysed, with only minor changes occurring in the C-terminal end of the protein.

When the genetic organisation of the *dcm* region is assessed it becomes apparent that large amounts of variation occur within this region. The phenomenon of recombination and insertion in the vicinity of the *dcm* gene has been previously reported in numerous *C. perfringens* plasmid studies (Gurjar *et al.*, 2010; Li *et al.*, 2013; Li *et al.*, 2007; Mehdizadeh Gohari *et al.*, 2016; Miyamoto *et al.*, 2002; Miyamoto *et al.*, 2006; Miyamoto *et al.*, 2008). The *dcm* region is a hotspot

for the insertion of IS-elements and pathogenicity loci on many pCW3-like plasmids. Frequently plasmid-encoded toxin genes are located in close proximity to insertion sequence elements such as IS*1151,* IS*1470,* IS*1469* and IS*406* (Billington *et al.*, 1998, Gurjar *et al.,* 2010, Sayeed *et al.*, 2007, Sayeed *et al.,* 2010). Is it possible that the *pcw350*-encoded transposase facilitates the large amounts of recombination and insertion that occur within this region, as evidenced by the duplication or even triplication of this gene? Or was the insertion of this transposase the catalyst, opening the door for the insertion of other mobile genetic elements into this region? These questions remain to be answered.

No previous work has examined the conservation or disruption of the genes commonly found distal to the *dcm* gene. The analysis conducted in this study suggests that many of the genes within this region are dispensable, as homologues of *pcw340, pcw345, pcw346* and *pcw347* are present on only a few of the plasmids analysed (Table 4.3 and Figure 4.1). Homologues of *dcm, pcw342, srm, pcw349* and *pcw350* are consistently found on other pCW3-like plasmids, suggesting their function is important to the biology of these plasmids. Further investigation into the function of these genes in pCW3 biology were attempted in this study, however mutant construction proved difficult and thus further analyses were curtailed. The bioinformatic work conducted within this study has highlighted the importance of some of the genes located within the *dcm* region and future studies should aim to further characterise this genetic region.

This study also demonstrated that the mutation of *srm* on pCW3, could be complemented by *srm* from other Tcp plasmids. The *srm* homologues assessed in this study were from the plasmid pJIR3844, which is harboured within the strain EHE-NE18 (Bannam *et al.*, 2011). This strain contains two other Tcp plasmids, pJIR3537 and pJIR3535, the latter of which does not possess a full length *srm* gene (Bannam *et al.*, 2011). It is postulated, in the context of this strain, that one Srm from pJIR3844 may assist in stabilisation of pJIR3535. This hypothesis is further supported by the difficulty experienced in obtaining a strain with pJIR3535 (or similar derivative) alone

without pJIR3844 following conjugation (Bannam *et al.*, 2011) (T. Watts, S. Revitt-Mills, V. Adams and J. Rood, unpublished). This theory suggests that the Tcp plasmids are able to share this vital stability machinery without the need for plasmid specificity; making this plasmid maintenance system different to other mechanisms, such as active partitioning, which requires identification of specific plasmids for effective plasmid maintenance.

The results of this study clearly demonstrate the involvement of multiple plasmid stability mechanisms to ensure the faithful inheritance of the *C. perfringens* plasmid pCW3. These findings suggest that Srm is essential to pCW3 plasmid stability and may constitute a new type of plasmid maintenance system, unique to the clostridia. The mechanism in which Srm mediates enhanced plasmid stability remains uncharacterised but may be involved in the regulation of *rep* gene expression. The results have shown that Srm is likely to be regulated by RegC. Overall the findings of this study have further defined the mechanisms by which the pCW3-like plasmids of *C. perfringens* stably maintain themselves within this pathogenic bacterium.

References

Adams, V., Watts, T. D., Bulach, D. M., Lyras, D. & Rood, J. I. (2015). Plasmid partitioning systems of conjugative plasmids from *Clostridium perfringens*. *Plasmid* **80**, 90-96.

Altschul, S. F., Gish, W., Miller, W., Myers, E. W. & Lipman, D. J. (1990). Basic local alignment search tool. *Journal of Molecular Biology* **215**, 403-410.

Aravind, L., Anantharaman, V., Balaji, S., Babu, M. M. & Iyer, L. M. (2005). The many faces of the helix-turn-helix domain: Transcription regulation and beyond. *FEMS Microbiology Reviews* **29**, 231-262.

Austin, S., Ziese, M. & Sternberg, N. (1981). A novel role for site-specific recombination in maintenance of bacterial replicons. *Cell* **25**, 729-736.

Bannam, T. L. & Rood, J. I. (1993). *Clostridium perfringens-Escherichia coli* shuttle vectors that carry single antibiotic resistance determinants. *Plasmid* **29**, 233-235.

Bannam, T. L., Teng, W. L., Bulach, D., Lyras, D. & Rood, J. I. (2006). Functional identification of conjugation and replication regions of the tetracycline resistance plasmid pCW3 from *Clostridium perfringens*. *Journal of Bacteriology* **188**, 4942-4951.

Bannam, T. L., Yan, X.-X., Harrison, P. F., Seemann, T., Keyburn, A. L., Stubenrauch, C., Weeramantri, L. H., Cheung, J. K., McClane, B. A., Boyce, J. D., Moore, R. J. & Rood, J. I. (2011). Necrotic enteritis-derived *Clostridium perfringens* strain with three closely related independently conjugative toxin and antibiotic resistance plasmids. *mBio* **2**: e00190-11.

Bantwal, R., Bannam, T. L., Porter, C. J., Quinsey, N. S., Lyras, D., Adams, V. & Rood, J. I. (2012). The peptidoglycan hydrolase TcpG is required for efficient conjugative transfer of pCW3 in *Clostridium perfringens*. *Plasmid* **67**, 139-147.

Bartolomé, B., Jubete, Y., Martínez, E. & de la Cruz, F. (1991). Construction and properties of a family of pACYC184-derived cloning vectors compatible with pBR322 and its derivatives. *Gene* **102**, 75-78.

Bedbrook, J. R. & Ausubel, F. M. (1976). Recombination between bacterial plasmids leading to the formation of plasmid multimers. *Cell* **9**, 707-716.

Benson, D. A., Cavanaugh, M., Clark, K., Karsch-Mizrachi, I., Lipman, D. J., Ostell, J. & Sayers, E. W. (2017). GenBank. *Nucleic Acids Research* **45**, D37-D42.

Billington, S.J., Wieckowski, E.U., Sarker, M.R., Bueschel, D., Songer, J.G., and McClane, B.A. (1998) *Clostridium perfringens* type E animal enteritis isolates with highly conserved, silent enterotoxin gene sequences. *Infection and Immunity* **66**: 4531-4536.

Bingle, L. E. H. & Thomas, C. M. (2001). Regulatory circuits for plasmid survival. *Current Opinion in Microbiology* **4**, 194-200.

Brantl, S. (2002). Antisense RNAs in plasmids: control of replication and maintenance. *Plasmid* **48**, 165-173.

Cheung, J. K., Awad, M. M., McGowan, S. & Rood, J. I. (2009). Functional analysis of the VirSR phosphorelay from *Clostridium perfringens*. *PLOS One* **4**, e5849.

Cheung, J. K., Keyburn, A. L., Carter, G. P., Lanckriet, A. L., Van Immerseel, F., Moore, R. J. & Rood, J. I. (2010). The VirSR two-component signal transduction system regulates NetB toxin production in *Clostridium perfringens*. *Infection and Immunity* **78**, 3064-3072.

Crooks, G. E., Hon, G., Chandonia, J.-M. & Brenner, S. E. (2004). WebLogo: a sequence logo generator. *Genome research* **14**, 1188-1190.

Del Solar, G. & Espinosa, M. (2000). Plasmid copy number control: an ever-growing story. *Molecular Microbiology* **37**, 492-500.

Dodd, I. B. & Egan, J. B. (1990). Improved detection of helix-turn-helix DNA-binding motifs in protein sequences. *Nucleic Acids Research* **18**, 5019-5026.

Dorman, C. J. & Deighan, P. (2003). Regulation of gene expression by histone-like proteins in bacteria. *Current Opinion in Genetics & Development* **13**, 179-184.

Ebersbach, G. & Gerdes, K. (2005). Plasmid segregation mechanisms. *Annual Review of Genetics* **39**, 453-479.

Gao, R., Mack, T. R. & Stock, A. M. (2007). Bacterial response regulators: versatile regulatory strategies from common domains. *Trends in Biochemical Sciences* **32**, 225-234.

Gerdes, K., Howard, M. & Szardenings, F. (2010). Pushing and pulling in prokaryotic DNA segregation. *Cell* **141**, 927-942.

Gerdes, K., Rasmussen, P. B. & Molin, S. (1986). Unique type of plasmid maintenance function: postsegregational killing of plasmid-free cells. *Proceedings of the National Academy of Sciences* **83**, 3116-3120.

Gurjar, A., Li, J. & McClane, B. A. (2010). Characterization of toxin plasmids in *Clostridium perfringens* type C isolates. *Infection and Immunity* **78**, 4860-4869.

Hughes, M. L., Poon, R., Adams, V., Sayeed, S., Saputo, J., Uzal, F. A., McClane, B. A. & Rood, J. I. (2007). Epsilon-toxin plasmids of *Clostridium perfringens* type D are conjugative. *Journal of Bacteriology* **189**, 7531-7538.

Hülter, N., Ilhan, J., Wein, T., Kadibalban, A. S., Hammerschmidt, K. & Dagan, T. (2017). An evolutionary perspective on plasmid lifestyle modes. *Current Opinion in Microbiology* **38**, 74-80.

Inoue, H., Nojima, H. & Okayama, H. (1990). High efficiency transformation of *Escherichia coli* with plasmids. *Gene* **96**, 23-28.

Iyer, L. M., Abhiman, S., Maxwell Burroughs, A. & Aravind, L. (2009). Amidoligases with ATP-grasp, glutamine synthetase-like and acetyltransferase-like domains: synthesis of novel metabolites and peptide modifications of proteins. *Molecular BioSystems* **5**, 1636-1660.

Iyer, L. M., Burroughs, A. M. & Aravind, L. (2008). Unraveling the biochemistry and provenance of pupylation: a prokaryotic analog of ubiquitination. In *Biology Direct*, p. 45.

Li, J., Adams, V., Bannam, T. L., Miyamoto, K., Garcia, J. P., Uzal, F. A., Rood, J. I. & McClane, B. A. (2013). Toxin plasmids of *Clostridium perfringens*. *Microbiology and Molecular Biology Reviews* **77**, 208-233.

Li, J., Miyamoto, K. & McClane, B. A. (2007). Comparison of virulence plasmids among *Clostridium perfringens* type E isolates. *Infection and Immunity* **75**, 1811-1819.

Lyristis, M., Bryant, A. E., Sloan, J., Awad, M. M., Nisbet, I. T., Stevens, D. L. & Rood, J. I. (1994). Identification and molecular analysis of a locus that regulates extracellular toxin production in *Clostridium perfringens*. *Molecular Microbiology* **12**, 761-777.

Marchler-Bauer, A., Bo, Y., Han, L., He, J., Lanczycki, C. J., Lu, S., Chitsaz, F., Derbyshire, M. K., Geer, R. C., Gonzales, N. R., Gwadz, M., Hurwitz, D. I., Lu, F., Marchler, G. H., Song, J. S., Thanki, N., Wang, Z., Yamashita, R. A., Zhang, D., Zheng, C., Geer, L. Y. & Bryant, S. H. (2017). CDD/SPARCLE: functional classification of proteins via subfamily domain architectures. *Nucleic Acids Research* **45**, D200-D203.

Marchler-Bauer, A., Derbyshire, M. K., Gonzales, N. R., Lu, S., Chitsaz, F., Geer, L. Y., Geer, R. C., He, J., Gwadz, M., Hurwitz, D. I., Lanczycki, C. J., Lu, F., Marchler, G. H., Song, J. S., Thanki, N., Wang, Z., Yamashita, R. A., Zhang, D., Zheng, C. & Bryant, S. H. (2015). CDD: NCBI's conserved domain database. *Nucleic Acids Research* **43**, D222-D226.

McWilliam, H., Li, W., Uludag, M., Squizzato, S., Park, Y. M., Buso, N., Cowley, A. P. & Lopez, R. (2013). Analysis tool web services from the EMBL-EBI. *Nucleic Acids Research* **41**, W597-W600.

Mehdizadeh Gohari, I., Kropinski, A. M., Weese, S. J., Parreira, V. R., Whitehead, A. E., Boerlin, P. & Prescott, J. F. (2016). Plasmid characterization and chromosome analysis of two *netF+ Clostridium perfringens* isolates associated with foal and canine necrotizing enteritis. *PLOS One* **11**, e0148344.

Mignot, T., Mock, M. & Fouet, A. (2003). A plasmid-encoded regulator couples the synthesis of toxins and surface structures in *Bacillus anthracis*. *Molecular Microbiology* **47**, 917-927.

Miroux, B. & Walker, J. E. (1996). Over-production of proteins in *Escherichia coli*: mutant hosts that allow synthesis of some membrane proteins and globular proteins at high levels. *Journal of Molecular Biology* **260**, 289-298.

Miyamoto, K., Chakrabarti, G., Morino, Y. & McClane, B. A. (2002). Organization of the plasmid *cpe* locus in *Clostridium perfringens* Type A isolates. *Infection and Immunity* **70**, 4261-4272.

Miyamoto, K., Fisher, D. J., Li, J., Sayeed, S., Akimoto, S. & McClane, B. A. (2006). Complete sequencing and diversity analysis of the enterotoxin-encoding plasmids in *Clostridium perfringens* type A non-food-borne human gastrointestinal disease isolates. *Journal of Bacteriology* **188**, 1585-1598.

Miyamoto, K., Li, J., Sayeed, S., Akimoto, S. & McClane, B. A. (2008). Sequencing and diversity analyses reveal extensive similarities between some epsilon-toxin-encoding plasmids and the pCPF5603 *Clostridium perfringens* enterotoxin plasmid. *Journal of Bacteriology* **190**, 7178-7188.

Nordström, K. (2006). Plasmid R1—Replication and its control. *Plasmid* **55**, 1-26.

Parreira, V. R., Costa, M., Eikmeyer, F., Blom, J. & Prescott, J. F. (2012). Sequence of two plasmids from *Clostridium perfringens* chicken necrotic enteritis isolates and comparison with *C. perfringens* conjugative plasmids. *PLOS One* **7**, e49753.

Parsons, J. A., Bannam, T. L., Devenish, R. J. & Rood, J. I. (2007). TcpA, an FtsK/SpoIIIE homolog, is essential for transfer of the conjugative plasmid pCW3 in *Clostridium perfringens*. *Journal of Bacteriology* **189**, 7782-7790.

Petersen, T. N., Brunak, S., von Heijne, G. & Nielsen, H. (2011). SignalP 4.0: discriminating signal peptides from transmembrane regions. *Nature Methods* **8**, 785.

Pinto, U. M., Pappas, K. M. & Winans, S. C. (2012). The ABCs of plasmid replication and segregation. *Nature Reviews Microbiology* **10**, 755.

Porter, C. J., Bantwal, R., Bannam, T. L., Rosado, C. J., Pearce, M. C., Adams, V., Lyras, D., Whisstock, J. C. & Rood, J. I. (2012). The conjugation protein TcpC from *Clostridium perfringens* is structurally related to the type IV secretion system protein VirB8 from Gram-negative bacteria. *Molecular Microbiology* **83**, 275-288.

Rood, J. I., Maher, E. A., Somers, E. B., Campos, E. & Duncan, C. L. (1978). Isolation and characterization of multiply antibiotic-resistant *Clostridium perfringens* strains from porcine feces. *Antimicrobial Agents and Chemotherapy* **13**, 871-880.

San Millan, A. & MacLean, R. C. (2017). Fitness costs of plasmids: A limit to plasmid transmission. *Microbiology Spectrum* **5**: MTBP-0016-2017.

Sayeed, S., Li, J., and McClane, B.A. (2007) Virulence plasmid diversity in *Clostridium perfringens* type D isolates. *Infection and Immunity* **75**: 2391-2398.

Sayeed, S., Li, J., and McClane, B.A. (2010) Characterization of virulence plasmid diversity among *Clostridium perfringens* type B isolates. *Infection and Immunity* **78**: 495-504.

Shimizu, T., Ohtani, K., Hirakawa, H., Ohshima, K., Yamashita, A., Shiba, T., Ogasawara, N., Hattori, M., Kuhara, S. & Hayashi, H. (2002). Complete genome sequence of *Clostridium perfringens*, an anaerobic flesh-eater. *Proceedings of the National Academy of Sciences* **99**, 996-1001.

Skarin, H. & Segerman, B. (2014). Plasmidome interchange between *Clostridium botulinum, Clostridium novyi* and *Clostridium haemolyticum* converts strains of independent lineages into distinctly different pathogens. *PLOS One* **9**, e107777.

Steen, J. A., Bannam, T. L., Teng, W. L., Devenish, R. J. & Rood, J. I. (2009). The putative coupling protein TcpA interacts with other pCW3-encoded proteins to form an essential part of the conjugation complex. *Journal of Bacteriology* **191**, 2926-2933.

Sullivan, M. J., Petty, N. K. & Beatson, S. A. (2011). Easyfig: a genome comparison visualizer. *Bioinformatics (Oxford, England)* **27**, 1009-1010.

Summers, D. K. (1991). The kinetics of plasmid loss. *Trends in Biotechnology* **9**, 273-278.

Teng, W. L., Bannam, T. L., Parsons, J. A. & Rood, J. I. (2008). Functional characterization and localization of the TcpH conjugation protein from *Clostridium perfringens*. *Journal of Bacteriology* **190**, 5075-5086.

Tolmasky, M. E. (2017). Plasmids. In *Reference Module in Life Sciences*: Elsevier.

Traore, D. A. K., Wisniewski, J. A., Flanigan, S. F., Conroy, P. J., Panjikar, S., Mok, Y.-F., Lao, C., Griffin, M. D. W., Adams, V., Rood, J. I. & Whisstock, J. C. (2018). Crystal structure of TcpK in complex with *oriT* DNA of the antibiotic resistance plasmid pCW3. *Nature Communications* **9**, 3732.

Wang, Y., Penkul, P. & Milstein, J. N. (2016). Quantitative localization microscopy reveals a novel organization of a high-copy number plasmid. *Biophysical Journal* **111**, 467-479.

Watts, T. D., Johanesen, P. A., Lyras, D., Rood, J. I. & Adams, V. (2017). Evidence that compatibility of closely related replicons in *Clostridium perfringens* depends on linkage to *parMRC*-like partitioning systems of different subfamilies. *Plasmid* **91**, 68-75.

Wisniewski, J. A., Teng, W. L., Bannam, T. L. & Rood, J. I. (2015a). Two novel membrane proteins, TcpD and TcpE, are essential for conjugative transfer of pCW3 in *Clostridium perfringens*. *Journal of Bacteriology* **197**, 774-781.

Wisniewski, J.A., Traore, D.A., Bannam, T.L., Lyras, D., Whisstock, J.C., and Rood, J.I. (2015b) TcpM, a novel relaxase that mediates transfer of large conjugative plasmids from *Clostridium perfringens*. *Molecular Microbiology* **99**: 884-896.

Zatyka, M., Jagura-Burdzy, G. & Thomas, C. M. (1994). Regulation of transfer genes of promiscuous IncPα plasmid RK2: repression of Tra1 region transcription both by relaxosome proteins and by the Tra2 regulator TrbA. *Microbiology* **140**, 2981-2990.

Chapter Five

Super-resolution microscopy reveals the spatial location of the Tcp conjugation proteins in *Clostridium perfringens*

Introduction

Conjugation is the primary means of horizontal gene transfer in bacteria and plays a critical role in the rapid dissemination of mobile genetic elements amongst prokaryotes (Grohmann *et al.*, 2017). The conjugative transfer of DNA relies on the contact-dependent translocation of protein and DNA substrates through a large multi-protein complex known as a conjugative type IV secretion system (T4SS) (Goessweiner-Mohr *et al.*, 2014). Conjugative T4SSs are present in both Gram-negative and Gram-positive bacteria and are comprised of two key components: the cytoplasmic DNA-processing relaxosome and the membrane-associated transfer apparatus, which are linked together by a coupling protein (Wallden *et al.*, 2010). The VirB/D4 T4SS of the Gram-negative plant pathogen *Agrobacterium tumefaciens* is currently the best characterised T4SS, encoding proteins universally conserved amongst Gram-negative T4SS, making it the archetypal transfer system (Waksman & Orlova, 2014). The *A. tumefaciens* T4SS is comprised of 12 proteins (VirB1-VirB11 and VirD4), that span the inner membrane, periplasm and outer membrane of the Gram-negative cell (Waksman & Orlova, 2014). The transfer systems of Gram-positive bacteria have similarity to their Gram-negative counterparts, although they do not encode homologues of the outer membrane channel components VirB7, VirB9 and VirB10 (Goessweiner-Mohr *et al.*, 2014). Additionally, in Gram-negative systems, cell-to-cell contact is promoted by pilus extensions, but no analogous structures have been identified in Gram-positive systems. Instead they are thought to mediate cell attachment through the production of surface adhesins (Bhatty *et al.*, 2013, Goessweiner-Mohr *et al.*, 2014).

The Gram-positive anaerobic pathogen *C. perfringens* harbours many of its disease-causing toxin genes on large conjugative plasmids (Bannam *et al.*, 2011, Brynestad *et al.*, 2001, Hughes *et al.*, 2007, Mehdizadeh Gohari *et al.*, 2016). The best characterised family of these plasmids is the pCW3-like plasmid family. Within the conserved genetic backbone of the pCW3-like plasmids is the novel *tcp* conjugation locus, which encodes several proteins that are functionally homologous

to those found in Gram-negative T4SS (Bannam *et al.*, 2006). The *tcp* locus is comprised of 12 genes, (*tcpK, tcpM* and *tcpA-tcpJ*) all of which are required for the efficient conjugative transfer of pCW3, except *tcpB, tcpI and tcpJ*, (Figure 5.1) (Bannam *et al.*, 2006, Parsons *et al.*, 2007, Porter *et al.*, 2012, Wisniewski *et al.*, 2015a, Bantwal *et al.*, 2012, Traore *et al.*, 2018, Wisniewski *et al.*, 2015b, Wisniewski & Rood, 2017).

The DNA processing machinery is comprised of TcpM and TcpK, which are encoded at the beginning of the *tcp* locus, on either side of the origin of transfer (*oriT*) (Traore *et al.*, 2018, Wisniewski *et al.*, 2015b). TcpM functions as an atypical relaxase, processing pCW3 DNA prior to transfer through a mechanism similar to tyrosine recombinase enzymes (Wisniewski *et al.*, 2015b). TcpK is a small DNA binding protein that interacts specifically with the *oriT* DNA and may function as an accessory factor for TcpM-mediated DNA processing (Traore *et al.*, 2018).

The transmembrane channel that spans from the donor cell into the recipient is formed primarily by the VirB8-like protein TcpC and the VirB6-like scaffold protein TcpH (Porter *et al.*, 2012, Teng *et al.*, 2008, Bannam *et al.*, 2006). Powering the transfer of plasmid DNA is the hexameric ATPase TcpF and the coupling protein TcpA (Bannam *et al.*, 2006, Parsons *et al.*, 2007, Steen *et al.*, 2009). Lastly, the peptidoglycan hydrolase enzyme TcpG functions to produce localised openings in the peptidoglycan layers of bacterial cells allowing for the effective transfer of pCW3 (Bantwal *et al.*, 2012).

Previously, wide-field fluorescence microscopy was used to visualise the location of several structural components of the Tcp conjugation system, however, the resolution of these images was limited (Wisniewski *et al.*, 2015a, Teng *et al.*, 2008). Nevertheless, fluorescence microscopy determined that the essential Tcp proteins TcpD, TcpE, TcpF and TcpH localised predominantly to the poles of the bacterial cells, suggesting that the conjugation event may occur at this location (Teng *et al.*, 2008, Wisniewski *et al.*, 2015a). Polar localisation of T4SS components is recognised as the consensus location for conjugation events in multiple organisms, including *A. tumefaciens*

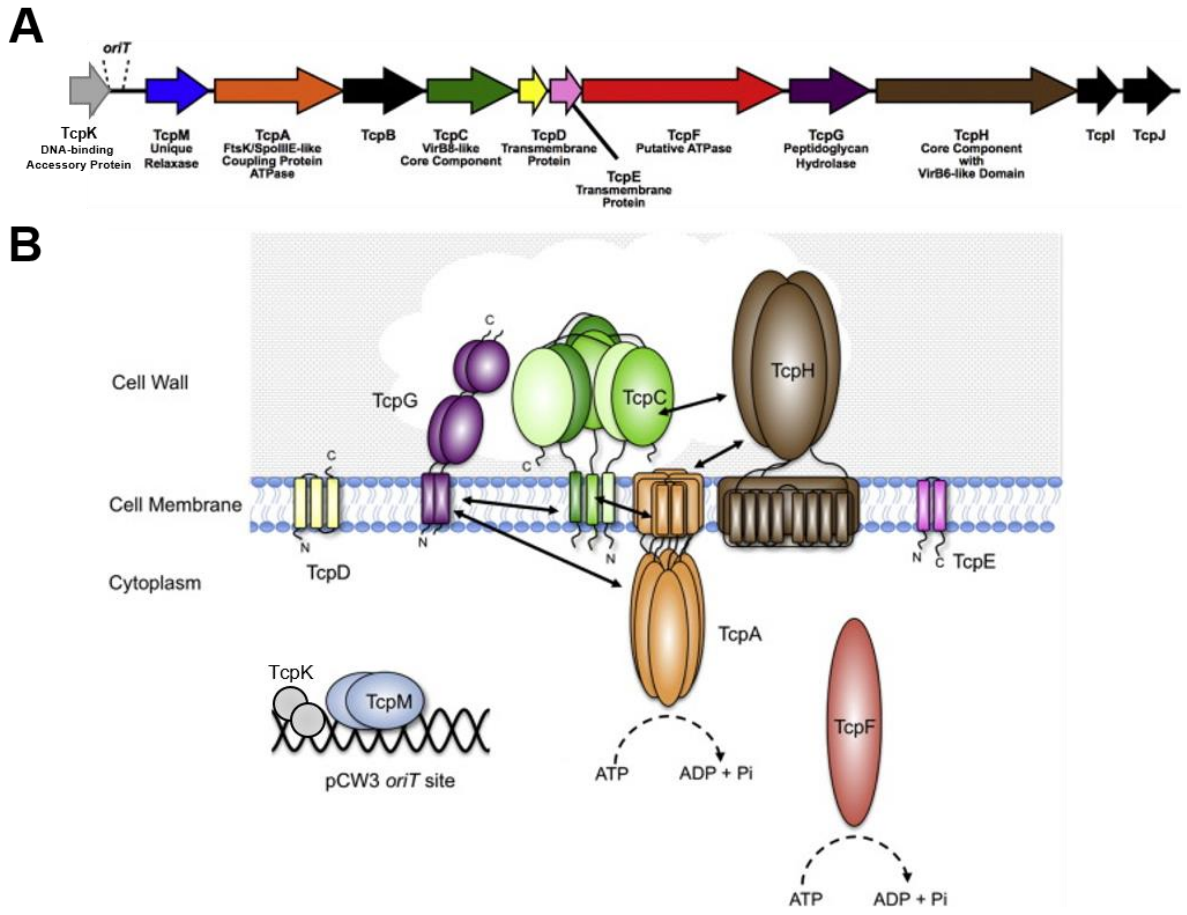

Figure 5.1: Schematic representation of the pCW3 *tcp* locus and Tcp conjugation system. **A.** The updated *tcp* locus: genes are denoted by the arrows. The name and proposed function of the encoded proteins are labelled below the respective gene. Genes not required for conjugative transfer are coloured black. Image taken from (Wisniewski & Rood, 2017) and adapted. **B.** Model of localisation and interactions of the pCW3 Tcp conjugation apparatus, as determined by protein interaction studies and bioinformatic analysis. Confirmed protein-protein interactions are denoted by the black arrows. Proteins are coloured corresponding to the gene shown in Figure 5.1A. Image taken from (Wisniewski & Rood, 2017) and adapted.

(Kumar & Das, 2002, Judd *et al.*, 2005) and *Legionella pneumophila* (Jeong *et al.*, 2017, Jeong *et al.*, 2018). However, improvements in imaging techniques now allows us to visualise proteins to a much higher resolution, sometimes even allowing for the identification of individual protein complexes on the surface of bacterial cells (Gunasinghe *et al.*, 2018, Gunasinghe *et al.*, 2017). As such, imaging of T4SS proteins at a higher resolution has now challenged the notion that conjugation occurs at the cell poles, and multiple complexes may form around the circumference of the cell (Aguilar *et al.*, 2011, Aguilar *et al.*, 2010).

To gain further insight into how the Tcp T4SS functions in *C. perfringens,* the localisation of several epitope tagged Tcp proteins using STimulated Emission Depletion (STED) super resolution microscopy was determined. This work showed that several of the Tcp proteins localise to different areas within the *C. perfringens* cell, with some proteins showing a strong polar localisation whereas others are more dispersed. These data support a model (Aguilar *et al.*, 2011) in which T4SS form in multiple sites to maximise conjugative interactions.

Materials and Methods

Bacterial strains, plasmids and culture conditions

C. perfringens strains and plasmids used in this study are listed in Table 5.1**.** *C. perfringens* and *E. coli* strains were cultured as described in Chapter Two.

Molecular Techniques

Plasmid DNA was extracted from *E. coli* using QIAprep Spin Miniprep kit (Qiagen) as outlined by the manufacturer. Crude *C. perfringens* DNA was obtained as previously described (Bannam *et al.*, 2006)**.** *E. coli* cells were made chemically competent and transformed as previously described (Inoue *et al.*, 1990). Oligonucleotides used in this study are listed in Table 5.2 and were synthesised by Integrated DNA Technologies (IDT) or Sigma. PCR amplification was performed

Table 5.1: Strains and plasmids used in this study

Strain	Description	Reference
E. coli		
DH5α	F-φ80*lacZ*ΔM15, Δ(*lac*ZYA-*argF*)U169, *rec*A1, *end*A1, *hsd*R17(r_k-, m_k+), *pho*A, *sup*E44, *thi*-1, *gyr*A96, *rel*A1 λ	Invitrogen/ Life Technologies
C. perfringens		
JIR325	Strain 13 derivative; Rif^R Nal^R	(Lyristis *et al.*, 1994)
JIR4195	JIR325(pCW3); Rif^R Nal^R Tc^R	(Hughes *et al.*, 2007)
JIR4394	Strain 13 derivative; Sm^R Chl^R	(Bannam *et al.*, 2006)
JIR4885	JIR4195(pJIR2902); Rif^R Nal^R Tc^R Em^R pCW3Δ*tcpH::erm*(Q)	(Bannam *et al.*, 2006)
JIR12051	JIR4195(pJIR3213); Rif^R Nal^R Tc^R Em^R pCW3Δ*tcpA::erm*(Q)	(Parsons *et al.*, 2007)
JIR12212	JIR4195(pJIR3440); Rif^R Nal^R Tc^R Em^R pCW3Δ*tcpD::erm*(Q)	(Wisniewski *et al.*, 2015a)
JIR12215	JIR4195(pJIR3442); Rif^R Nal^R Tc^R Em^R pCW3Δ*tcpE::erm*(Q)	(Wisniewski *et al.*, 2015a)
JIR12540	JIR4195(pJIR3760); Rif^R Nal^R Tc^R Em^R pCW3Ω*tcpM*::targetron (TT)	(Wisniewski *et al.*, 2015b)
JIR13063	JIR4195(pJIR4349); Rif^R Nal^R Tc^R Em^R pCW3Ω*tcpK*::targetron (TT)	(Traore *et al.*, 2018)
Plasmids		
pCW3	Conjugative tetracycline resistance plasmid	(Rood *et al.*, 1978)
pT7-Blue3	*E. coli* cloning vector, *bla*$^+$, f1 origin, pUC origin, *lacZ* α-peptide	Novagen
pJIR2902	pCW3Δ*tcpH::erm*(Q)	(Bannam *et al.*, 2006)
pJIR3213	pCW3Δ*tcpA::erm*(Q)	(Parsons *et al.*, 2007)
pJIR3422	*E. coli-C. perfringens* shuttle vector; lacZ α-peptide, Cm^R	(Adams *et al.*, 2014)
pJIR3440	pCW3Δ*tcpD*::*erm*(Q)	(Wisniewski *et al.*, 2015a)
pJIR3442	pCW3Δ*tcpE::erm*(Q)	(Wisniewski *et al.*, 2015a)
pJIR3757	pJIR3422(BamHI/Asp718)ΩJRP4048/JRP4489 (BamHI/Asp718; 451 bp, pCW3) *tcpE*-HA complementation vector	(Wisniewski *et al.*, 2015a)

pJIR3760	pCW3Ω*tcpM*:: TT	(Wisniewski *et al.*, 2015b)
pJIR4204	pJIR3422(BamHI/Asp718)ΩJRP4046/JRP4728 (BamHI/Asp718; 450 bp, pCW3) *tcpD*-G_6-HA complementation vector	(Wisniewski *et al.*, 2015a)
pJIR4349	pCW3Ω*tcpK*:: TT	(Traore *et al.*, 2018)
pJIR4644	pT7-Blue3 (EcoRI) ΩJRP6570/JRP6571 (798 bp, pCW3) *tcpK*-G_6-HA, blunt cloning vector	This study
pJIR4645	pT7-Blue3 (EcoRI) ΩJRP6572/JRP6573 (305 bp, pCW3) *tcpM*-G_6-HA, blunt cloning vector	This study
pJIR4655	pJIR3422(BamHI/Asp718) (BamHI/Asp718; 798 bp, pJIR4644) *tcpK*-G_6-HA complementation vector	This study
pJIR4657	pJIR3422(BamHI/Asp718) (BamHI/Asp718; 305 bp, pJIR4645) *tcpM*-G_6-HA complementation vector	This study
pJIR4843	pJIR3422(BamHI/Asp718) ΩJRP7059/JRP7060 (BamHI/Asp718; 2521 bp, pCW3) *tcpH*-G_6-HA complementation vector	C. Lao, V. Adams, J. Rood, unpublished
pJIR4844	pJIR3422(BamHI/SphI) ΩJRP6265/JRP6240 (BamHI/SphI; 1703 bp, pCW3) *tcpA*-G_6-FLAG complementation vector	This study

Chl^R- potassium chlorate resistance, Cm^R- chloramphenicol resistance, Em^R- erythromycin resistance, Nal^R- nalidixic acid resistance, Rif^R – rifampicin resistance, Sm^R- streptomycin resistance, Tc^R- tetracycline resistance, Tm^R – thiamphenicol resistance.

Table 5.2: Oligonucleotides used in this study.

Name	Sequence (5'-3')	Purpose
JRP6570	GCGGGATCCATGAAAGATTTAAATTTATATGCAAAA GAATTAGTTG	Forward oligo, to construct *tcpK*-G_6-HA complementation vector
JRP6571	GGGGTACCTTAAGCATAATCTGGAACATCATATGGAT ATCCACCCCCGCCTCCCCCCTCTAAATAGAGCCTTTTT AAAATACTATATGAGC	Reverse oligo, to construct *tcpK*-G_6-HA complementation vector
JRP6572	GCGGGATCCATGAATATATTTAATTTAAAAAAAGAA ATGAAAAATATTATTTATTCTG	Forward oligo, to construct *tcpM*-G_6-HA complementation vector
JRP6573	GGGGTACCTTAAGCATAATCTGGAACATCATATGGAT ATCCACCCCCGCCTCCCCCAACTTTAATCTTACTATTC AAATAAATCTTAGTAGTGTC	Reverse oligo, to construct *tcpM*-G_6-HA complementation vector
JRP6265	ATTACGGCATGCTAGAAGCGACACTAC	Forward oligo, to construct *tcpA*-FLAG complementation vector
JRP6240	TTGGATCCTCACTTATCGTCATCATCTTTATAATCTT CATAATCATCATTTATAGTTGATTTTAG	Reverse oligo, to construct *tcpA*-FLAG complementation vector

using *Taq* (Roche) or Phusion Polymerase (NEB). PCR products were purified using QIAquick PCR purification kit (Qiagen). Restriction enzymes were used according to the manufacturer's instructions (Roche and NEB). Sequencing was performed using Prism BigDye Terminator mix (Applied Biosystems) and separated using an Applied Biosystems 3730S capillary sequencer. Sequences were analysed using Vector NTI (Invitrogen).

Construction of epitope tagged complementation vectors

To generate C-terminal haemagglutinin (HA)-tagged *tcpM, tcpK* and *tcpH* complementation vectors, wild-type genes were PCR amplified with gene specific reverse primers that encoded a hexaglycine polylinker and the HA sequence. The PCR products were individually cloned into the blunt cloning vector pT7-Blue3 (Novagen) as per the manufacturer's instructions. *tcpM* and *tcpK* fragments were subcloned into the BamHI/Asp718 sites of pJIR3422, to construct pJIR4657 and pJIR4655, respectively. The PCR product generated for *tcpH* was cloned into the BamHI/Asp718 sites of pJIR3422, to produce pJIR4843. A C-terminal FLAG octapeptide-tagged *tcpA* complementation vector was constructed by amplifying the wild-type *tcpA* gene with a reverse primer that encoded the FLAG sequence. The $tcpA_{\mathrm{FLAG}}$ PCR product was cloned into the BamHI/SphI sites of pJIR3422 generating, pJIR4847. The complementation plasmids were confirmed by restriction digestion and sequence analysis. These plasmids were introduced into *C. perfringens* using electroporation, and transformants were selected using nutrient agar supplemented with Tm. The presence of the complementation plasmids was confirmed by restriction analysis and sequencing following plasmid rescue in *E. coli.*

Conjugation assays

Conjugative transfer experiments were conducted as mixed plate mating on solid media as previously described (Rood *et al.*, 1978, Rood, 1983). A spontaneous Sm^R Chl^R resistant derivative of strain 13, JIR4394, was used as a recipient. Transconjugant cells were selected on NA

supplemented with Sm, Chl and Tc. The conjugation frequency is described as the number of transconjugant cells per donor cell.

Immunofluorescence microscopy

Immunofluorescence was performed as previously described (Wisniewski *et al.*, 2015a, Teng *et al.*, 2008) with minor modifications. *C. perfringens* cells from an overnight agar plate were resuspended in 500 µl of phosphate buffered saline (PBS; pH 7.4). Cells were centrifuged at 4, 000 x g for 2 mins. Cells were fixed in 1 mL of ice cold methanol (Amresco) for 20 mins at -20°C, washed with PBS and, where applicable, permeablised in 0.001% (v/v) Triton-X-100 (Sigma) for 15 min. Cells were washed in PBS and resuspended in 100-500 µl of GTE (50mM Glucose, 20mM Tris-HCl, 10mM EDTA; pH 7.5) supplemented with 1 mg/ml lysostaphin (Sigma) and 10mg/ml lysozyme (Amresco). The cell suspension was incubated for 1-2 hrs at 37°C. Following permeabilization, 2 µl of cell suspension was spread onto a 0.1% poly-L-lysine (Sigma) coated coverslip (Zeiss). The cells were blocked in 2% (w/v) bovine serum albumin (BSA) (Sigma) in PBS. Cells were either treated with anti-HA mouse monoclonal antibodies (1:100 dilution in PBS) overnight at 4°C or OctA-Probe (H-5) mouse monoclonal antibodies (1:100 dilution in PBS) for 1-2 hrs. After washing three times in PBS, cells were treated with 5% (v/v) normal goat serum (Invitrogen) in PBS for 30 mins. The cells were then incubated in the dark with either a combination of Abberior STAR 635 anti-mouse monoclonal antibody (1:500 dilution in PBS; Abberior) and 1 µg/mL Rhodamine B (Sigma) in PBS, or AlexaFluor568 goat anti-mouse monoclonal antibody (1:500 dilution in PBS; Thermo Fisher Scientific) with 1 µg/ml SYTO™9 (Thermo Fisher Scientific) for 1-2 hrs. Cells were then washed three times with PBS and mounted onto a microscope slide with Prolong™ Gold Antifade Mountant (Invitrogen).

To assess effective cell labelling, the stained cells were observed by using an Olympus BX60 wide-field fluorescence microscope with a 100x oil immersion objective. Images were captured by

using a SPOT RT3 digital camera with SPOT Basic for image capture (Scitech, Australia). Images were pseudo-coloured as indicated in figures using FIJI (Schneider *et al.*, 2012).

The stained cells were observed by using an Abberior STED Super-Resolution Microscope with a 100x oil immersion lens (UPlanSApo). Images were captured by using IMSpector control software. Images were merged and pseudo-coloured (red for rhodamine B and green for Abberior STAR 635 or blue for SYTO9 and yellow for AlexaFluor568) using FIJI (Schneider *et al.*, 2012). Animated Z-stack images were merged, pseudo-coloured as above, converted to RGB stacks and saved as animated gifs using FIJI (Schneider *et al.*, 2012).

Image analysis

Quantitative analysis of individual protein foci was conducted using Cell Profiler (Lamprecht *et al.*, 2007). Prior to analysis, grouped Rhodamine B images of the cells and labelled protein 'spot' images were processed using FIJI (Schneider *et al.*, 2012). Rhodamine B labelled cell images were used to define the parent cell area. To reduce background signals, protein 'spot' images were filtered using Gaussian Blur (sigma value: 1.5) and further defined using the plugin MorphoLibJ grey attribute filtering TopHat function at a value between 20-60. The processed images were then analysed in Cell Profiler, which grouped 'spots' according to the parent cell. The number of 'spots' per parent cell area (pixels) was calculated. The data were then transformed to μm^2 according to the pixel depth of recorded images and the number of 'spots' normalised to 1 μm^2. Data were plotted for each individual cell using GraphPad prism and statistical analysis was performed on normalised data using the Mann-Whitney *u*-test, with statistical significance determined as $p < 0.05$.

Results

Transfer capacity of epitope-tagged fusion proteins

An immunofluorescence approach was used to localise Tcp proteins within *C. perfringens* cells. Unfortunately, due to the poor availability and specificity of primary antibodies raised to various Tcp proteins (Teng *et al.*, 2008, Porter *et al.*, 2012) the cellular localisation using native proteins was unable to be assessed. Instead epitope-tagged derivatives of various Tcp proteins were utilised and their cellular localisation was investigated using commercially available epitope tag-specific antibodies. The use of epitope-tagged derivatives has been previously used to determine the localisation of two Tcp proteins, TcpD and TcpE (Wisniewski *et al.*, 2015a). However, it was noted that the addition of the epitope-tag to the C-terminus of TcpD rendered the protein non-functional (Wisniewski *et al.*, 2015a). It was only when a flexible hexaglycine (G_6) linker was located proximal to the epitope-tag that the protein was functional. Therefore, in this study complementation vectors were constructed with a C-terminal G_6 linker followed by a haemagglutanin (HA) epitope-tag for the TcpK, TcpM and TcpH proteins. For TcpA a C-terminal FLAG octapeptide-tag without a linker was used. The use of a different epitope-tag for TcpA allowed for future use in double labelling experiments, looking at more than one Tcp protein within the cell. To ensure that the epitope-tagged Tcp derivatives were functional prior to localisation studies, the ability of the tagged derivatives to complement their respective mutant strains was analysed (Figure 5.2). In this study, TcpD and TcpE epitope-tagged strains were reconstructed, and thus the ability of the reconstructed strains to complement conjugation was also assessed. All of the tagged derivatives restored conjugation efficiencies to levels similar to wild-type (Figure 5.2). These results showed that the epitope-tagged derivatives were functional and could be used to determine their subcellular location.

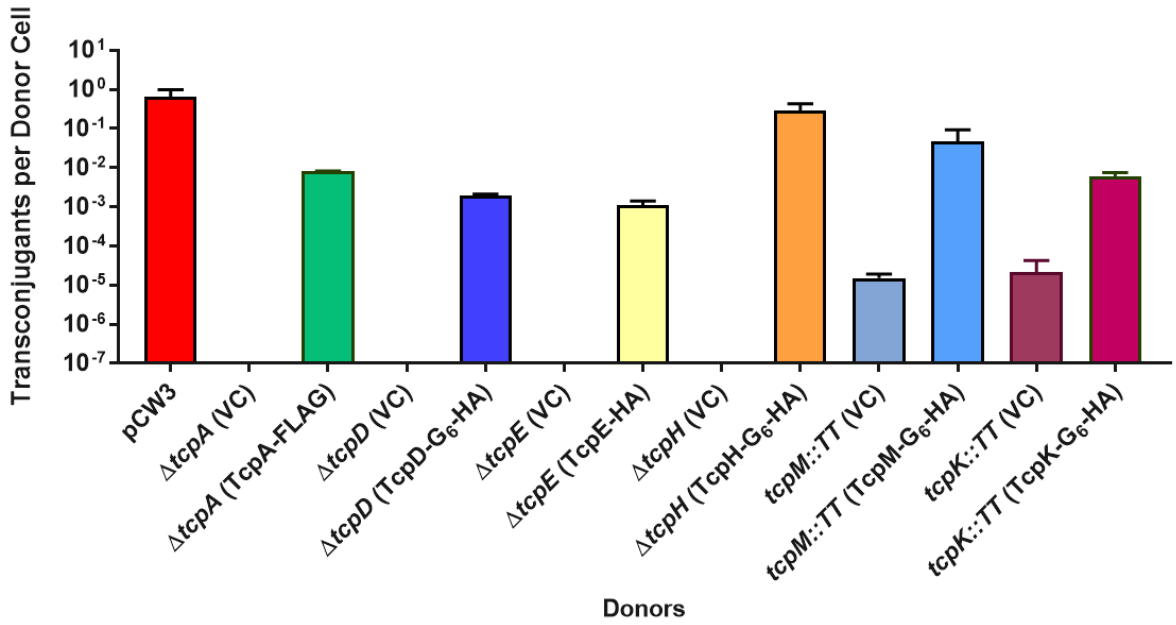

Figure 5.2: Conjugation frequencies of complemented pCW3 mutant strains. Complementation vectors encoding epitope-tagged derivatives of TcpA, TcpD, TcpE, TcpH, TcpM and TcpK were introduced into each respective mutant strain. The ability of tagged derivatives to complement the respective mutation was assessed in an overnight mating assay. Mixed plate matings were conducted using JIR4195 derived strains as donors and the isogenic strain 13 derivative JIR4394 as a recipient. Donor strains are labelled on the X-axis and wild type pCW3 is denoted as pCW3. The conjugation frequency is described as the number of transconjugants cells per donor cell. Donors are shown on the x-axis. Donors are all isogenic derivatives of JIR4195. The means are shown based on the results of at least two replicates.

pCW3 relaxosome proteins are dispersed throughout the cytoplasm

Initial studies were aimed to determine the subcellular location of the relaxosome components TcpM and TcpK. TcpM is a novel relaxase protein, required for the efficient transfer of pCW3 (Wisniewski *et al.*, 2015b) and TcpM (31.2 kDa) does not possess any putative transmembrane domains and is expected to be cytoplasmic (Wisniewski *et al.*, 2015b). Functionally, TcpM has been shown to bind to the pCW3 *oriT* as well as to relax supercoiled DNA (Wisniewski *et al.*, 2015b). TcpK is a small DNA binding protein (12.4 kDa), that is necessary for efficient conjugative transfer of pCW3 (Traore *et al.*, 2018). TcpK binds as dimers to regions within the *oriT* referred to as TcpK boxes and is thought to act as an accessory factor to the relaxase TcpM (Traore *et al.*, 2018). The location of TcpM-G_6-HA and TcpK-G_6-HA in the respective mutant *C. perfringens* cells was probed using immunofluorescence and STED super resolution microscopy. Both TcpM-G_6-HA and TcpK-G_6-HA localised throughout the cytoplasm of the cell (Figure 5.3 and Figure 5.4). TcpK-G_6-HA was more diffuse than TcpM, with only a few punctate foci observed. By contrast, TcpM-G_6-HA formed noticeable foci throughout the cytoplasm of the cell. To increase the depth of field and observe the distribution of both proteins within the volume of the cell, z-stack images were taken. Animated z-stacks clearly demonstrate the disperse intracellular localisation of TcpM-G_6-HA (Figure 5.5- https://monash.figshare.com/s/bdbef2fa804eb6a0c1c6). Similarly, animated z-stack images accentuate the diffuse cytoplasmic localisation of TcpK-G_6-HA (Figure 5.6- https://monash.figshare.com/s/1d956d8dddfc4987a456). In control experiments, where no primary antibody was added, little or no far-red fluorescence (pseudo-coloured green) was observed for either preparation, indicating that the labelling observed was specific for the HA-tag epitope (Figure 5.7 C and E).

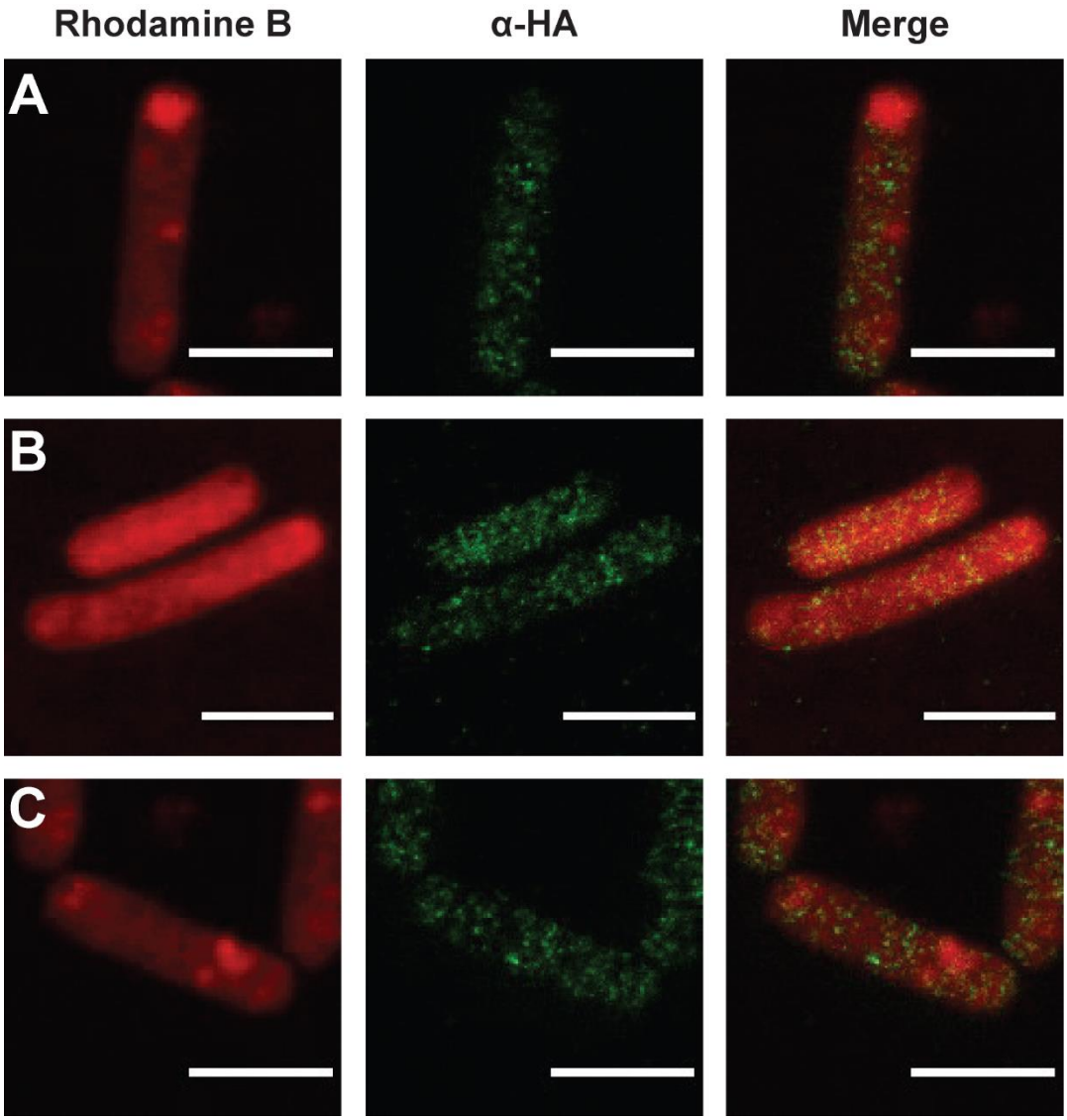

Figure 5.3: Localisation of TcpM-G_6-HA in *C. perfringens*. Localisation of TcpM-G_6-HA was determined by probing *C. perfringens* cells complemented with a HA-tagged TcpM derivative using primary antibodies to the HA epitope tag followed by staining with Abberior STAR 635 anti-mouse secondary (green) and the cellular dye Rhodamine B (red). Images were collected using an Abberior STED Microscope. Shown (**A, B, C**.) are representative images from three replicate experiments. Scale bar 2 µm.

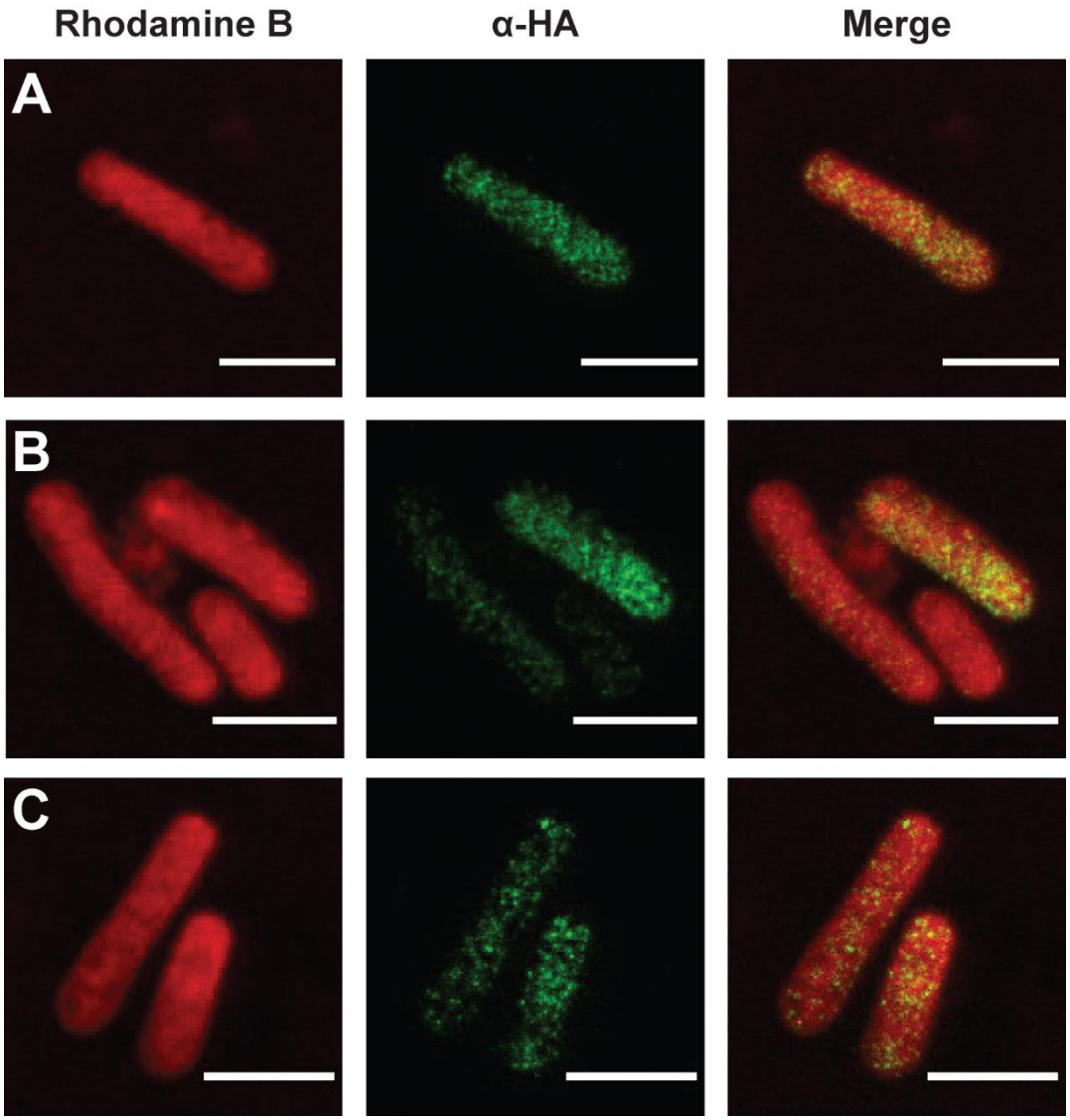

Figure 5.4: Localisation of TcpK-G_6-HA in *C. perfringens* cells. Localisation of TcpK-G_6-HA was determined by probing *C. perfringens* cells complemented with an HA-tagged TcpK derivative with primary antibodies to the HA epitope tag followed by staining with Abberior STAR 635 anti-mouse secondary (green) and the cellular dye Rhodamine B (red). Images were collected using an Abberior STED Microscope. Scale bar is 2 μm. Shown (**A, B, C**) are representative images from three replicate experiments.

A Available at: https://monash.figshare.com/s/bdbef2fa804eb6a0c1c6

B

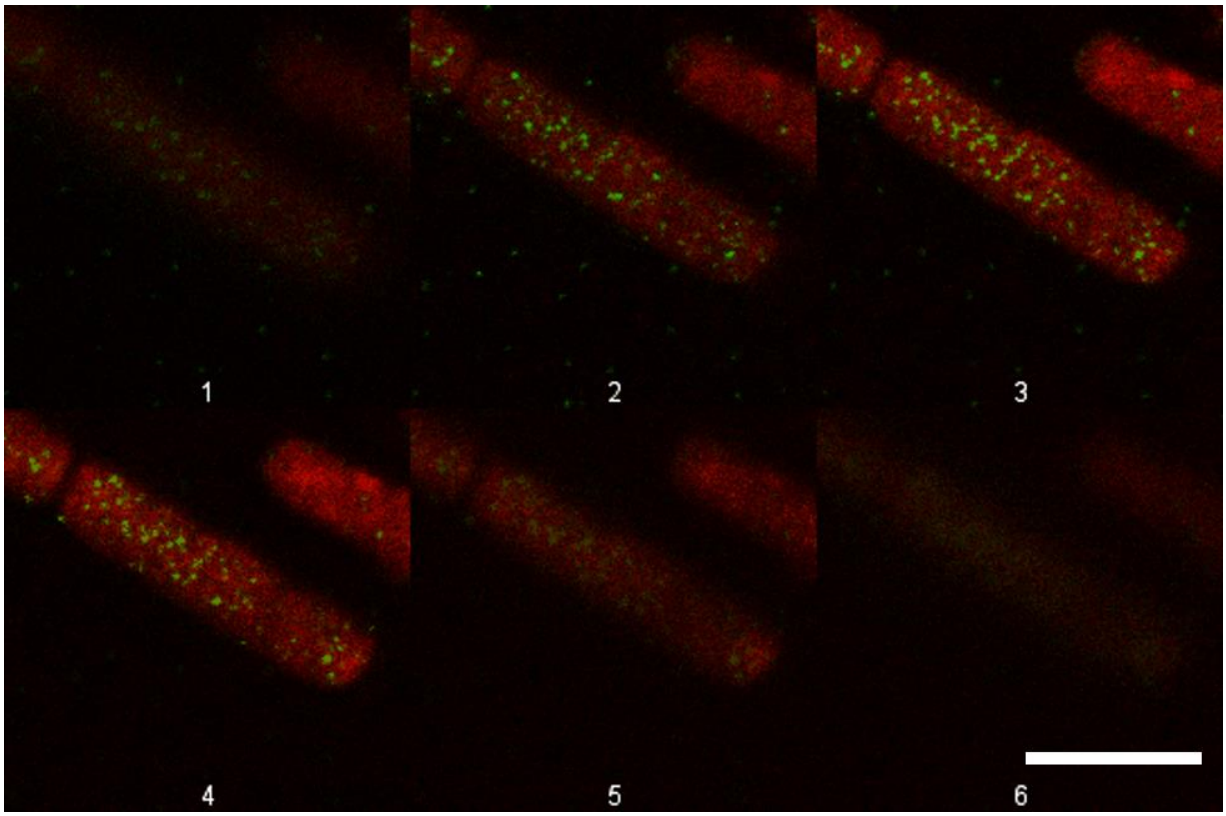

Figure 5.5: Animated and montage images of z-stack collections demonstrating localisation of TcpM-G_6-HA in *C. perfringens*. Localisation of TcpM-G_6-HA was determined by probing *C. perfringens* cells complemented with an HA-tagged TcpM derivative with primary antibodies to the HA epitope tag followed by staining with Abberior STAR 635 anti-mouse secondary (green) and the cellular dye Rhodamine B (red). Z-stack slices were obtained at optical depth changes of 200 nm and were collected using an Abberior STED Microscope. These data were representative of results obtained from three replicate experiments. Shown is the montage breakdown (**B**) of six z- slices (1-6) used for the animated z-stack (**A**) available at the link above. Scale bar is 2 µm

A Available at: https://monash.figshare.com/s/1d956d8dddfc4987a456

B

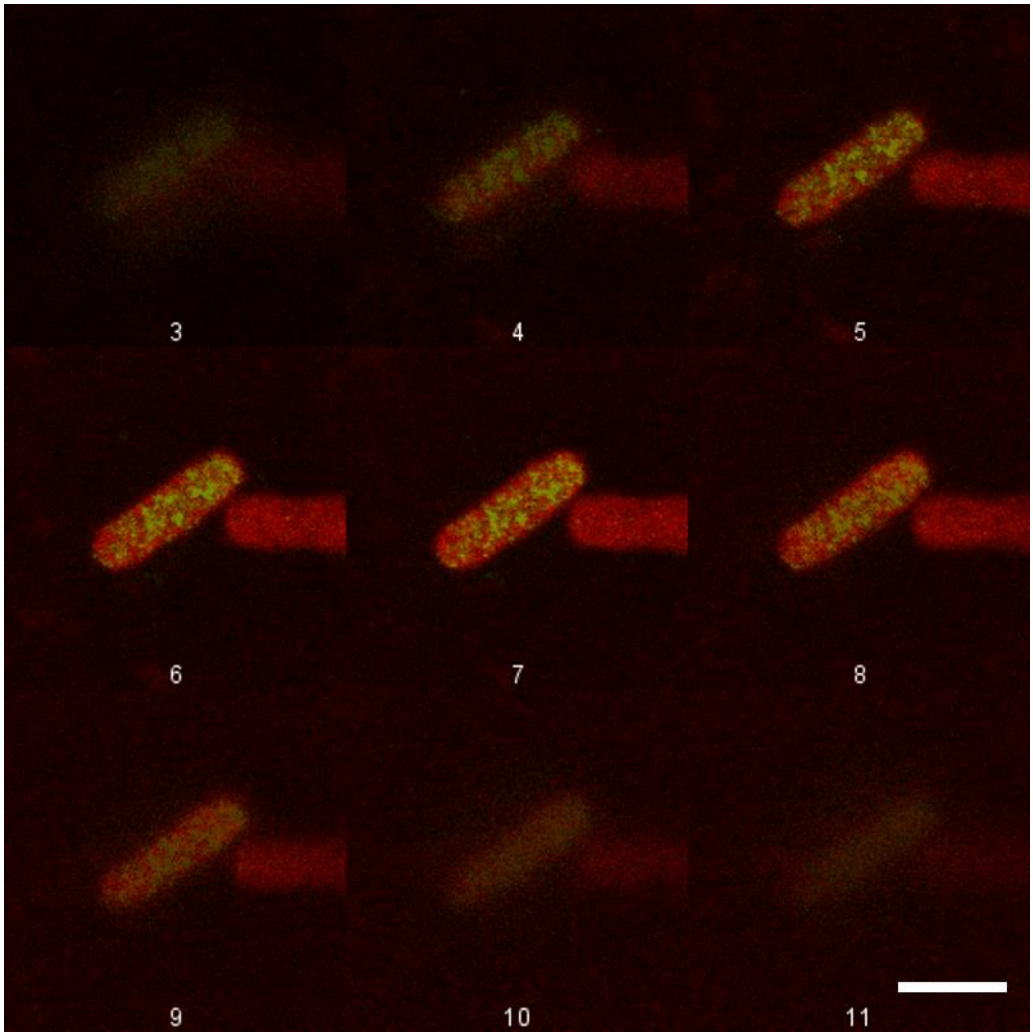

Figure 5.6: Animated and montage images of z-stack collection demonstrating localisation of TcpK-G_6-HA in *C. perfringens*. Localisation of TcpK-G_6-HA was determined by probing *C. perfringens* cells complemented with an HA-tagged TcpK derivative with primary antibodies to the HA epitope tag followed by staining with an Abberior STAR 635 anti-mouse secondary (green) and the cellular dye Rhodamine B (red). Z-stack slices were obtained at optical depth changes of 200 nm and were collected using an Abberior STED Microscope. This data is representative of results obtained from three replicate experiments. Shown is the montage breakdown (**B**) of nine z- slices (3-11) used for the animated z-stack (**A**) available at the link above. Scale bar is 2 µm.

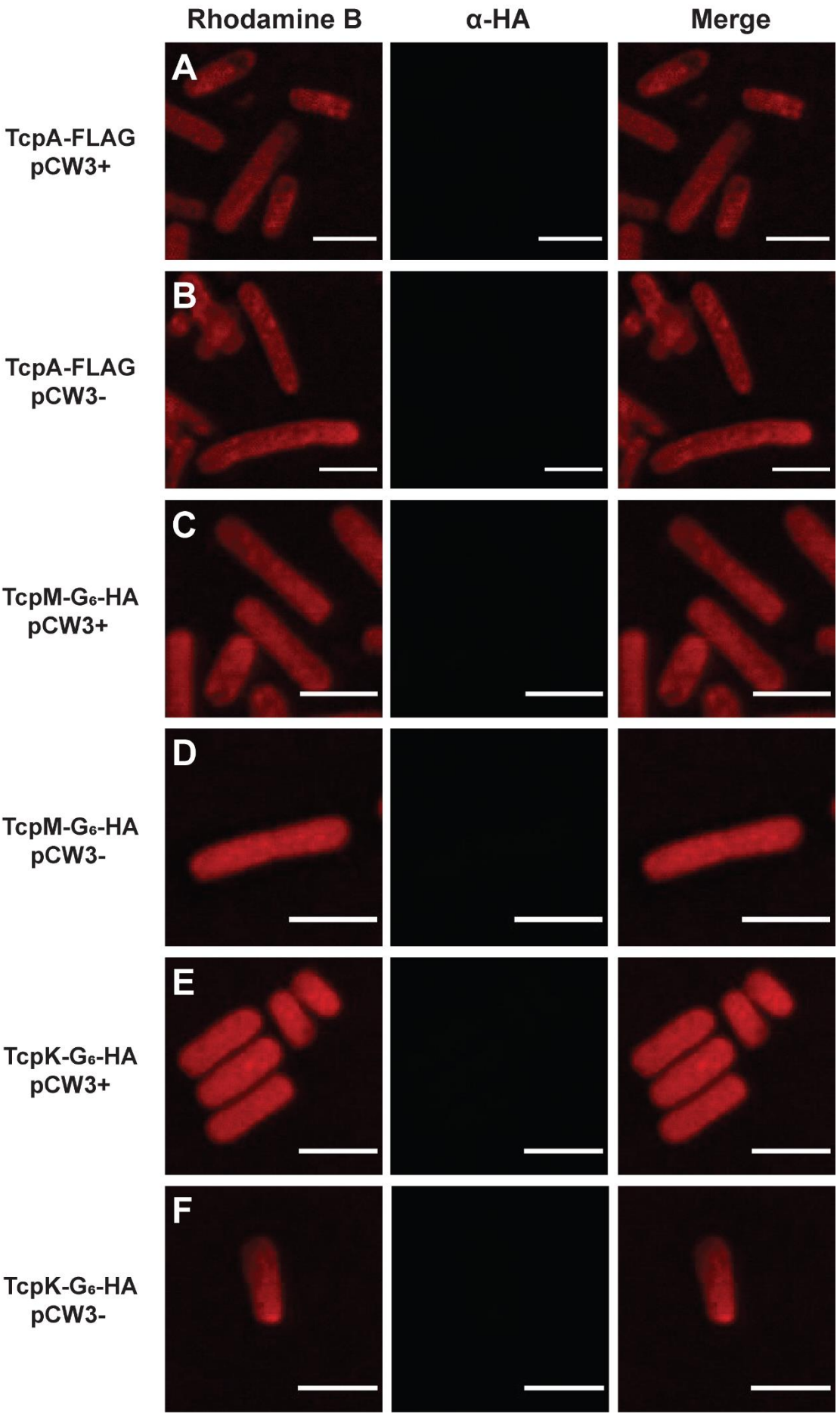
Rhodamine B
α-HA
Merge
A
TcpA-FLAG
pCW3+
B
TcpA-FLAG
pCW3-
C
TcpM-G6-HA
pCW3+
D
TcpM-G6-HA
pCW3-
E
TcpK-G6-HA
pCW3+
F
TcpK-G6-HA
pCW3-

Figure 5.7: Controls without primary antibody for TcpA, TcpM and TcpK complementation strains. To confirm specific antibody labelling, *C. perfringens* cells complemented with HA-tagged TcpA, TcpM and TcpK derivatives were not labelled with primary antibodies to either the HA- or FLAG-epitope tags. Staining with Abberior STAR 635 anti-mouse secondary (green) and the cellular dye Rhodamine B (red) was conducted as described. **A and B.** Breakdown schematics of fluorescence patterns of cells expressing TcpA-FLAG in the presence (**A**) and absence (**B**) of pCW3 are shown. **C and D.** The fluorescence captured from cells expressing TcpM-G_6-HA in the presence (**C**) and absence (**D**) of pCW3. **E and F.** The fluorescence captured from cells expressing TcpK-G_6-HA in the presence (**C**) and absence (**D**) of pCW3. Images were collected using an Abberior STED Microscope. Scale bar 2µm. Shown are representative images from at least two replicate experiments.

TcpM and TcpK localisation patterns do not change in the absence of pCW3.

To assess if the localisation of either TcpM or TcpK requires other factors from pCW3, HA-tagged TcpM and TcpK complementation vectors were introduced into the pCW3-negative strain JIR325. The location of the proteins was examined as before. The general localisation pattern of TcpM-G_6-HA did not alter when pCW3 was absent (Figure 5.8). A similar phenotype was observed for TcpK-G_6-HA (Figure 5.9). Control experiments confirmed specific anti-HA labelling (Figure 5.7 D and F).

The coupling protein, TcpA, localises throughout the cell membrane independently of other pCW3 proteins

T4SS coupling proteins are integral membrane proteins that interact with both DNA processing components of the T4SS machinery, as well as the multi-protein transfer complex (Gomis-Rüth *et al.*, 2002). The Tcp coupling protein, TcpA, has two N-terminal transmembrane domains that are required for efficient conjugative transfer as well as facilitating interactions with other Tcp proteins (Parsons *et al.*, 2007, Steen *et al.*, 2009). TcpA-FLAG localised in punctate foci, randomly distributed around the cell surface (Figure 5.10). This distribution pattern did not change when pCW3 was absent (Figure 5.11). Analysis of localisation using z-stacks suggests a membrane association of TcpA-FLAG (Figure 5.12 https://monash.figshare.com/s/ffcaae59bc452b706339). Quantitative analysis showed that the average number of TcpA-FLAG foci present on cells when pCW3 was also present was significantly higher (9.27±0.42 foci per μm^2) than when pCW3 was absent (6.78±0.44) ($p=0.0025$) (Figure 5.13). These data strongly suggest that the localisation of TcpA within the membrane does not require pCW3-associated factors, however, these factors may be required for the expression or stability of TcpA.

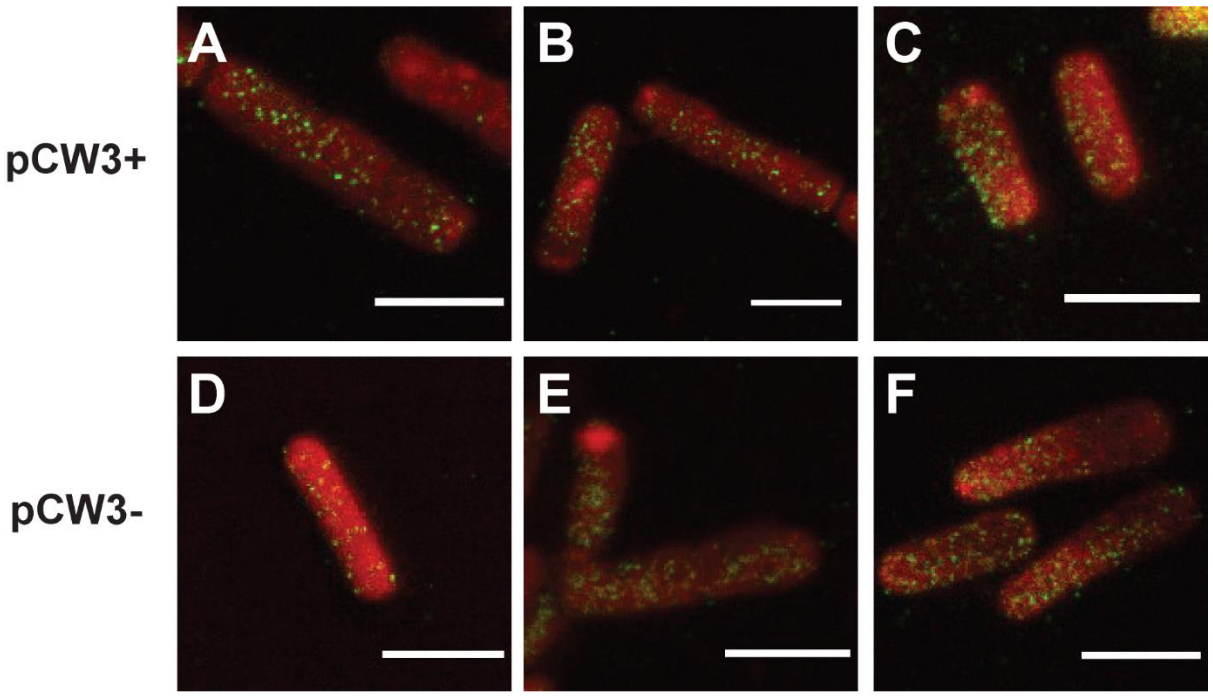

Figure 5.8: Localisation of TcpM-G_6-HA in the presence and absence of pCW3. A complementation vector encoding TcpM- G_6-HA was introduced into the pCW3-negative strain JIR325. The localisation of TcpM-G_6-HA was determined by probing *C. perfringens* cells (±pCW3) with primary antibodies to the HA epitope tag followed by staining with Abberior STAR 635 anti-mouse secondary (green) and the cellular dye Rhodamine B (red). Shown are three representative images from three replicate experiments showing the localisation of TcpM-G_6-HA in the presence (**A, B, C**) and absence (**D, E, F**) of pCW3. Images were collected using an Abberior STED Microscope. Scale bar is 2 μm.

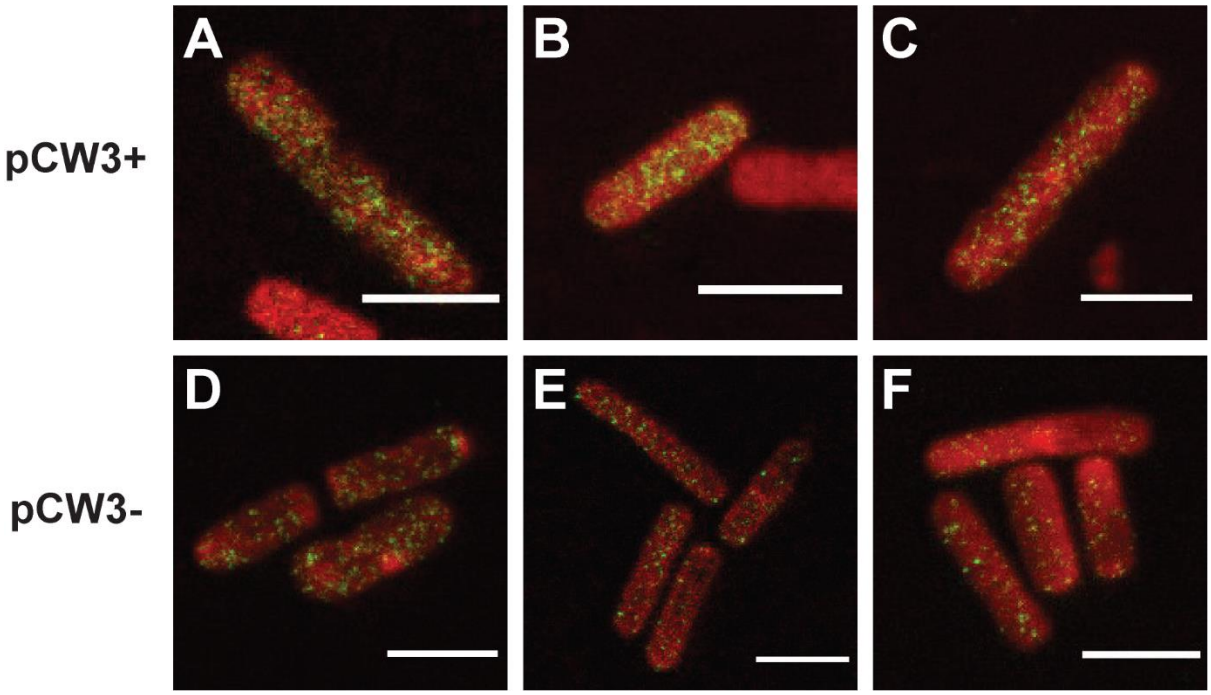

Figure 5.9: Localisation of TcpK-G_6-HA in the presence and absence of pCW3. A complementation vector encoding TcpK- G_6-HA was introduced into the pCW3-negative strain JIR325. The localisation of TcpK-G_6-HA was determined by probing *C. perfringens* cells (±pCW3) with primary antibodies to the HA epitope tag followed by staining with Abberior STAR 635 anti-mouse secondary (green) and the cellular dye Rhodamine B (red). Shown are three representative images from three replicate experiments showing the localisation of TcpK-G_6-HA in the presence (**A, B, C**) and absence (**D, E, F**) of pCW3. Images were collected using an Abberior STED Microscope. Scale bar is 2 µm.

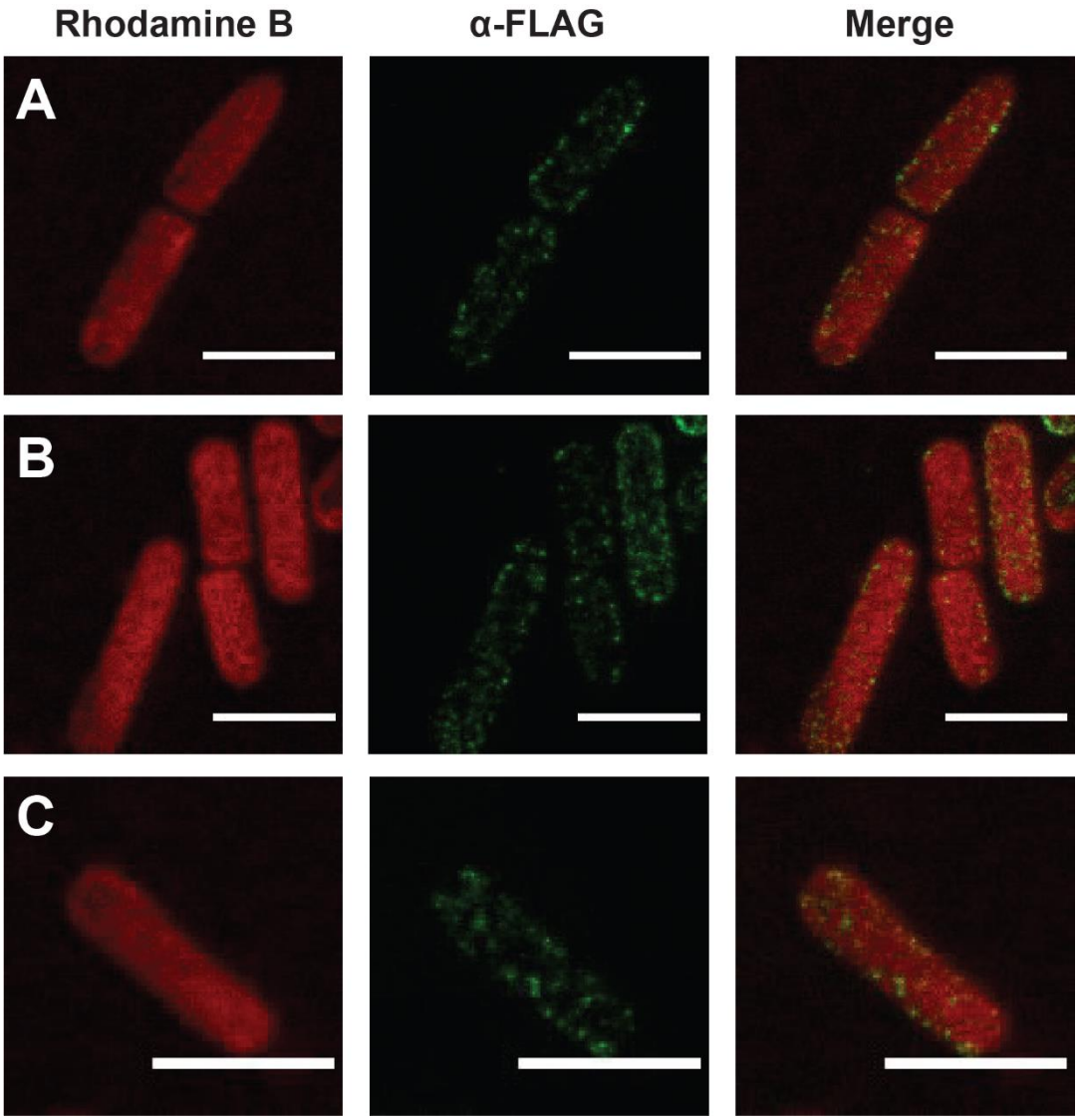

Figure 5.10: Localisation of TcpA-FLAG in *C. perfringens*. Localisation of TcpA-FLAG was determined by probing *C. perfringens* cells (pCW3Ω*tcpM*::TT) complemented with a FLAG-tagged TcpA derivative with primary antibodies to the FLAG epitope tag followed by staining with Abberior STAR 635 anti-mouse secondary (green) and the cellular dye Rhodamine B (red). Images were collected using an Abberior STED Microscope. Shown are representative images (**A, B, C**.) from three replicate experiments. Scale bar is 2 μm.

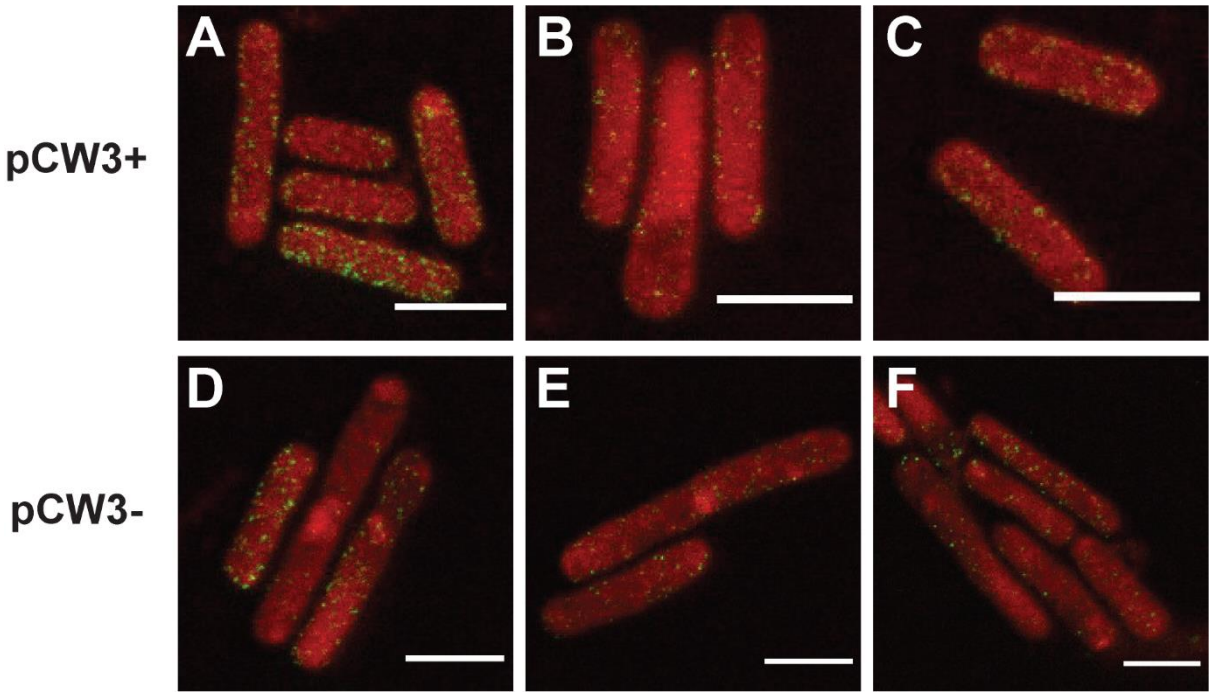

Figure 5.11: Localisation of TcpA-FLAG in the presence and absence of pCW3. A complementation vector encoding TcpA-FLAG was introduced into the pCW3-negative strain JIR325. The localisation of TcpA-FLAG was determined by probing *C. perfringens* cells (±pCW3) with primary antibodies to the FLAG epitope tag followed by staining with Abberior STAR 635 anti-mouse secondary (green) and the cellular dye Rhodamine B (red). Shown are three representative images from two replicate experiments showing the localisation of TcpA-FLAG in the presence (**A, B, C**) and absence (**D, E, F**) of pCW3. Images were collected using the Abberior STED Microscope. Scale bar is 2 μm.

A Available at: https://monash.figshare.com/s/ffcaae59bc452b706339

B

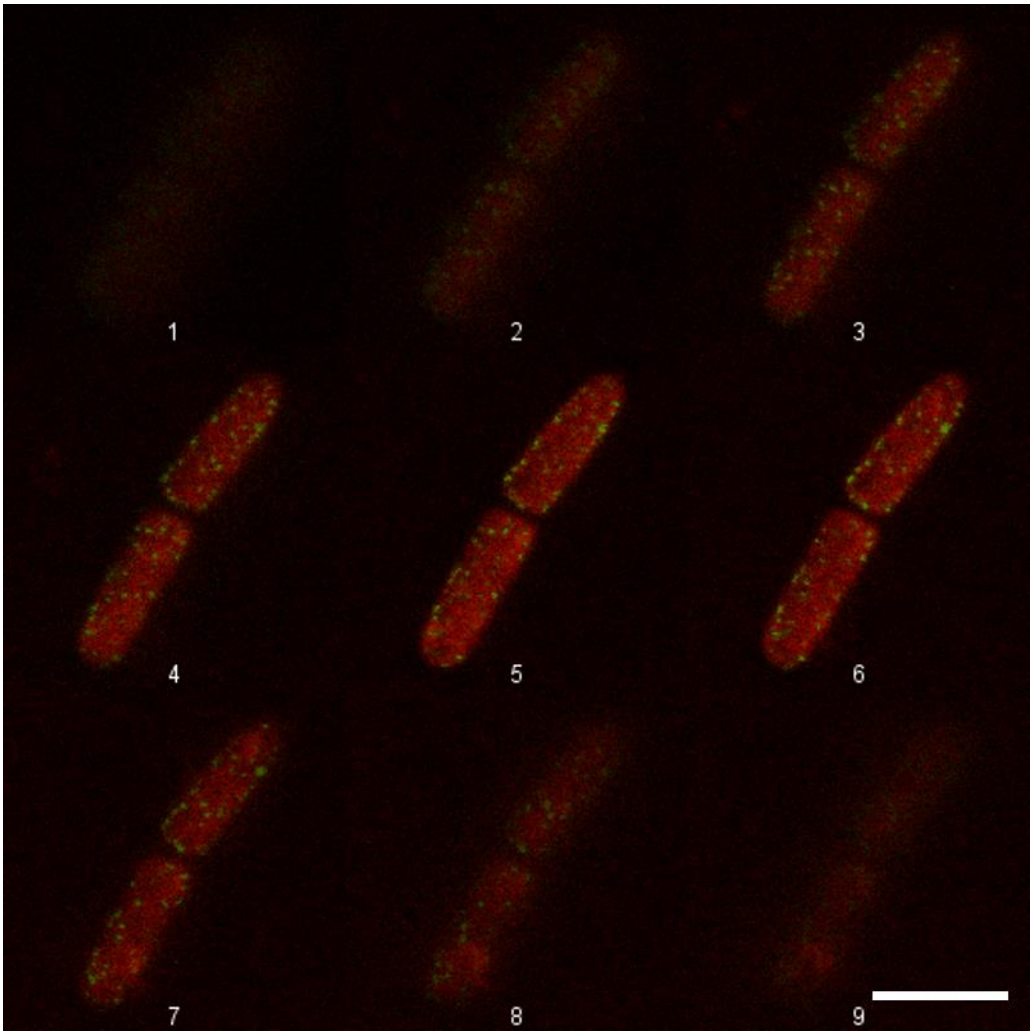

Figure 5.12: Animated and montage images of z-stack collection demonstrating localisation of TcpA-FLAG in *C. perfringens*. Localisation of TcpA-FLAG was determined by probing *C. perfringens* cells complemented with a FLAG-tagged TcpA derivative with primary antibodies to the FLAG epitope tag followed by staining with Abberior STAR 635 anti-mouse secondary (green) and the cellular dye Rhodamine B (red). Z-stack slices were obtained at optical depth changes of 200 nm and were collected using an Abberior STED Microscope. These data are representative of results obtained from three replicate experiments. Shown is the montage breakdown (**B**) of nine z- slices (1-9) used for the animated z-stack (**A**) available at the link above.

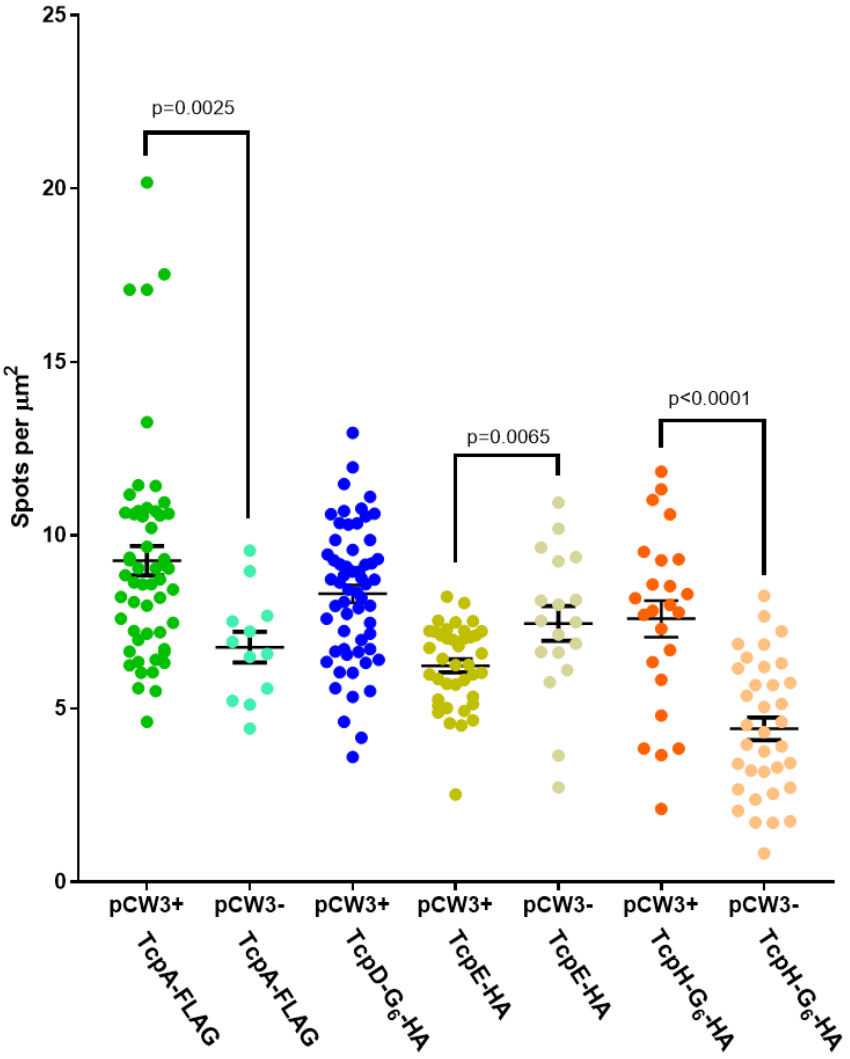

Figure 5.13: Distribution of epitope-tagged Tcp proteins on the surface of *C. perfringens* cells. Foci (spots) were counted on the surface of *C. perfringens* cells expressing TcpA-FLAG, TcpD-G_6-HA, TcpE-HA and TcpH-G_6-HA in the presence and absence of pCW3 (except for TcpD-G6-HA, which was only imaged in the presence of pCW3). Values were normalised to the number of spots per µm^2. Errors bars represent mean ± SEM. Each dot represents data obtained for a single cell, shown are data obtained from at least two replicate experiments. Comparisons of significance are reported using Mann-Whitney *u*-test.

Components of the multi-protein transmembrane transfer complex localise in various positions throughout the cell

Other researchers in this laboratory have previously reported that TcpD, TcpE, TcpF and TcpH, localised predominantly to the cell poles (Wisniewski *et al.*, 2015a, Teng *et al.*, 2008). With the significant advances in imaging technology since these studies were conducted, this study examined the subcellular localisation of these proteins using super resolution microscopy. TcpD is a small protein with three predicted transmembrane domains (Wisniewski *et al.*, 2015a). Although this protein is essential for pCW3 conjugation, the precise mechanism of action has not yet been elucidated, however, it is hypothesised to form a critical component of the transfer complex (Wisniewski *et al.*, 2015a). Previous work using conventional wide-field fluorescence microscopy demonstrated TcpD-G_6-HA localised predominantly at the poles of *C. perfringens* cells (Wisniewski *et al.*, 2015a). Indeed, during this study when cells were labelled and imaged using wide-field fluorescence microscopy, strong polar signals were observed (Figure 5.14). However, STED immunofluorescent detection of TcpD-G_6-HA revealed that, in addition to localisation to the cell poles (Figure 5.15A), the protein was dispersed throughout the membrane of the cell (Figure 5.15 B and C). Polar localisation, whether at a single or both poles, was observed in 28% of cells imaged (Table 5.3). TcpD-G_6-HA foci were detected in high numbers on the surface of the cells, with 8.3±0.25 foci per μm^2. Attempts were made to image the localisation pattern of TcpD-G_6-HA in the absence of pCW3, however expression of the epitope tagged protein in this strain was too low for immunofluorescent detection. This low-level expression of TcpD-G_6-HA in strains without pCW3 has been previously reported for this construct (Wisniewski *et al.*, 2015a). Control experiments confirmed specific protein labelling (Figure 5.16)

TcpE is another small protein that is essential for pCW3 conjugation. TcpE has two putative transmembrane domains and was previously reported to localise predominantly to the cell poles (Wisniewski *et al.*, 2015a). Detection of TcpE-HA in *C. perfringens* cells using STED microscopy

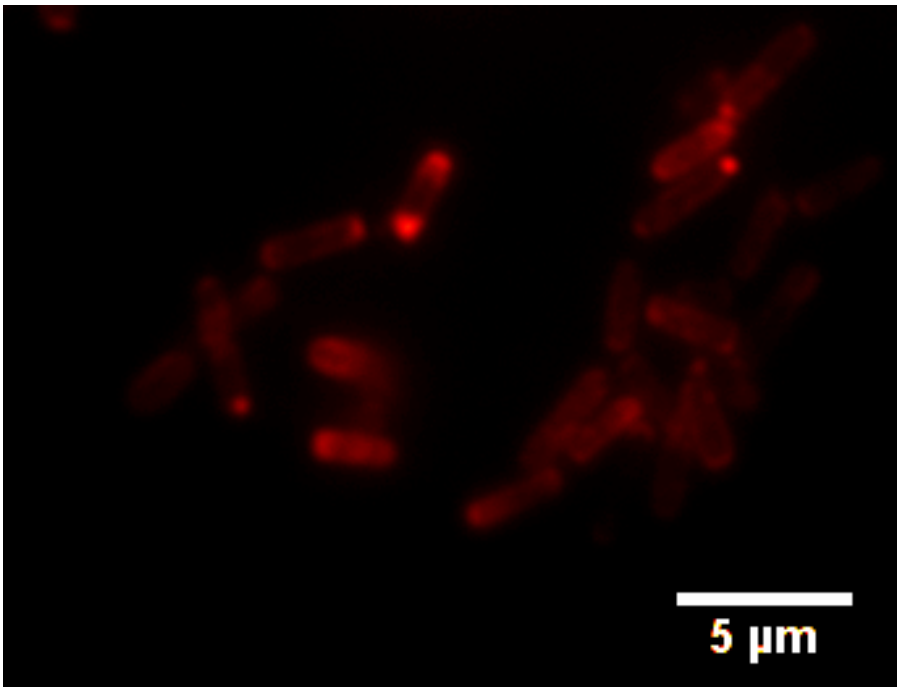

Figure 5.14: Localisation of TcpD HA-tagged derivative in *C. perfringens* using conventional wide-field fluorescence microscopy. *C. perfringens* cells were labelled using monoclonal anti-HA mouse primary antibodies, followed by goat anti-mouse AlexaFluor568 conjugated secondary antibodies. Images were collected using SPOT basic software on an Olympus BX60 fluorescence microscope. Shown is a representative image of at least two replicate experiments.

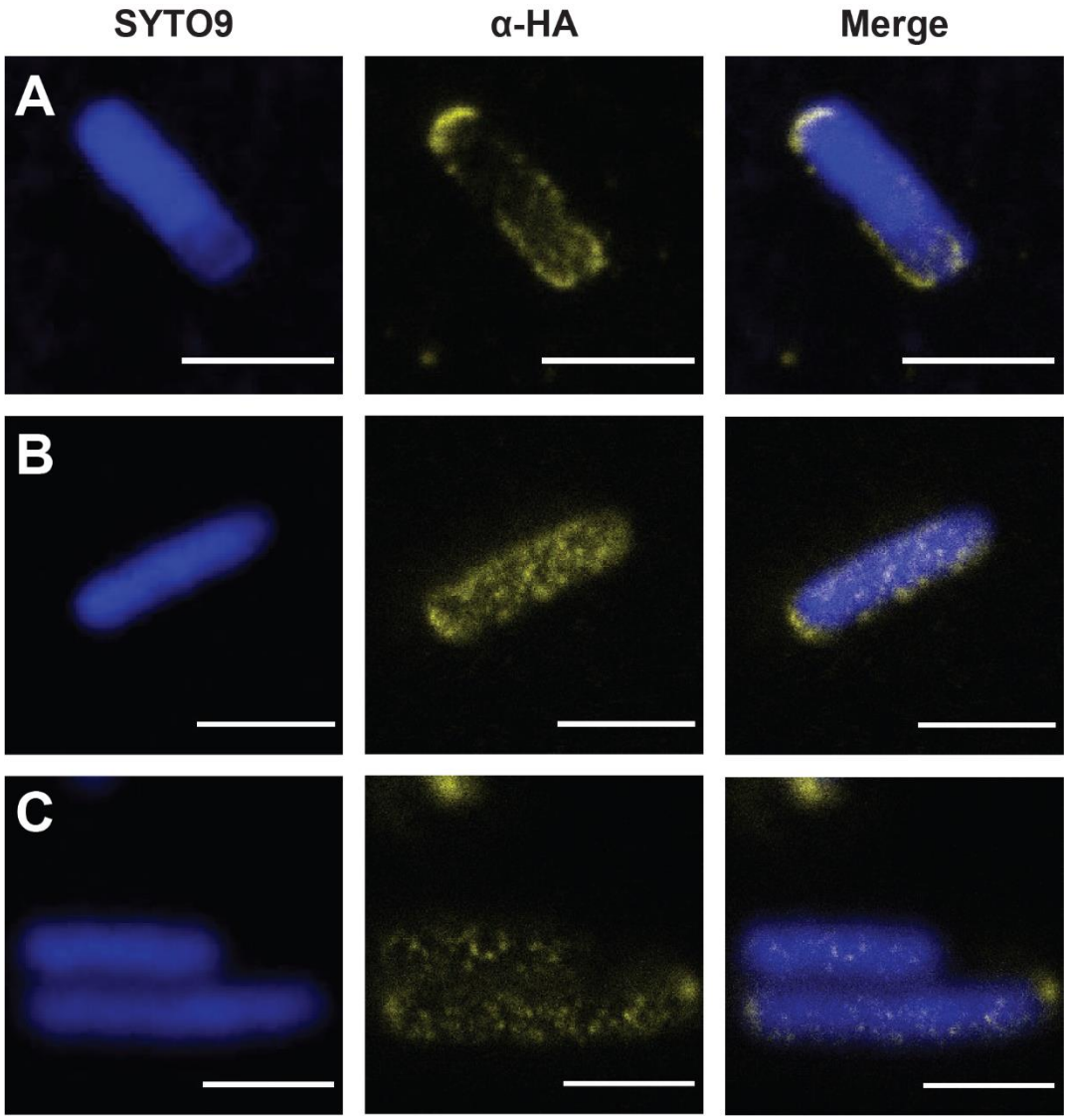

Figure 5.15: Localisation of TcpD-G_6-HA in *C. perfringens*. Localisation of TcpD-G_6-HA was determined by probing *C. perfringens* cells (containing pCW3Δ*tcpD*) complemented with a HA-tagged TcpD derivative with primary antibodies to the HA epitope tag followed by staining with AlexaFluor568 goat anti-mouse secondary (yellow) and the DNA dye SYTO™9 (blue). The SYTO9 stain was used to visualise the cells in these preparations as no other appropriate cellular dye (ie. Rhodamine B) was available at the time of image collection. Images were collected using an Abberior STED Microscope. Shown (**A, B, C**) are representative images from two replicate experiments. Scale bar is 2 μm.

Table 5.3: Protein localisation patterns observed for labelled cells expressing TcpD-G_6-HA, TcpE-HA and TcpH-G_6-HA in the presence and absence of pCW3.

		% of cells with protein localisation pattern (total no. of cells):						
		Total	**Single Pole**	**Both Poles**	**Banded**	**Dispersed**	**One cluster/ring**	**≥ 2 clusters/rings**
TcpD- G_6-HA	**pCW3+**	148	18 (26)	10 (15)	n/a	72 (107)	n/a	n/a
TcpE-HA	**pCW3+**	121	n/a	n/a	n/a	36 (43)	52 (63)	12 (15)
	pCW3-	43	n/a	n/a	n/a	93 (40)	7 (3)	0 (0)
TcpH-G_6-HA	**pCW3+**	74	30 (22)	12 (9)	7 (5)	51 (38)	n/a	n/a
	pCW3-	93	2.2 (2)	0 (0)	1 (1)	96.8 (90)	n/a	n/a

n/a- not applicable

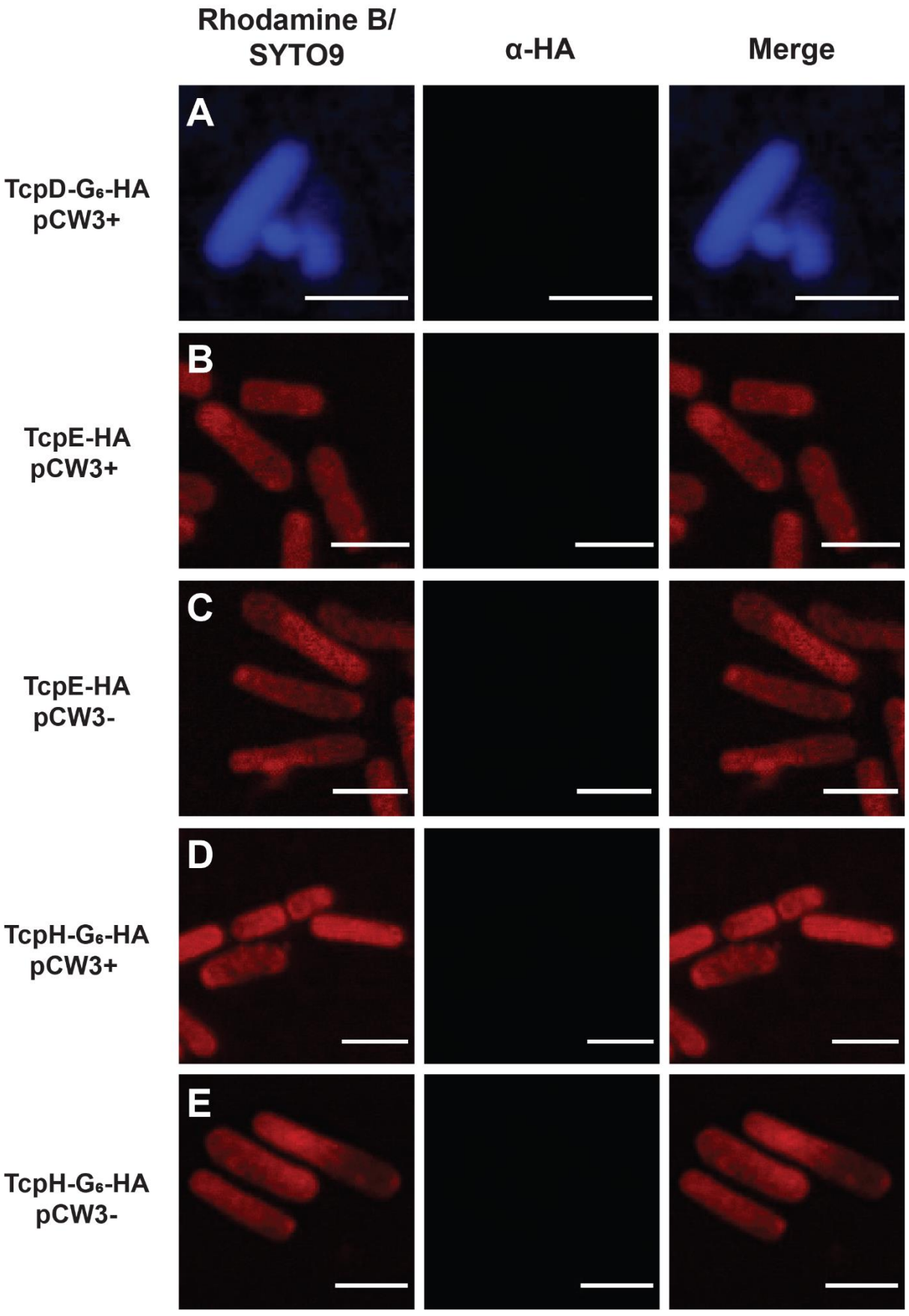
Rhodamine B/
SYTO9
α-HA
Merge
A
TcpD-G6-HA
pCW3+
B
TcpE-HA
pCW3+
C
TcpE-HA
pCW3-
D
TcpH-G6-HA
pCW3+
E
TcpH-G6-HA
pCW3-

Figure 5.16: No primary antibody controls for TcpD, TcpE and TcpH complementation strains. To confirm specific antibody labelling, respective mutant *C. perfringens* cells complemented with HA-tagged TcpD, TcpE and TcpH derivatives were not labelled with primary antibodies to the HA-epitope tag. Staining with either SYTO™9 (blue) and AlexaFluor568 anti-mouse secondary (yellow) or Abberior STAR 635 anti-mouse secondary (green) and the cellular dye Rhodamine B (red) was conducted as per previous experiments. **A.** Breakdown schematics of fluorescence patterns of cells expressing TcpD-G_6-HA in the presence of pCW3 are shown. **B and C.** The fluorescence captured from cells expressing TcpE-HA in the presence (**B**) and absence (**C**) of pCW3. **D and E.** The fluorescence captured from cells expressing TcpH-G_6-HA in the presence (**D**) and absence (**E**) of pCW3. Images were collected using an Abberior STED Microscope. Scale bar is 2 μm. Shown are representative images from three replicate experiments.

revealed that TcpE did not localise to the cell poles as expected. Instead TcpE-HA formed multiple foci around the membrane (Figure 5.17). Additionally, TcpE-HA was also present in large clusters on the surface of the cell. In some cells, the TcpE clusters appeared to form ring-like structures (white arrows, Figure 5.17). Quantitative analysis determined that at least one cluster or ring structure occurred in 52% of labelled cells (Table 5.3). A small percentage of cells (10%) had two or more ring structures present. In the absence of pCW3, TcpE-HA localised in fewer punctate spots around the membrane (Figure 5.18), large clusters were only observed in 7% of cells imaged (Table 5.3). No cells with more than one cluster were observed. This finding suggests that the large TcpE clusters may rely on other pCW3-encoded factors for efficient formation.

As yet, no specific function in conjugation has been described for TcpE although it is essential to the conjugation process (Wisniewski *et al.*, 2015a). The formation of these large clusters on the membrane of the bacterial cell may hint at a potential function of TcpE as an adhesion factor. Gram-positive conjugation systems are hypothesised to utilise adhesion factors to facilitate cell-to-cell contact (Bhatty *et al.*, 2013). We hypothesised that the TcpE clusters may function as short non-fimbiral adhesins. As short adhesins can be shielded by the presence of a polysaccharide capsule (Schembri *et al.*, 2004) we investigated if the *C. perfringens* capsule is perturbed at the site of the TcpE clusters. To investigate this theory, *C. perfringens* pCW3Δ*tcpE* cells expressing TcpE-HA from a complementation vector were labelled with the DNA dye SYTO9, the capsule was labelled with Alexa-Fluor555-conjugated wheat germ agglutinin (WGA555) and TcpE-HA was immunolabelled with Abberior STAR635 secondary antibody. STED analysis revealed that the capsule was not altered at the sites where TcpE-HA clusters were present (Figure 5.19). These results indicate that TcpE clusters do not lead to gross capsular disruption.

TcpH is a large membrane protein that is essential for pCW3 conjugative transfer. TcpH is hypothesised to form the primary component of the membrane associated transfer complex, due to the presence of eight predicted transmembrane domains (Bannam *et al.*, 2006). Previous work

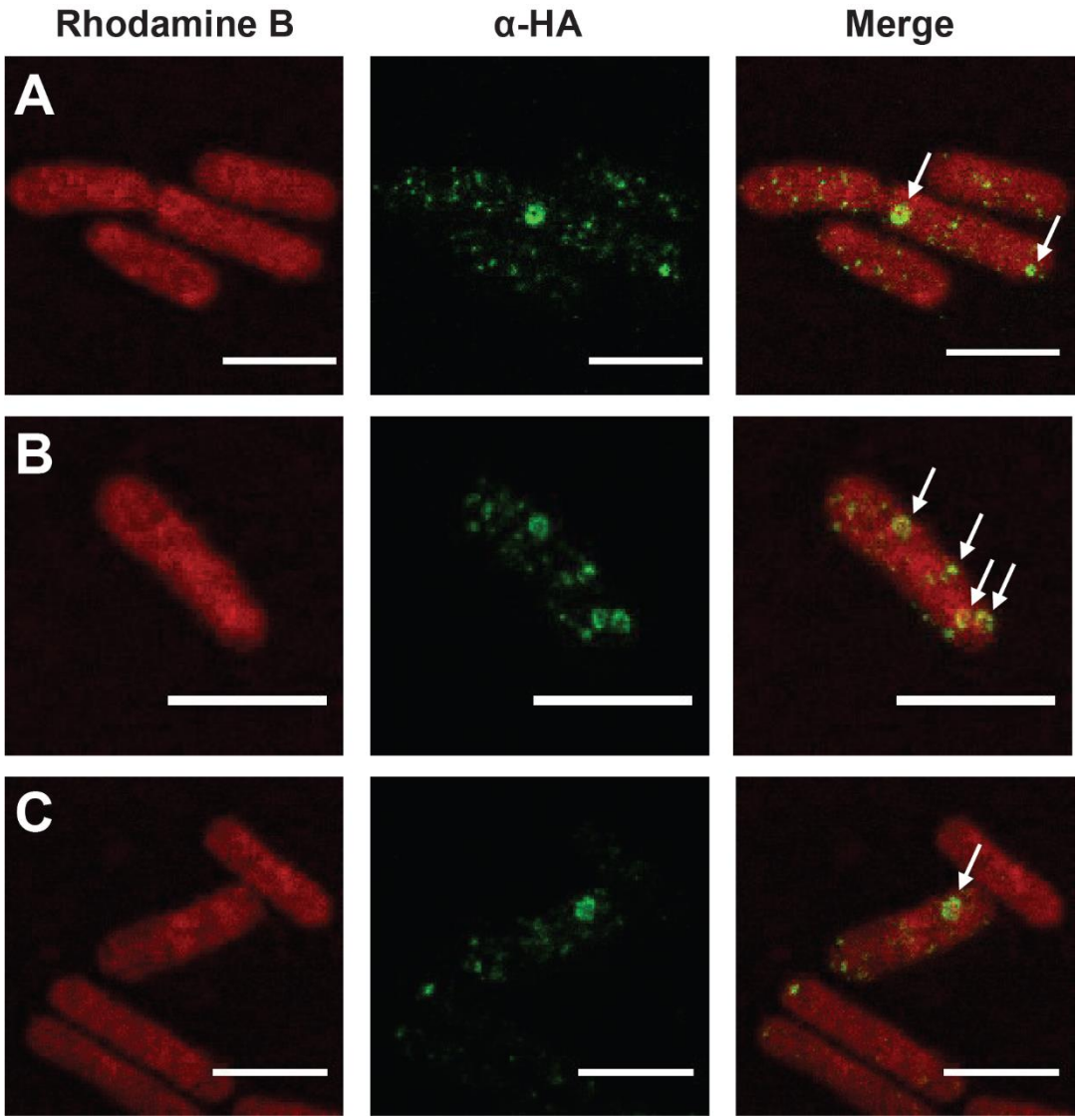

Figure 5.17: STED immunofluorescence imaging of *C. perfringens* cells expressing TcpE-HA. Localisation of TcpE-HA was determined by probing pCW3Δ*tcpE C. perfringens* cells complemented with a HA-tagged TcpE derivative with primary antibodies to the HA epitope tag followed by staining with Abberior STAR 635 anti-mouse secondary (green) and the cellular dye Rhodamine B (red). Ring-like structures are indicated by the white arrows. Images were collected using an Abberior STED Microscope. Shown are representative images (**A, B, C**) from three replicate experiments. Images were collected using the Abberior STED Microscope. Scale bar is 2 μm.

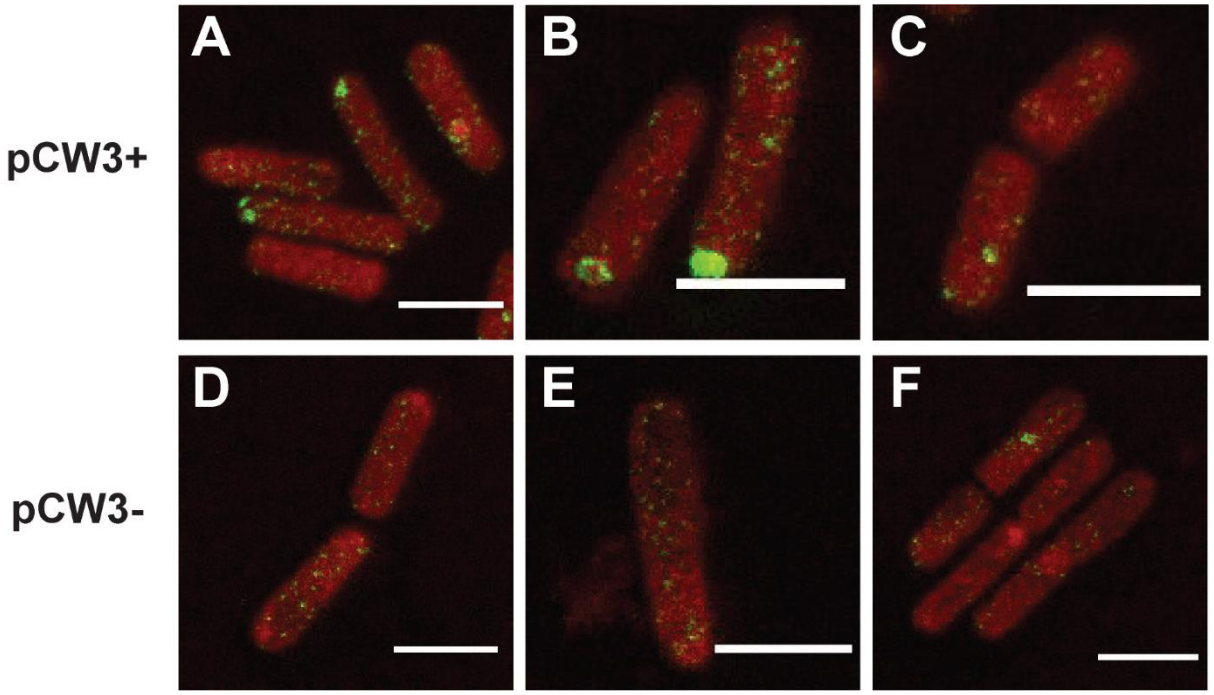

Figure 5.18: Localisation of TcpE-HA in the presence and absence of pCW3. A complementation vector encoding TcpE-HA was introduced into the pCW3-negative strain JIR325. The localisation of TcpE-HA was determined by probing *C. perfringens* cells (±pCW3) with primary antibodies to the HA epitope tag followed by staining with Abberior STAR 635 anti-mouse secondary (green) and the cellular dye Rhodamine B (red). Shown are three representative images from two replicate experiments showing the localisation of TcpE-HA in the presence (**A, B, C**) and absence (**D, E, F**) of pCW3. Images were collected using an Abberior STED Microscope. Scale bar is 2 μm.

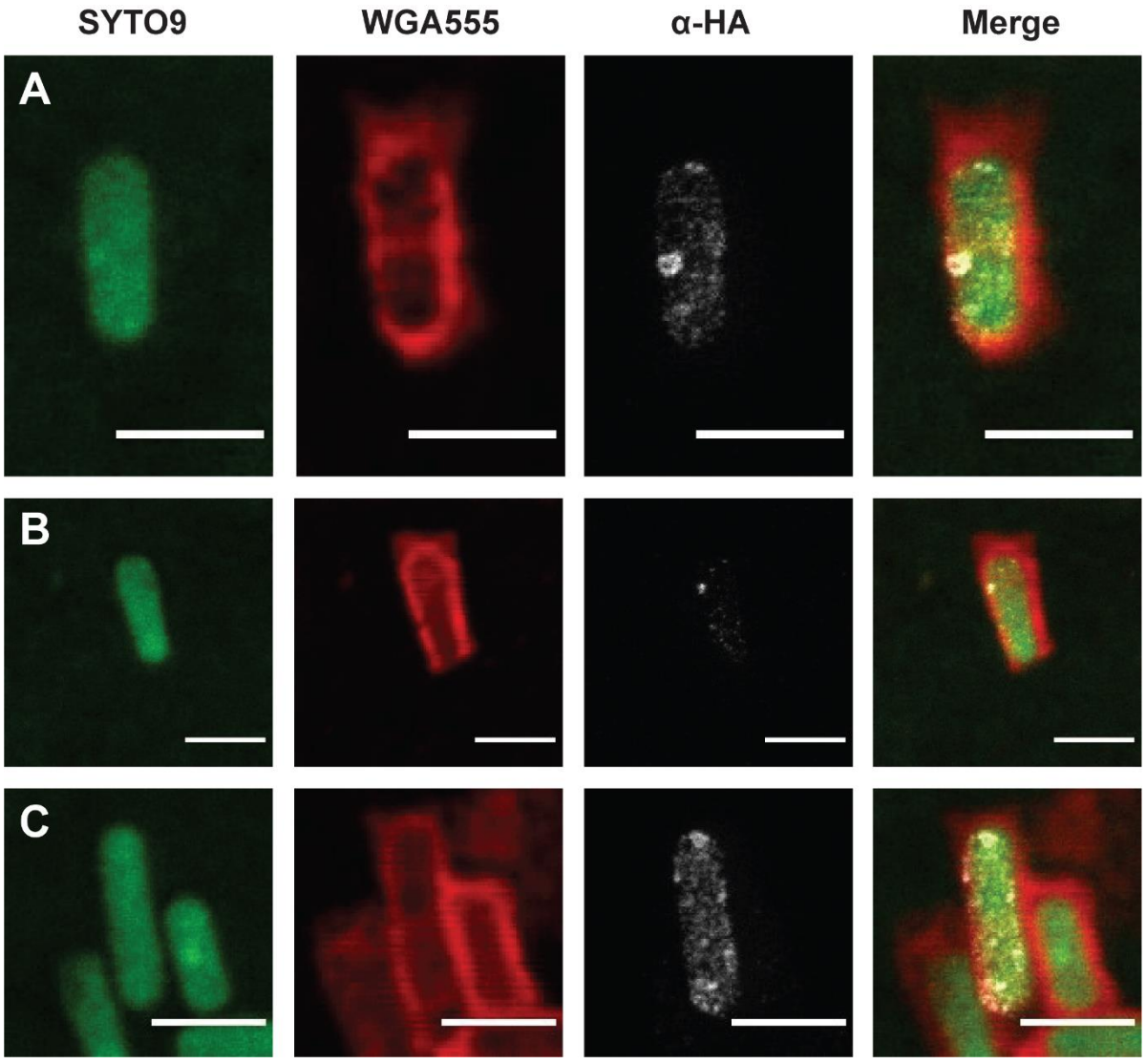
SYTO9
WGA555
α-HA
Merge
A
B
C

Figure 5.19: Localisation of TcpE-HA clusters with labelled capsule. The localisation of TcpE-HA was determined by probing *C. perfringens* cells containing pCW3Δ*tcpE* with primary antibodies to the HA epitope tag. Cells were subsequently stained with Abberior STAR 635 anti-mouse secondary (grey) along with the DNA dye SYTO9 (green) and AlexaFluor555 conjugated wheat germ agglutinin (WGA555; red). Shown are three representative channel breakdown images (**A, B, C**) from two replicate experiments. Shown are the localisations of TcpE-HA (grey), the body of the cell as shown by *C. perfringens* nucleic acids (green) and the *C. perfringens* capsule (red). Images were collected using an Abberior STED Microscope, SYTO9 and WGA555 images shown here were captured using the STED microscope confocal setting because of photobleaching induced by the STED laser. Scale bar is 2 μm

has determined that native TcpH localised primarily to the cell poles (Teng *et al.*, 2008). Super resolution microscopy confirmed that epitope tagged TcpH also localised to the cell poles (Figure 5.20 A and B). Control experiments confirmed specific protein labelling (Figure 5.16). TcpH-G_6-HA also demonstrated a dispersed distribution (Figure 5.20D) amongst the membrane at a density of 7.6±0.52 foci per μm^2 (Figure 5.13) and, in a subset of cells, also formed banded patterns around the membrane of the cell (Figure 5.20C). Quantitative analysis determined that TcpH-G_6-HA localised to the poles in 42% of cells when pCW3 was present, however polar localisation was only observed in 2.2% cells when pCW3 was absent (Table 5.3). In the cells without pCW3, TcpH-G_6-HA demonstrated a predominantly dispersed localisation throughout the membrane (Figure 5.21). The density of dispersed TcpH-G_6-HA foci when pCW3 was present was significantly higher (7.6±0.52 foci per μm^2, $p<0.0001$) than when pCW3 was absent (4.6±0.38) (Figure 5.13). These data indicate that TcpH may require other components from pCW3 for efficient localisation to the cell poles.

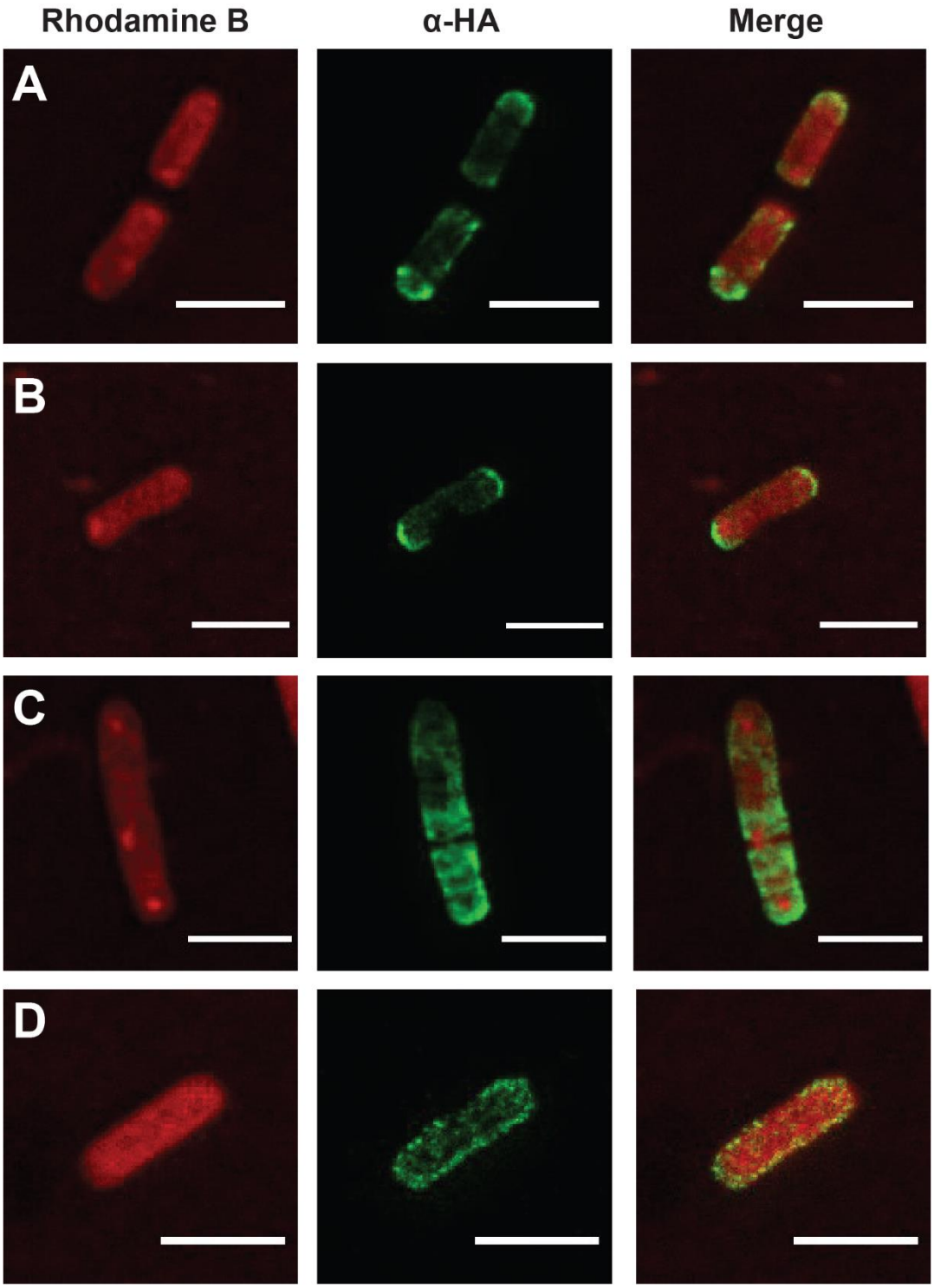
Rhodamine B
α-HA
Merge
A
B
C
D

Figure 5.20: TcpH-G_6-HA localisation patterns. Localisation of TcpH-G_6-HA was determined by probing *C. perfringens* cells complemented with a HA-tagged TcpH derivative with primary antibodies to the HA epitope tag followed by staining with Abberior STAR 635 anti-mouse secondary (green) and the cellular dye Rhodamine B (red). Shown are channel breakdown images of representative cells with TcpH-G_6-HA localisations at a single pole (**A**), both poles (**B**), banded (**C**) and dispersed (**D**). Images were collected using an Abberior STED Microscope. Scale bar is 2 μm.

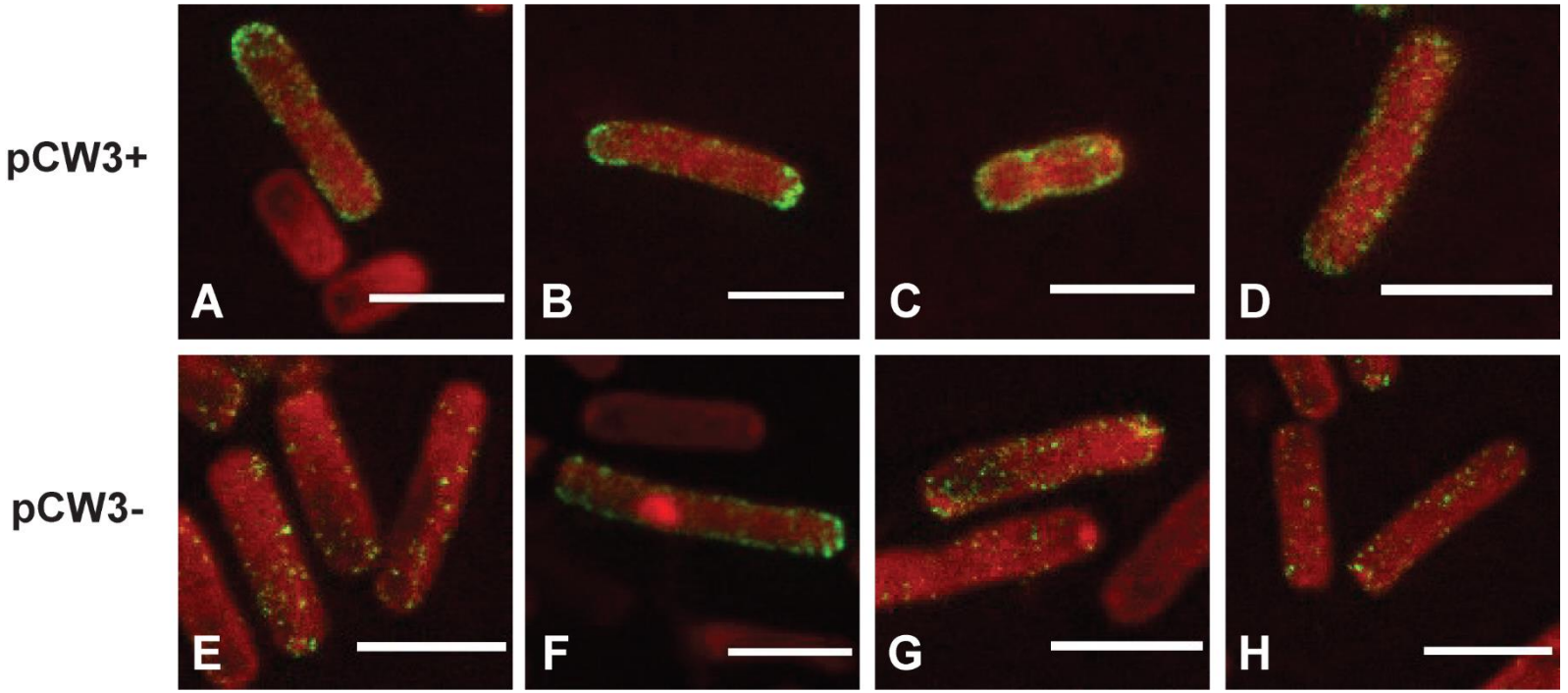

Figure 5.21: STED immunofluorescence imaging of *C. perfringens* cells expressing TcpH-G_6-HA with and without the presence of pCW3. A complementation vector encoding TcpH-G_6-HA was introduced into the pCW3-negative strain JIR325. The localisation of TcpH-G_6-HA was determined by probing *C. perfringens* cells (±pCW3) with primary antibodies to the HA epitope tag followed by staining with Abberior STAR 635 anti-mouse secondary (green) and the cellular dye Rhodamine B (red). Shown in the top panels (**A-D**) are representative cells with TcpH-G_6-HA localisations at a single pole (**A**), both poles (**B**), banded (**C**) and dispersed (**D**) observed in three replicate experiments. The bottom panels (**E-H**) are representative images of the localisation of TcpH-G_6-HA in the absence of pCW3 from three replicate experiments. Images were collected using an Abberior STED Microscope. Scale bar is 2 μm.

Discussion

In this study, the subcellular localisation of six highly conserved Tcp proteins was examined using super-resolution microscopy. Analysis of epitope-tagged proteins *in situ* allowed us to determine the spatial organisation of the Tcp components TcpA, TcpD, TcpE, TcpH, TcpM and TcpK, providing insight into the location and organisation of the *C. perfringens* Tcp conjugative T4SS. STED super-resolution microscopy maximised the resolution of images collected and built upon previous imaging data (Teng *et al.*, 2008, Wisniewski *et al.*, 2015a). This approach allowed the visualisation of the location of individual protein foci on the surface of the cell and revealed that the small membrane protein TcpE formed large ring-like clusters within the membrane (Figure 5.16).

TcpE is essential for conjugative transfer (Wisniewski *et al.*, 2015a) and TcpE-like proteins are a unique feature of the MPF_{FA} class of conjugative T4SS. They form their own family of conjugation related proteins, as they do not share homology to conjugation proteins from any other known conjugation class (Guglielmini *et al.*, 2014). Subcellular localisation studies demonstrated that TcpE did not localise to the cell pole as previously described (Wisniewski *et al.*, 2015a), instead it formed ring-like clusters in various positions on the surface of the bacterial cell that did not alter the gross appearance of the capsule at these sites (Figure 5.18). As yet, the precise function of TcpE in pCW3 conjugation has not been elucidated. Previous bioinformatic analysis of TcpE identified no functional domains other than two putative transmembrane domains, providing no hints as to its potential function (Wisniewski *et al.*, 2015a). Based on the observations of large clusters on the surface of the *C. perfringens* cells during this study it is postulated that the TcpE clusters may function as adhesins, facilitating cell-to-cell contact. In a recent study, two plasmid-encoded adhesins, Pep and the VirB5 homologue TraC, were shown *via* 3D-SIM super resolution microscopy to form punctate clusters on the surface of *E. coli* cells (González-Rivera *et al.*, 2018). Although the work on these two proteins utilised super resolution microscopy, the resolution of individual bacterial cells was too low to identify if either adhesin molecule forms ring-like clusters. However, the results presented in this chapter provide evidence that TcpE molecules can form higher order complexes (foci) on the surface of bacterial cells.

In other Gram-positive T4SS, surface adhesin molecules are typically large proteins attached to the cell wall *via* sortase recognition of C-terminal LPXTG motifs (Alvarez-Martinez & Christie, 2009, Bhatty *et al.*, 2013). The pheromone-inducible conjugation system of the *Enterococcus faecalis* plasmid pCF10 utilises three large proteins, PrgA (previously named Sec10), PrgB (previously named Asc10) and PrgC, to facilitate cellular aggregation and attachment (Bhatty *et al.*, 2015, Olmsted *et al.*, 1991, Alvarez-Martinez & Christie, 2009). Immunogold labelling and electron microscopy demonstrated that PrgA and PrgB have a dispersed membrane localisation, although no apparent protein clustering was observed (Olmsted *et al.*, 1993). Similarly, the broad host range plasmid pIP501 is hypothesised to utilise TraO (previously annotated as Orf15), a protein structurally similar to PrgB, to mediate contact with recipient cells (Goessweiner-Mohr *et al.*, 2013, Alvarez-Martinez & Christie, 2009, Grohmann *et al.*, 2017). With respect to the Tcp conjugation system, it is possible that TcpE could function as an adhesin. However, as many other Gram-positive T4SS utilise large LPXTG containing proteins for adhesion, a more likely option is that the LPXTG containing, large collagen adhesin-like protein CnaC, encoded upstream of the *tcp* locus, mediates cell-to-cell interactions. Unlike PrgB, mutation of *cnaC* on pCW3 reduced but did not abolish conjugation, suggesting in addition to CnaC, other adhesins may be promoting cell-to-cell contact (S. Revitt-Mills, V. Adams and J. Rood, unpublished).

The effective formation of TcpE clusters appears to require the presence of pCW3, as clusters were present in 64% of cells containing pCW3 whereas only 7% of cells had identifiable TcpE clusters when pCW3 was absent (Table 5.3). In the VirB/VirD4 T4SS from *A. tumefaciens*, it has been reported that correct localisation of T4SS proteins requires only the presence of the ATPase VirB8 (Judd *et al.*, 2005). VirB8 is hypothesised to function as a scaffolding factor, facilitating the correct construction of the T4SS. The requirement of VirB8 or a homologue for correct protein localisation has been observed in both Gram-negative and Gram-positive conjugation systems, highlighting the importance of VirB8 in conjugation complex formation (Leonetti *et al.*, 2015, Judd *et al.*, 2005). The structural VirB8 homologue, TcpC, is required for the efficient conjugative transfer of pCW3, as deletion resulted in a reduction in conjugation frequency by five orders of magnitude (Porter *et al.*, 2012). The observation of some

clustered TcpE foci in the absence of pCW3 does indicate that these structures can form independently of pCW3 factors and may explain why mutation of TcpC does not abrogate conjugation. In this model, TcpC may function as an assembly factor or scaffolding protein, assisting efficient formation of the conjugation apparatus, however, it is not essential. If TcpC does function as an assembly factor this premise predicts that TcpC should localise to various sites within the membrane independently of other components from the Tcp conjugation system. Indeed, cell fractionation studies have determined that TcpC localises to the membrane independent of other conjugation related proteins, supporting this hypothesis (Porter *et al.*, 2012). Although no direct interaction of TcpC and TcpE has been demonstrated (Wisniewski *et al.*, 2015a, Porter *et al.*, 2012), it remains possible that these proteins interact to form the Tcp conjugation apparatus. This theory is further supported by evidence that TcpC interacts with other Tcp proteins TcpA, TcpH and TcpG (Porter *et al.*, 2012, Steen *et al.*, 2009, Teng *et al.*, 2008). To date, the cellular localisation of TcpC has not been determined. It would be valuable to assess if TcpC co-localised with other Tcp proteins, supporting the hypothesis that TcpC may contribute to the assembly of the Tcp conjugation apparatus.

Localisation studies also revealed for the first time the subcellular localisation of the key relaxosome proteins, TcpM and TcpK (Figures 5.3 and 5.4 respectively) and the membrane-associated coupling protein TcpA (Figure 5.10). Both the relaxase, TcpM, and relaxosome accessory protein, TcpK, demonstrated a dispersed cytoplasmic localisation. TcpM formed notable punctate foci throughout the cytoplasm, independent of other pCW3-associated factors. Other relaxase enzymes such as PcfG from the *E. faecalis* plasmid pCF10 and VirD2 from the *A. tumefaciens* T4SS form punctate foci within the cytoplasm of the cell (Chen *et al.*, 2008, Aguilar *et al.*, 2010). In these systems, however, relaxase foci appear to be associated with the membrane of the cell, despite the lack of transmembrane domains within these proteins. Cell fractionation studies confirmed the membrane association of the PcfG relaxase, which is thought to interact with the membrane via peripheral interactions (Chen *et al.*, 2008). Membrane association appears to be common amongst relaxase proteins, however, z-stack image collection clearly shows TcpM to be located throughout the entire cytoplasm and not showing any

noticeable accumulation at the membrane. It is likely that TcpM does interact with membrane proteins at some point during the conjugation process, since TcpM is hypothesised to be transferred into the recipient cell along with covalently attached plasmid DNA (Wisniewski *et al.*, 2015b, Lanka & Wilkins, 1995).

TcpK is a small accessory protein that is necessary for conjugative transfer (Traore *et al.*, 2018). Although biochemical analysis has demonstrated specific binding to TcpK boxes located within the pCW3 *oriT* site, the precise mechanism of action of TcpK in pCW3 conjugation remains unknown (Traore *et al.*, 2018). This study demonstrated that TcpK may rely on the presence of pCW3 factors for the dispersed localisation pattern observed, as when pCW3 is absent, the concentration of TcpK protein is low. When pCW3 is present within the *C. perfringens* cell it is possible that TcpK interaction with pCW3 DNA occurs, resulting in the diffuse localisation. To confirm the *in vivo* interactions, elucidation of the cellular location of pCW3 DNA is required. It remains possible that the differences in localisation profiles may be due to potential instability of TcpK in the absence of other pCW3 encoded proteins, as was reported for TcpD (Wisniewski *et al.*, 2015a). Destabilisation of T4SS proteins in the absence of other T4SS components has also been described for the *Legionella pneumophila* Dot/Icm T4SS (Sexton *et al.*, 2004). These findings highlight the importance of other components for the formation of stable T4SS. To determine if the differences observed in TcpK distribution patterns are due to protein instability or lower levels of protein expression in the absence of other pCW3-encoded proteins, the levels of TcpK production in the presence and absence of pCW3 should be elucidated. The diffuse localisation of TcpM and TcpK throughout the cytoplasm indicates that DNA processing reactions can occur anywhere throughout the cell, suggesting that the starting steps of the conjugation process are not spatially limited to certain locales within the bacterial cell.

In this study, the pCW3 coupling protein TcpA was shown to form multiple foci around the membrane of the bacterial cell, with no discernible pattern of distribution (Figure 5.10). Coupling proteins typically possess one or more transmembrane domains (Gomis-Ruth *et al.*, 2004, Alvarez-Martinez & Christie, 2009), which aid in localising the protein to the cell wall, where the transfer apparatus is formed. TcpA

has two transmembrane domains and was hypothesised to localise in the membrane (Parsons *et al.*, 2007), which was confirmed through super resolution immunofluorescence microscopy in the current study. The subcellular localisation of coupling proteins in T4SS remains controversial. Previous localisation studies on the coupling proteins VirD4 (Kumar & Das, 2002), TraG (Gunton *et al.*, 2005), PcfC (Chen *et al.*, 2008) and TrwB (Segura *et al.*, 2014) have demonstrated variable patterns in cellular distribution. VirD4 and TrwB were shown to localise primarily to the cell poles independently of the presence of other respective conjugation proteins (Kumar & Das, 2002, Segura *et al.*, 2014). By contrast, TraG and PcfC were shown to form numerous fluorescent foci around the membrane of the cell, with no discernible pattern of distribution (Chen *et al.*, 2008, Segura *et al.*, 2014). In a later study, using fluorescence deconvolution microscopy, GFP-fused VirD4 was shown to form helical arrays around the membrane of the *A. tumefaciens* cell (Aguilar *et al.*, 2010). The location of the coupling protein may be specific to the conjugative element in question or even the resolution of the method of detection that is used. Immunofluorescence super resolution microscopy of TcpA clearly demonstrated a non-polar dispersed membrane localisation, which is in agreement with what was seen for TraG, PcfC and more recently VirD4 (Gunton *et al.*, 2005, Chen *et al.*, 2008, Aguilar *et al.*, 2010). This dispersed membrane localisation may increase the likelihood of interactions with the diffusely located relaxosome components TcpM and TcpK. Although no protein-protein interactions between relaxosome and coupling protein components have been demonstrated, this scenario is plausible since relaxase-bound DNA requires interaction with the coupling protein for its transport through the transmembrane transfer complex (Lanka & Wilkins, 1995, Llosa *et al.*, 2002).

Finally, the small membrane protein TcpD and VirB6-like structural protein TcpH clearly demonstrated a polar localisation (Figures 5.15 and 5.19, respectively). Effective polar positioning of TcpH requires the presence of pCW3 factors; polar fluorescence was only observed in 2.2% of the population without pCW3, in comparison to 42% with pCW3. Many previous studies on the localisation of various T4SS components provide evidence that the conjugation event occurs at the cell poles (Teng *et al.*, 2008, Judd *et al.*, 2005, Berkmen *et al.*, 2010, Jeong *et al.*, 2017, Jeong *et al.*, 2018, Leonetti *et al.*, 2015). Why does

this event occur at the poles? Bacterial membranes are dynamic and complex structures, and as such the composition of cell membranes differs at the bacterial poles (Howell & Brown, 2016, Bowman *et al.*, 2011). The composition of the membrane may affect the conjugation process. For example, the efficiency of conjugative transfer of the integrative conjugative element ICE*Bs*1 was altered by changing phospholipid compositions of the bacterial membrane (Johnson & Grossman, 2016). Similar observations were made for ICE*St*3 (Dahmane *et al.*, 2018). These findings support the notion that cell wall composition plays a critical role in facilitating effective conjugative transfer and may explain why conjugation is thought to occur at the cell poles.

For conjugation to occur at the poles, the proteins must first localise to this subcellular domain. The precise mechanisms governing subcellular distribution of T4SS components remains unknown. Some studies propose that mechanisms involving bacterial cytoskeletal components and cell wall synthesis machinery may aide in polar localisation (Chen *et al.*, 2008, Aguilar *et al.*, 2010). Bacterial cytoskeletal components such as the actin-homologue MreB and ATPase MinD are known to target proteins to the cell poles (Carballido-López, 2006, Lutkenhaus, 2012). These proteins form dynamic helical arrays within the inner face of the membrane, playing an important role in the determination of bacterial shape and cytoskeletal structure (Laloux & Jacobs-Wagner, 2014). Some studies have demonstrated co-localisation of actin-like homologues with T4SS proteins, inferring that the localisation of the T4SS is associated with the cytoskeletal bacterial scaffold (Aguilar *et al.*, 2010). Other studies have been unable to demonstrate similar co-localisation. Therefore, more work is required to determine how T4SS proteins are positioned within the cell. As the polar localisation of TcpH was reduced in the absence of pCW3, it is likely that TcpH polar positioning is facilitated by pCW3-encoded factors. However, it is possible that the polar localisation of TcpH may be influenced by cytoskeletal structures.

More recent studies have challenged the notion that T4SSs localise and function primarily at the cell poles. Studies conducted on the T4SS of *A. tumefaciens* determined that multiple components of this system form helical arrays around the circumference of the cell (Aguilar *et al.*, 2011, Aguilar *et al.*, 2010). 3D deconvolution microscopy techniques were used to image the subcellular localisation of various

A. tumefaciens T4SS proteins. In these studies proteins that had previously been described as having a polar localisation were identified as multiple foci throughout the cell membrane (Aguilar *et al.*, 2010, Aguilar *et al.*, 2011). Subsequently, a new model for subcellular localisation of the Vir-T4SS was proposed, whereby multiple T4SS are assembled throughout the membrane of the bacterial cell, which maximises the chances of donor-recipient cell interaction and conjugation occurring.

In addition to their polar localisation, both TcpD and TcpH were present as distinct foci on the surface of the bacterial cell, with no discernible bias toward any particular cellular location. TcpH was also observed in a banded, almost helical pattern in a subset of cells. The multiple localisation patterns observed for these two proteins may be growth phase dependent, as the cells imaged in this study were not normalised to a specific growth phase. A study conducted on the Dot/Icm T4SS of *L. pneumophila* determined that complex localisation was closely linked to cell division and age (Jeong *et al.*, 2017). Another study conducted on the T4SS of *Coxiella burnetii* hypothesised that bipolar localisation of the T4SS correlates with cells approaching cell division (Luedtke *et al.*, 2010). As such, bipolar localisation would ensure that both daughter cell progeny possess functional secretion systems following cell division. It is postulated that the dispersed localisation observed for TcpD and TcpH is indeed the regular positioning of these proteins. The formation of multiple T4SS on the entire surface of the bacterial cell would increase the potential of interactions with a recipient cell. The cells with a banded TcpH pattern may have been captured in the process of localising T4SS components to the poles prior to cell division. Cells with protein localisation at a single pole were observed for both proteins and in the cells captured in Figure 5.19A, it appears these cells have just undergone cell division.

A model for the conjugative transfer of pCW3 in *C. perfringens* can be proposed based on the results of this study. The data demonstrated the dispersed localisation of membrane proteins TcpD, TcpE and TcpH, which are thought to comprise some of the structural components of the transfer apparatus. As such, it is hypothesised that Tcp conjugation complexes form at multiple positions around the cell, maximising the chance of interactions with recipient cells. Either as a function of cell growth or protein accumulation due to age, the scaffold proteins TcpD and TcpH accumulate at the poles in some cells. At

this position they could potentially contribute to polar conjugation events. TcpE could potentially function as an adhesion factor, facilitating cell-to-cell contact, although it is more likely that TcpE functions as a structural component. The TcpE rings could provide structural support for the multi-protein transfer apparatus. In agreement with the notion that multiple Tcp apparatuses are formed around the membrane of the cell, the relaxosome components TcpM and TcpK were dispersed throughout the cytoplasm. This localisation suggests that relaxosome processing of plasmid DNA could occur anywhere within the cytoplasm. Following processing, the relaxase-bound plasmid DNA could interact with the coupling protein TcpA, which is diffusely located throughout the membrane. TcpA is known to interact with the structural components TcpC and TcpH, which would facilitate the transfer of plasmid DNA into recipient cells.

There are limitations involved in this proposed model. The data obtained in this study involved determining the localisation of the various Tcp proteins expressed *in trans* under control of the strong clostridial promoter, P_{attCI}. It is likely that the levels of Tcp protein produced were much higher than wild-type levels and as such the observed localisations may be an artefact of over expression, particularly with respect to the formation of the large clusters observed for TcpE. However, the localisation patterns of overexpressed, epitope-tagged TcpH were similar to those observed previously for native TcpH (Teng *et al.*, 2008). This observation indicates that the patterns observed in this study may not be completely perturbed by overexpression. Quantitative analysis of protein foci on the surface of the cells involved capturing images on a single z-plane. Whilst efforts were made to image cells labelled for membrane-associated proteins at the top of the cell to infer a normalised area of analysis, capture of all proteins at this site cannot be guaranteed, potentially skewing the data. Future work should aim to overcome these limitations to provide a more robust analysis of the localisation of the Tcp conjugation apparatus, as discussed in Chapter Six.

This study has successfully developed a robust method for the visualisation of epitope-tagged proteins within fixed *C. perfringens* cells using STED super-resolution microscopy. The improved resolution obtained in this study allowed new conclusions about protein localisation to be drawn. This finding

highlights the importance of re-visiting and revising past conclusions as technology continues to improve, which will allow us to gain a better understanding of how these systems work. In addition, this study demonstrated that the Tcp conjugation proteins have variable and dispersed localisations which forms the basis of the proposed Tcp conjugation model, whereby multiple complexes form around the periphery of the cell, maximising the occurrence of conjugation events. Overall, these findings have provided further insights into the mechanism of conjugative transfer within the Gram-positive pathogen *C. perfringens.*

References

Adams, V., Bantwal, R., Stevenson, L., Cheung, J.K., Awad, M.M., Nicholson, J., Carter, G.P., Mackin, K.E., Rood, J.I., and Lyras, D. (2014) Utility of the Clostridial site-specific recombinase TnpX to clone toxic-product-encoding genes and selectively remove genomic DNA fragments. *Applied and Environmental Microbiology* **80**: 3597-3603.

Aguilar, J., Cameron, T.A., Zupan, J., and Zambryski, P. (2011) Membrane and core periplasmic *Agrobacterium tumefaciens* virulence Type IV secretion system components localize to multiple sites around the bacterial perimeter during lateral attachment to plant cells. *mBio* **2**: e00218-11.

Aguilar, J., Zupan, J., Cameron, T.A., and Zambryski, P.C. (2010) *Agrobacterium* type IV secretion system and its substrates form helical arrays around the circumference of *virulence*-induced cells. *Proceedings of the National Academy of Sciences* **107**: 3758-3763.

Alvarez-Martinez, C.E., and Christie, P.J. (2009) Biological diversity of prokaryotic type IV secretion systems. *Microbiology and Molecular Biology Reviews* **73**: 775-808.

Bannam, T.L., Teng, W.L., Bulach, D., Lyras, D., and Rood, J.I. (2006) Functional identification of conjugation and replication regions of the tetracycline resistance plasmid pCW3 from *Clostridium perfringens*. *Journal of Bacteriology* **188**: 4942-4951.

Bannam, T.L., Yan, X.-X., Harrison, P.F., Seemann, T., Keyburn, A.L., Stubenrauch, C., Weeramantri, L.H., Cheung, J.K., McClane, B.A., Boyce, J.D., Moore, R.J., and Rood, J.I. (2011) Necrotic enteritis-derived *Clostridium perfringens* strain with three closely related independently conjugative toxin and antibiotic resistance plasmids. *mBio* **2**: e00190-11.

Bantwal, R., Bannam, T.L., Porter, C.J., Quinsey, N.S., Lyras, D., Adams, V., and Rood, J.I. (2012) The peptidoglycan hydrolase TcpG is required for efficient conjugative transfer of pCW3 in *Clostridium perfringens*. *Plasmid* **67**: 139-147.

Berkmen, M.B., Lee, C.A., Loveday, E.-K., and Grossman, A.D. (2010) Polar positioning of a conjugation protein from the integrative and conjugative element ICE*Bs1* of *Bacillus subtilis*. *Journal of Bacteriology* **192**: 38-45.

Bhatty, M., Cruz, M.R., Frank, K.L., Laverde Gomez, J.A., Andrade, F., Garsin, D.A., Dunny, G.M., Kaplan, H.B., and Christie, P.J. (2015) *Enterococcus faecalis* pCF10-encoded surface proteins PrgA, PrgB (aggregation substance) and PrgC contribute to plasmid transfer, biofilm formation and virulence. *Molecular Microbiology* **95**: 660-677.

Bhatty, M., Laverde Gomez, J.A., and Christie, P.J. (2013) The expanding bacterial type IV secretion lexicon. *Research in Microbiology* **164**: 620-639.

Bowman, G.R., Lyuksyutova, A.I., and Shapiro, L. (2011) Bacterial polarity. *Current Opinion in Cell Biology* **23**: 71-77.

Brynestad, S., Sarker, M.R., McClane, B.A., Granum, P.E., and Rood, J.I. (2001) Enterotoxin plasmid from *Clostridium perfringens* is conjugative. *Infection and Immunity* **69**: 3483-3487.

Carballido-López, R. (2006) The bacterial actin-like cytoskeleton. *Microbiology and Molecular Biology Reviews* **70**: 888-909.

Chen, Y., Zhang, X., Manias, D., Yeo, H.-J., Dunny, G.M., and Christie, P.J. (2008) *Enterococcus faecalis* PcfC, a spatially localized substrate receptor for Type IV secretion of the pCF10 transfer intermediate. *Journal of Bacteriology* **190**: 3632-3645.

Dahmane, N., Robert, E., Deschamps, J., Meylheuc, T., Delorme, C., Briandet, R., Leblond-Bourget, N., Guédon, E., and Payot, S. (2018) Impact of cell surface molecules on conjugative transfer of the integrative and conjugative element ICE*St3* of *Streptococcus thermophilus*. *Applied and Environmental Microbiology* **84**: e02109-02117.

Goessweiner-Mohr, N., Arends, K., Keller, W., and Grohmann, E. (2013) Conjugative type IV secretion systems in Gram-positive bacteria. *Plasmid* **70**: 289-302.

Goessweiner-Mohr, N., Arends, K., Keller, W., and Grohmann, E. (2014) Conjugation in Gram-positive bacteria. *Microbiology Spectrum* **2**: PLAS-0004-2013.

Gomis-Rüth, F.X., de la Cruz, F., and Coll, M. (2002) Structure and role of coupling proteins in conjugal DNA transfer. *Research in Microbiology* **153**: 199-204.

Gomis-Ruth, F.X., Sola, M., Cruz, F.d.l., and Coll, M. (2004) Coupling factors in macromolecular Type-IV secretion machineries. *Current Pharmaceutical Design* **10**: 1551-1565.

González-Rivera, C., Khara, P., Awad, D., Patel, R., Li, Y.G., Bogisch, M., and Christie, P.J. (2018) Two pKM101-encoded proteins, the pilus-tip protein TraC and Pep, assemble on the *Escherichia coli* cell surface as adhesins required for efficient conjugative DNA transfer. *Molecular Microbiology* **111**: 96-117.

Grohmann, E., Keller, W., and Muth, G., (2017) Mechanisms of conjugative transfer and Type IV secretion-mediated effector transport in Gram-positive bacteria. In: Type IV Secretion in Gram-Negative and Gram-Positive Bacteria. S. Backert & E. Grohmann (eds). Cham: Springer International Publishing, pp. 115-141.

Guglielmini, J., Néron, B., Abby, S.S., Garcillán-Barcia, M.P., la Cruz, F.d., and Rocha, E.P.C. (2014) Key components of the eight classes of type IV secretion systems involved in bacterial conjugation or protein secretion. *Nucleic Acids Research* **42**: 5715-5727.

Gunasinghe, S.D., Shiota, T., Stubenrauch, C.J., Schulze, K.E., Webb, C.T., Fulcher, A.J., Dunstan, R.A., Hay, I.D., Naderer, T., Whelan, D.R., Bell, T.D.M., Elgass, K.D., Strugnell, R.A., and Lithgow, T. (2018) The WD40 protein BamB mediates coupling of BAM complexes into assembly precincts in the bacterial outer membrane. *Cell Reports* **23**: 2782-2794.

Gunasinghe, S.D., Webb, C.T., Elgass, K.D., Hay, I.D., and Lithgow, T. (2017) Super-resolution imaging of protein secretion systems and the cell surface of Gram-negative bacteria. *Frontiers in Cellular and Infection Microbiology* **7**: 220.

Gunton, J.E., Gilmour, M.W., Alonso, G., and Taylor, D.E. (2005) Subcellular localization and functional domains of the coupling protein, TraG, from IncHI1 plasmid R27. *Microbiology* **151**: 3549-3561.

Howell, M., and Brown, P.J.B. (2016) Building the bacterial cell wall at the pole. *Current Opinion in Microbiology* **34**: 53-59.

Hughes, M.L., Poon, R., Adams, V., Sayeed, S., Saputo, J., Uzal, F.A., McClane, B.A., and Rood, J.I. (2007) Epsilon-toxin plasmids of *Clostridium perfringens* type D are conjugative. *Journal of Bacteriology* **189**: 7531-7538.

Inoue, H., Nojima, H., and Okayama, H. (1990) High efficiency transformation of *Escherichia coli* with plasmids. *Gene* **96**: 23-28.

Jeong, K.C., Ghosal, D., Chang, Y.-W., Jensen, G.J., and Vogel, J.P. (2017) Polar delivery of *Legionella* type IV secretion system substrates is essential for virulence. *Proceedings of the National Academy of Sciences* **114**: 8077-8082.

Jeong, K.C., Gyore, J., Teng, L., Ghosal, D., Jensen, G.J., and Vogel, J.P. (2018) Polar targeting and assembly of the *Legionella* Dot/Icm type IV secretion system (T4SS) by T6SS-related components. *bioRxiv*.

Johnson, C.M., and Grossman, A.D. (2016) The composition of the cell envelope affects conjugation in *Bacillus subtilis*. *Journal of Bacteriology* **198**: 1241-1249.

Judd, P.K., Kumar, R.B., and Das, A. (2005) Spatial location and requirements for the assembly of the *Agrobacterium tumefaciens* type IV secretion apparatus. *Proceedings of the National Academy of Sciences* **102**: 11498-11503.

Kumar, R.B., and Das, A. (2002) Polar location and functional domains of the *Agrobacterium tumefaciens* DNA transfer protein VirD4. *Molecular Microbiology* **43**: 1523-1532.

Laloux, G., and Jacobs-Wagner, C. (2014) How do bacteria localize proteins to the cell pole? *Journal of Cell Science* **127**: 11-19.

Lamprecht, M.R., Sabatini, D.M., and Carpenter, A.E. (2007) CellProfiler™: free, versatile software for automated biological image analysis. *BioTechniques* **42**: 71-75.

Lanka, E., and Wilkins, B.M. (1995) DNA processing reactions in bacterial conjugation. *Annual Reviews Biochemistry* **64**: 141-169.

Leonetti, C.T., Hamada, M.A., Laurer, S.J., Broulidakis, M.P., Swerdlow, K.J., Lee, C.A., Grossman, A.D., and Berkmen, M.B. (2015) Critical components of the conjugation machinery of the integrative and conjugative element ICE*Bs1* of *Bacillus subtilis*. *Journal of Bacteriology* **197**: 2558-2567.

Llosa, M., Gomis-Rüth, F.X., Coll, M., and Cruz, F.d.l. (2002) Bacterial conjugation: a two-step mechanism for DNA transport. *Molecular Microbiology* **45**: 1-8.

Lobato-Márquez, D., Molina-García, L., Moreno-Córdoba, I., García-Del Portillo, F., and Díaz-Orejas, R. (2016) Stabilization of the virulence plasmid pSLT of *Salmonella* Typhimurium by three maintenance systems and its evaluation by using a new stability test. *Frontiers in Molecular Biosciences* **3**: 66-66.

Low, H.H., Gubellini, F., Rivera-Calzada, A., Braun, N., Connery, S., Dujeancourt, A., Lu, F., Redzej, A., Fronzes, R., Orlova, E.V., and Waksman, G. (2014) Structure of a type IV secretion system. *Nature* **508**: 550-553.

Luedtke, B.E., Morgan, J.K., and Shaw, E.I. (2010) Polar localization of the *Coxiella burnetii* type IVB secretion system. *FEMS Microbiology Letters* **305**: 177-183.

Lutkenhaus, J. (2012) The ParA/MinD family puts things in their place. *Trends in Microbiology* **20**: 411-418.

Lyristis, M., Bryant, A.E., Sloan, J., Awad, M.M., Nisbet, I.T., Stevens, D.L., and Rood, J.I. (1994) Identification and molecular analysis of a locus that regulates extracellular toxin production in *Clostridium perfringens*. *Molecular Microbiology* **12**: 761-777.

Mehdizadeh Gohari, I., Kropinski, A.M., Weese, S.J., Parreira, V.R., Whitehead, A.E., Boerlin, P., and Prescott, J.F. (2016) Plasmid characterization and chromosome analysis of two *netF*+ *Clostridium perfringens* isolates associated with foal and canine necrotizing enteritis. *PLOS One* **11**: e0148344.

Olmsted, S.B., Erlandsen, S.L., Dunny, G.M., and Wells, C.L. (1993) High-resolution visualization by field emission scanning electron microscopy of *Enterococcus faecalis* surface proteins encoded by the pheromone-inducible conjugative plasmid pCF10. *Journal of Bacteriology* **175**: 6229-6237.

Olmsted, S.B., Kao, S.M., van Putte, L.J., Gallo, J.C., and Dunny, G.M. (1991) Role of the pheromone-inducible surface protein Asc10 in mating aggregate formation and conjugal transfer of the *Enterococcus faecalis* plasmid pCF10. *Journal of Bacteriology* **173**: 7665-7672.

Parsons, J.A., Bannam, T.L., Devenish, R.J., and Rood, J.I. (2007) TcpA, an FtsK/SpoIIIE homolog, is essential for transfer of the conjugative plasmid pCW3 in *Clostridium perfringens*. *Journal of Bacteriology* **189**: 7782-7790.

Porter, C.J., Bantwal, R., Bannam, T.L., Rosado, C.J., Pearce, M.C., Adams, V., Lyras, D., Whisstock, J.C., and Rood, J.I. (2012) The conjugation protein TcpC from *Clostridium perfringens* is structurally related to the type IV secretion system protein VirB8 from Gram-negative bacteria. *Molecular Microbiology* **83**: 275-288.

Ragonese, H., Haisch, D., Villareal, E., Choi, J.-H., and Matson, S.W. (2007) The F plasmid-encoded TraM protein stimulates relaxosome-mediated cleavage at *oriT* through an interaction with TraI. *Molecular Microbiology* **63**: 1173-1184.

Rood, J.I. (1983) Transferable tetracycline resistance in *Clostridium perfringens* strains of porcine origin. *Canadian Journal of Microbiology* **29**: 1241-1246.

Rood, J.I., Maher, E.A., Somers, E.B., Campos, E., and Duncan, C.L. (1978) Isolation and characterization of multiply antibiotic-resistant *Clostridium perfringens* strains from porcine feces. *Antimicrobial Agents and Chemotherapy* **13**: 871-880.

Schembri, M.A., Dalsgaard, D., and Klemm, P. (2004) Capsule shields the function of short bacterial adhesins. *Journal of Bacteriology* **186**: 1249-1257.

Schneider, C.A., Rasband, W.S., and Eliceiri, K.W. (2012) NIH Image to ImageJ: 25 years of image analysis. *Nature Methods* **9**: 671-675.

Segura, R.L., Águila-Arcos, S., Ugarte-Uribe, B., Vecino, A.J., de la Cruz, F., Goñi, F.M., and Alkorta, I. (2014) Subcellular location of the coupling protein TrwB and the role of its transmembrane domain. *Biochimica et Biophysica Acta (BBA) - Biomembranes* **1838**: 223-230.

Sexton, J.A., Miller, J.L., Yoneda, A., Kehl-Fie, T.E., and Vogel, J.P. (2004) *Legionella pneumophila* DotU and IcmF are required for stability of the Dot/Icm complex. *Infection and Immunity* **72**: 5983-5992.

Steen, J.A., Bannam, T.L., Teng, W.L., Devenish, R.J., and Rood, J.I. (2009) The putative coupling protein TcpA interacts with other pCW3-encoded proteins to form an essential part of the conjugation complex. *Journal of Bacteriology* **191**: 2926-2933.

Teng, W.L., Bannam, T.L., Parsons, J.A., and Rood, J.I. (2008) Functional characterization and localization of the TcpH conjugation protein from *Clostridium perfringens*. *Journal of Bacteriology* **190**: 5075-5086.

Traore, D.A.K., Wisniewski, J.A., Flanigan, S.F., Conroy, P.J., Panjikar, S., Mok, Y.-F., Lao, C., Griffin, M.D.W., Adams, V., Rood, J.I., and Whisstock, J.C. (2018) Crystal structure of TcpK in complex with *oriT* DNA of the antibiotic resistance plasmid pCW3. *Nature Communications* **9**: 3732.

Waksman, G., and Orlova, E.V. (2014) Structural organisation of the type IV secretion systems. *Current Opinion in Microbiology* **17**: 24-31.

Wallden, K., Rivera-Calzada, A., and Waksman, G. (2010) Microreview: Type IV secretion systems: versatility and diversity in function. *Cell Microbiol* **12**: 1203-1212.

Wisniewski, J.A., and Rood, J.I. (2017) The Tcp conjugation system of *Clostridium perfringens*. *Plasmid* **91**: 28-36.

Wisniewski, J.A., Teng, W.L., Bannam, T.L., and Rood, J.I. (2015a) Two novel membrane proteins, TcpD and TcpE, are essential for conjugative transfer of pCW3 in *Clostridium perfringens*. *Journal of Bacteriology* **197**: 774-781.

Wisniewski, J.A., Traore, D.A., Bannam, T.L., Lyras, D., Whisstock, J.C., and Rood, J.I. (2015b) TcpM, a novel relaxase that mediates transfer of large conjugative plasmids from *Clostridium perfringens*. *Molecular Microbiology* **99**: 884-896.

Chapter Six

Discussion

In this study multiple aspects of the biology of the *C. perfringens* Tcp plasmids have been examined, with a specific focus on conjugation and plasmid stability. The pathogenic bacterium *C. perfringens* harbours many of its disease-producing toxin genes on highly stable, conjugative Tcp plasmids. Ensuring the maintenance of these plasmids in a host in the absence of selective pressure is required to preserve the potential of these cells to cause tissue damage that results in disease (Sengupta & Austin, 2011). To minimise plasmid loss, plasmids can encode genetic systems that ensure their stability within a host (Sengupta & Austin, 2011). Whilst important studies on the partitioning system of the Tcp plasmids have been conducted (Adams *et al.*, 2015, Watts *et al.*, 2017), little information regarding the genetic and mechanistic basis of other stability mechanisms utilised by this family of plasmids are known.

The carriage of toxin genes on conjugative plasmids allows for the efficient transfer of virulence factors between *C. perfringens* cells. Many studies have identified key components of the Tcp conjugation apparatus (Parsons *et al.*, 2007, Steen *et al.*, 2009, Porter *et al.*, 2012, Wisniewski *et al.*, 2015a, Bannam *et al.*, 2006, Bantwal *et al.*, 2012, Teng *et al.*, 2008, Traore *et al.*, 2018, Wisniewski *et al.*, 2015b), but little is known about whether all of the factors involved in conjugation have been identified and where in the cell this event occurs. The work presented in this thesis has contributed to the knowledge of both of these critical aspects of Tcp plasmid biology.

Expanding the *tcp* conjugation locus of pCW3

Many of the genes present on pCW3 have remained largely uncharacterised, since they encode hypothetical proteins (Bannam *et al.*, 2006). This study aimed to examine the involvement of these conserved genes in key aspects of plasmid biology, including conjugation and plasmid stability.

Following bioinformatic analysis of the uncharacterised CnaC region, located upstream of the *tcp* locus, the involvement of these genes in pCW3 conjugation was examined through the

construction of mutants. Mutation of *srtD* and *tcpN* resulted in a significant reduction of conjugative efficiency in both intrastrain and interstrain mating. To confirm the phenotypes observed, various *in trans* complementation strategies were employed. However, none of the complementation methods attempted in this study were successful, suggesting that either these gene are not able to be complemented *in trans*, or that a secondary mutation may have resulted in the conjugation phenotypes. Whilst it is possible that a secondary mutation has occurred, the construction of genetically confirmed, independent mutants of both genes and the demonstration that these mutants had the same phenotypes makes this scenario unlikely. Despite difficulties in complementing the mutants, these results provided evidence of the involvement of both *srtD* and *tcpN* in pCW3 conjugation.

Future experiments should aim to confirm the involvement of *srtD* and *tcpN* in conjugation through alternative complementation strategies, such as *in trans* complementation using a native promoter or *in cis* complementation *via* a genetic knock-in, as discussed in Chapter Two. Following complementation, future studies should aim to identify the protein targets of SrtD, potentially providing insight into how the Tcp conjugation system facilitates cell-to-cell contact with the recipient. Sortase protein targets are primarily identified through bioinformatic analysis, searching for protein sequences that possess the sortase recognition motif (LPXTG), followed by a hydrophobic region and a charged C-terminal tail (Clancy *et al.*, 2010). The only identified protein encoded on pCW3 that possesses some of these characteristics is CnaC, making it a likely target of SrtD (Bannam *et al.*, 2006). However, identification through bioinformatic screening alone could limit the discovery of targets that do not fall into the consensus target protein parameters. The identification of SrtD targets could be achieved through a more sensitive method such as the examination of the differences in membrane protein composition between the wild type and the sortase mutant *via* mass spectrometry (MS). This approach has been used successfully to identify the substrates of two sortases from *Listeria monocytogenes* (Pucciarelli *et al.*, 2005).

The mechanism of action of SrtD should also be investigated. Many studies have analysed sortase activity and substrate specificity i*n vitro* using recombinant sortase protein and short synthetic peptides that contain putative sortase recognition motifs or mutated derivatives (Suryadinata *et al.*, 2015, van Leeuwen *et al.*, 2014). In these studies, the ability of the sortase enzyme to link the synthetic peptides to peptidoglycan substrates has been analysed using SDS-PAGE and Western blotting (Suryadinata *et al.*, 2015), or MOLDI-ToF MS (van Leeuwen *et al.*, 2014). Determination of the SrtD activity and recognition sequence using similar techniques could confirm CnaC as the SrtD target. Additionally, elucidation of SrtD tag preferences may also assist in identification of other plasmid- or host-encoded protein targets.

Studies should also aim to characterise the function of the protein encoded by *tcpN,* as bioinformatic analysis provides no insights. One avenue of investigation would be structural analysis using X-ray crystallography. Structural analysis of another pCW3-encoded protein, TcpC, demonstrated structural homology to the VirB8 protein from *Agrobacterium tumefaciens*, despite the absence of any significant amino acid similarity between the two proteins (Porter *et al.*, 2012). It remains possible that many of the proteins encoded on pCW3 do not share significant amino acid homology to proteins of known function but may fold and act in very similar ways. Since TcpN is involved in conjugation, determination of the location within the cell, as was investigated for other Tcp proteins in Chapter Five, may provide insight into putative functions. Additionally, elucidating protein-protein interactions between TcpN and other Tcp proteins could identify a potential role for TcpN in the conjugation complex. Elucidating these protein interactions could be achieved using methods such as bacterial-two-hybrid, as has been used for other Tcp proteins (Steen *et al.*, 2009, Porter *et al.*, 2012, Teng *et al.*, 2008), or through more sensitive approaches using recombinant proteins and techniques such as biolayer interferometry (BLItz)(Sultana & Lee, 2015) or surface plasmon resonance (SPR)(Drescher *et al.*, 2018). Elucidation of TcpN structure, protein interactions and location would allow for a better understanding of how this protein functions in Tcp conjugation.

Characterisation of an essential stability factor of pCW3, ResP

In addition to being conjugative, many plasmids of the pCW3 family appear to be stable without selection (Watts *et al.*, 2017)(S. Revitt-Mills, V. Adams, D. Lyras and J. Rood, unpublished). To better understand how the Tcp family of plasmids are maintained within *C. perfringens* cells without the need for constant selection, the mechanisms of pCW3-like plasmid stability must be further characterised. Some maintenance mechanisms utilised by these plasmids have been identified, including a ParMRC-like active partitioning system (Adams *et al.*, 2015, Watts *et al.*, 2017) and putative regulatory proteins (T. Stent, X. Han, V. Adams, R. Moore and J. Rood, unpublished) but there remain large gaps in our knowledge.

The *resP* gene was predicted to encode a serine recombinase and to function as part of a plasmid multimer resolution system (Bannam *et al.*, 2006). To investigate the requirement of *resP* in pCW3 stability, mutants were constructed, and plasmid stability assessed. Deletion of *resP* resulted in an unstable plasmid phenotype, which was rescued by complementation *in trans*, confirming the involvement of *resP* in pCW3 stability. Bioinformatic analysis identified the putative pCW3 *res* site, and the ability of ResP to recognise and recombine DNA containing these directly repeated *res* sites was examined in an excision assay. The results demonstrated that ResP is essential for pCW3 plasmid stability and is a highly efficient recombinase, likely to constitute a multimer resolution system that is conserved amongst the pCW3-like plasmids of *C. perfringens*.

This study has determined that ResP is required for pCW3 stability, however, questions remain regarding its mechanism of action and confirmation of involvement in a multimer resolution system. Future work should examine the role of ResP in multimer formation and resolution in the context of pCW3. Pulsed-field gel electrophoresis has been used successfully in other studies to confirm the production of large plasmid multimers (Kusano *et al.*, 1989). Attempts to confirm pCW3 multimer formation in *resP* mutants using this method were made in this study, however, the results were inconclusive. It was postulated that multimer formation of pCW3-like plasmids

may be a low frequency event, as evidenced by the gradual loss of the mutant plasmid observed in stability assays, thus making detection difficult using the current method. In future, optimisation of sample preparation, electrophoresis and detection methods may assist in better visualisation of pCW3 plasmid multimers. Alternatively, other studies have assayed multimer resolution using small, high-copy number vector systems, which allow for easy visualisation of multimeric plasmid forms (LeBard *et al.*, 2008). Similar experiments could be conducted using some of the vectors constructed as part of the excision assay preformed in this study (Chapter Three). In these experiments, plasmid multimer formation could be investigated using an *E. coli* *recA*$^{+}$ background, comparing the proportions of plasmid DNA forms of *res* containing plasmids encoding ResP and a ResP knockout derivative.

A unique feature of a multimer resolution system is the specificity of the recombination reaction through the recognition of a recombination site, *res*. The putative pCW3 *res* site identified in this study was typical of that of other serine recombinases (Figure 3.9). However, the location of the putative cleavage dinucleotide within the inverted repeat closest to the *resP* gene implies that the orientation of these sites is reversed compared to other characterised systems, whereby site I (cleavage site) is located closest to the resolvase gene and site III (accessory site) is furthest from the *resP* gene. Whilst it is postulated that the dinucleotide present in the inverted repeat closest to the *resP* gene is the recombination site within the pCW3 *res*, until the cleavage site is determined experimentally, it cannot be rule out that ResP may cleave and recombine DNA at a different dinucleotide sequence. Techniques such as DNase I footprinting have been previously used to assess binding of Res proteins to the inverted repeats of their cognate *res* sites (Grindley *et al.*, 1982, Rowland *et al.*, 2002, Eberl *et al.*, 1994, LeBard *et al.*, 2008). Although this technique is robust, a more sensitive method, such as surface plasmon resonance (SPR), could be used to examine the binding sites and binding kinetics of the pCW3 ResP proteins.

To determine the ResP cleavage site within *res*, a site-directed mutagenesis approach, similar to that used in the study of the site-specific recombinase TnpX (Crellin & Rood, 1997), could be used. In this study, to determine the specificity of TnpX enzyme. the putative dinucleotide sequence of the transposon Tn*4451* was mutated and the ability of TnpX to excise the transposon was assessed (Crellin & Rood, 1997). This would be an excellent avenue to explore in future works.

The recognition and recombination of multiple *res* sites on a single plasmid molecule is typical of resolvase enzymes, however, since pCW3 ResP is predicted to have a serine recombinase domain it would be pertinent to assess if ResP functions solely as a resolvase or can invert DNA sequences. Recombinase enzymes of the serine recombinase family rely on the recognition of directly repeated *res* sites and resolves DNA into two separate molecules (Grindley *et al.*, 2006). Conversely, invertase enzymes of the same family recognise and function on *res* sites that are inverted, resulting in DNA recombination that reverses the sequence between the two sites (Johnson, 2015). To assess if ResP can invert DNA sequences future work should utilise a reporter assay system, using a phenotypic expression plasmid with the promoter reversed and harboured between two inverted *res* sites. If ResP were able to invert DNA, an inversion between the two *res* sites would place the promoter in the correct orientation for the reporter protein expression. Experiments proposed in this discussion would help firmly establish the role of ResP in pCW3-like plasmid multimer resolution and provide insight into the characteristics of this system.

The novel *srm* gene is involved in the stability of pCW3

Further expanding on the mechanisms of pCW3 plasmid stability, this study identified a novel gene that was essential for the stability of pCW3 (Chapter Four). The gene, *srm,* is located within the conserved genetic region of pCW3 located downstream of *dcm*. *srm* is found on almost all pCW3-like plasmids and some plasmids carry multiple copies. Bioinformatic analysis of the putative Srm protein predicted a Hin-like HTH domain in the C-terminal portion of the protein. The presence of this domain indicates that Srm may bind to DNA and could potentially function

as a regulatory protein. Mutation of *srm* on pCW3 resulted in an unstable plasmid phenotype, which was rescued upon complementation *in trans*, confirming the essential role of Srm in pCW3 stability. Two Srm homologues from another pCW3-like plasmid were also able to complement the pCW3 *srm* mutation, suggesting that the mechanism by which Srm functions is not plasmid specific. Overall these findings have identified and characterised a novel gene involved in the stability of pCW3-like plasmids.

The mechanism by which Srm modulates plasmid stability remains unknown, since bioinformatic analysis and preliminary biochemical studies have not definitively established a putative function for Srm. Future work should attempt to establish Srm function through determination of its protein structure through X-ray crystallography. This avenue of experimentation was attempted in this study, however, protein expression and purification experiments require further optimisation. Future work on optimisation of these techniques may aid in the determination of Srm structure, providing valuable insight into protein function.

The presence of a putative Hin-like HTH domain, although not essential for Srm function, does suggest that Srm may work as a regulatory protein. If Srm is indeed a regulator of stability functions, it would be imperative to determine its precise regulatory targets. Methods such as RNA-sequencing (RNA-seq) and chromatin immunoprecipitation- sequencing (ChIP-seq) could be employed (Furey, 2012, Wang *et al.*, 2009). RNA-seq analysis could be used to compare RNA transcripts between the wild type and *srm* mutants, which would establish target transcripts that may be regulated by Srm. There are some limitations in the analysis of transcript levels between strains if the plasmid copy number is altered by the mutation in question. Differences in plasmid copy numbers, and thus plasmid transcript levels, make the normalisation of data challenging, since it would be difficult to ascertain if differences in transcript levels are conferred by the mutation or through changes in plasmid copy number. As the changes in pCW3 copy number are minimal in *srm* mutants (Figure 4. 9) it is possible that this plasmid copy number difference may

not affect RNA-seq analysis. ChIP-seq is another method that could be used to identify Srm targets. ChIP-seq combines immunoprecipitation and sequencing techniques to identify DNA targets for DNA-associated proteins (Furey, 2012). If Srm binds DNA, ChIP-seq could identify the genetic regions to which it binds, providing insight into the targets of Srm regulation.

It is hypothesised that Srm may facilitate auxiliary interactions that regulate *rep* or rep_{AS} transcription. To investigate this postulate the amount of *rep* and rep_{AS} transcript produced in the wild type, *srm* mutant and complemented strains could be evaluated *via* Northern blotting or transcriptomics analysis, as mentioned above. Alternatively, Srm regulation of *rep* and other transcripts could be assayed using a plasmid reporter system. For example, a chloramphenicol reporter assay was used to demonstrate autoregulation of the pSK41 *res* transcript by the Res protein (LeBard *et al.*, 2008).

This study determined the existence of a potential regulatory circuit utilised by pCW3 to ensure plasmid stability, whereby the putative regulator, RegC, regulates plasmid stability through Srm (Figure 4.12). Previous work has shown that mutation of *regC* results in a dramatic reduction in plasmid stability, which can be rescued by *in trans* complementation (T. Stent, X. Han, V. Adams, R. Moore and J. Rood, unpublished). In this study, complementation of the *regC* mutant with *srm* restored plasmid stability to levels similar to wild type, suggesting that the stability phenotype observed in the *regC* mutant strain was due, at least in part, to a dysregulation of *srm*.

Based on current knowledge, a model of this regulatory pathway can be proposed (Figure 6.1). Since RegC has organisational similarity to the transcriptional repressor LexA, it is assumed that this protein functions as a negative regulator. For this model to fit the data obtained in this study, RegC-mediated regulation of *srm* is proposed to function through a putative intermediate repressor, denoted "SrmR" with the R referring to repressor. It is assumed that Srm is an activator of positive stability functions, as the data obtained in this study suggests Srm has a positive effect on plasmid stability. SrmR is hypothesised to act directly to repress *srm* transcription. In wild

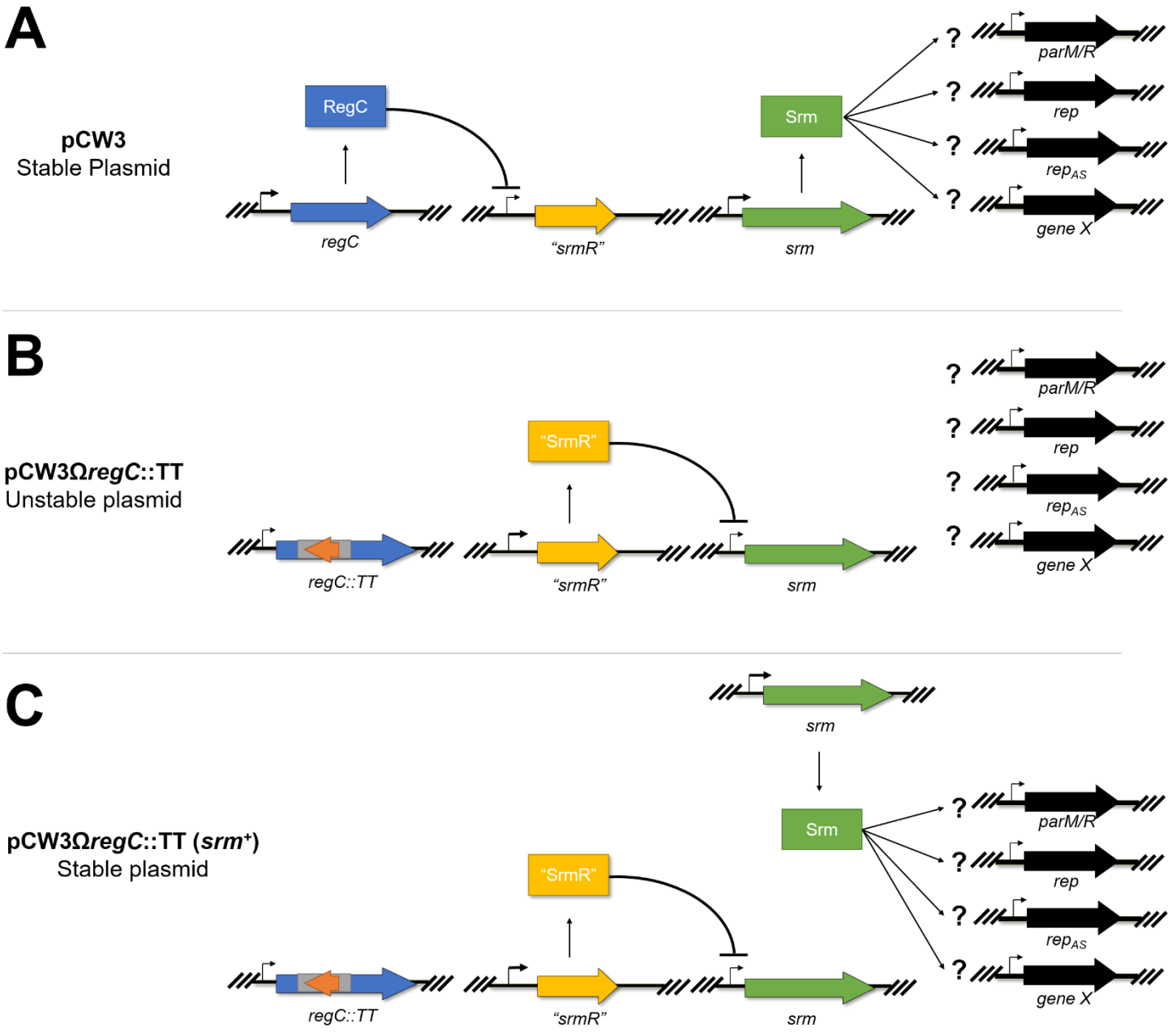
A
pCW3
Stable Plasmid
RegC
Srm
regC
"srmR"
srm
parM/R
rep
repAS
gene X
B
pCW3ΩregC::TT
Unstable plasmid
"SrmR"
regC::TT
"srmR"
srm
parM/R
rep
repAS
gene X
C
pCW3ΩregC::TT (srm+)
Stable plasmid
srm
Srm
"SrmR"
regC::TT
"srmR"
srm
parM/R
rep
repAS
gene X

Figure 6.1: Proposed model of RegC mechanistic control. Schematic representation of the regulatory pathway involving RegC and Srm. ORFs are shown as thick coloured arrows. Proteins are depicted as boxes and are labelled accordingly. **A.** The RegC regulation pathway for wild type pCW3. RegC regulates Srm production through the direct regulation of a putative *srm* repressor. RegC binds upstream of the repressor gene, blocking transcription. This allows for the transcription of *srm* mRNA. Expression of the Srm protein results in a stable plasmid phenotype through an unknown mechanism. In this model, Srm is hypothesised to act on several plasmid genes thought to be important for plasmid stability, shown as black ORFS, including active partitioning (*parMRC*), replication (*rep* or rep_{AS}) or through another unknown mechanism (*gene X*). **B.** The RegC regulation pathway in the *regC* mutant. Here, the *srm* repressor is expressed, which ultimately blocks effective expression of *srm.* The result is an unstable plasmid phenotype. **C.** The RegC regulation pathway for the *regC* mutant, complemented *in trans* with *srm*. When *srm* is provided on a multicopy vector, the expression of Srm partially complements the plasmid stability phenotype.

type pCW3 (Figure 6.1A), RegC is expressed at normal levels and represses the expression of *srmR*, allowing for the expression of Srm, which establishes a stable plasmid phenotype through an unknown mechanism. In this model Srm is hypothesised to act on other plasmid stability mechanisms, such as active partitioning (*parMRC*), replication (*rep* or rep_{AS}) or through an unidentified mechanism (*gene X*). In the *regC* mutant (Figure 6.1 B), *srmR* is no longer repressed by RegC, is expressed and SrmR subsequently represses the transcription of *srm.* Repression of *srm* results in an unstable plasmid phenotype. Plasmid stability can be rescued in this strain following complementation with *srm* on a multi-copy vector (Figure 6.1 C). The *srm* gene is present in the *C. perfringens* cell at a level that is not effectively repressed by SrmR. Srm is therefore produced from the over-expression vector, and regulates the stability pathway as normal, resulting in a stable plasmid. The slight loss of the pCW3 *regC* plasmid later in the stability assay (Figure 4.12) indicates that RegC most likely regulates other stability mechanisms, which were not complemented by addition of the *srm* gene. This model requires validation through additional experiments to examine this complex regulatory system.

Localisation of various Tcp conjugation apparatus components using super-resolution microscopy

The pCW3-like plasmids of *C. perfringens* utilise the Tcp conjugation machinery to transfer plasmid DNA between bacterial cells. Previous studies (Teng *et al.*, 2008, Wisniewski *et al.*, 2015a) have determined the location of some key components of the Tcp conjugation apparatus within the *C. perfringens* cell, however, the resolution has been limited. In this study the locations of functional epitope-tagged derivatives of six Tcp proteins were determined using StimulaTed Emission Depletion (STED) super resolution microscopy building upon previous observations about Tcp protein cellular localisation (Chapter Five). This work determined that the small membrane protein TcpE formed ring-like clusters in various positions on the surface of the bacterial cell. Proteins TcpD and TcpH demonstrated variable patterns of localisation, with many cells indicating a polar localisation, similar to what has been observed previously for both proteins (Wisniewski *et al.*, 2015a, Teng *et al.*, 2008). The relaxosome proteins TcpK and TcpM were dispersed throughout the cytoplasm. Whereas the coupling protein, TcpA,

was present around the periphery of the cell. Through the use of super resolution microscopy, the location of individual protein spots were mapped on the bacterial cell, providing valuable insight into the cellular location of the Tcp conjugation process.

This study demonstrated that the Tcp conjugation proteins have variable and dispersed localisations. From these observations a model for Tcp conjugation was proposed, whereby multiple complexes form around the periphery of the cell, maximising the possibility of encountering a suitable recipient cell and therefore conjugative transfer. To confirm this model, future work would involve co-localisation of multiple Tcp proteins. Using methods similar to those developed in this study, FLAG-tagged TcpA could be visualised in the same cell as HA-tagged TcpD, TcpE, TcpH, TcpM or TcpK, since the antibodies for the FLAG and HA epitope tags are compatible for dual labelling experiments (Li, 2010). However, all the epitope tagged proteins used in this study are harboured on vectors with the same antibiotic resistance profiles, meaning they are not appropriate for strain construction. Efforts would have to be made to construct strains with epitope-tagged proteins encoded on the same vector or on multiple compatible vectors. Alternatively, epitope tags could be introduced onto pCW3. This approach would allow for the detection of Tcp proteins at native expression levels, potentially overcoming limitations involved with protein overexpression from multi-copy vectors. The co-localisation of Tcp proteins would confirm complex formation at the multiple foci throughout *C. perfringens* cells that were observed in this study.

To further understand the Tcp conjugation process, elucidation of the cellular location of pCW3 DNA is required. Previous studies have utilised fluorescently labelled LacO-LacI operator systems to specifically label plasmid DNA in the cell (Bauer *et al.*, 2011, Berkmen *et al.*, 2010, Lawley *et al.*, 2002, Lawley & Taylor, 2003). The LacO array and *lacI* genes are inserted into the DNA molecule of interest. In these systems, the LacO cassette is comprised of tandem repeats of the lactose operator and the fluorescently tagged LacI (usually green fluorescent protein, GFP) binds to the operator repeats, which clusters the fluorescence signal to the position of the DNA molecule. Unfortunately, effective folding of GFP requires oxygen (Heim *et al.*, 1994), and *C. perfringens* is an anaerobic organism. Only a few fluorescent protein tags are amenable for use in anaerobic environments, such as the iLOV proteins

(Chapman *et al.*, 2008). The visualisation of plasmid DNA in *C. perfringens* using this technique would require the development of a new LacO/LacI-iLOV array and optimisation of microscopy techniques. Ultimately visualisation of the conjugation process in live cells would be beneficial for the understanding of the Tcp conjugation process. To achieve this objective, the development of *C. perfringens* live-cell imaging techniques utilising fluorescent labelling that is functional in the absence of oxygen would be required. This is an achievable goal, but a large body of work is required to reach it. The live visualisation of the pCW3 plasmid DNA alongside Tcp proteins would help answer several questions about the conjugation system used by these plasmids, such as (i) does TcpM co-transfer through the conjugation apparatus into the recipient cell with plasmid DNA? and (ii) for strains that harbour multiple Tcp plasmids, do these plasmids share conjugation machinery for transfer or are they transferred separately through their own machinery?

Conclusions

This thesis presents an analysis of several key aspects of *C. perfringens* pCW3-like plasmid biology, specifically plasmid stability and conjugation. The results of these studies have expanded the *tcp* conjugation locus to include a putative sortase encoded by *srtD* and a protein of unknown function encoded by *tcpN*. This thesis has also identified and examined a putative multimer resolution system, encoded by the gene *resP*, and a novel stability mechanism mediated by Srm, both of which are essential for pCW3 stability. Lastly, the results of this study have provided new and invaluable insight into the spatial location of the Tcp conjugation event using super-resolution microscopy techniques. Overall, this body of work has provided useful insights into the mechanisms of stability and conjugation used by the pCW3-like family of plasmids and has provided a platform for future research into the maintenance and spread of toxin and antibiotic resistance plasmids among *C. perfringens* populations.

References

Adams, V., Watts, T.D., Bulach, D.M., Lyras, D., and Rood, J.I. (2015) Plasmid partitioning systems of conjugative plasmids from *Clostridium perfringens*. *Plasmid* **80**: 90-96.

Bannam, T.L., Teng, W.L., Bulach, D., Lyras, D., and Rood, J.I. (2006) Functional identification of conjugation and replication regions of the tetracycline resistance plasmid pCW3 from *Clostridium perfringens*. *Journal of Bacteriology* **188**: 4942-4951.

Bantwal, R., Bannam, T.L., Porter, C.J., Quinsey, N.S., Lyras, D., Adams, V., and Rood, J.I. (2012) The peptidoglycan hydrolase TcpG is required for efficient conjugative transfer of pCW3 in *Clostridium perfringens*. *Plasmid* **67**: 139-147.

Bauer, T., Rösch, T., Itaya, M., and Graumann, P.L. (2011) Localization pattern of conjugation machinery in a Gram-positive bacterium. *Journal of Bacteriology* **193**: 6244-6256.

Berkmen, M.B., Lee, C.A., Loveday, E.-K., and Grossman, A.D. (2010) Polar positioning of a conjugation protein from the integrative and conjugative element ICE*Bs1* of *Bacillus subtilis*. *Journal of Bacteriology* **192**: 38-45.

Chapman, S., Faulkner, C., Kaiserli, E., Garcia-Mata, C., Savenkov, E.I., Roberts, A.G., Oparka, K.J., and Christie, J.M. (2008) The photoreversible fluorescent protein iLOV outperforms GFP as a reporter of plant virus infection. *Proceedings of the National Academy of Sciences* **105**: 20038-20043.

Clancy, K.W., Melvin, J.A., and McCafferty, D.G. (2010) Sortase transpeptidases: Insights into mechanism, substrate specificity, and inhibition. *Peptide Science* **94**: 385-396.

Crellin, P.K., and Rood, J.I. (1997) The resolvase/invertase domain of the site-specific recombinase TnpX is functional and recognizes a target sequence that resembles the junction of the circular form of the *Clostridium perfringens* transposon Tn*4451*. *Journal of Bacteriology* **179**: 5148-5156.

Drescher, D.G., Selvakumar, D., and Drescher, M.J., (2018) Analysis of protein interactions by surface plasmon resonance. In: Advances in Protein Chemistry and Structural Biology. R. Donev (ed). Academic Press, pp. 1-30.

Eberl, L., Kristensen, C.S., Givskov, M., Grohmann, E., Gerlitz, M., and Schwab, H. (1994) Analysis of the multimer resolution system encoded by the *parCBA* operon of broad-host-range plasmid RP4. *Molecular Microbiology* **12**: 131-141.

Furey, T.S. (2012) ChIP-seq and beyond: new and improved methodologies to detect and characterize protein-DNA interactions. *Nature Reviews Genetics* **13**: 840-852.

Grindley, N.D.F., Lauth, M.R., Wells, R.G., Wityk, R.J., Salvo, J.J., and Reed, R.R. (1982) Transposon-mediated site-specific recombination: Identification of three binding sites for resolvase at the *res* sites of *γδ* and Tn*3*. *Cell* **30**: 19-27.

Grindley, N.D.F., Whiteson, K.L., and Rice, P.A. (2006) Mechanisms of site-specific recombination. *Annual Review of Biochemistry* **75**: 567-605.

Heim, R., Prasher, D.C., and Tsien, R.Y. (1994) Wavelength mutations and posttranslational autoxidation of green fluorescent protein. *Proceedings of the National Academy of Sciences* **91**: 12501-12504.

Johnson, R.C. (2015) Site-specific DNA inversion by serine recombinases. *Microbiology Spectrum* **3**: 1-36.

Kusano, K., Nakayama, K., and Nakayama, H. (1989) Plasmid-mediated lethality and plasmid multimer formation in an *Escherichia coli recBC sbcBC* mutant. Involvement of RecF recombination pathway genes. *Journal of Molecular Biology* **209**: 623-634.

Lawley, T.D., Gordon, G.S., Wright, A., and Taylor, D.E. (2002) Bacterial conjugative transfer: visualization of successful mating pairs and plasmid establishment in live *Escherichia coli*. *Molecular Microbiology* **44**: 947-956.

Lawley, T.D., and Taylor, D.E. (2003) Characterization of the double-partitioning modules of R27: Correlating plasmid stability with plasmid localization. *Journal of Bacteriology* **185**: 3060-3067.

LeBard, R.J., Jensen, S.O., Arnaiz, I.A., Skurray, R.A., and Firth, N. (2008) A multimer resolution system contributes to segregational stability of the prototypical staphylococcal conjugative multiresistance plasmid pSK41. *FEMS Microbiology Letters* **284**: 58-67.

Li, Y. (2010) Commonly used tag combinations for tandem affinity purification. *Biotechnology and Applied Biochemistry* **55**: 73-83.

Parsons, J.A., Bannam, T.L., Devenish, R.J., and Rood, J.I. (2007) TcpA, an FtsK/SpoIIIE homolog, is essential for transfer of the conjugative plasmid pCW3 in *Clostridium perfringens*. *Journal of Bacteriology* **189**: 7782-7790.

Porter, C.J., Bantwal, R., Bannam, T.L., Rosado, C.J., Pearce, M.C., Adams, V., Lyras, D., Whisstock, J.C., and Rood, J.I. (2012) The conjugation protein TcpC from *Clostridium perfringens* is structurally related to the type IV secretion system protein VirB8 from Gram-negative bacteria. *Molecular Microbiology* **83**: 275-288.

Pucciarelli, M.G., Calvo, E., Sabet, C., Bierne, H., Cossart, P., and García-del Portillo, F. (2005) Identification of substrates of the *Listeria monocytogenes* sortases A and B by a non-gel proteomic analysis. *Proteomics* **5**: 4808-4817.

Rowland, S.-J., Stark, W.M., and Boocock, M.R. (2002) Sin recombinase from *Staphylococcus aureus*: synaptic complex architecture and transposon targeting. *Molecular Microbiology* **44**: 607-619.

Sengupta, M., and Austin, S. (2011) Prevalence and significance of plasmid maintenance functions in the virulence plasmids of pathogenic bacteria. *Infection and Immunity* **79**: 2502-2509.

Steen, J.A., Bannam, T.L., Teng, W.L., Devenish, R.J., and Rood, J.I. (2009) The putative coupling protein TcpA interacts with other pCW3-encoded proteins to form an essential part of the conjugation complex. *Journal of Bacteriology* **191**: 2926-2933.

Sultana, A., and Lee, J.E. (2015) Measuring protein-protein and protein-nucleic acid interactions by biolayer interferometry. *Current Protocols in Protein Science* **79**: 19.25. 11-19.25. 26.

Suryadinata, R., Seabrook, S.A., Adams, T.E., Nuttall, S.D., and Peat, T.S. (2015) Structural and biochemical analyses of a *Clostridium perfringens* sortase D transpeptidase. *Acta Crystallographica Section D: Biological Crystallography* **71**: 1505-1513.

Teng, W.L., Bannam, T.L., Parsons, J.A., and Rood, J.I. (2008) Functional characterization and localization of the TcpH conjugation protein from *Clostridium perfringens*. *Journal of Bacteriology* **190**: 5075-5086.

Traore, D.A.K., Wisniewski, J.A., Flanigan, S.F., Conroy, P.J., Panjikar, S., Mok, Y.-F., Lao, C., Griffin, M.D.W., Adams, V., Rood, J.I., and Whisstock, J.C. (2018) Crystal structure of TcpK in complex with *oriT* DNA of the antibiotic resistance plasmid pCW3. *Nature Communications* **9**: 3732.

van Leeuwen, H.C., Klychnikov, O.I., Menks, M.A.C., Kuijper, E.J., Drijfhout, J.W., and Hensbergen, P.J. (2014) *Clostridium difficile* sortase recognizes a (S/P)PXTG sequence motif and can accommodate diaminopimelic acid as a substrate for transpeptidation. *FEBS Letters* **588**: 4325-4333.

Wang, Z., Gerstein, M., and Snyder, M. (2009) RNA-Seq: a revolutionary tool for transcriptomics. *Nature Reviews Genetics* **10**: 57.

Watts, T.D., Johanesen, P.A., Lyras, D., Rood, J.I., and Adams, V. (2017) Evidence that compatibility of closely related replicons in *Clostridium perfringens* depends on linkage to *parMRC*-like partitioning systems of different subfamilies. *Plasmid* **91**: 68-75.

Wisniewski, J.A., Teng, W.L., Bannam, T.L., and Rood, J.I. (2015a) Two novel membrane proteins, TcpD and TcpE, are essential for conjugative transfer of pCW3 in *Clostridium perfringens*. *Journal of Bacteriology* **197**: 774-781.

Wisniewski, J.A., Traore, D.A., Bannam, T.L., Lyras, D., Whisstock, J.C., and Rood, J.I. (2015b) TcpM, a novel relaxase that mediates transfer of large conjugative plasmids from *Clostridium perfringens*. *Molecular Microbiology* **99**: 884-896.

Supplementary Data

Supplementary Table 1: List of *E. coli* strains used in this thesis

Strain	Description	Reference
DH5α	F-φ80*lacZ*ΔM15, Δ(*lac*ZYA-*argF*)U169, *rec*A1, *end*A1, *hsd*R17(r_k-, m_k+), *pho*A, *sup*E44, *thi*-1, *gyr*A96, *rel*A1 λ	Invitrogen/ Life Technologies
DH12S	φ80*lacZ*ΔM15, *mcrA* Δ(*mrr-hsdRMS-mcrBC*), *araD139* Δ(*ara, leu*)7697, Δ(*lacX74 galU galK rpsL)* (Str^R) *nupG, recA1/F,' proAB+, lacI*^{q}ZΔM15	Invitrogen/ Life Technologies
C41 (DE3)	BL21(DE3) derivative	(Miroux & Walker, 1996)

Supplementary Table 2: List of *C. perfringens* strains used in this thesis

Strain	Description	Reference
JIR39	Strain CW362 derivative, Sm^R Chl^R	(Johanesen *et al.*, 2001)
JIR325	Strain 13 derivative; Rif^R Nal^R	(Lyristis *et al.*, 1994)
JIR4195	JIR325 (pCW3); Rif^R Nal^R Tc^R	(Hughes *et al.*, 2007)
JIR4394	Strain 13 derivative; Sm^R Chl^R	(Bannam *et al.*, 2006)
JIR4885	JIR4195(pJIR2902); Rif^R Nal^R Tc^R Em^R pCW3Δ*tcpH::erm*(Q)	(Bannam *et al.*, 2006)
JIR12540	JIR4195(pJIR3760); Rif^R Nal^R Tc^R Em^R pCW3Ω*tcpM*::targetron (TT)	(Wisniewski *et al.*, 2015b)
JIR13063	JIR4195(pJIR4349); Rif^R Nal^R Tc^R Em^R pCW3Ω*tcpK*::targetron (TT)	(Traore *et al.*, 2018)
JIR13187	JIR4195(pJIR4851); Rif^R Nal^R Tc^R Em^R pCW3Ω*regC::*targetron(TT), independent mutant	T. Stent, X. Han, V. Adams, R. Moore and J. Rood, unpublished
JIR13211	JIR325(pCP13)$^-$; Rif^R Nal^R JIR325 cured of pCP13	(Watts *et al.*, 2019)
JIR13224	JIR13211(pCW3); Rif^R Nal^R Tc^R	This study
JIR13252	JIR13211(pJIR4521); Rif^R Nal^R Tc^R Em^R pCW3Δ*pcw321::erm*(Q)	This study

JIR13253	JIR13211(pJIR4522); Rif^R Nal^R Tc^R Em^R pCW3Δ*pcw321::erm*(Q), independent mutant	This study
JIR13254	JIR13211(pJIR4523); Rif^R Nal^R Tc^R Em^R pCW3Δ*pcw322::erm*(Q)	This study
JIR13255	JIR13211(pJIR4524); Rif^R Nal^R Tc^R Em^R pCW3Δ*pcw322::erm*(Q), independent mutant	This study
JIR13256	JIR13211(pJIR4525); Rif^R Nal^R Tc^R Em^R pCW3Δ*srtD::erm*(Q)	This study
JIR13257	JIR13211(pJIR4526); Rif^R Nal^R Tc^R Em^R pCW3Δ*srtD::erm*(Q), independent mutant	This study
JIR13258	JIR13211(pJIR4527); Rif^R Nal^R Tc^R Em^R pCW3Δ*tcpN::erm*(Q)	This study
JIR13259	JIR13211(pJIR4528); Rif^R Nal^R Tc^R Em^R pCW3Δ*tcpN::erm*(Q) (Q), independent mutant	This study
JIR13321	JIR13211(pJIR4583); Rif^R Nal^R Tc^R Em^R pCW3Δ*pcw325::erm*(Q)	This study
JIR13338	JIR4195(pJIR4593); Rif^R Nal^R Tc^R Em^R pCW3Δ*srm::erm*(Q)	This study
JIR13390	JIR4195(pJIR4621); Rif^R Nal^R Tc^R Em^R pCW3Δ*srm::erm*(Q), independent mutant	This study
JIR13587	JIR4195(pJIR4796); Rif^R Nal^R Tc^R Em^R pCW3Δ*resP::erm*(Q)	This study
JIR13588	JIR4195(pJIR4797); Rif^R Nal^R Tc^R Em^R pCW3Δ*resP::erm*(Q), independent mutant	This study

Amp^R- ampicillin resistance, Chl^R- potassium chlorate resistance, Cm^R- chloramphenicol resistance, Em^R- erythromycin resistance, Kn^R- kanamycin resistance, Nal^R- nalidixic acid resistance, Rif^R – rifampicin resistance, Sm^R- streptomycin resistance, Tc^R- tetracycline resistance, Tm^R – thiamphenicol resistance.

Supplementary Table 3: List of plasmids used in this thesis

Plasmid	Description	Reference
pET22b+	*E. coli* expression vector, C-terminal His_6-Tag	Invitrogen
pSU39	*E. coli* cloning vector, Kan^R	(Bartolomé *et al.*, 1991)

pT7-Blue	*E. coli* cloning vector, f1 origin, pUC origin, *lacZ* α-peptide, Amp^R	Novagen
pJIR750	*E. coli-C. perfringens* shuttle vector, Cm^R	(Bannam & Rood, 1993)
pCW3	Conjugative tetracycline resistance plasmid	(Rood *et al.*, 1978)
pJIR2715	Base plasmid for the construction of *C. perfringens* suicide vectors, Em^R Cm^R	(Bannam *et al.*, 2006)
pJIR2902	pCW3Δ*tcpH::erm*(Q)	(Bannam *et al.*, 2006)
pJIR3213	pCW3Δ*tcpA::erm*(Q)	(Parsons *et al.*, 2007)
pJIR3422	pJIR750*ΩattCI, E. coli-C. perfringens* shuttle and expression vector, Cm^R	(Adams *et al.*, 2014, Bantwal *et al.*, 2012)
pJIR3440	pCW3Δ*tcpD*::*erm*(Q)	(Wisniewski *et al.*, 2015a)
pJIR3442	pCW3Δ*tcpE::erm*(Q)	(Wisniewski *et al.*, 2015a)
pJIR3562	Clostridial targetron vector with P_{tet}, *ermB*-RAM	(Cheung *et al.*, 2010)
pJIR3566	Clostridial TargeTron vector, pMTL9361 derivative, *lacZ* α-peptide, Cm^R	(Cheung *et al.*, 2010)
pJIR3757	pJIR3422(BamHI/Asp718)ΩJRP4048/JRP4489 (BamHI/Asp718; 451 bp, pCW3) *tcpE*-HA complementation vector	(Wisniewski *et al.*, 2015a)
pJIR3760	pCW3Ω*tcpM*:: TT	(Wisniewski *et al.*, 2015b)
pJIR3844	Cpb2-toxin plasmid from EHE-NE-18	(Bannam *et al.*, 2011)
pJIR4067	Group II intron of pJIR3562 retargeted to the 152/153 site of *regC* gene	T. Stent, X. Han, V. Adams, R. Moore and J. Rood, unpublished
pJIR4204	pJIR3422(BamHI/Asp718)ΩJRP4046/JRP4728 (BamHI/Asp718; 450 bp, pCW3) *tcpD*-G_6-HA complementation vector	(Wisniewski *et al.*, 2015a)
pJIR4349	pCW3Ω*tcpK*:: TT	(Traore *et al.*, 2018)
pJIR4353	pJIR750(Asp718/BamHI) ΩJRP5350/JRP5350 BamHI/Asp7118; 1200bp, pCW3) *regC* complementation vector	T. Stent, X. Han, V. Adams, R. Moore and J. Rood, unpublished

pJIR4503	pJIR2715 (XhoI/SacI) ΩJRP6249/JRP6250 (XhoI/SacI; 2817 bp, pCW3) downstream of *pcw321*	This study
pJIR4504	pJIR2715 (XhoI/SacI) ΩJRP6249/JRP6251 (XhoI/SacI; 2550 bp, pCW3) downstream of *pcw322*	This study
pJIR4505	pJIR2715 (XhoI/SacI) ΩJRP6249/JRP6252 (XhoI/SacI; 1894 bp, pCW3) downstream of *srtD*	This study
pJIR4506	pJIR2715 (XhoI/SacI) ΩJRP6249/JRP6253 (XhoI/SacI; 1583 bp, pCW3) downstream of *tcpN*	This study
pJIR4507	pJIR2715 (XhoI/SacI) ΩJRP6249/JRP6254 (XhoI/SacI; 2550 bp, pCW3) downstream of *pcw325*	This study
pJIR4508	pJIR4503 (SphI/BamHI) ΩJRP6243/JRP6244 (SphI/BamHI; 1556 bp, pCW3) *pcw321* suicide vector	This study
pJIR4509	pJIR4504 (SphI/BamHI) ΩJRP6243/JRP6245 (SphI/BamHI; 1704 bp, pCW3) *pcw322* suicide vector	This study
pJIR4510	pJIR4506 (SphI/BamHI) ΩJRP6243/JRP6247 (SphI/BamHI; 2626 bp, pCW3) *tcpN* suicide vector	This study
pJIR4511	pJIR4507 (SphI/BamHI) ΩJRP6243/JRP6248 (SphI/BamHI; 2932 bp, pCW3) *pcw325* suicide vector	This study
pJIR4515	pJIR4505 (SphI/BamHI) ΩJRP6243/JRP6246 (SphI/BamHI; 1971 bp, pCW3) *srtD* suicide vector	This study
pJIR4521	pCW3Δ*pcw321::erm*(Q)	Transformation of JIR13224 with pJIR4508
pJIR4522	pCW3Δ*pcw321::erm*(Q), independent mutant	Transformation of JIR13224 with pJIR4508

pJIR4523	pCW3Δ*pcw322::erm*(Q)	Transformation of JIR13224 with pJIR4509
pJIR4524	pCW3Δ*pcw322::erm*(Q), independent mutant	Transformation of JIR13224 with pJIR4509
pJIR4525	pCW3Δ*srtD::erm*(Q)	Transformation of JIR13224 with pJIR4515
pJIR4526	pCW3Δ*srtD::erm*(Q), independent mutant	Transformation of JIR13224 with pJIR4515
pJIR4527	pCW3Δ *tcpN::erm*(Q)	Transformation of JIR13224 with pJIR4510
pJIR4528	pCW3Δ *tcpN::erm*(Q), independent mutant	Transformation of JIR13224 with pJIR4510
pJIR4545	pT7Blue (EcoRV) ΩJRP6372/JRP6373 (661 bp, pCW3) *srtD+*	This study
pJIR4546	pT7Blue (EcoRV) ΩJRP6375/JRP6375 (316 bp, pCW3) *tcpN*	This study
pJIR4547	pJIR3422 (PstI/BamHI) ΩpJIR4545 (PstI/BamHI; 661 bp, pCW3), *srtD* complementation vector	This study
pJIR4549	pJIR3422 (PstI/BamHI) ΩpJIR4546 (PstI/BamHI; 316 bp, pCW3), *tcpN* complementation vector	This study
pJIR4557	pJIR2715 (BamHI/Asp718) ΩJRP6414/JRP6418 BamHI/Asp718; 1643 bp, pCW3) downstream of *srm*	This study
pJIR4583	pCW3Δ*pcw325::erm*(Q)	Transformation of JIR13224 with pJIR4511

pJIR4584	pT7Blue (EcoRV) ΩJRP6472/JRP6475 (970 bp, pCW3) *srtD+, tcpN+*	This study
pJIR4586	pJIR3566 (BamHI/Asp718) ΩJRP6450/JRP6451 (BamHI/Asp718; 1688 bp, pCW3) *pCW321* to *pcw325* knock-in vector	This study
pJIR4587	pJIR3422 (PstI/BamHI) ΩJRP6450/JRP6449 (PstI/BamHI; 1687 bp, pCW3) *pcw321* to *pcw325* complementation vector	This study
pJIR4588	pJIR3422 (PstI/BamHI) ΩpJIR4584 (PstI/BamHI; 970 bp, pCW3), *srtD* and *tcpN* double complementation vector	This study
pJIR4591	pJIR4557 (XhoI/EagI) ΩJRP6413/JRP6417 XhoI/EagI; 1851 bp, pCW3), *srm* suicide vector	This study
pJIR4593	pCW3Δ*srm::erm*(Q)	Transformation of JIR4195 with pJIR4591. This study
pJIR4621	pCW3Δ*srm::erm*(Q), independent mutant	Transformation of JIR4195 with pJIR4591 This study
pJIR4640	pT7-Blue (EcoRV) ΩJRP6563/JRP6564 (1615 bp, pCW3), *pCW347⁺, srm⁺*	This study
pJIR4641	pT7-Blue (EcoRV) ΩJRP6565/JRP6564 (1485 bp, pCW3), *srm⁺*	This study
pJIR4644	pT7-Blue3 (EcoRI) ΩJRP6570/JRP6571 (798 bp, pCW3) *tcpK*-G_6-HA, blunt cloning vector	This study
pJIR4645	pT7-Blue3 (EcoRI) ΩJRP6572/JRP6573 (305 bp, pCW3) *tcpM*-G_6-HA, blunt cloning vector	This study
pJIR4653	pJIR750 (BamHI/Asp718) pJIR4640 (BamHI/Asp718; 1615 bp) *pCW347⁺, srm⁺* complementation vector	This study

pJIR4654	pJIR750 (BamHI/Asp718) pJIR4641 (BamHI/Asp718; 1485 bp) *srm*$^{+}$ complementation vector	This study
pJIR4655	pJIR3422(BamHI/Asp718) (BamHI/Asp718; 798 bp, pJIR4644) *tcpK*-G_6-HA complementation vector	This study
pJIR4657	pJIR3422(BamHI/Asp718) (BamHI/Asp718; 305 bp, pJIR4645) *tcpM*-G_6-HA complementation vector	This study
pJIR4704	pT7-Blue (EcoRV) ΩJRP6564/JRP6638 (1180 bp, pCW3), $srm_{1\text{-}256}^{+}$	This study
pJIR4706	pJIR750 (BamHI/Asp718) pJIR4704 (BamHI/Asp718; 1180 bp) $srm_{1\text{-}256}^{+}$ complementation vector	This study
pJIR4724	pET22b+ (XhoI/NdeI) Ω JRP6670/JRP6671 (XhoI/NdeI; 902 bp, pCW3) Srm expression vector	This study
pJIR4794	pJIR2715 (EcoRI/XbaI) ΩJRP6797/JRP6798 (EcoRI/XbaI; 2039 bp, pCW3) downstream of *resP*	This study
pJIR4795	pJIR4794 (Asp718/BamHI) ΩJRP6799/JRP6800 (Asp718/BamHI; 1764 bp, pCW3), *resP* suicide vector	This study
pJIR4796	pCW3Δ*resP::erm*(Q)	Transformation of JIR4195 with pJIR4794
pJIR4797	pCW3Δ*resP::erm*(Q), independent mutant	Transformation of JIR4195 with pJIR4794
pJIR4798	pJIR750 (BamHI/Asp718) ΩJRP6844/JRP6845 (BamHI/Asp718; 1196 bp, pCW3) *resP*$^{+}$ complementation vector	This study
pJIR4800	pET22b+ (XhoI/NdeI) ΩJRP6783/JRP6670 (XhoI/NdeI; 770bp, pCW3) $Srm_{1\text{-}256}$ expression vector without putative HTH domain	This study

pJIR4809	pJIR750 (BamHI/Asp718) ΩJRP7195/JRP7196(BamHI/Asp718; 1117 bp, pJIR3844) *resP*$_{pJIR3844^+}$ complementation vector	This study
pJIR4810	pJIR750 (Asp718/BamHI) ΩJRP6866/JRP6867 (Asp718/BamHI; 744 bp; pCP13) *resP*$_{pCP13^+}$ complementation vector	This study
pJIR4812	pJIR750 (BamHI/Asp718) ΩJRP6564/JRP6865 (BamHI/Asp718; 1467 bp, pJIR3844) *srm*$_{pJIR3844\_45^+}$ complementation vector	This study
pJIR4813	pJIR750 (BamHI/Asp718) ΩJRP6564/JRP6864 (BamHI/Asp718; 1363 bp, pJIR3844) *srm*$_{pJIR3844\_56^+}$ complementation vector	This study
pJIR4833	pJIR2715 (Asp718/BamHI) ΩJRP7126/JRP7127 (Asp718/BamHI; 1176 bp, pCW3) Excision assay vector with one *res* site	This study
pJIR4834	pJIR4833 (XhoI/SacI) ΩJRP7128/JRP7129 (XhoI/SacI; 1176 bp, pCW3) Excision assay vector with two *res* sites flanking *erm*(Q)	This study
pJIR4835	pSU39 (Asp718/BamHI) ΩJRP6845/JRP6844 (Asp718/BamHI; 1196 bp, pCW3) ResP expression plasmid for excision assay	This study
pJIR4843	pJIR3422(BamHI/Asp718) ΩJRP7059/JRP7060 (BamHI/Asp718; 2521 bp, pCW3) *tcpH*-G_6-HA complementation vector	C. Lao, V. Adams, J. Rood, unpublished
pJIR4844	pJIR3422(BamHI/SphI) ΩJRP6265/JRP6240 (BamHI/SphI; 1703 bp, pCW3) *tcpA*-G_6-FLAG complementation vector	This study
pJIR4851	pCW3Ω*regC*::targetron (TT)	T. Stent, X. Han, V. Adams, R. Moore and J. Rood, unpublished

Amp^R- ampicillin resistance, Chl^R- potassium chlorate resistance, Cm^R- chloramphenicol resistance, Em^R- erythromycin resistance, Kn^R- kanamycin resistance, Nal^R- nalidixic acid resistance, Rif^R – rifampicin resistance, Sm^R- streptomycin resistance, Tc^R- tetracycline resistance, Tm^R – thiamphenicol resistance.